이학박사 학위논문

세포기반분석법을 통한
생체시계 조절자의 개발 및 적용 연구

Development of circadian clock modulator

and its application

2014 년 2 월

서울대학교 대학원

생명과학부

전 승 국

세포기반분석법을 통한
생체시계 조절자의 개발 및 적용 연구

Development of circadian clock modulator

and its application

지도교수 김 경 진

이 논문을 이학박사 학위논문으로 제출함
2013년 12월

서울대학교 대학원
생명과학부
전 승 국

전 승 국의 이학박사 학위논문을 인준함

2013년 12월

위 원 장 정 진 하 (인)
부위원장 김 경 진 (인)
위 원 이 건 수 (인)
위 원 최 석 우 (인)
위 원 선 웅 (인)

Development of circadian clock modulator

and its application

A dissertation submitted in partial fulfillment
of the requirement for the degree of

DOCTOR OF PHILOSOPHY

to the Faculty of
School of Biological Sciences
at
Seoul National University
by
Sung Kook Chun

Date Approved

Dec, 2013

ABSTRACT

In mammals, circadian rhythms are found in almost all of biological processes. Based on the physiological and clinical importance of circadian rhythms, identification of novel drugs that can modulate circadian clock is an immerging field. However, small molecule modulators that enhance E box-mediated transcriptional activity have not been reported yet. In Chapter 1, I identified and characterized a novel small molecule KS15 that directly binds to cryptochromes (CRYs) and inhibits its repressive function. In Chapter 2, I investigated the effect of KS15 on proliferation, chemosensitivity and metastatic activity of human breast cancer cells as an application study.

1. In Chapter 1, I aimed to identify novel small molecule modulator influencing the molecular feedback loop of the circadian clock. I designed two-step cell-based screening strategy based on E-box-mediated transcriptional activity to test more than 1,000 drug-like compounds. As a result, KS15 was selected as the most promising drug candidate. I then performed pull-down assays with the biotinylated KS15 and found that both cryptochrome 1 and 2 (CRY1/2), are molecular targets of KS15. In accordance with the binding property, KS15 enhanced E-box-mediated transcription in a CRY1/2-dependent manner, and more importantly, it

attenuated the circadian oscillation of Per2-Luc and Bmal1-dLuc activities in cultured fibroblasts, indicating that KS15 can functionally inhibit the effects of CRY1/2 in the molecular circadian clockwork. Finally, intracerebral injection of KS15 *in vivo* shows delayed phase and lengthened period of circadian rhythm. The present study describes the first novel chemical inhibitor of CRY1/2 that inhibits the repressive function of CRY1/2, thereby modulates circadian clock both *in vitro* and *in vivo*.

2. In Chapter 2, based on recent studies that CRY1/2 are involved in the onset of human breast cancer, I evaluated the anti-tumor activity of KS15 on human breast cancer cells in vitro. First, I treated KS15 in various concentrations to human breast cancer cells (MCF-7 and MDA-MB-231) as well as to a normal mammary epithelial cell (MCF10A). As a result, KS15 inhibited the proliferation of MCF-7 cell line in a dose-dependent manner, but not in other cell lines. Also, sensitivities for the anti-tumor drugs were enhanced only in MCF-7 when co-treated with KS15. On the other hand, adhesion ability on extracellular matrix and metastatic activity were not significantly affected by treatment of KS15. These findings suggest that pharmacological inhibition of CRYs has an anti-proliferative effect and increasing chemosensitivity to anti-tumor drugs on a specific type of breast cancer. It appears that KS15 has the potential to be a candidate for anti-

tumor drugs or an adjuvant to treatment of breast cancer.

In conclusion, I discovered the first novel chemical inhibitor (KS15) of CRY1/2 that inhibits the repressive function of CRY1/2, thereby activating E-box-mediated transcription regulated by CLOCK:BMAL1 heterodimer. As an application study, I evaluated anti-tumor activity of KS15 on proliferation and chemosensitivity of MCF-7 cells. Further investigation on the detailed mechanism and optimization of this anti-tumor activity of KS15 in needed to develop a novel therapeutic drug for breast cancer.

Key words: Cryptochrome (CRY); Circadian rhythm; Small molecule; Cell-based screening; Chemical biology; Breast cancer; Anti-tumor activity

CONTENTS

Page

Chapter 2. Evaluation of anti-tumor activity of Cryptochrome inhibitor on human breast cancer cell lines

LIST OF FIGURES AND TABLES

Background and Purpose

Background and Purpose

1. Mammalian circadian clock

1.1. Circadian rhythm and biological clock

Most living organisms on earth, from cyanobacteria to mammals, have been exposed to day and night cycle due to the earth's rotation. Thus, most organisms have developed an internal time-keeping system, referred to as the 'biological clock' (Dunlap, 1999; Reppert, 1998), to anticipate to these cyclic environmental changes. In mammals, biological clock regulates various essential physiologies and behaviors and therefore, many biological processes display clear daily oscillation. For example, sleep-wake cycles, core body temperature, blood pressure and glucose level as well as hormone levels show robust circadian rhythm. Thus, biological clock allows the organism to prepare for the changes in the environment. Also, this innate time-keeping system provides internal time cues to ensure that a certain physiological change takes place in coordination with others (Gachon et al., 2004). In mammals, the circadian timing is regulated by a hierarchical assembly of multiple oscillators, in which the hypothalamic suprachiasmatic nucleus (SCN) serves as the central pacemaker. (Moore and Silver, 1998; Silver et al., 1996) Most peripheral organs, as well as

extra-SCN brain regions, possess their own molecular oscillators, and these are referred to as peripheral clocks. These clocks have molecular makeup that is similar to the SCN master clock (Lamia et al., 2008; Son et al 2008; Zhang et al., 2010). These oscillators have two general characteristics: First, they are self-sustained and approximately 24-hour rhythm in constant conditions; rhythmicity persists even in the absence of environmental cues such as light. Moreover, oscillation can be observed in dissociated cells from brain (Welsh et al., 1995) as well as in fibroblasts (Balsalobre et al., 1998). Second, autonomous clock can be synchronized by external signals such as light, temperature, or social cues like feeding schedules and maintain the timekeeping system of organism through phase shift and resetting of internal clock. (Reppert and Weaver, 2002; Schibler and Sassone-Corsi, 2002; Schibler et al., 2003).

1.2. Regulation of circadian clock in mammals

Regulation of circadian rhythm in mammal is hierarchical in structure with the master pacemaker located in the SCN of the anterior hypothalamus. SCN is composed by approximately 20,000 neurons and entrained to external light-dark cycle by receiving photic input through the retinohypothalamic tract (RHT). SCN produces a rhythmic output which is composed of neural and hormonal signals that influence physiology and

behavior (Schibler and Sassone-Corsi, 2002). This master pacemaker coordinates countless peripheral clocks within various tissue and cell types. In general, the molecular clock machinery of oscillators within the SCN and the periphery are very similar. The main difference between master and peripheral clocks is how they are synchronized and influenced by various signals. The SCN is entrained by light received through the retina while the peripheral oscillators are often adjusted by chemical signals or by feeding (Dallmann et al., 2012). Elimination of the SCN disrupts circadian rhythm of behavior and hormonal output such as sleep-wake cycle and corticosterone release. Furthermore, implantation of SCN to SCN-lesioned animals rescued circadian pattern in behavior (Ralph et al., 1990; Kriegsfeld et al., 2004). Desynchrony between intrinsic and environmental rhythms has been found to render shortened lifespan in mice (Davidson et al., 2006).

1.3. Molecular mechanism of circadian clock in mammals

The autonomous and self-sustainable nature of circadian timing mainly depends on the molecular circadian clockwork, which is comprised of a subset of clock genes (Fig 1). The clock gene products cooperatively control the rhythmicity of gene expression, primarily by two interlocked positive and negative transcriptional/translational feedback loops (Balsalobre et al., 1998; Bunger et al., 2000; Hogenesch et al., 1998;

Takahata et al., 1998; Gekakis et al., 1998). Circadian Locomotor Output Cycle Kaput (CLOCK) and Brain-Muscle-Arnt-Like protein 1 (BMAL1), which belong to the basic helix-loop-helix–Period-ARNT-SIM (bHLH–PAS) transcription factor superfamily, form a heterodimer to recognize E-box elements on the promoter region of downstream genes, including *Periods* (*Pers*) and *Cryptochromes* (*Crys*), and subsequently activate their transcription. PERs and CRYs proteins translocate into the nucleus and suppress CLOCK:BMAL1-mediated transcription by forming a negative complex that completes the core feedback loop (Jin et al., 1999; Kume et al., 1999; Sangoram et al., 1998). Proteins from core clock genes are not only regulated by transcriptional feedback but also by various post-translational regulations including phosphorylation and ubiquitination. For example, CRYs have been shown to be phosphorylated by AMP-activated kinase AMPK (Lamia et al., 2009) prior to ubiquitination by the F-box E3 ligase FBXL3 (Siepka et al., 2007; Busino et al., 2007). Likewise, phosphorylation by Casein kinase I primes PER proteins for ubiquitination and proteosomal degradation (Chiu et al., 2011). Also, CLOCK and BMAL1 are target of various modifications including phosphorylation, acetylation, ubiquitination (Tamaru et al., 2009; Hirayama et al., 2007; Yoshitane et al., 2009; Kwon et al., 2006). Moreover, a small ubiquitin-related modifier (SUMO)-mediated modification of BMAL1 has also been proposed as another important post-translational regulatory mechanism (Cardone et al.,

Figure 1. Mammalian molecular circadian clockwork. CLOCK and BMAL1 form heterodimer and induce the expression of negative regulators, *Period* and *Cryptochrome* genes by binding to the E-box element in their promoter. PER and CRY form a complex and translocate into the nucleus to inhibit CLOCK/BMAL1-mediated transcription. The CLOCK/BMAL1 heterodimer also induce the transcription of nuclear receptor RORα and REV-ERBα. They control Bmal1 gene expression by binding to ROR response element (RRE) in Bmal1 promoter. RORα activates transcription of *Bmal1* gene, whereas REV-ERBα inhibits *Bmal1* transcription. Also, post-translational modifications of clock genes are also important issue for regulating activity of molecular clockwork. Various kinds of modifications, such as phosphorylation (P), ubiquitination (Ub), Acetylation (A), and SUMOrylation (S) are occurred in core clock genes like CLOCK, BMAL1, PER1/2 and CRY1/2. These modifications regulate their activity and stability and theirby modulate overall activity of molecular circadian clockwork.

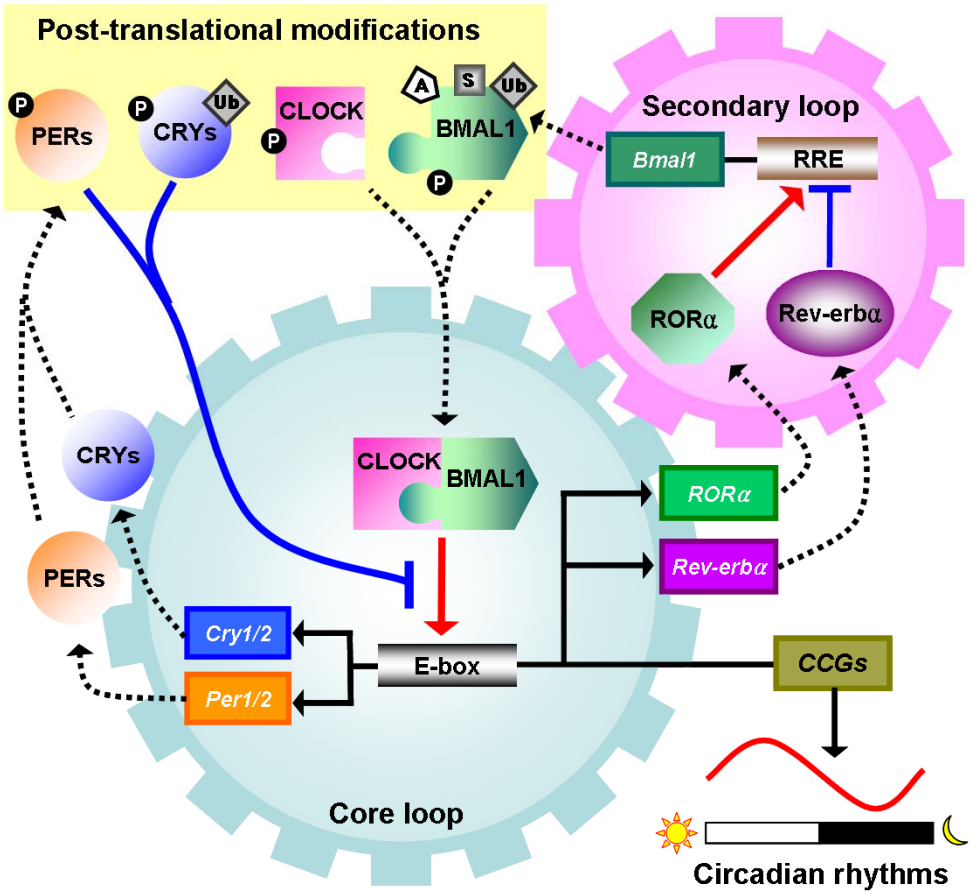
Post-translational modifications
PERs
CRYs
Ub
CLOCK
BMAL1
A
S
Ub
Secondary loop
Bmal1
RRE
RORα
Rev-erbα
CRYs
CLOCK
BMAL1
RORα
Rev-erbα
PERs
Cry1/2
Per1/2
E-box
CCGs
Core loop
Circadian rhythms

2005; Lee et al., 2008). On the other hand, a secondary loop composed of nuclear receptors, including RAR-related Orphan Receptors (RORs) and REV-ERBs, stabilizes the normal cycling of the core clock loop**.** REV-ERBα/β proteins are transcriptional repressors that compete with the RORs in such a manner as to regulate periodic *Bmal1* gene transcription. The RORs and REV-ERBs are also activated by CLOCK:BMAL1-mediated transcription, and this links the secondary loop with the core loop of the circadian molecular clock. (Ueda et al., 2002; Preitner et al., 2002; Bugge et al., 2012; Cho et al., 2012) Taken together, this self-sustained, cell autonomous circadian oscillator is maintained in nearly all mammalian cells and drives physiological alterations by controlling genes that are responsive to components of the molecular circadian clockwork.

2. Disturbance of circadian rhythm and its related disorder

2.1. Disruption of circadian rhythm and its related disorders

Disruption of normal circadian cycling has long been believed to be intimately linked to the onset of various human diseases, including metabolic and mood disorders, cardiovascular diseases, and cancer

(Takahashi et al., 2008; Kondratova and Kondratov, 2012; Maury et al., 2010; Park et al., 2012). People in modern lifestyle especially in highly industrialized society can be easily exposed to these disturbing stimuli for circadian clock system including artificial lights, night feeding, or social activity such as shift work. These are common causes of disturbances in the circadian clock system.

Exposure to light, especially at night, is the most powerful and well-known stimulus for disruption of circadian rhythm. Studies with animal models are providing the consequence of light exposure at night and indicate deleterious effects on behavior and physiology such as accelerated aging, tumorigenesis, propensity to obesity and anxiety-like and depressive-like behaviors (Grone et al., 2011; Shuboni and Yan, 2010; Ohta et al., 2005). Disturbance of circadian rhythms by exposure to various intensities of artificial light also has negative physiological effect in humans (Navara and Nelson, 2007). All this together conforms that the disruption of circadian rhythms consequent to an overexposure to the artificial light may lead to behavioral and physiological dysfunction.

Besides photic signals, there are also non-photic entraining stimuli influencing the biological clock as zeitgebers, such as those given by feeding schedules and physical activity (Dallmann and Mrosovsky, 2006;

Stephan, 2002). Such stimuli can also give temporal signals to the SCN, although they are weak as compared with light inputs (Emens et al., 2005). Although they do not override the light/dark cycle for the adjustment of the SCN, non-photic stimuli, especially food, contribute as potent synchronizers of cells and organs in the periphery, driving them out of phase from the signals transmitted by the SCN, thus resulting in internal desynchrony (Escobar et al., 2009; Hara et al., 2001; Mistlberger and Skene, 2004).

In humans, social activity also acts as important zeitgeber influencing the biological clock. The development of modern technology has promoted a relative independency of social and work activities from the environmental light/dark cycle. Some examples of modern-life habits that alter our biological rhythms are given by the long flights across the continents (jet-lag), shift work, night work, and so forth (Waterhouse et al*.,* 2007; Spiegel et al*.,* 1996; Davis et al., 2001). Animal models simulating similar conditions as night work have confirmed the deleterious effects of activity during the resting hours and circadian desynchrony (Ribeiro et al., 1998; Salgado-Delgado et al*.,* 2008; Salgado-Delgado et al., 2010; Nagano et al., 2003). Even more, the proportion of individuals that stay awake for long intervals in the night, engaged in leisure activities, has importantly increased and has become an important health problem (Pauley, 2004). Exposure to

nontraditional work schedules has been linked with increased risks of colorectal (Schernhammer et al., 2003), breast (Schernhammer et al., 2006), lymphatic (Lahti et al., 2008), and prostate (Kubo et al., 2006) cancers, as well as with obesity (Karlsson et al., 2001), diabetes (Morikawa et al., 2005), stroke (Karlsson et al., 2005), coronary heart disease, atherosclerosis, and heart attack (Tenkanen et al., 1998; Haupt et al., 2008). Individuals reporting poor or disturbed sleep, including shift workers, show increased incidences of diabetes and risk factors for the development of cardiovascular disease (Spiegel et al., 2009). Although the detailed mechanisms for these correlations between shift work exposure and disease are largely unknown, these evidences suggested that disruption of endogenous circadian clock by unnatural activity rhythm is clinically important risk factors.

2.2. Role of circadian clock genes in cancer

Disruption of circadian rhythms is associated with various forms of cancer in humans. Epidemiological studies have revealed that human night-shift workers show an increased risk of breast, colon, lung, endometrial and prostate cancer, hepatocellular carcinoma and non-

Hodgkin's lymphoma (Hansen, 2001; Davis et al., 2001). Loss of circadian rhythm is also associated with accelerated tumor growth in both rodents and human cancer patients (Flipski et al., 2002; Sephton et al., 2000). These findings raise a question of how circadian dysfunction increases the risk of cancers.

There is increasing evidence that links dysfunction of the clockwork with the pathogenesis of cancer. Both positive and negative loops of the molecular clock are involved in cell cycle control. For example, BMAL1 suppresses proto-oncogene c-myc but stimulates the tumor suppressor Wee1 (Fu et al., 2002; Fu et al., 2005). CRY2 indirectly regulates the intra S-check point (Unsal-Kacmaz et al., 2007 ; Unsal-Kacmaz et al., 2005), and PER1 directly interacts with ATM in response to γ-radiation in vitro (Gery et al., 2006). In mice, mutation in Per2 leads to deregulation of DNA-damage response and increased neoplastic growth (Fu et al., 2002; Fu et al., 2005). In humans, deregulation or polymorphism of Per1, Per2, Cry2, Npas2 and Clock is associated with acute myelogenous leukemia, hepatocellular carcinoma, breast, lung, endometrial and pancreatic cancers, and non-Hodgkin's lymphoma (Echave and Nash, 1970; Hoffman et al., 2009; Marino et al., 2008; Zhu et al., 2007; Gery et al., 2005; Chen et al., 2005; Gery et al., 2007; Shih et al., 2006; Pogue-Geile et al., 2006). There

is increasing evidence that links dysfunction of the clockwork with the pathogenesis of cancer. For example, decreased expression levels of Per1 and Per2 genes are observed in sporadic and familiar breast cancers when compared with normal breast tissues. The Per1 gene shows lower expression levels in familiar forms of breast cancer when compared with sporadic forms, suggesting that a potential deregulation of the circadian clock may contribute to the inherited form of the diseases.

3. Pharmacological modulation of circadian rhythm

3.1. Choronopharmacology and circadian rhythm

Recent advances in understanding the molecular control of circadian rhythms and subsequent signaling pathways have allowed for new therapeutic targets to be identified as well as for a better understanding of how to more efficaciously utilize current drugs. In addition to playing a key role in normal physiology and behavior, aberrations in the circadian rhythm are associated with the pathophysiology of diseases including diabetes, cardiovascular disease, psychological disorders and various autoimmune diseases/inflammation (Rybak et al., 2007; Solt et al., 2012), the potency

and efficacy of many drugs is associated with the circadian rhythmicity of expression of their molecular targets and cellular biochemical signals (Ohdo, 2010). A significant fraction of genes are expressed in a circadian fashion (Yan et al., 2008) including many drug targets and drug metabolizing enzymes yielding potential differences in efficacy/side effects based on time of day administration. Applying the knowledge of circadian function and regulation to the relevance of disease has enabled a chronotherapy approach in the timing of administration of conventional drugs in order to synchronize the rhythms in disease activity with the efficacy of the drug. Furthermore, recent advances in targeting the protein components involved in maintenance of the core circadian rhythm have allowed us to examine pharmacological alteration of the core rhythm to examine potential utility for treatment of disease.

3.2. Discovery of small molecule modifiers of circadian clock

Whereas classical genetics produces inherited changes in the sequence and/or abundance of the target protein, most synthetic small molecule modifiers allosterically alter the protein in a reversible, time-controlled and dose-dependent manner. Small molecules may also bind to a particular

domain and consequently modulate the cognate function of a multi-domain protein, leaving the other parts of the protein and associated functions intact. If the binding surface is conserved among multiple paralogous proteins, small molecules can concurrently regulate their activities to circumvent functional redundancy commonly observed in classical genetic studies. Thus, the small molecule-based chemical genetic approach is a powerful tool to perturb the system of interest (Hirota and Kay, 2009; Lehar et al., 2008). Two complementary methods have been utilized to identify small molecule modifiers of the clock. The first approach, based on phenotypic functional assays, interrogates broad chemical space via screening of diverse chemical libraries. In published studies, the reporter assays involved stable cell lines expressing either luciferase alone from an exogenous Bmal1 promoter (Hirota et al., 2012; Lee et al., 2011; Hirota et al., 2010) or PER2::luciferase fusion proteins from the endogenous Per2 promoter (Chen et al., 2012) corresponding to mRNA or protein rhythm, respectively. Bioluminescence is monitored over several days in the so-called kinetic, as opposed to end-point, assay to visualize circadian reporter rhythms. Changes in key clock parameters, including period, phase, and amplitude, can then be measured to identify small molecule modifiers. In these screens, small molecule modifiers may act on an intracellular target

in the upstream input pathway, the core oscillator, or any output pathways with feedback regulatory functions, such as metabolism. Furthermore, novel screening assays targeting additional clock regulatory pathways will likely lead to an enriched repertoire of clock modifiers.

Small molecule modifiers can also be identified based on direct interaction with particular clock proteins or regulatory factors. For example, IC261 and CKI-7 have been shown to lengthen the clock period as expected from their known CKI inhibitory activities (Eide et al., 2005; Vanselow et al., 2006). On the other hand, to generate novel and/or improved ligands for a particular target, it is often necessary to conduct deliberate chemical derivatization of small molecule analogs based on prior knowledge of known ligands and/or binding cavity structures (Vougogiannopoulou et al., 2008). An interesting example is the development of a selective inhibitor of casein kinase Iε, PF-4800567 which confers 20-fold selective inhibition over CKIδ (Walton et al., 2009; Badura et al., 2007; Meng et al., 2010). More recently, this approach has been successfully applied to the nuclear hormone receptors REV-ERBs and RORs, which constitute the stabilization loop of the core oscillator (Solt et al., 2011). Whereas the endogenous ligands are known for these proteins (heme and cholesterols respectively) (Raghuram et al., 2007 ; Yin et al.,

2007 ; Kallen et al., 2004), small molecule ligands are highly desirable to circumvent intracellular complications that altering metabolites commonly incurs, including nonspecific actions, cytotoxicity and redox imbalance (Grant et al., 2010). Starting with privileged scaffolds known to target ligand binding domains of nuclear hormone receptors, investigators were able to identify tertiary amines with three lipophilic substituents as agonists of REV-ERBa (Meng et al., 2008; Gibbs et al., 2012; Solt et al., 2012). Novel RORa/c ligands, most of them sulfonamide derivatives, have also been shown to modulate hepatic metabolism (Wang et al., 2010; Kumar et al., 2011) or to attenuate expression of downstream cytokines and alleviate autoimmune disease symptoms (Kumar et al., 2010; Solt et al., 2011). However, the role of the clock in these settings is currently unknown. In an attempt to correlate bona fide clock effects of small molecules with physiological consequences, I describe below known small molecule clock modifiers based on their activities in modifying the three major clock characteristics, namely period, phase, and amplitude. The classification is based on their primary, most pronounced phenotype since many small molecules are able to co-regulate more than one clock parameter.

4. Purpose

As described above, the circadian clock is a biological process that has physiological and clinical importance. However, the development of small molecule modulators that directly target the core clock machinery of molecular circadian clock has only been recently initiated. In the present study, I aimed to identify novel small molecule modulators influencing the molecular feedback loop of the circadian clock and to discover its clinical implication.

Chapter 1 is designed to identify and characterize a novel circadian clock modulator (KS15) that directly targets Cryptochromes (CRYs) in the molecular circadian clockwork.

Chapter 2 is focused on a potential clinical application of the newly developed circadian modulator. Recent studies suggest that epidemiology of human breast cancer is closely related to disturbance of circadian rhythm. Based on these studies, I hypothesized whether KS15 would affect to regulate induction and progression of human breast cancer. To prove this, I treated KS15 on human breast cancer cell lines and investigated the anti-tumor effect of KS15.

CHAPTER 1

Identification and characterization of a novel small compound modulator that can affect molecular circadian clock, Cryptochrome 1/2

ABSTRACT

Circadian rhythms, biological oscillations with a period of about 24 hours, are maintained by a genetically determined innate time-keeping system called the molecular circadian clockwork. Despite the physiological and clinical importance of the circadian clock, the development of small molecule modulators that directly target the core clock machinery has only been recently initiated. In the present study, I aimed to identify novel small molecule modulators influencing the molecular feedback loop of the circadian clock. I designed two-step cell-based screening strategy based on E-box-mediated transcriptional activity to test more than 1,000 drug-like compounds. As a result, a derivative of 2-ethoxypropanoic acid designated as KS15 was selected as the most promising candidate in terms of both efficacy and potency. I then performed pull-down assays with the biotinylated KS15 and found that both cryptochrome 1 and 2 (CRY1/2), key negative components of the mammalian circadian clock are molecular targets of KS15. In accordance with the binding property, KS15 enhanced E-box-mediated transcription in a CRY1/2-dependent manner, and more importantly, it attenuated the circadian oscillation of Per2-Luc and Bmal1-dLuc activities in cultured fibroblasts, indicating that KS15 can functionally inhibit the activities of CRY1/2 in the molecular circadian clockwork. In addition, intracerebral injection of KS15 *in vivo* caused delay of phase and lengthened period of activity rhythm. In conclusion, the present study describes the first novel chemical inhibitor of CRY1/2 that inhibits the repressive function of CRY1/2, thereby activating CLOCK-BMAL1-evoked E-box-mediated transcription. Further optimizations and subsequent

functional studies about this compound may lead to development of efficient therapeutic strategies for a variety of physiological and metabolic disorders with circadian natures.

Keywords: Cryptochrome; Circadian rhythm; Small molecule; Cell-based screening; Chemical biology

INTRODUCTION

Circadian rhythms with an approximate 24-hour period are found in most biological processes, such as core body temperature, hormone levels, and metabolism, as well as the sleep-wake and activity cycles. To anticipate cyclic environmental changes and coordinate both physiology and behavior so they occur at the appropriate time of day, most organisms from cyanobacteria to mammals have developed an internal time-keeping system referred to as the circadian clock. The mammalian system of circadian timing is organized in a hierarchy of multiple oscillators, in which the hypothalamic suprachiasmatic nucleus (SCN) serves as the central pacemaker (Moore and Silver, 1998; Silver et al., 1996). Most peripheral organs, as well as extra-SCN brain regions, possess their own molecular oscillators, and these are referred to as peripheral clocks. These clocks have molecular makeup that is similar to the SCN master clock (Lamia et al., 2008; Son et al., 2008; Zhang et al., 2010).

Disruption of normal circadian cycling has long been believed to be intimately linked to the onset of various human diseases, including metabolic and mood disorders, cardiovascular diseases, and cancer. Inappropriate light exposure, nighttime food intake, and misalignment of internal and external cycles, such as due to jet lag and shift work, are common causes of disturbances in the circadian clock system (Takahashi et al., 2008; Kondratova and Kondratov, 2012; Maury et al., 2010; Park et al., 2012).

The autonomous and self-sustainable nature of circadian timing mainly depends on the molecular circadian clockwork, which is comprised of a subset of clock genes. The clock gene products cooperatively control the rhythmicity of gene expression, primarily by two interlocked positive and negative transcriptional/translational feedback loops (Balsalobre et al., 1998; Bunger et al., 2000; Hogenesch et al., 1998; Takahata et al., 1998; Gekakis et al., 1998). Circadian Locomotor Output Cycle Kaput (CLOCK) and Brain-Muscle-Arnt-Like protein 1 (BMAL1), which belong to the basic helix-loop-helix–Period-ARNT-SIM (bHLH–PAS) transcription factor superfamily, form a heterodimer to recognize E-box elements on the promoter region of downstream genes, including *Periods* (*Pers*) and *Cryptochromes* (*Crys*), and subsequently activate their transcription. PERs and CRYs proteins translocate into the nucleus and suppress CLOCK:BMAL1-mediated transcription by forming a negative complex that completes the core feedback loop (Jin et al., 1999; Kume et al., 1999; Sangoram et al., 1998). In addition, a secondary loop composed of nuclear receptors, including RAR-related Orphan Receptors (RORs) and REV-ERBs, stabilizes the normal cycling of the core clock loop**.** REV-ERBα/β proteins are transcriptional repressors that compete with the RORs in such a manner as to regulate periodic *Bmal1* gene transcription. The RORs and REV-ERBs are also activated by CLOCK:BMAL1-mediated transcription, and this links the secondary loop with the core loop of the circadian molecular clock (Ueda et al., 2002; Preitner et al., 2002; Bugge et al., 2012; Cho et al., 2012).

Both synthetic compounds and endogenous small molecules have recently been identified as circadian clock modulators. Heme (Raghuram et al., 2007), cAMP (O'Neill et al., 2008) , and NAD (Nakahata et al., 2009; Ramsey et al., 2009) have been shown to affect the periodicity of molecular circadian clock. Synthetic REV-ERBα modulators, including GSK4112 (Grant et al., 2010), SR8278 (Kojetin et al., 2011), SR9009, and SR9011 (Solt et al., 2012), as well as casein kinase I inhibitors such as longdaysin (Hirota et al., 2010) and LH846 (Lee et al., 2011), were recently identified as promising molecular clock modulators. However, despite the physiological and clinical importance of circadian rhythms, small molecule modulators that enhance E box-mediated transcriptional activity have not been reported yet. Notably, the very recently developed compound KL001 is the only one that was reported as a small molecule directly targeting the core clock machinery, but it represses core loop activity by strengthening the negative functions of CRY1/2 (Hirota et al., 2012). In the present study, I identified and characterized a novel small molecule that directly binds to CRY1/2 and inhibits its repressive function, thereby activating E-box-mediated transcriptional activity. This small molecule has a distinct scaffold containing 2-ethoxypropanoic acid and two aryl rings connected by an oxime ether linker, compared with KL001, which has a carbazole scaffold (Hirota et al., 2012).

MATERIALS AND METHODS

Stable transfection Twenty-four hours before transfection, NIH3T3 and Y1 cells (1×10^6 cells per dish) were seeded in 35-mm culture dishes. Cells were co-transfected with luciferase reporter constructs (E-box-Luc or Per2-Luc for NIH3T3 and StARp-Luc for Y1) using Lipofectamine-PLUS reagent (Invitrogen) and a neomycin resistant plasmid (pcDNA3.1) at a molar ratio of 3:1. Two days after transfection, G-418 was added at a final concentration of 1 mg/mL. During 3-weeks of selection, the concentration of G-418 gradually reduced to 250 μg/mL. When resistant colonies became visible, stable transfection was verified by measuring bioluminescence with Cellgraph (ATTO, Tokyo, Japan). Colonies with sufficient luciferase activities were then trypsinized and clonally propagated. Cells were maintained in the culture medium containing G-418 at a final concentration of 100 μg/mL and luciferase activities were measured at every passage.

Luciferase Reporter Assay Stably transfected cells were plated in 48-well plates 12 hours before treatment. After 24 hour of treatment, cells were harvested and lysed with Passive Lysis Buffer (Promega, Madison, WI). Luciferase activities were examined with a commercial reporter assay reagent (Promega) according to the manufacturer's instructions and normalized by protein content, which were measured using Bradford protein assay reagent (Bio-Rad, Hercules, CA). At 24 hours before transfection, MEFs were seeded in 24-well culture plates at 1×10^5 cells/well. Cells were then transiently co-transfected with E-box-Luc (250

ng/well) and a control plasmid (promoterless renilla luciferase expression plasmid, 750 ng/well) using Metafectene easy reagent (Biontex, Martinsried, Germany). Twenty-four hours after transfection, cells were synchronized by a brief treatment with 100 nM dexamethasone (DEX) for 2 hours and then further cultivated for 12 hours. Thereafter, the indicated chemicals were treated for 24 hours and subsequently subjected to luciferase assays with Dual Luciferase Reporter reagent (Promega). E-box-driven firefly luciferase activities were normalized by renilla luciferase levels.

Synthesis Biotin-Conjugated KS15 To a solution of KS15 (62.7 mg, 0.149 mmol) and *N*-(5-aminopentyl)biotinamide trifluoroacetate salt (20.3 mg, 0.0520 mmol) in DMF (2 mL) were added 1-ethyl-3-(3-dimethylaminopropyl)carbodiimide (57.1 mg, 0.298 mmol), triethylamine (0.04 mL, 0.298 mmol) and 1-hydroxybenzotriazole (40.3 mg, 0.298 mmol), and the reaction mixture was stirred at 50 ˚C for 8 h. Then the reaction mixture was cooled to ambient temperature, and the solvent was evaporated *in vacuo*. The residue was diluted with EtOAc, washed with H_2O and brine, dried over $MgSO_4$, filtered, and concentrated *in vacuo*. The resulting residue was purified by flash column chromatography on silica gel (MeOH:CH_2Cl_2 = 1:10) to obtain the biotin-conjugated KS15 (8.2 mg, 23%) as a white solid. FT-IR (thin film, neat) ν_{max} 3297, 3082, 2928, 2859, 1701, 1650, 1535, 1487, 1461, 1403, 1368, 1331 cm^{-1}; ^1H NMR ($CDCl_3$, 400 MHz) δ 7.47 (m, 2H), 7.45 (s, 2H), 7.27 (s, 1H), 7.25 (s, 1H), 7.21 (m, 1H), 6.55 (m, 1H), 5.96 (m, 1H), 5.94 (s, 1H), 5.17 (s, 1H), 5.15 (s, 2H), 4.47 (m, 1H), 4.28 (m, 1H), 3.90 (m, 1H), 3.45 (m, 1H), 3.38 (m, 1H), 3.15 (m, 7H),

2.87 (m, 2H), 2.70 (d, 1H, *J* = 12.7 Hz), 2.22 (s, 3H), 2.17 (t, 2H, *J* = 7.3 Hz), 1.66 (m, 8H), 1.44 (m, 4H), 1.09 (t, 3H, *J* = 7.0 Hz); ^{13}C NMR ($CDCl_3$, 100 MHz) δ 173.0, 172.1, 163.5, 155.3, 137.7, 137.2, 136.2, 131.5, 131.5, 130.5, 129.8, 129.8, 128.2, 127.4, 124.3, 121.6, 81.2, 75.3, 66.6, 61.8, 60.1, 55.5, 40.5, 39.2, 38.9, 38.5, 35.9, 29.7, 29.3, 29.0, 28.1, 25.6, 23.9, 15.2, 12.9; LRMS (FAB) *m*/*z* 730 (M + H^+). HRMS (FAB) calcd for $C_{35}H_{49}BrN_5O_5S$ (M + H^+), 730.2638; found, 730.2638.

Pull-Down Assay HEK293T cells (2 × 10^7 cells per dish) were seeded in 100-mm culture dishes and transiently transfected with CMV promoter-driven expression constructs harboring mouse or human core clock proteins with the indicated epitope-tags (myc-CLOCK, myc-BMAL1, V5-PER1, V5-PER2, flag-CRY1, or flag-CRY2; 32 μg per dish). After 48 hour of transfection, cells were harvested with ice-cold lysis buffer [50 mM Tris (pH 7.4), 2 mM EDTA, 1 mM $MgCl_2$, 0.2% NP-40, 0.1% sodium deoxycholate, 1 mM sodium orthovanadate, 1 mM sodium fluoride, and protease inhibitor cocktail (Sigma−Aldrich, St. Louis, MO)]. Lysates were prepared by sonication followed by centrifugation (7000 × g) at 4 °C for 10 min. The resulting supernatants were diluted with ice-cold 2× binding buffer [100 mM Tris-HCl (pH 7.4), 300 mM NaCl, 0.2% NP-40, 2 mM sodium orthovanadate, 2 mM sodium fluoride and protease inhibitor], pre-cleared with 200 μL (50% slurry) of NeutroAvidin Agarose resin (Thermo Scientific, NYSE, TMO, USA) and then subjected to the pull-down assay. Lysates were incubated at 4 °C with rotation for preclearing. After incubation, beads were removed by centrifugation. The remaining supernatant was split into four samples and

treated with a series of compound mixes: a) only DMSO b) Bait (20 μM), c) Bait 20 μM + KS15 40 μM, and d) Bait (20 μM) + KS16 (40 μM). The final concentration of DMSO was 0.5%. After 30-min incubation with the compounds as indicated, the chemical-bound proteins were isolated by incubating them with activated NeutroAvidin Agarose for 2 hours at 4 °C with continuous agitation. The beads were washed six times with 1× binding buffer, and the bound proteins were eluted with sodium dodecyl sulfate (SDS) sample buffer. The pulled-down samples were separated by SDS-PAGE (8%) and transferred to a PVDF membrane (Millipore, Billerica, MA, USA). Immunoblot analyses were carried out with anti-myc (9E10, Santa Cruz Biotechnology, Santa Cruz , CA, USA), anti-V5 (V8137, Sigma−Aldrich) or anti-flag (M2, Sigma−Aldrich).

Preparation of Purified CRY1 Protein HEK293T cells (2 × 10^7 cells per dish) were seeded in 100-mm culture dishes, and transiently transfected with CMV promoter-driven expression constructs harboring human CRY1 proteins with FLAG and hexa-histidine tag (32 μg per dish). After 48 hour after transfection, cells were harvested with ice-cold lysis buffer [20 mM Tris (pH 7.4), 500 mM NaCl, 5 mM imidazole, 2 mM β-mercaptoethnol, 1% NP-40, 0.1% SDS and protease inhibitor cocktail (Sigma−Aldrich)]. Lysates were prepared by sonication followed by centrifugation (7000 × g) at 4 °C for 10 min. The resulting supernatants were diluted ten times with ice-cold binding buffer [20 mM Tris (pH 7.4), 500 mM NaCl, 5 mM imidazole, 2 mM β-mercaptoethnol, 0.45% NP-40, and protease inhibitor cocktail] and subjected to affinity chromatography using His-Bind Agarose Resin (ELPIS

biotech, Daejeon, Korea). After washing with 10 column volumes of binding buffer, hCRY1 proteins were eluted by using elution buffer [10 mM Tris (pH 7.4), 250 mM NaCl, 500 mM imidazole, and protease inhibitor cocktail]. A single fraction with highest purity was dialyzed against dialysis buffer [10 mM Tris (pH 7.4), 250 mM NaCl, 1 mM phenylmethanesulfonyl fluoride] and used for pull-down assay.

RNA Isolation and RT-PCR mRNA expression analyses were performed as previously described with certain modifications.[2] WT and *Cry1/2*$^{-/-}$ MEFs were suspended and seeded in 6-well culture plates. Cells were synchronized with 100 nM DEX and then changed to normal culture medium. Twelve hours after synchronization, drugs were administrated for a further 24 hours and then harvested. Total RNA was isolated with a single-step acid guanidinium thiocyanate-phenol-chloroform method. Then, 2 μg of each RNA sample were subjected to reverse transcription with MMLV-reverse transcriptase (Promega). mRNA expression profiles were analyzed by quantitative real-time PCR in the presence of SYBR Green I (Sigma−Aldrich). TATA box-binding protein (TBP) was used as an internal control gene transcript. The primer sequences used for real-time RT-PCR were as follows: Per1 up, 5′-GTG TCG TGA TTA AAT TAG TCA G-3′; Per1 dn, 5′-ACC ACT CAT GTC TGG GCC-3′; Per2 up, 5’-ATG CTC GCC ATC CAC AAG A-3′; Per2 dn, 5′-GCG GAA TCG AAT GGG AGA AT-3′; Rev-erbα up, 5′-AGG GCA CAA GCA ACA TTA CC-3′; Rev-erbα dn, 5′-CAC AGG CGT GCA CTC CAT AG-3′; TBP up, 5′-GGG AGA ATC ATG GAC CAG AA-3′; and TBP dn, 5′-CCG TAA GGC ATC ATT GGA CT-3′.

Real-Time Bioluminescence Monitoring Per2-Luc-expressing cells were plated in 35-mm dishes. Cells were synchronized by a treatment with 200 nM DEX for 2 hours, and then the medium was replaced with recording medium [Dulbecco's modified Eagle medium (DMEM) supplemented with 5% fetal bovine serum (FBS), 100 U/mL penicillin/streptomycin, and 0.1 mM luciferin (Promega)] with vehicle (0.2% DMSO) or 20 μM KS15. Light emission was integrated for 1 min at intervals of 10 min using a dish-type wheeled luminometer (Kronos-Dio, ATTO).

Statistical Analysis The CLUSTER (Veldhuis, University of Virginia, Charlottesville, VA) statistical pulse analysis program was used to identify the exact peak timing of Per2-Luc fibroblasts. The number of points for the peak and nadir were set as 3, and both of the T-scores for increase and decrease were set as 3.00. Statistical significance was assessed by Student's *t*-test and is indicated as follows: *, †: $p < 0.05$ and **, ††: $p < 0.01$.

Preparation of ΔCC-Tail Mutant of hCRY1/2 Expression Plasmid Flag−myc−His-tagged human CRY1 and CRY2 expression plasmids were obtained from Addgene (hCRY1: #25843, hCRY2: #25842). The putative coiled-coil (CC) region of hCRY1 and hCRY2 was identified based on the sequence homology of CC regions in mCRY1 and mCRY2, which were defined in a previous study[38]. To generate ΔCC-Tail Mutant of hCRY1/2, we designed the following primers for cloning: 5'- GAT ATC GCC ACC ATG

GGG GTG AAC GCC GTG CAC -3' (hCRY1 mutant, forward), 5'- TCT AGA CAT TGG TTT AGG ATA ATT AAC TCC -3' (hCRY1 mutannt, reverse), 5'- GAT ATC GCC ACC ATG GCG GCG ACT GTG GC -3' (hCRY2 mutant, forward), 5'- TCT AGA GCG CGA AAG CTG CTG GTA AAT C -3' (hCRY2 mutannt, reverse). The forward primer was designed to start before the EcoRV restriction site at the upstream of start codon in the original plasmid. The reverse primer was designed to target immediately before the CC region and harboring the XbaI restriction site, resulting in truncation of the C-terminal region. A PCR-amplified construct was subcloned into a pGEM-T easy vector (Promega) and replaced wild-type hCRY1 or hCRY2 within the original plasmid by using EcoRV/XbaI.

Preparation of ΔCC-Tail Mutant of hCRY1/2 Expression Plasmid To examine the dose-response activity of these compounds on PPAR mediated transcriptional activity, 100 ng per well of DR1-Luc plasmid (a luciferase reporter driven by synthetic promoter containing multiple PPAR responsive elements) and a control plasmid (promoterless renilla luciferase expression plasmid, 500 ng per well) were transfected into NIH3T3 mouse fibroblast cell line and treated with various concentrations of compounds. After 24-hour incubation, cells were harvested and lysed with Passive Lysis Buffer (Promega) and subsequently subjected to luciferase assays with Dual Luciferase Reporter reagent (Promega) according to the manufacturer’s instructions. Luciferase activities were normalized by renilla luciferase levels.

Animal care and handling Wild-type male C57BL/6J mice at 9-12 weeks of ages were obtained from the Laboratoy Animal Center at Seoul National University. Mice were kept in temperature-controlled (22~23˚C) quarters under a 12-hr light and 12-hr dark (LD) photoperiod (light-on at 8:00 a.m.), with standard mouse chow and water availavle *ad libitum*. For dark-dark (DD) conditions, mice were kept in contrast darkness for the indicated duration from the light-off time. Home-cage activities and body temperatures were simultaneously monitored using a VitalView® data acquisition for more than 10-days under LD conditions. All animal procedures were approved by the institutional Animal Care and Use Committee of Seoul National University.

Cannula implantation and microinjection of KS15. Mice were anesthetized with sodium pentobarbital (50 mg/kg, i.p.), mounted on a stereotaxic apparatus (David Kopf Instruments, Tujunga, CA), and unilaterally implanted with 26-gauge stainless steel cannula (model C315G; Plastic Products, Roanoke, VA) into the lateral ventricle (AP -0.4 mm, ML 1.0 mm, DV -1.7 mm). A 32-gauge dummy cannula was inserted into guide cannula to prevent clogging. Two jewelry screws were implanted over the skull to serve as anchors, and the whole assembly was affixed on the skull with dental cement. Mice were given at least 1 week to recover before experimentation. After completion of the experiments, correct placement of the injection cannula tips was verified in all animals. For this purpose, brains were removed from animals and fixed overnight in PBS/4% paraformaldehyde. The fixed brains were coronally sectioned into 100-μm

thicknesses using a vibratome (World Precision Instruments, Sarasota, FL). Sections were then stained with cresyl violet and examined under light microscopy. KS15 dissolved in DMSO (8.4 μg / μl) was administrated unilaterally into the LV via a 33-gauge injector cannula (C315I; Plastic Products) attached to a 10-μl Hamilton syringe. A solution containing 4.2 μg of KS15 in 0.5 μl DMSO was administered. After administration, injector cannula was left in place for an additional minute to allow the solution to diffuse away from the tip.

Circadian Activity Measurements Wheel running activity was recorded at 6-minute intervals using an ER-4000 system (Mini-Mitter) supplemented with a wheel running assembly. For quantitative and statistical analysis, the raw data files generated by VitalView Version 4.0 data acquisition system (Mini-Mitter) were converted to data sets that can readily be applied to the software provided in the textbook, *Circadian Physiology* (CRC Press, Taylor & Francis Group, Boca Raton, FL). The length of periods from each groups were determined by the cosinor fitting analysis of 10-day profiles during entrainment period (light:dark = 12 hrs:12 hrs) and free running period (FRP) in constant dark, as well as post-injection period. Activity onset was characterized by an initial period of activity that: (1) exceeded 10% of the maximum rate for the day; (2) was preceded by at least 4 hours of activity quiescence; and (3) was followed by at least 60 minutes of sustained activity. Phase-shifts were calculated as the difference between the expected times of activity onset from profiles of FRP and actual activity onset timing in post-injection period.

RESULTS

Screen for E-box-mediated transcription modulator

To identify a novel synthetic circadian modulator, I designed a two-step cell-based screening method based on a luciferase reporter system. First, the CLOCK:BMAL1 heterodimer-responsive luciferase reporters were stably expressed in cultured cell lines based on the previous findings of our group. (Son et al., 2008). An artificial reporter (designated as E-box-Luc) was produced by incorporating two E-box elements originated from the mouse steroidogenic acute regulatory protein (StAR) promoter upstream of the SV40 minimal promoter-driven luciferase reporter. The E-box-Luc reporter was then stably expressed in NIH3T3 mouse fibroblasts. To test the effect on the endogenous clock-controlled promoter activities in parallel, mouse StAR promoter-driven luciferase (StAR-Luc) reporter activities were examined in Y1 mouse adrenocortical cell line. Expression profiles of luciferase reporters in these cell lines were verified by bioluminescence imaging device (Cellgraph, ATTO) (Fig 2). Both cell lines expressing luciferase reporters were cultured on 24-well plates for 24 hours, and then treated with 20 μM of more than 1,000 different drug-like compounds. Luciferase activities were analyzed after 24 hours of treatment (Fig 3 and Fig 4). As a result, 72 compounds were finally identified as E-box mediated transcription modulator that either enhanced or suppressed luciferase activities in both reporters (Fig 5). These 72 compounds were proceeding into further verification of compound effect in secondary screening step.

For the second screening, the effects of the selected compounds on E-box-mediated transcriptional activities were compared in mouse embryonic fibroblasts (MEFs) derived from wild-type (WT) and *Bmal1*-deficient mouse to select for compounds dependent on the CLOCK:BMAL1 heterodimer. Both types of MEF cells were synchronized by treatment with 100 nM dexamethasone (DEX) for 2 hours. After 12 hours of further incubation, the selected compounds were treated at 20 μM each for 24 hours. As a result, the compounds KS11a, KS11b, KS15, and KS16 were structurally similar and were shown to BMAL1-dependently enhance E-box-mediated transcription (Fig 6). These compounds were prepared according to the procedures that previously reported (Suh et al., 2008). The intermediate, 3-(3-acetylphenyl)-2-ethoxypropanoic acid is a racemate that was synthesized from commercially available 3-acetylbenzonitrile and then coupled with (*R*)-2-phenylglycinol, followed by chiral resolution. The optically pure (*R*)-3-(3-acetylphenyl)-2-ethoxypropanoic acid was converted into a variety of oxime ethers by condensation with benzyloxy amines. The selected compounds were further tested to determine the potency and dose-response using E-box-Luc-expressing fibroblasts. Efficacy was determined by calculating the maximum change in the luciferase activity at given concentrations. Potency was determined by deducing the EC_{50} from the dose-response curve (Fig 7 and Table 1). I also tested the analogs that both conformationally restricted isoxazoline analogs or stereoisomers containing *(S)*-ethoxypropanoic acid, but they only slightly enhanced E-box-mediated transcription at 20 μM (Fig 7 and Table 1). Among the tested compounds, KS15 was ultimately selected as the E-box-mediated

transcription modulator that was most promising in terms of efficacy and potency.

CRY1/2 are molecular targets of KS15

In the next set of experiments, I sought to identify a molecular target of KS15. I hypothesized that enhanced E-box-mediated transcription is likely to be due to direct binding of KS15 to its target clock protein. In collaboration with professor Youn-Ger Suh and his colleagues, I prepared a biotin-conjugated version of KS15 for pull-down assays, which was conveniently prepared by coupling the carboxyl group of KS15 with a commercially available biotin tag tethered with the amide linker. Derivatives of KS15 with a methyl ester or hexyl amide substituent at the same position (Fig 9) also enhanced E-box-mediated transcriptional activity (Fig 10), suggesting that biotin conjugated probe has same activity of KS15. Then, I carried out pull-down assays using this biotin-conjugated probe as bait in clock protein-expressing HEK293T cell lysates. HEK293T cells were transiently transfected with the tagged core clock proteins-expressing constructs, and cell lysates were prepared 48 hours after transfection and incubated with 20 μM biotin-conjugated KS15 (i.e., the bait) for 30 min in the absence or presence of 40 μM free competitors, and then the bound complexes were isolated by incubating them with avidin-coated beads for 2 hours at 4 °C. The bound proteins were then detected by immunoblotting with tag-specific antibodies. As shown in Figure 11, the biotin-conjugated chemical probe KS15 specifically bound to both CRY1 and CRY2 (Fig 11A),

but not to CLOCK, BMAL1 or PERs amongst the tested core clock proteins (Fig 11B). CRYs binding with biotin-conjugated probe were severely blocked in the presence of free KS15, while KS16, a structural analog of KS15 with weak potency, failed to interrupt CRY binding (Fig 11A). Biotin-conjugated probe also bound to purified CRY1 protein (Fig 12). Moreover, I generated functionally inactive mutants of CRYs and used it in a pull-down assay to find out whether KS15 interacts with an important functional structure/domain of CRYs. The CRYs are composed of highly conserved N-terminal photolyase homology region (PHR) and variable C-terminal extension domain, the tails (Chaves et al., 2006; Partch et al., 2005; Lin et al., 2005; Todo et al., 1996). Also, putative coiled-coil (CC) domain resides in the beginning of C-terminal tail and highly conserved even between CRY1 and CRY2 (Fig 13) (Chaves et al., 2006; Partch et al., 2005). Previous studies suggested that the C-terminal tail, including the CC domain, of CRYs is important for nuclear localization and interaction with other core clock proteins, such as PERs and BMAL1 (Chaves et al., 2006; van der Schalie et al., 2007; Czarna et al., 2011). Also, C-terminal tail is target site of phosphorylation by glycogen synthase kinase-3β (GSK3β) or mitogen-activated protein kinase (MAPK) and regulates stability of CRYs (Harada et al., 2005; Sanada et al., 2004). Based on these findings, I constructed mutants of human CRY1 and CRY2 with truncation of the C-terminal tail and putative CC domain (ΔCC-tail) (Fig 13). Unlike wild-type, both ΔCC-tail mutants of CRY1 and CRY2 were failed to bind biotin-conjugated KS15 (Fig 14). Taken together, these data suggest that KS15 selectively and directly interacts with CRY proteins.

CRYs play a crucial role in the clock gene expression cycle by forming inhibitory complexes with the CLOCK:BMAL1 heterodimer, thus repressing their transcriptional activities (Kume et al., 1999). Because KS15 binds to both CRY1/2, I examined whether the effect of KS15 on the E-box-mediated transcription depends on CRY1/2. WT or *Cry1/2*-knockout MEFs synchronized by DEX treatment were treated with 6.7 μM of KS15, KS16 or KS25 for 24 hours. The effect of KS15 on E-box-mediated transcription, as determined by the E-box-Luc reporter construct, was significantly attenuated in CRY1/2-deficient MEFs (Fig 15A). More importantly, KS15-induced *Per1*, *Per2*, and *Rev-erbα* mRNA expression but these inductions were disappeared in the absence of endogenous CRY1/2 (Fig 15B, C, D). In contrast, the less potent analogs KS16 and KS25 only marginally influenced E-box-mediated transcription, as well as endogenous clock gene expression. In good agreement with the binding assay, these results demonstrate that CRY1/2 are molecular targets of KS15.

Modulation of molecular clock activity by KS15

After identifying binding target of KS15, I examined whether KS15 modulates the circadian periodicity of clock-controlled gene transcription. For this purpose, stable NIH3T3-originated cell line bearing the mouse *Per2* promoter-driven luciferase reporter (Per2-Luc) was synchronized by treatment with DEX, and emitted bioluminescence in the presence of luciferin substrate was non-invasively monitored every 10 min for 96 hours. After synchronization, vehicle (0.2% DMSO) or KS15 (6.7 or 20 μM) was

included in the media (Fig 16). The relative amplitudes of the rhythms were significantly attenuated in a dose-dependent manner, although the periods were not significantly altered (Fig 16 and Table 2). Because the areas under the curves (AUCs) were also changed in same way, it can be postulated that KS15 inhibited CRY-mediated repression of CLOCK:BMAL1 heterodimer transcriptional activities. I also established another stable fibroblast cell line bearing the mouse *Bmal1* promoter-driven destabilized luciferase reporter (Bmal1-dLuc) and analyzed activity in the same way (Fig 17). Like Per2-Luc, the rhythms of Bmal1−dLuc were also attenuated in the presence of KS15 without significantly changing the periods (Fig 17 and Table 3). In addition, I examined the effect of CRY1/2 knockdown on circadian periodicity compared with the effect of KS15 to investigate more detailed mechanism of KS15's action, Small hairpin RNA expression vectors (shRNA) were used for knock down of CRY1/2 expression after verification (Fig 18). As a result, single knockdown of CRY1 or CRY2 altered period length of Bmal1-dLuc reporter activity rhythm, while knockdown of both CRY1/2 severely attenuated amplitude of the rhythm (Fig 19 and Table 3). Moreover, knockdown of CRY1/2 attenuated Bmal1-dLuc reporter activity rhythm in dose-dependent manner without significantly changing the period length (Fig 19 and Table 4). Considering that CRYs are key negative regulators of molecular circadian clockwork (Kume et al., 1999), these findings strongly suggest that the binding of KS15 to both CRY1/2 attenuates circadian clockwork oscillation by inhibiting negative regulators in the core molecular feedback loop.

Modulation of circadian rhythm by KS15 *in vivo*

Finally, I sought to investigate effect of KS15 on circadian rhythms *in vivo*. For this purpose, I designed a set of experiments that monitoring changes of daily activity rhythm of mouse after the intracerebroventricular (ICV) microinjection of KS15. For this purpose, a guide cannula was implanted unilaterally into wild-type male C27/B6 mouse that targeting lateral ventricles of brain. After 1 week of recovery, mice were entrained with normal 12-hr light:12-hr dark cycle with wheel running assembly. By then, free running period (FRP) were monitored in constant dark condition. Then, vehicle (100% DMSO 0.5 μl) or KS15 (4.2 μg in 0.5 μl of DMSO) were administrated by single ICV microinjection through the implanted cannula at two hour before activity onset. After administration, daily activity rhythms in constant dark were monitored another 10 days. As a result, administration of KS15 caused the delay of the activity rhythm than vehicle treated group (Fig 21). KS15 also cause nearly one hour shift of circadian phase than vehicle injected group. These data suggested that ICV administration of KS15 can modulate circadian rhythms *in vivo*.

Figure 2. Establishment of stable cell lines with CLOCK:BMAL1 heterodimer responsive luciferase reporters. (A) Schematic diagram of the promoter region of the mouse StAR gene (-2517 to -1). Previous studies suggested that two E-box elements within the distal region to of the mouse StAR promoter were directly regulated by the CLOCK:BMAL1 heterodimer. (Son et al., 2008) (B) Schematic diagram of transfected cell lines with stable luciferase expression of StARp-Luc and E-box-Luc reporters. E-box-Luc was produced by incorporating two E-box elements originated from the distal region of StAR promoter (around -2140) with SV40 minimal promoter-driven luciferase reporter. The E-box-Luc reporter was then stably expressed in NIH3T3 mouse fibroblasts. StARp-Luc was produced by conjucating 2.5 kb of mouse StAR promoter with luciferase reporter. StARp-Luc was transfected into Y1 mouse adrenocortical cell line for tissue-specificity issue (Y1:StARp-Luc) while E-box-Luc was transfected into NIH3T3 fibroblast cell line (NIH3T3:E-box-Luc) (C) Bioluminescence imaging of cell lines with stable expression of luciferase reporters. Images from NIH3T3:E-box-Luc (upper panel) and Y1:StARp-Luc (lower panel) are presented with both light field image (left) and bioluminescence imaging with pseudocolor coding (right).

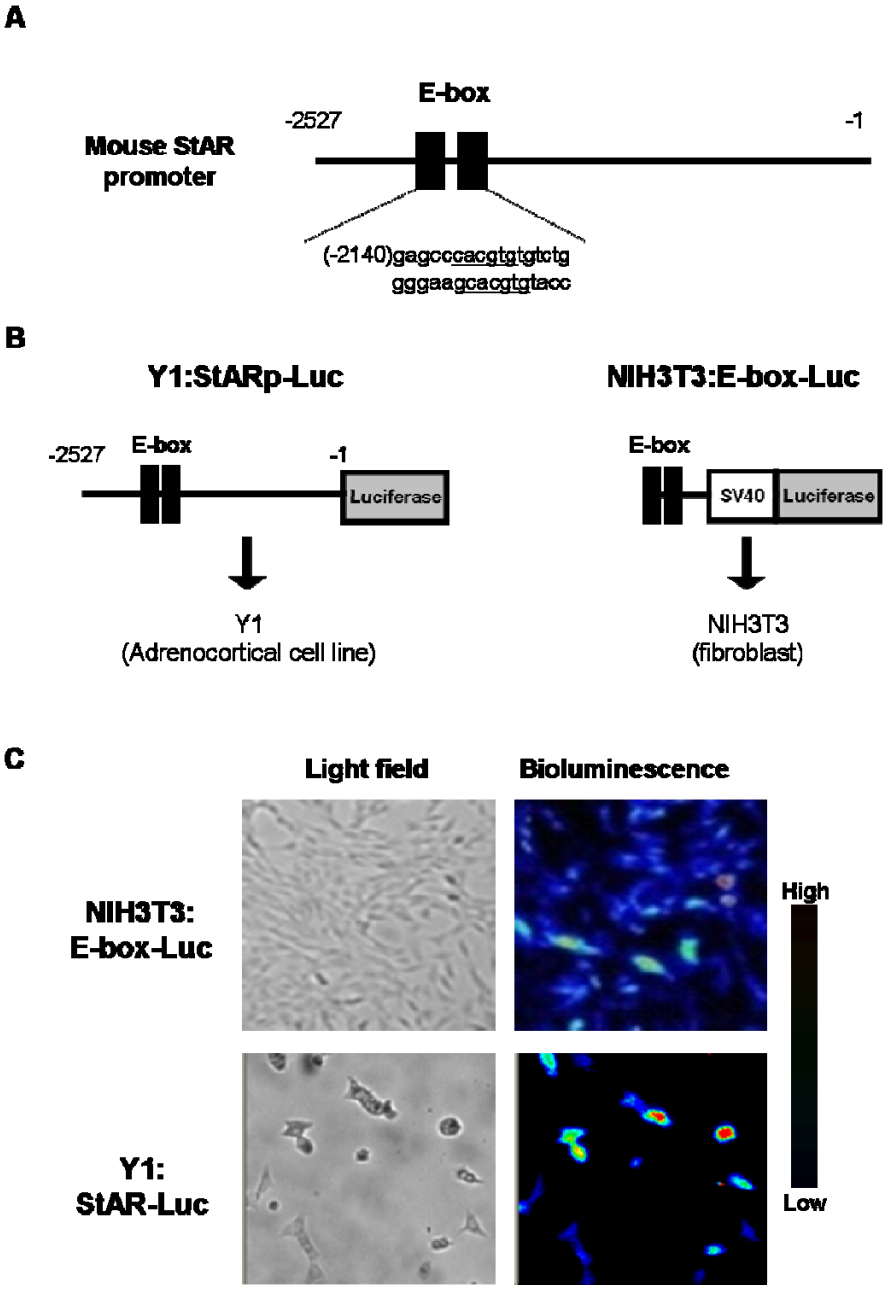
A
E-box
-2527
-1
Mouse StAR promoter
(-2140)gagcccacgtgtgtctg
gggaagcacgtgtacc
B
Y1:StARp-Luc
NIH3T3:E-box-Luc
-2527
E-box
-1
Luciferase
E-box
SV40
Luciferase
Y1
(Adrenocortical cell line)
NIH3T3
(fibroblast)
C
Light field
Bioluminescence
NIH3T3:
E-box-Luc
Y1:
StAR-Luc
High
Low

Figure 3. The primary screening of chemical library by using NIH3T3:E-box-Luc. (A) The distribution of the total 1172 compounds treated to NIH3T3:E-box-Luc stable cell. Changes of luciferase activity caused by compound treatment were normalized by vehicle (0.2% DMSO) treated group and results were presented in scatter plot. The compounds with significant fold change (over 50%) were presented in following colors: over 50% (blue dots), over 100% (orange dots) and over 200% (brown dots) (B) The distribution of whole chemical library presented on a pie graph (left panel). Compounds with inducing effect were shown in orange color, while compounds with inhibiting effect were shown in blue color. The compounds causing cell damage were shown in gray. Also, total chemicals were divided into two pie graphs (right panel). Induction group (compounds with enhancing activity) is composed two groups (over 100% fold change was presented orange color and over 50% change was presented light orange color). Repression group (compounds with repressive activity) is composed of three categories (over 200% fold change was presented dark blue, over 100% fold change was blue and over 50% fold change was presented light blue).

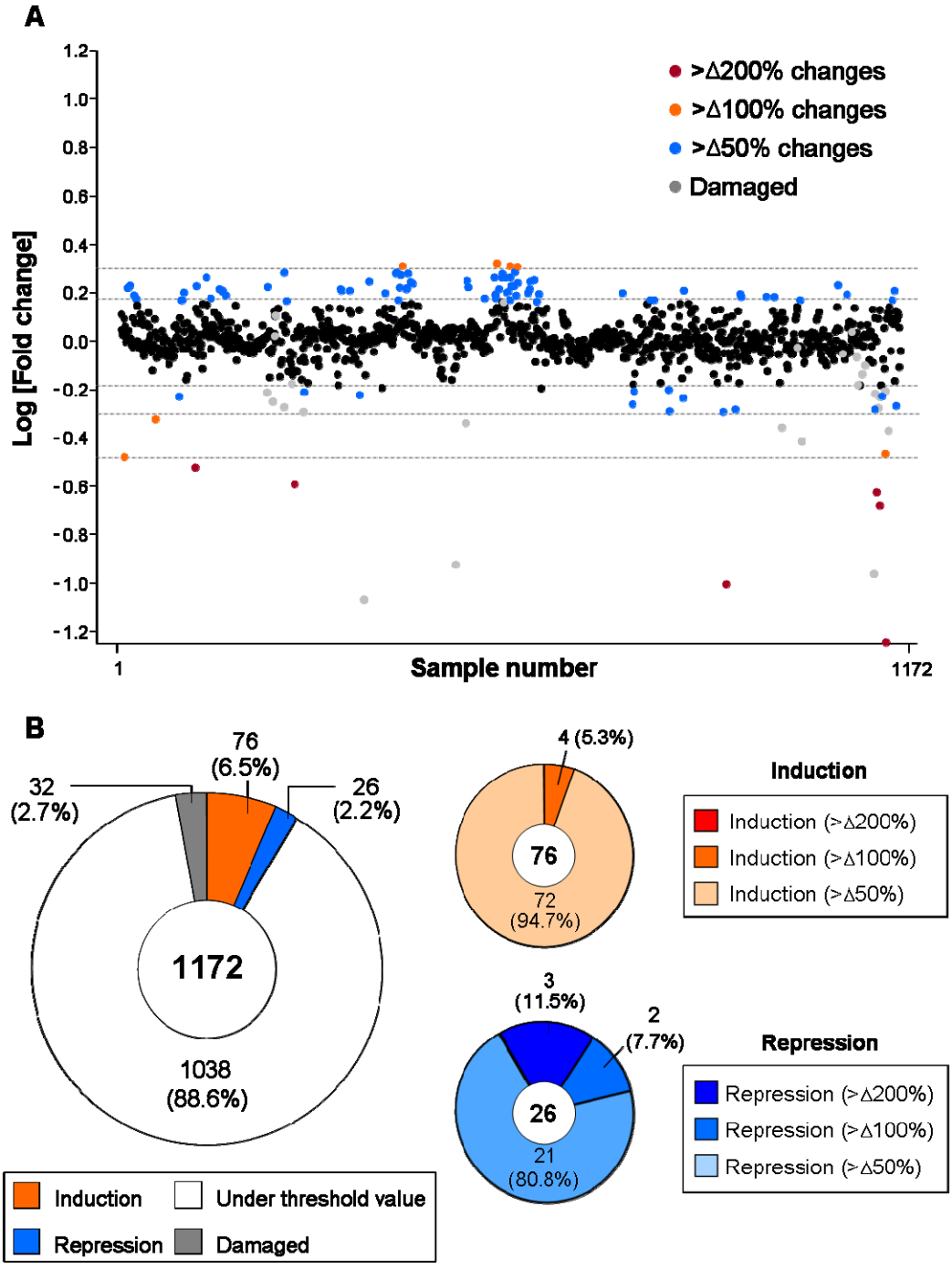
A
>Δ200% changes
>Δ100% changes
>Δ50% changes
Damaged
Log [Fold change]
1.2
1.0
0.8
0.6
0.4
0.2
0.0
-0.2
-0.4
-0.6
-0.8
-1.0
-1.2
1
Sample number
1172
B
76
(6.5%)
32
(2.7%)
26
(2.2%)
1172
1038
(88.6%)
Induction
Under threshold value
Repression
Damaged
4 (5.3%)
76
72
(94.7%)
Induction
Induction (>Δ200%)
Induction (>Δ100%)
Induction (>Δ50%)
3
(11.5%)
2
(7.7%)
26
21
(80.8%)
Repression
Repression (>Δ200%)
Repression (>Δ100%)
Repression (>Δ50%)

Figure 4. The primary screening of chemical library by using Y1:StARp-Luc. (A) The distribution of the total 1172 compounds treated to Y1:StARp-Luc stable cell. Changes of luciferase activity caused by compound treatment were normalized by vehicle (0.2% DMSO) treated group and results were presented in scatter plot. The compounds with significant fold change (over 50%) were presented in following colors: over 50% (blue dots), over 100% (orange dots) and over 200% (brown dots) (B) The distribution of whole chemical library presented on a pie graph (left panel). Compounds with inducing effect were shown in orange color, while compounds with inhibiting effect were shown in blue color. The compounds causing cell damage were shown in gray. Also, total chemicals were divided into two pie graphs (right panel). Induction group (compounds with enhancing activity) is composed three groups (over 200% fold change was presented red color, over 100% fold change was presented orange color and over 50% change was presented light orange color). Repression group (compounds with repressive activity) is also composed of three categories (over 200% fold change was presented dark blue, over 100% fold change was blue and over 50% fold change was presented light blue).

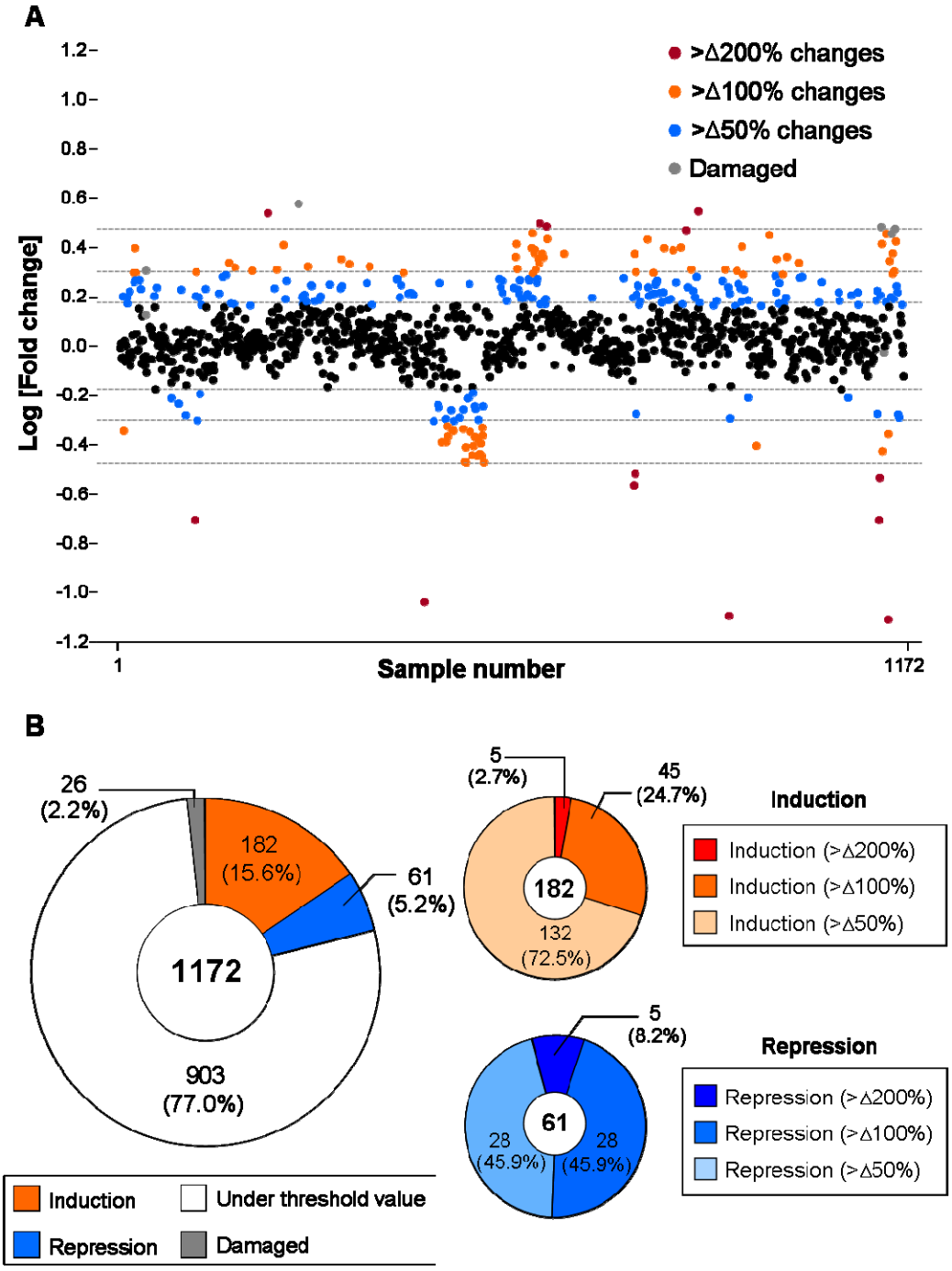
A
>Δ200% changes
>Δ100% changes
>Δ50% changes
Damaged
Log [Fold change]
1.2
1.0
0.8
0.6
0.4
0.2
0.0
-0.2
-0.4
-0.6
-0.8
-1.0
-1.2
1
Sample number
1172
B
26
(2.2%)
182
(15.6%)
61
(5.2%)
1172
903
(77.0%)
Induction
Under threshold value
Repression
Damaged
5
(2.7%)
45
(24.7%)
182
132
(72.5%)
Induction
Induction (>Δ200%)
Induction (>Δ100%)
Induction (>Δ50%)
5
(8.2%)
61
28
(45.9%)
28
(45.9%)
Repression
Repression (>Δ200%)
Repression (>Δ100%)
Repression (>Δ50%)

Figure 5. Selection of hit compounds from primary screening. Hit compounds from primary screening were identified by selecting the compounds that shows enhancing or repressing activities on both reporter systems in same direction. Comparing results from two reporters system, 50 compounds were finally identified as hit compounds with induction effect on both reporters, while 12 compounds were selected as hit compounds with repressive effect on both reporters.


Induction
E-box-Luc
(76 species)
StARp-Luc
(182 species)
24
52
130
Repression
E-box-Luc
(26 species)
StARp-Luc
(61 species)
6
20
41

Figure 6. Identification of the hit compounds by two-step cell-based screening strategy. (A) Representative group of compounds (KS11a-16, KS25) from primary screening. These compounds identified as significantly enhancing both E-box-Luc activities in NIH3T3 cells and StARp-Luc in Y1 cells. (B) Comparison of the effects of KS11a-16 and 25 on E-box-Luc activities in WT and BMAL1-deficient MEFs (*$p < 0.05$, **$p < 0.01$, compared with vehicle (0.1% DMSO)-treated groups (VEH); †$p < 0.05$, ††$p < 0.01$ compared with WT MEF). Data are presented as the mean ± S.E.M. ($n = 3$ for each group). Note that KS11a, KS11b, KS15, and KS16 were found to enhance E-box-mediated transcription in a BMAL1-dependent manner. (C) Structure of KS11a-b, KS15 and KS16.

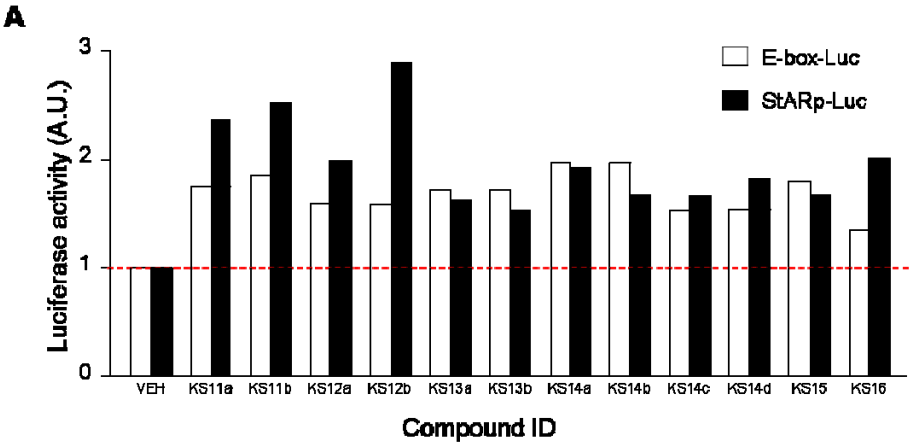
A
Luciferase activity (A.U.)
E-box-Luc
StARp-Luc
VEH
KS11a
KS11b
KS12a
KS12b
KS13a
KS13b
KS14a
KS14b
KS14c
KS14d
KS15
KS16
Compound ID

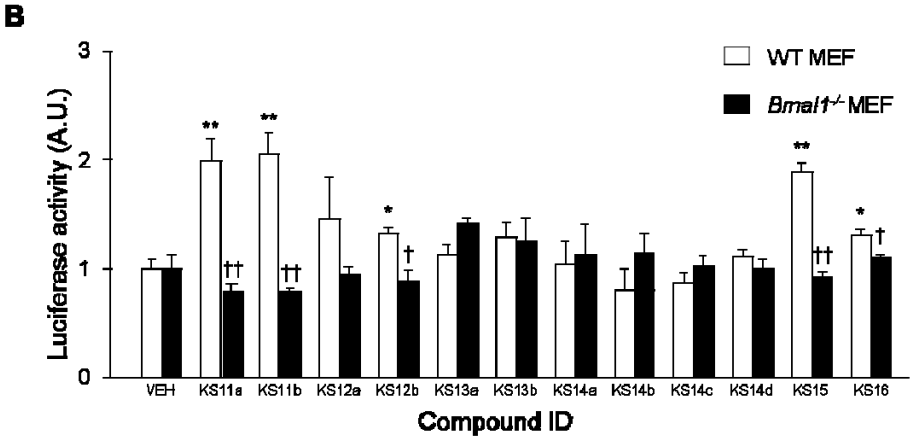
B
Luciferase activity (A.U.)
WT MEF
Bmal1-/- MEF
Compound ID

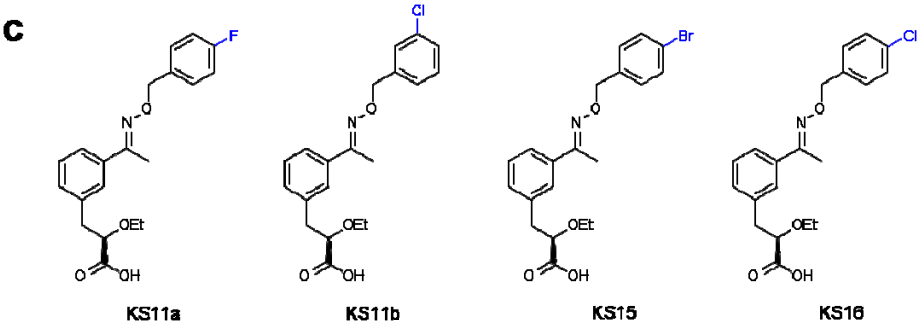
C
KS11a
KS11b
KS15
KS16

Figure 7. Structures and effects of the selected compounds to E-box-mediated transcription. (A) Chemical structure of the selected compounds (**11a**, **11b**, **15**, **16**, and **25**) and their stereoisomers (**11a', 11b'** and **15'**) containing *(S)*-ethoxypropanoic acid**.** (B, C) Dose-response curves of E-box-mediated transcription for the selected compounds (B) and their stereoisomers (C). Data are presented as mean ± S.E.M. (n = 3).

A

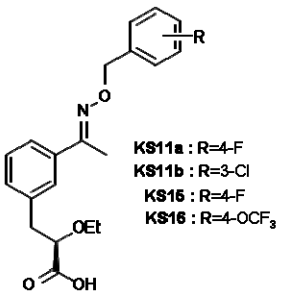

KS11a : R=4-F
KS11b : R=3-Cl
KS15 : R=4-F
KS16 : R=4-OCF3

KS11a, KS11b, KS15, KS16

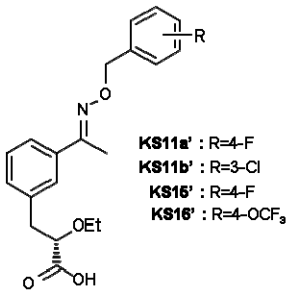

KS11a' : R=4-F
KS11b' : R=3-Cl
KS15' : R=4-F
KS16' : R=4-OCF3

KS11a', KS11b', KS15', KS16'

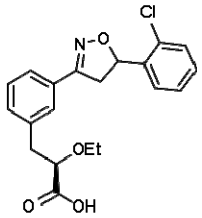

KS25

B

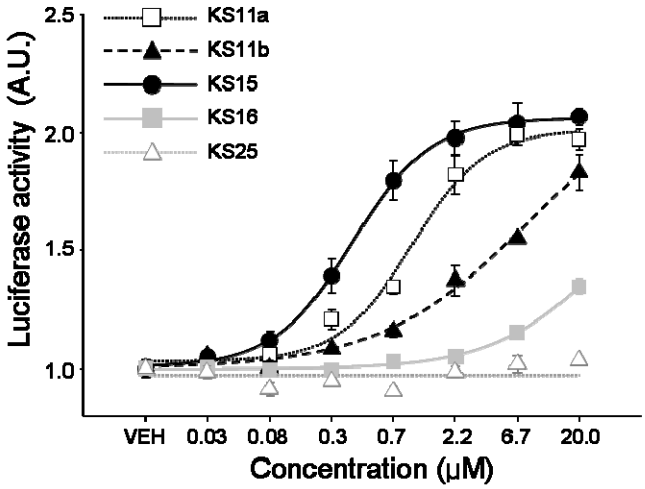

C

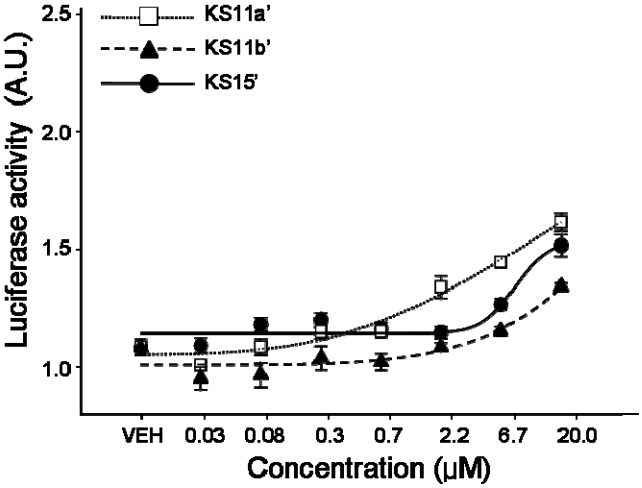

Table 1. Efficacy and potency of the selected analogs in enhancing E-box-Luc activity. KS11a, KS11b, KS15, KS16 and their structural analogs were tested to analyze dose-response curves for E-box-mediated transcription by using NIH3T3:E-box-Luc stable cell line. Efficacy and potency were determined by calculating the maximum change and EC_{50} values from the dose-response curve. Maximum response (MAX.) expressed as the percentage of the vehicle-treated group. EC50 values were calculated with a logistic 4-parametric equation using the mean values of its intrinsic activation. “ND” means that EC_{50} values were not determined within the tested dosages.

ID	Structure	R	Max. (%)	EC_{50} (μM)
11a	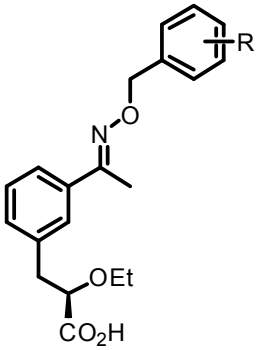	-F (p)	200.55	1.25
11b		-Cl (m)	192.40	2.22
15		-Br (p)	220.98	0.49
16		$-OCF_3$ (p)	140.93	ND
17		-H	193.12	4.02
18		-I (p)	195.94	1.91
19		-Cl (p)	208.10	4.77
20		-OH (p)	138.88	ND
21		-OMe (p)	221.80	3.79
22		$-CF_3$ (p)	143.07	ND
23	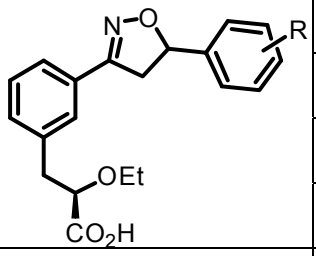	-F (p)	116.20	ND
24		-Cl (m)	99.48	ND
25		-Cl (o)	100.70	ND
26		$-CF_3$ (p)	103.86	ND
11a'	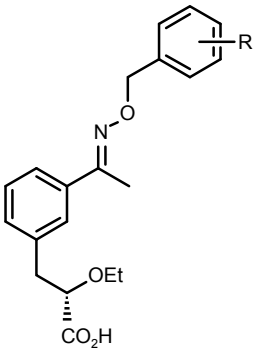	-F (p)	155.30	ND
11b'		-Cl (m)	126.77	ND
15'		-Br (p)	145.05	ND

Figure 8. Dose-response and potency of the selected compounds and their stereoisomers on Peroxisome proliferator-activated receptor (PPAR) mediated transcriptional activity. To examine the dose-response activity of these compounds on PPAR mediated transcriptional activity, DR1-Luc plasmid (a luciferase reporter driven by synthetic promoter containing multiple PPAR responsive elements) and a control plasmid (promoterless renilla luciferase expression plasmid) was transfected into NIH3T3 cells and treated with various concentrations of these compounds. After 24-hour incubation, cells were analyzed by luciferase assay. Dose-response curves of PPAR mediated transcriptional activity for the selected compounds (A) and their stereoisomers (B). Data are presented as mean ± S.E.M. (n = 5).

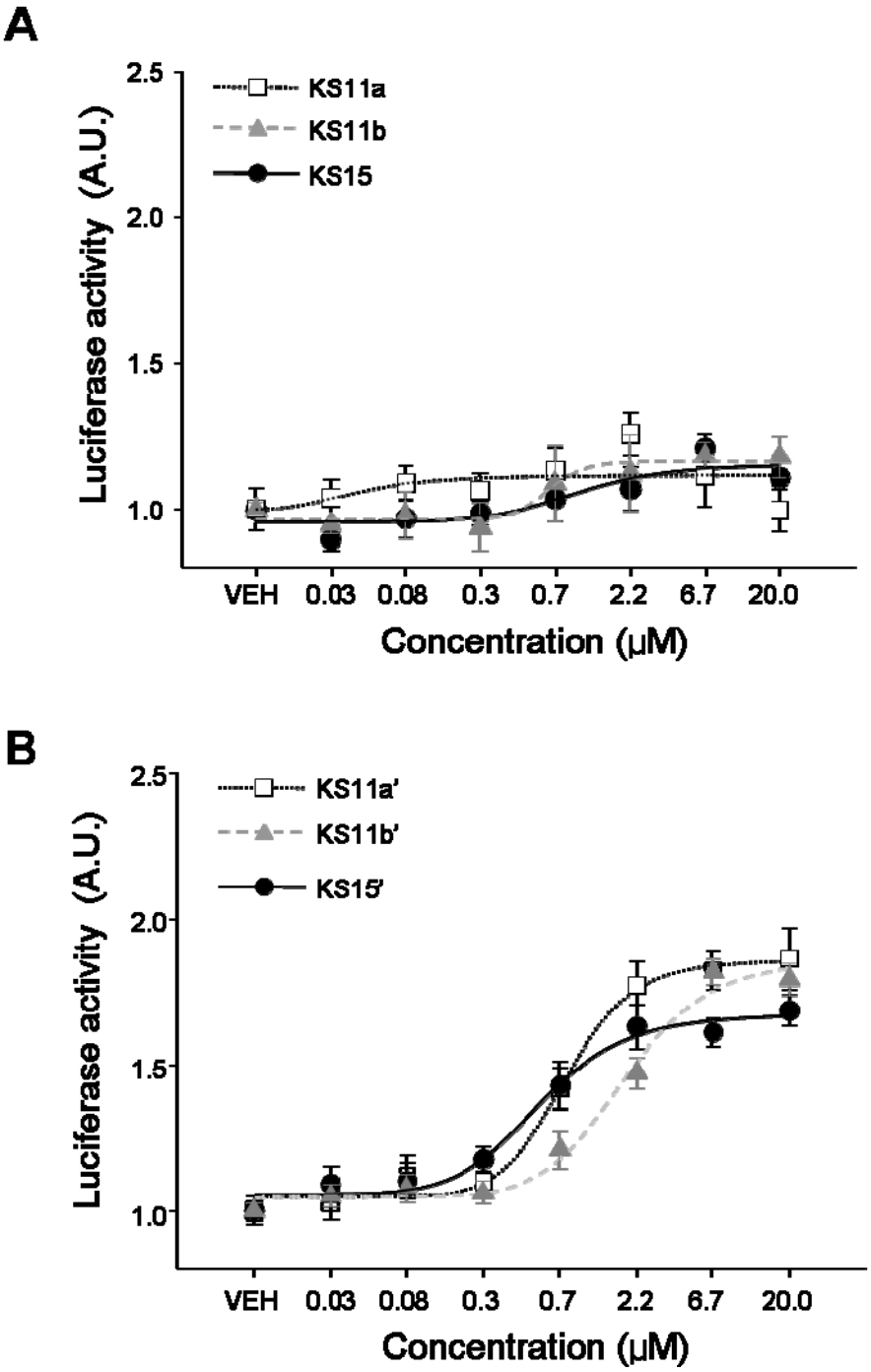
A
2.5
2.0
1.5
1.0
Luciferase activity (A.U.)
KS11a
KS11b
KS15
VEH
0.03
0.08
0.3
0.7
2.2
6.7
20.0
Concentration (μM)
B
2.5
2.0
1.5
1.0
Luciferase activity (A.U.)
KS11a'
KS11b'
KS15'
VEH
0.03
0.08
0.3
0.7
2.2
6.7
20.0
Concentration (μM)

Figure 9. Chemical structure of the derivatives of KS15 with linker from the process of biotinylation. (A) Structure of the original KS15 and its derivatives. The carboxyl group in KS15 was substituted with methyl ester (KS15a) or Hexyl amid (KS15b), the same as the biotin-conjugated probe. (B) Structure of biotin-conjugated KS15.

A

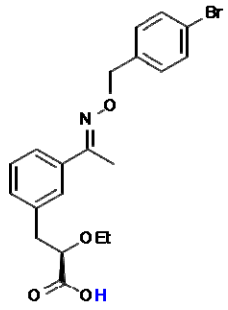

KS15

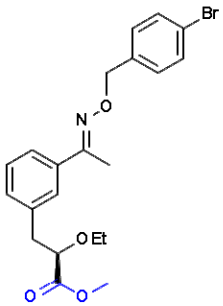

KS15a: Methyl ester

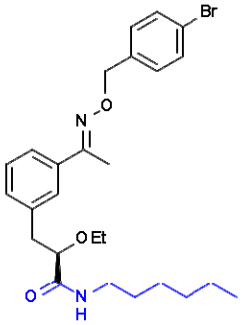

KS15b: Hexyl amide

B

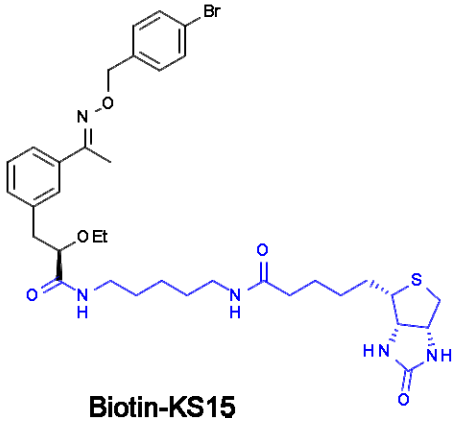

Biotin-KS15

Figure 10. Dose response and potency of the derivatives of KS15 with linker. To examine the dose-response activity of these derivatives on E-box mediated transcription, fibroblast cells stably expressing (A) E-box-Luc or (B) Per2-Luc were treated with various concentrations of these compounds. After 24-hour incubation, cells were analyzed by luciferase assay. Data are presented as mean ± S.E.M. (n = 3).

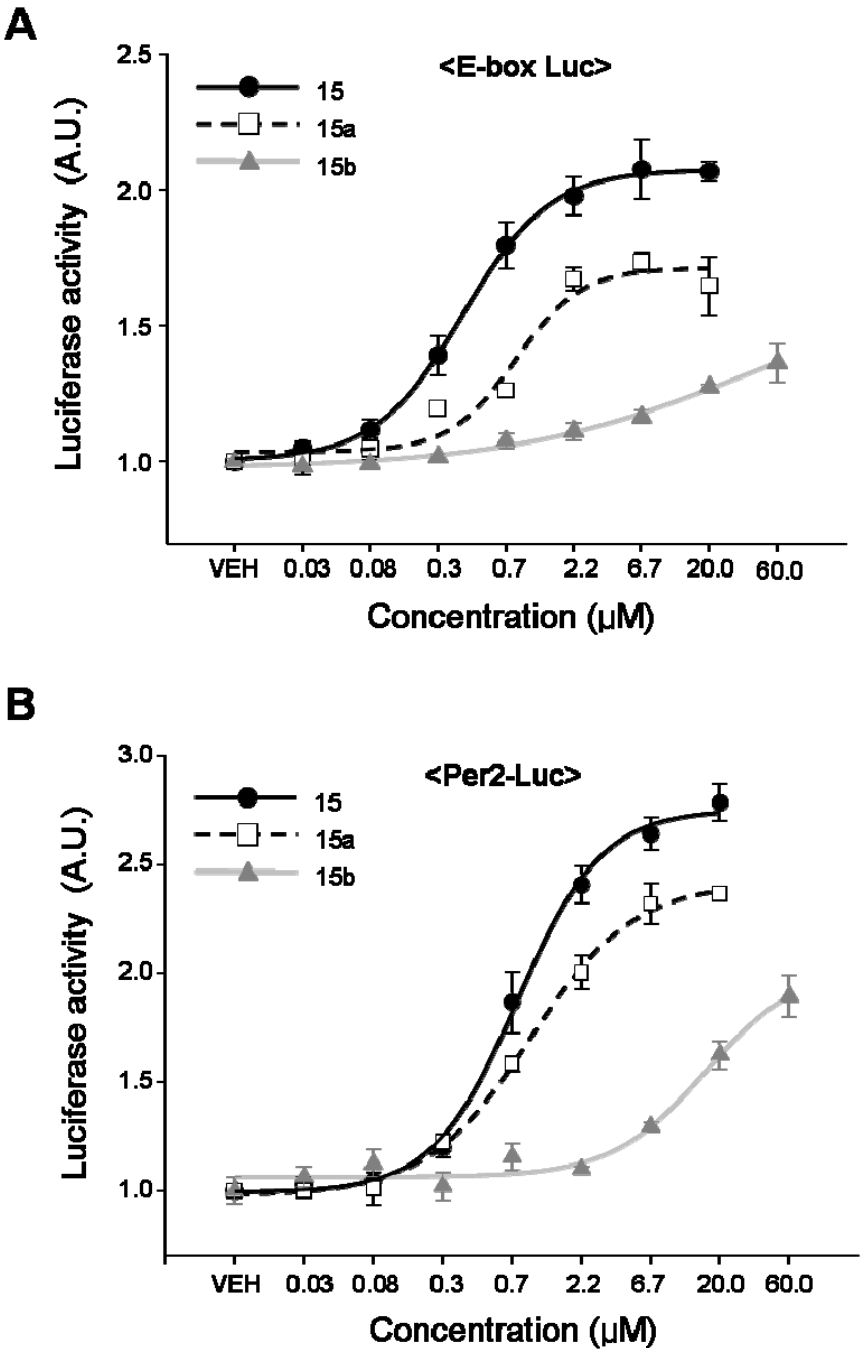
A
<E-box Luc>
15
15a
15b
Luciferase activity (A.U.)
2.5
2.0
1.5
1.0
VEH 0.03 0.08 0.3 0.7 2.2 6.7 20.0 60.0
Concentration (μM)
B
<Per2-Luc>
15
15a
15b
Luciferase activity (A.U.)
3.0
2.5
2.0
1.5
1.0
VEH 0.03 0.08 0.3 0.7 2.2 6.7 20.0 60.0
Concentration (μM)

Figure 11. Identification of binding target of KS15. (A) Pull-down assay of CRY1/2-expressing HEK293T cell lysates. KS15 and KS16 were added for competition. (B) Pull-down assays of core clock proteins. Myc-CLOCK, myc-BMAL1, and V5-PER1/2 were not pulled-down by biotin-conjugated KS15. Bound proteins were visualized by western blot using specific antibodies for the epitopes (anti-FLAG for CRY1/2, anti-myc for CLOCK and BMAL1 and anti-V5 for PER1/2).

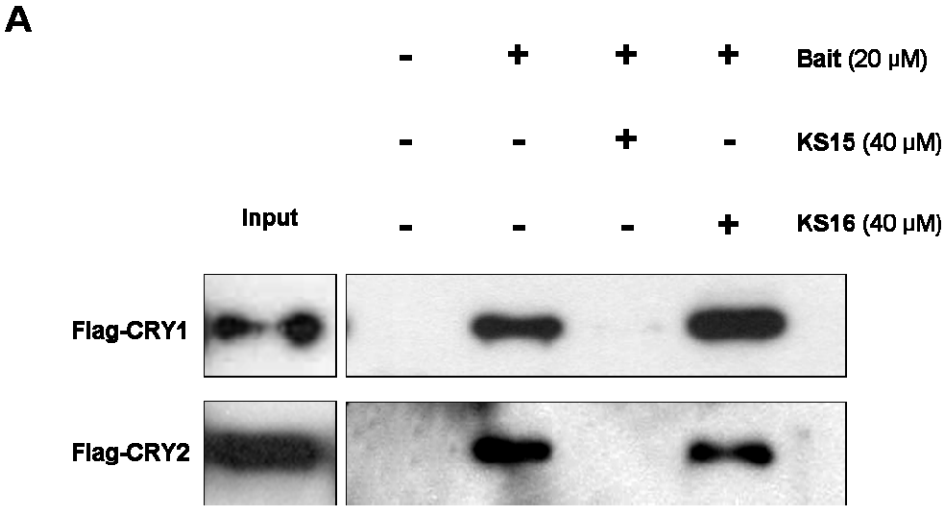
A
- + + + Bait (20 μM)
- - + - KS15 (40 μM)
Input - - - + KS16 (40 μM)
Flag-CRY1
Flag-CRY2

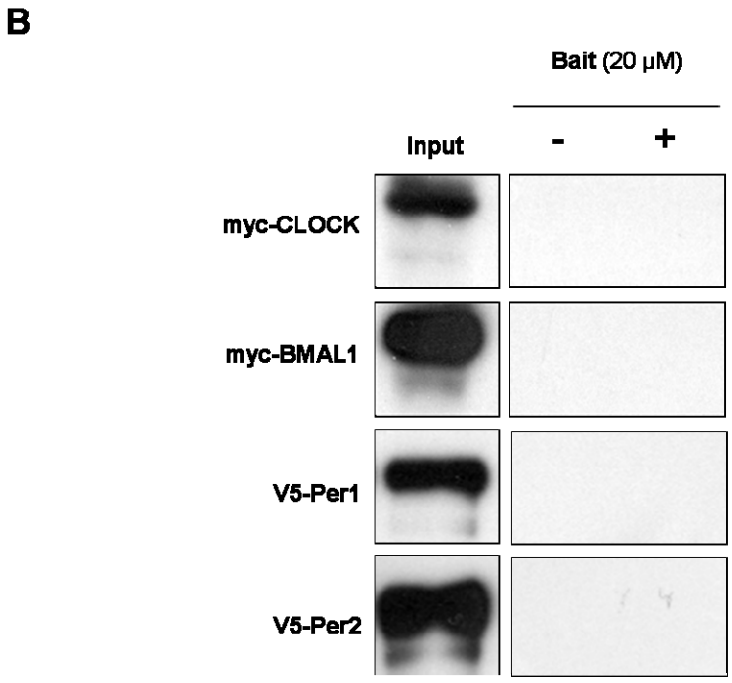
B
Bait (20 μM)
Input - +
myc-CLOCK
myc-BMAL1
V5-Per1
V5-Per2

Figure 12. Pull-down assay of purified CRY1 protein. (A) Purification of CRY1 protein expressed in mammalian cells. Purified CRY1 protein was visualized by Coomassie blue staining (left, CBB staining) or immunolabeling with an anti-FLAG antibody (Right, WB: anti-FLAG). Arrows indicate purified CRY1. More purified fraction of eluate (E2) was used for further experiments. I: Input, F: Flow-through, E1: Eluate fraction 1, E2: Eluate fraction 2. (B) Pull-down assay of purified CRY1 protein. KS15 and KS16 were added for competition.

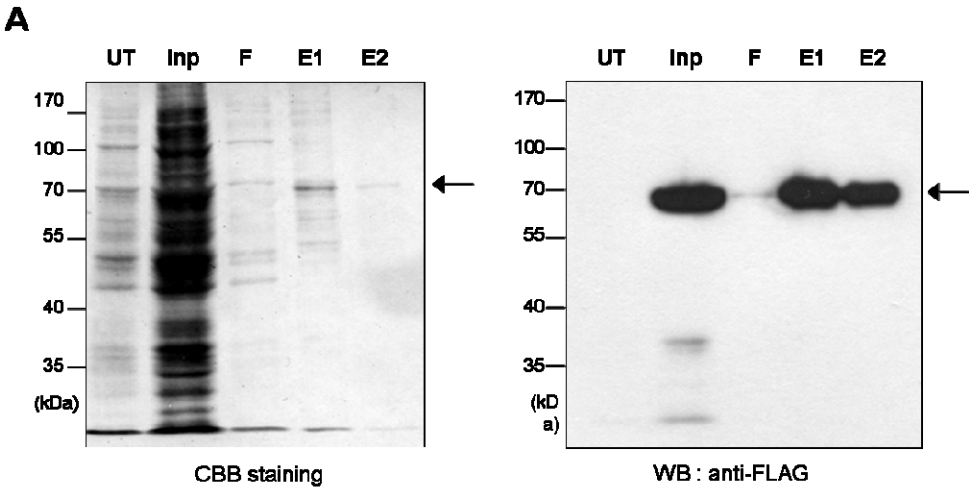
A
UT
Inp
F
E1
E2
170
100
70
55
40
35
(kDa)
CBB staining
WB : anti-FLAG
B
Input
2%
1%
Bait (20 μM)
KS15 (40 μM)
KS16 (40 μM)
Flag-CRY1

Figure 13. Structure of wild-type and functionally inactive mutant (ΔCC-tail) of human CRY1 (hCRY1) and CRY2 (hCRY2) (A) Schematic diagram of the wild-type and ΔCC-tail mutant of hCRY1/2. The N-terminal photolyase-like domain of CRYs are evolutionally conserved, and amino acid sequence homology between hCRY1 and hCRY2 is more than 80%, but the C-terminal extension domains of hCRY1/2 lack sequence homology. The putative coiled-coil domain (CC domain) within hCRY1 and hCRY2 reside at the start of the C-terminal extension domain. (B) Sequence alignment of the mouse and human CRYs: mouse CRYs (mCRYs) and human CRYs (hCRYs). We analyzed sequence homology of mouse and human CRYs by using CLUSTAL Omega (1.2.0) multiple sequence alignment software (Sievers et al., 2011). Putative CC domain and C-terminal extension domain of human CRYs were identified by comparing with predicted C-terminal structure of mCRY1/2 in previous study (Czarna et al., 2011). Unlike C-terminal extension domains, predicted CC domains are highly conserved among the species and subtypes.

A

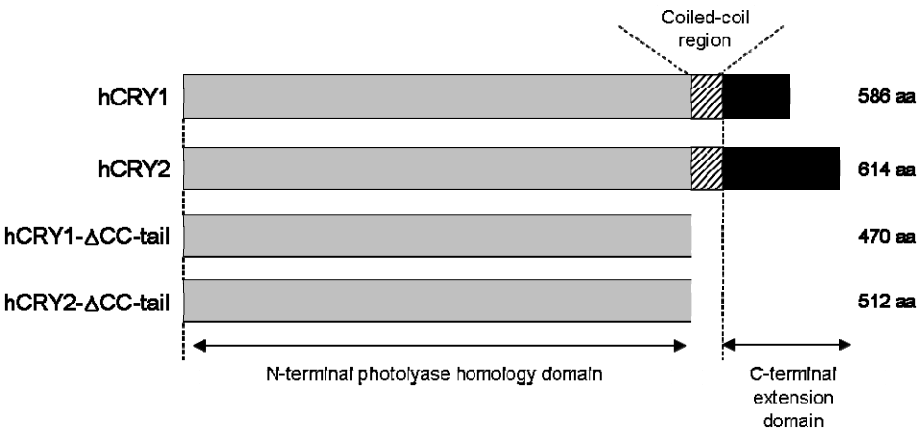
Coiled-coil region
hCRY1
586 aa
hCRY2
614 aa
hCRY1-ΔCC-tail
470 aa
hCRY2-ΔCC-tail
512 aa
N-terminal photolyase homology domain
C-terminal extension domain

B

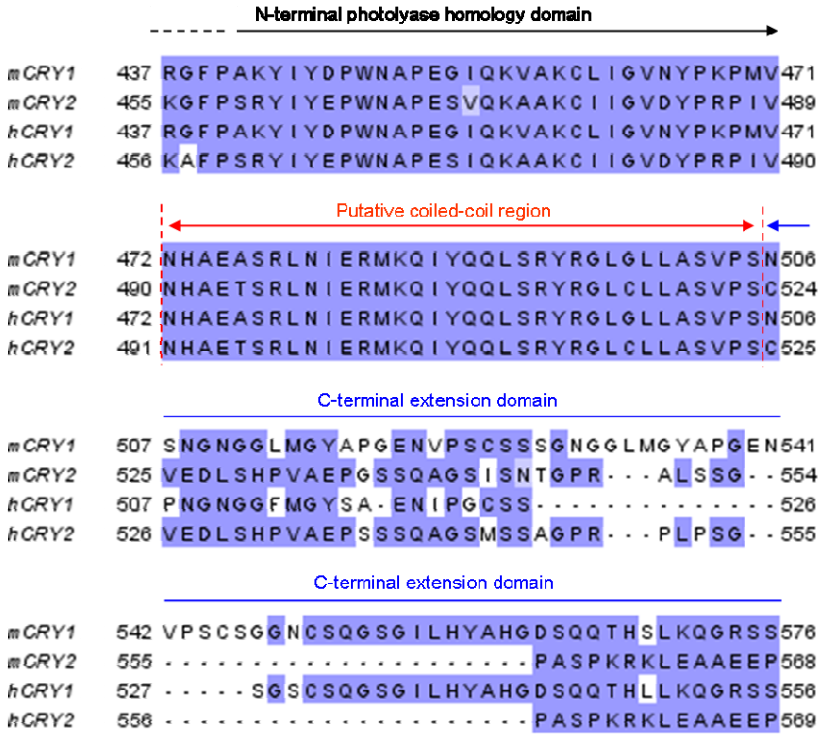
N-terminal photolyase homology domain
mCRY1 437 RGFPAKYIYDPWNAPEGIQKVAKCLIGVNYPKPMV 471
mCRY2 455 KGFPSRYIYEPWNAPESVQKAAKCIIGVDYPRPIV 489
hCRY1 437 RGFPAKYIYDPWNAPEGIQKVAKCLIGVNYPKPMV 471
hCRY2 456 KAFPSRYIYEPWNAPESIQKAAKCIIGVDYPRPIV 490
Putative coiled-coil region
mCRY1 472 NHAEASRLNIERMKQIYQQLSRYRGLGLLASVPSN 506
mCRY2 490 NHAETSRLNIERMKQIYQQLSRYRGLCLLASVPSC 524
hCRY1 472 NHAEASRLNIERMKQIYQQLSRYRGLGLLASVPSN 506
hCRY2 491 NHAETSRLNIERMKQIYQQLSRYRGLCLLASVPSC 525
C-terminal extension domain
mCRY1 507 SNGNGGLMGYAPGENVPSCSSSGNGGLMGYAPGEN 541
mCRY2 525 VEDLSHPVAEPGSSQAGSISNTGPR---ALSSG--554
hCRY1 507 PNGNGGFMGYSA-ENIPGCSS--------------526
hCRY2 526 VEDLSHPVAEPSSSQAGSMSSAGPR---PLPSG--555
C-terminal extension domain
mCRY1 542 VPSCSGGNCSQGSGILHYAHGDSQQTHSLKQGRSS 576
mCRY2 555 ----------PASPKRKLEAAEEP 568
hCRY1 527 -----SGSCSQGSGILHYAHGDSQQTHLLKQGRSS 556
hCRY2 556 ----------PASPKRKLEAAEEP 569

Figure 14. Pull-down assay of mutant CRY1/2. Wild-type and ΔCC-tail mutant of CRY1/2 were individually transfected into HEK293T cell. Whole-cell lysates were harvested for pull-down assay. Note that both ΔCC-tail mutant of CRY1/2 were failed to interact with biotin-conjugated KS15, while wild-type of CRY1/2 successfully bind with bait. V: vehicle (DMSO), B: bait.

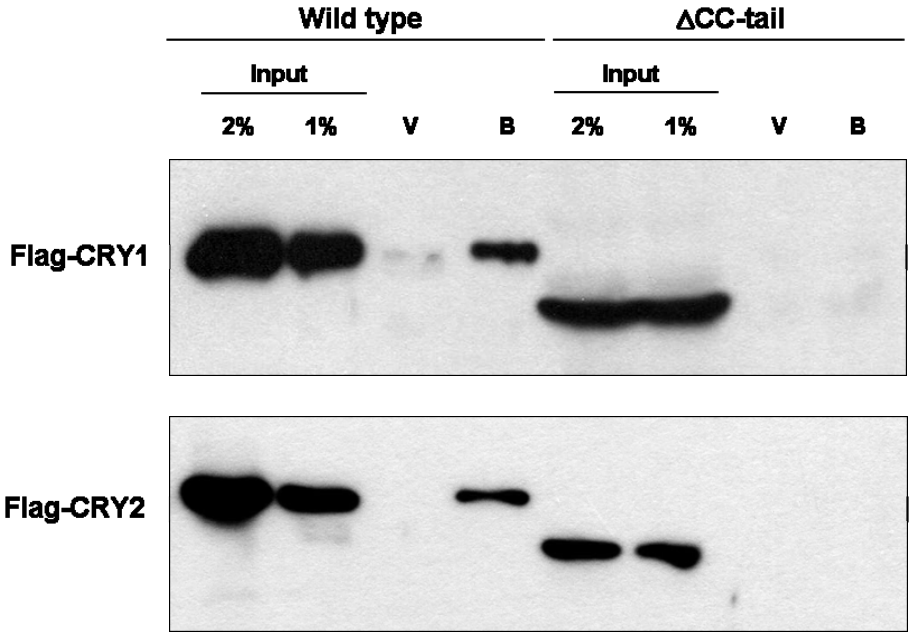
Wild type
ΔCC-tail
Input
Input
2%
1%
V
B
2%
1%
V
B
Flag-CRY1
Flag-CRY2

Figure 15. CRYs-dependent actions of KS15. (A) E-box-Luc reporter activity. Relative *Per1* (B), *Per2* (C) and *Rev-erbα* (D) mRNA expression in WT or CRYs-deficient MEF. ***p* < 0.01 *vs.* Vehicle, ††*p* < 0.01 *vs.* WT with the same treatment. Data are presented as mean ± S.E.M. (n = 4 for each group).

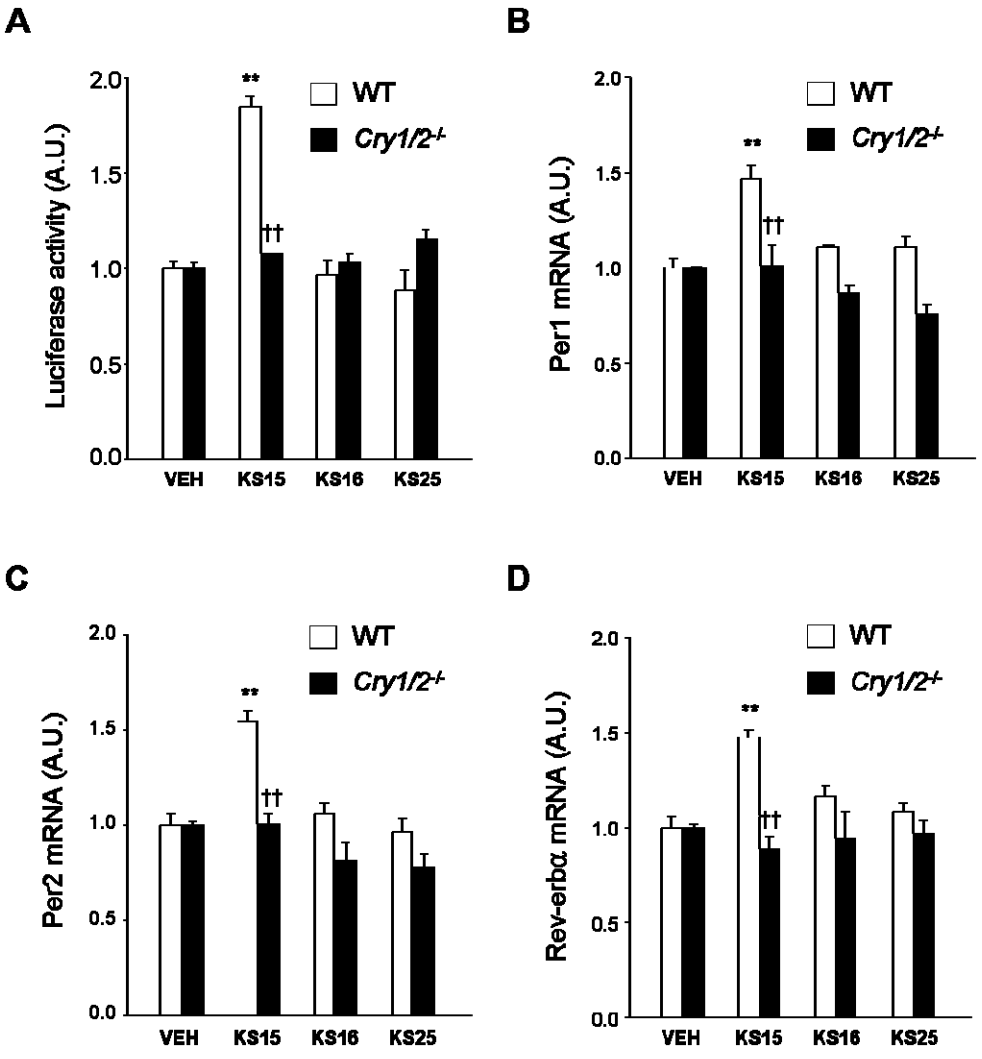
A
B
C
D
WT
Cry1/2-/-
Luciferase activity (A.U.)
Per1 mRNA (A.U.)
Per2 mRNA (A.U.)
Rev-erbα mRNA (A.U.)
2.0
1.5
1.0
0.5
0.0
**
††
VEH
KS15
KS16
KS25

Figure 16. Effect of KS15 on the oscillation of Per2-Luc in fibroblasts. The results of real-time bioluminescence recording are represented in (A) raw or (B) detrended data format. Treatment of KS15 after synchronized by dexamethasone (DEX) decreased Per2-Luc oscillation amplitude compared to the vehicle group. Data are representative of at least five independent experiments.

A

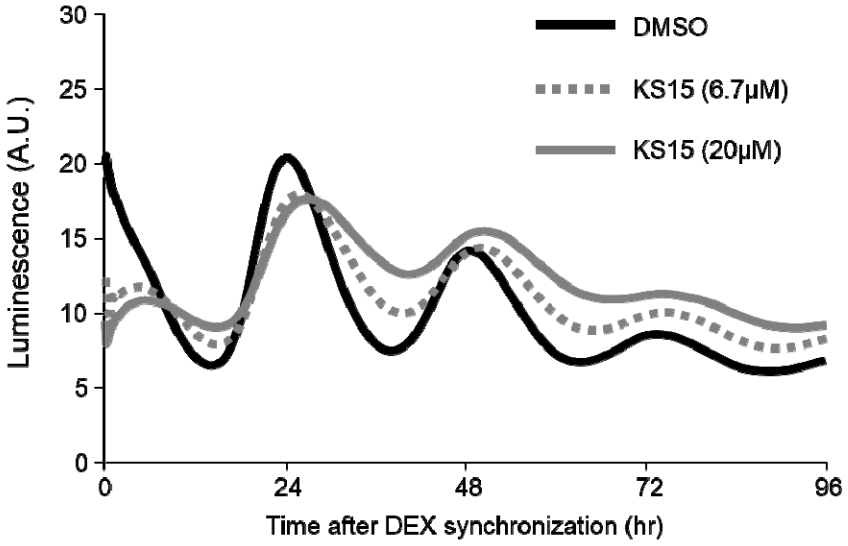
30
25
20
15
10
5
0
Luminescence (A.U.)
0
24
48
72
96
Time after DEX synchronization (hr)
DMSO
KS15 (6.7μM)
KS15 (20μM)

B

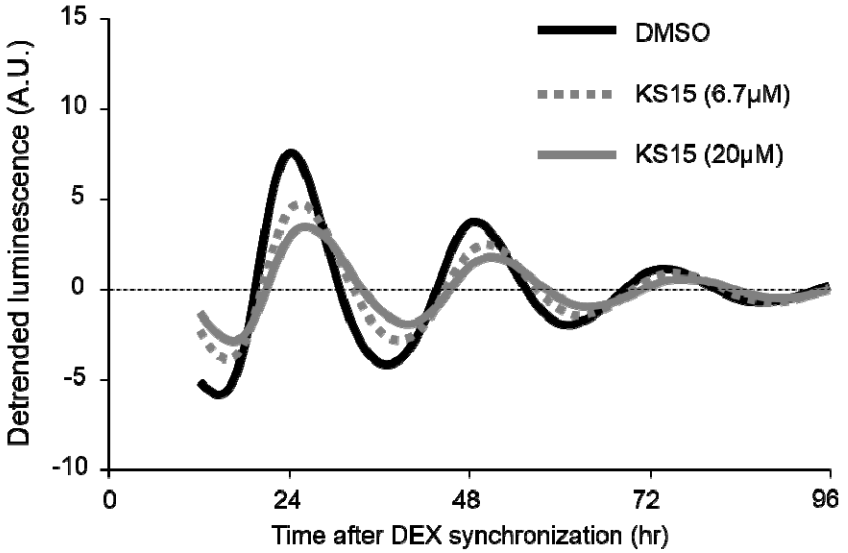
15
10
5
0
-5
-10
Detrended luminescence (A.U.)
0
24
48
72
96
Time after DEX synchronization (hr)
DMSO
KS15 (6.7μM)
KS15 (20μM)

Table 2. Circadian oscillation of Per2-Luc in fibroblasts following treatment with KS15. Statistical analysis of circadian profiles generated by Per2-Luc reporters in fibroblast cell. Average periods were calculated as the mean ± S.E.M. of the inter-peak intervals among the four peaks. Relative amplitudes were calculated as the mean ± S.E.M. of each peak's amplitudes, which were normalized by the amplitudes of the vehicle-treated group. Areas under the curves (AUC) represent the percentage of the vehicle-treated group in raw data format. Each experiment was repeated five times.

Compound	Concentration	Period (hour)	Relative amplitude (%)	AUC (%)
Vehicle (DMSO)	0.20%	24.1 ± 0.03	100	100
KS15	6.7 μM	23.9 ± 0.07	54.2 ± 3.9	111.3 ± 3.0
	20 μM	23.7 ± 0.08	42.6 ± 3.5	115.9 ± 1.7

Figure 17. Effect of KS15 on the oscillation of Bmal1-dLuc in fibroblasts. The results of real-time bioluminescence recording are represented in (A) raw or (B) detrended data format. Treatment of KS15 after DEX synchronization decreased Bmal1-dLuc oscillation amplitude compared to the vehicle group. Data are representative of at least three independent experiments.

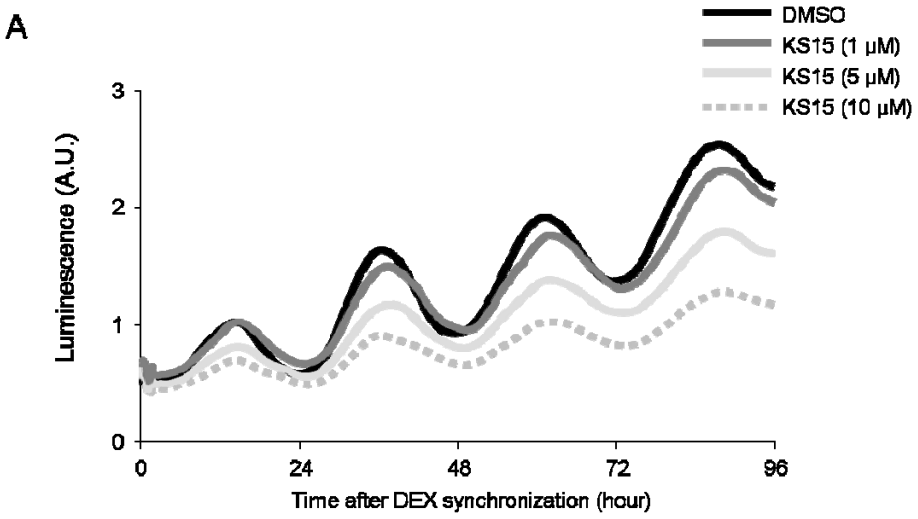
A
DMSO
KS15 (1 μM)
KS15 (5 μM)
KS15 (10 μM)
Luminescence (A.U.)
3
2
1
0
0
24
48
72
96
Time after DEX synchronization (hour)

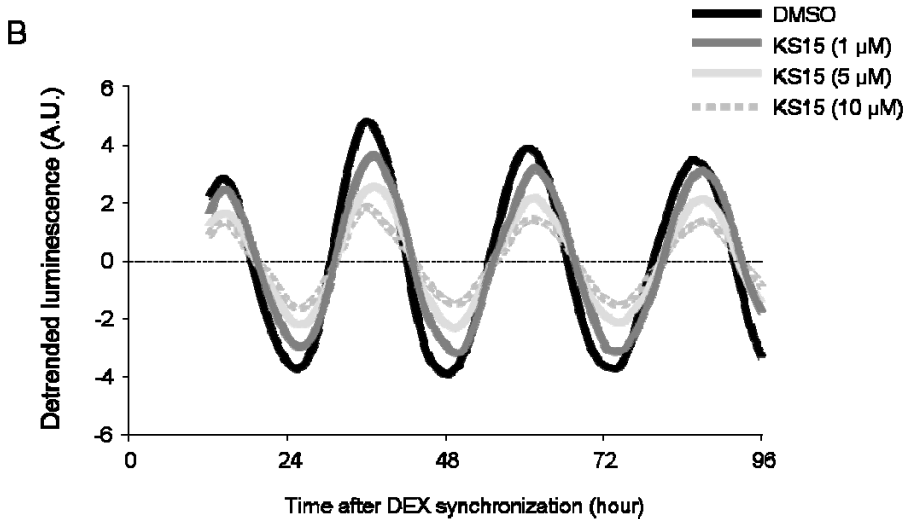
B
DMSO
KS15 (1 μM)
KS15 (5 μM)
KS15 (10 μM)
Detrended luminescence (A.U.)
6
4
2
0
-2
-4
-6
0
24
48
72
96
Time after DEX synchronization (hour)

Table 3. Circadian oscillation of Bmal1-dLuc in fibroblasts following treatment with KS15. Statistical analysis of circadian profiles generated by Bmal1-dLuc reporters in fibroblast cell. Average periods were calculated as the mean ± S.E.M. of the inter-peak intervals among the four peaks. Relative amplitudes were calculated as the mean ± S.E.M. of each peak's amplitudes, which were normalized by the amplitudes of the vehicle-treated group. AUC represent the percentage of the vehicle-treated group in raw data format. Each experiment was repeated three times.

Compound	Concentration	Period (hour)	Relative amplitude (%)	AUC (%)
Vehicle (DMSO)	0.20%	24.6 ± 0.1	100	100
KS15	1 μM	24.5 ± 0.2	71.5 ± 8.3	90.3 ± 2.6
	5 μM	24.5 ± 0.04	60.8 ± 2.9	81.8 ± 2.2
	10 μM	24.1 ± 0.2	39.0 ± 1.7	69.4 ± 3.9

Figure 18. Effect of shCRY1/2 on E-box mediated transcription. E-box-Luc reporter and shCRY1/2 constructs (sc-44835-SH and sc-44836-SH, Santa Cruz Biotechnology) were co-transfected in cultured fibroblasts (NIH3T3) and incubated for 48 hours. Each plasmids were transfected 100 ng per well. After that, cells were harvested and analyzed with luciferase assays. Data are presented as mean ± S.E.M. (n = 3). **: $p < 0.01$ compared with cells transfected with the blank construct.

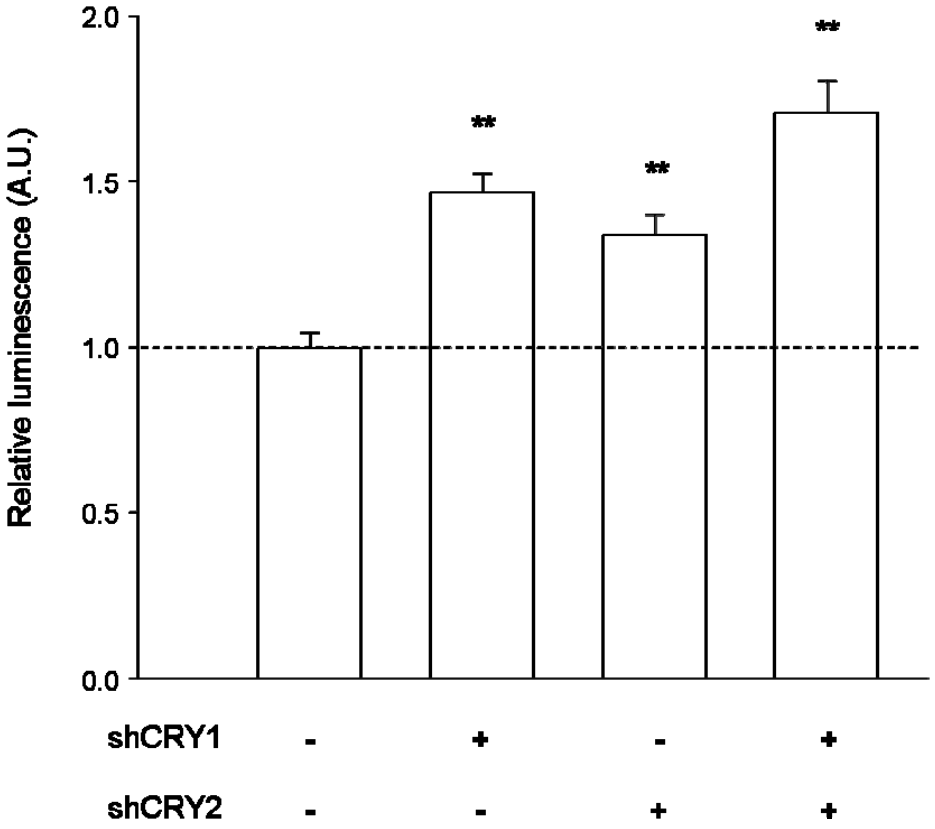
2.0
1.5
1.0
0.5
0.0
Relative luminescence (A.U.)
**
**
**
shCRY1 - + - +
shCRY2 - - + +

Figure 19. The effect of CRY subtype knockdown on Bmal1-dLuc oscillation in fibroblasts. Bmal1-dLuc reporter and shRNA constructs were co-transfected in cultured fibroblasts (NIH3T3) and incubated for 48 hours. Then, cells were synchronized by treatment with DEX, and emitting bioluminescence in the presence of the luciferin substrate was monitored every 10 min for 96 hours. The real-time bioluminescence recording results are represented in raw (A) and detrended data (B) formats. pU6 plasmid was co-transfected with Bmal1-dLuc as a blank construct. Data are representative of at least three independent experiments.

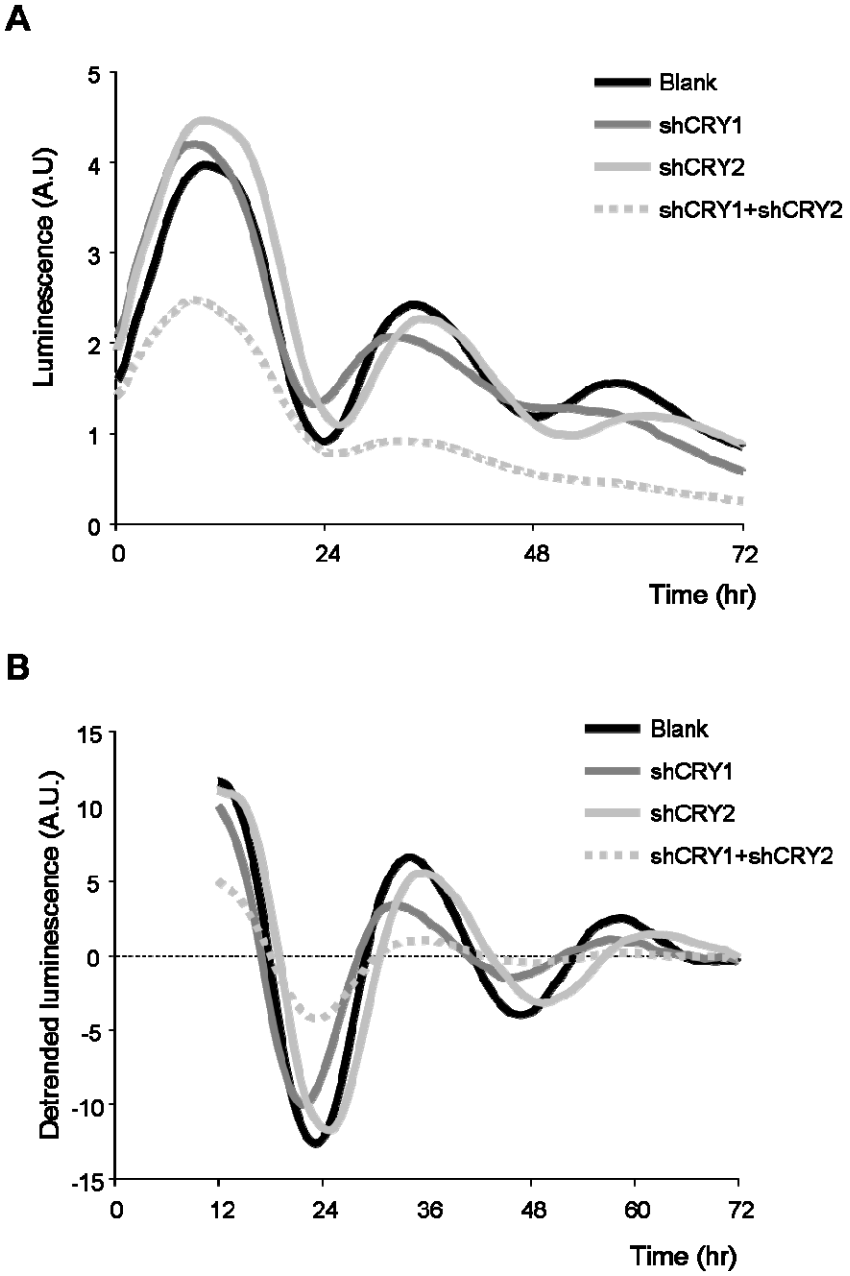
A
Luminescence (A.U)
5
4
3
2
1
0
0
24
48
72
Time (hr)
Blank
shCRY1
shCRY2
shCRY1+shCRY2
B
Detrended luminescence (A.U.)
15
10
5
0
-5
-10
-15
0
12
24
36
48
60
72
Time (hr)
Blank
shCRY1
shCRY2
shCRY1+shCRY2

Table 4. Circadian oscillation of Bmal1-dLuc with co-transfection of shCRY1/2. Statistical analysis of circadian profiles generated by Bmal1-dLuc reporters in fibroblast cell following co-transfection with shCRY1 or shCRY2. Note that single transfection of shCRY1 or shCRY2 were mainly affect on period length whereas co-transfection of shCRY1/2 were not significantly alter period length but severely repressed amplitude of the rhythm. Average periods were calculated as the mean ± S.E.M. of the inter-peak intervals among the four peaks. Relative amplitudes were calculated as the mean ± S.E.M. of each peak's amplitudes, which were normalized by the amplitudes of the vehicle-treated group. AUC represent the percentage of the vehicle-treated group in raw data format. Each experiment was repeated three times.

Construct	Amounts	Period (hour)	Relative amplitude (%)	AUC (%)
Blank	-	23.3 ± 0.2	100	100
shCRY1	200 ng	22.1 ± 0.2	81.6 ± 6.6	83.1 ± 3.8
shCRY2	200 ng	24.9 ± 0.4	96.7 ± 3.4	93.8 ± 2.9
shCRY1 +shCRY2	100 ng + 100 ng	23.6 ± 0.3	46.9 ± 2.8	51.3 ± 1.9

Figure 20. The dose-dependent effect of CRY1/2 double knockdown on Bmal1-dLuc oscillation in fibroblast. Gradually increasing total amounts of shRNA of CRY1/2 were monitored to examine the dose-dependent effect of shCRY1/2 (shCRY1:shCRY2 = 1:1). Procedures for transfection, synchronization and bioluminescence monitoring were same as the experiments in Fig 18. The real-time bioluminescence recording results are represented in raw (A) and detrended data (B) formats. Data are representative of at least three independent experiments.

A

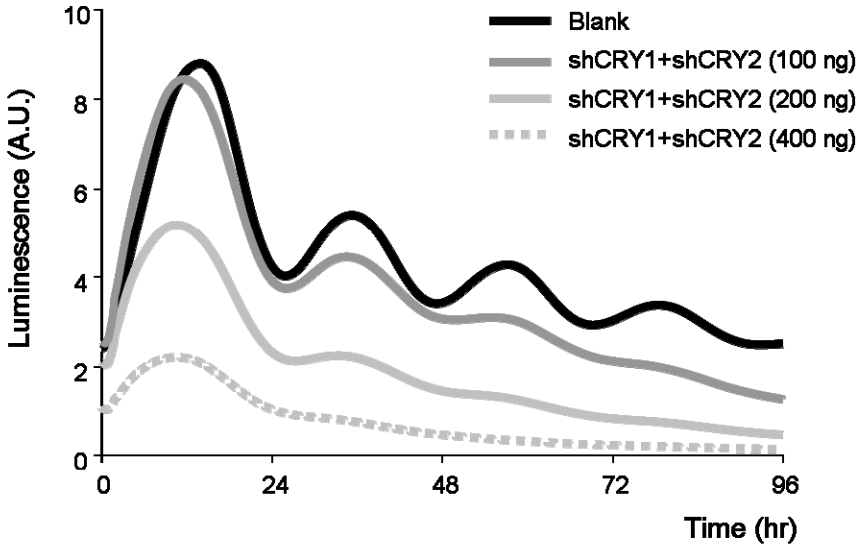
Blank
shCRY1+shCRY2 (100 ng)
shCRY1+shCRY2 (200 ng)
shCRY1+shCRY2 (400 ng)
Luminescence (A.U.)
10
8
6
4
2
0
0
24
48
72
96
Time (hr)

B

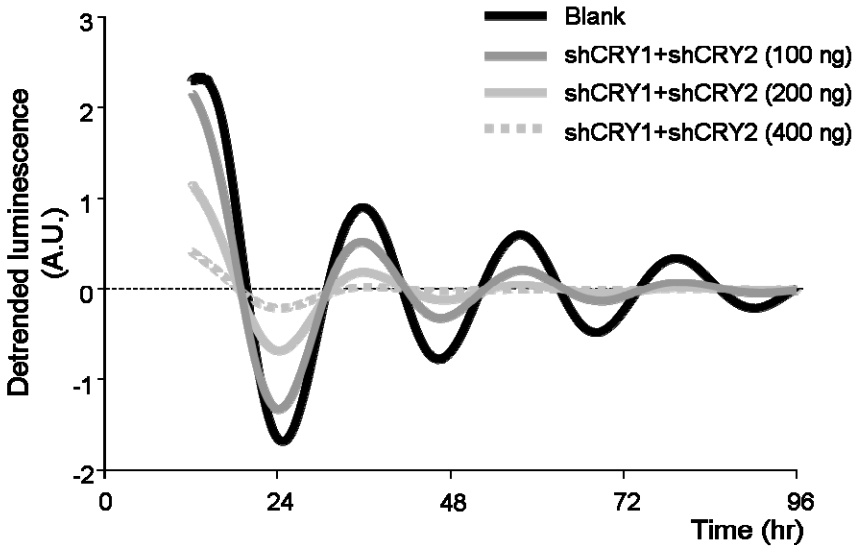
Blank
shCRY1+shCRY2 (100 ng)
shCRY1+shCRY2 (200 ng)
shCRY1+shCRY2 (400 ng)
Detrended luminescence (A.U.)
3
2
1
0
-1
-2
0
24
48
72
96
Time (hr)

Table 5. The dose-dependent effect of CRY1/2 double knockdown on Bmal1-dLuc oscillation in fibroblast. Statistical analysis of circadian profiles that generated by Bmal1-dLuc reporter in fibroblast following co-transfection of both shCRY1 and shCRY2. Note that shCRY1/2 mainly affect on amplitude of Bmal1-dLuc rhythm in dose-dependent manner while period length were not significantly altered. Average periods were calculated as the mean ± S.E.M. of the inter-peak intervals among the four peaks. Relative amplitudes were calculated as the mean ± S.E.M. of each peak's amplitudes, which were normalized by the amplitudes of the vehicle-treated group. AUC represent the percentage of the vehicle-treated group in raw data format. Each experiment was repeated three times.

Construct	Amount	Period (hour)	Relative amplitude (%)	AUC (%)
Blank	-	23.6 ± 0.1	100	100
shCRY1 +shCRY2	100 ng (50 ng + 50 ng)	23.7 ± 0.07	61.9 ± 6.6	74.5 ± 2.7
	200 ng (100 ng + 100 ng)	24.4 ± 0.1	41.2 ± 6.8	51.6 ± 2.1
	400 ng (200 ng + 200 ng)	23.8 ± 0.3	30.3 ± 6.4	26.5 ± 2.9

Figure 21. *In vivo* administration of KS15. Intracerebroventricular (ICV) microinjection of KS15 alters period and phase of activity rhythm. DMSO (vehicle, 0.5 μl) or KS15 (140 μg / kg) of were administrated into mice by single ICV bolus microinjection at two hour before activity onset. (A) Representative 30-day wheel-running double-plot actograms. After 10 days under normal light:dark = 12 hours:12 hours (LD), recording of 10 days under constant dark (FRP, Free-running period), and 10 days after injection of DMSO or KS15 (ICV injection) were shown here. The constant dark phases are illustrated by gray shadows and timings of injection are marked in blank circles within the image. (B) Periods from wheel running activity rhythm of mice with DMSO or KS15 injection. Periods of activity rhythms were determined by the cosinor fitting analysis of 7-day profiles during FRP and post-injection profiles (ICV injection). (**:$p<0.01$ vs vehicle administrated group) (C) Phase-shifts profiles induced by injection of DMSO or KS15. (*:$p<0.05$ vs vehicle administrated group) (D) Relative wheel running activity during FRP and post-injection period. Wheel running activity during entrainment period defined as 100%. All data were presented as the mean ± S.E.M. from three independent experiments.

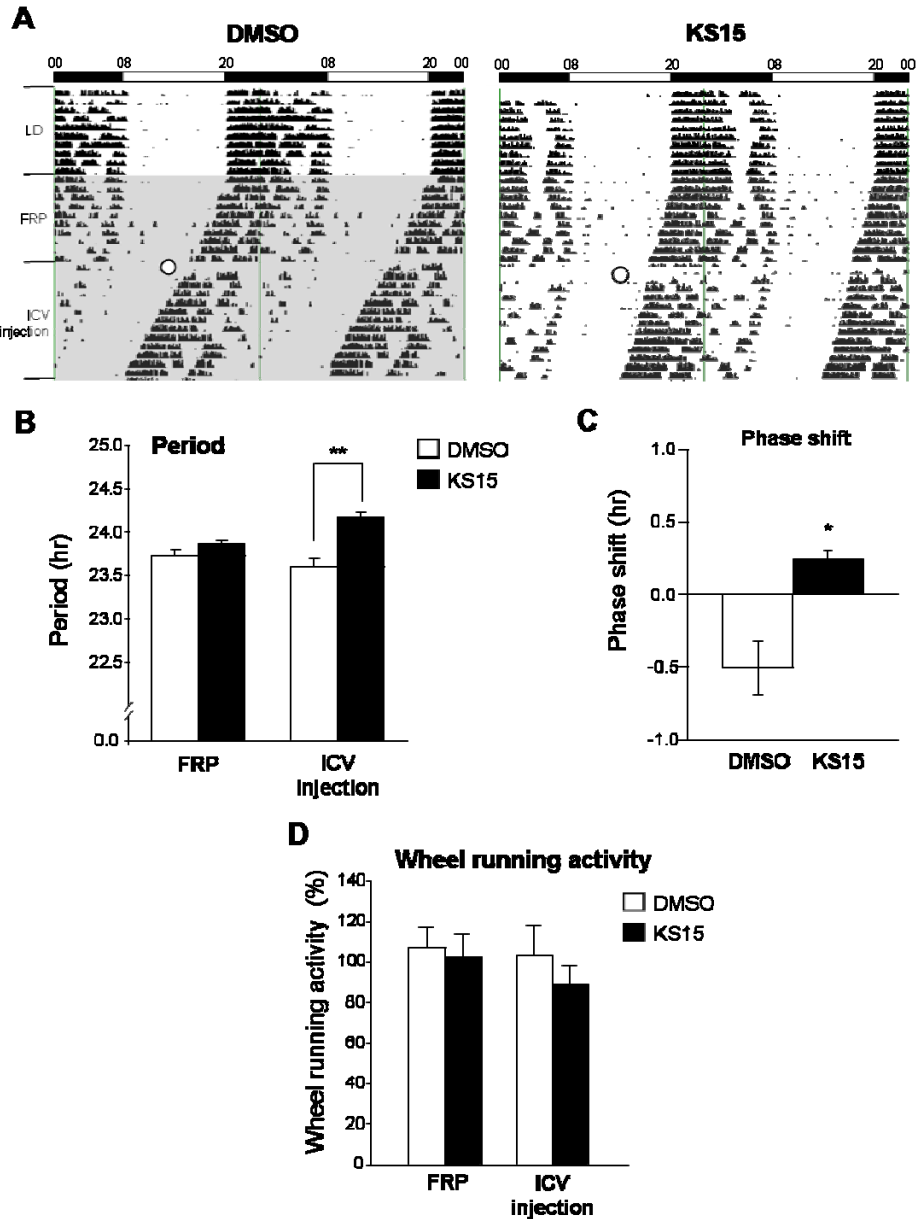
A
DMSO
KS15
00
08
20
08
20
00
LD
FRP
ICV injection
B
Period
**
DMSO
KS15
Period (hr)
25.0
24.5
24.0
23.5
23.0
22.5
0.0
FRP
ICV injection
C
Phase shift
*
Phase shift (hr)
1.0
0.5
0.0
-0.5
-1.0
DMSO
KS15
D
Wheel running activity
Wheel running activity (%)
140
120
100
80
60
40
20
0
DMSO
KS15
FRP
ICV injection

DISCUSSION

The present study was designed to develop a novel synthetic modulator for core clock genes and their functions. In last decades, several synthetic compounds were identified as circadian clock modulators. For example, several agonists and antagonists of REV-ERBα were identified recently and those modulators were used for many physiological and clinical research. SR9009 and SR9011 were identified as REV-ERBα/β agonists and *in vivo* application of these agonists induced enhancement of metabolic functions under normal light-dark cycle as well as affect circadian rhythm without light cues (Solt et al., 2012). This study suggests that circadian clock and its regulatory mechanisms can be novel therapeutic targets for treatment of circadian rhythm-related disorders. However, despite the physiological and clinical importance of circadian rhythms, synthetic compounds that directly regulate E-box mediated transcriptional activity have not been reported yet. Development of circadian clock modulator is immerging field during last decades and many compounds were reported as circadian clock modulator. However, most of them were targeting other than core clock genes (CLOCK, BMAL1, PER1/2, CRY1/2) (Chen et al., 2013). In the present study, I identified and characterized a novel small molecule called as KS15 that directly binds to CRY1/2 and inhibits its repressive function, thereby activating E-box-mediated transcriptional activity. Periodic gene transcription by the CLOCK:BMAL1 heterodimer plays a pivotal role in the cyclic mRNA accumulation of numerous clock-controlled genes, as well as core clock components, such as *Pers* and *Crys*. Therefore, KS15 can be a

novel approach for studying detailed mechanism as well as investigating implication of molecular circadian clockwork on physiology and behavior.

To discover a novel small molecule modulator of the molecular clock, I designed a new cell-based screening method based on E-box-mediated transcriptional activity, the main output of molecular circadian clock. In this method, I used the artificial luciferase reporters selectively regulated by CLOCK:BMAL1 heterodimer and the cultured cell lines with stable expression of these reporters. Establishment of stable cell lines is an important strategy because these stable cell lines are ready-to-use materials for massive screening of chemical library. I also designed the secondary screening step by using BMAL1 knock-out fibroblasts for optimizing selectivity of hit chemicals. Taken together, this two-step screening strategy is a highly efficient method for development of a novel circadian clock modulator.

It should be noted that the hit chemicals (KS11a, KS11b, KS15) from the screening turned out to be stereoisomers of PPAR (peroxisomal proliferator-activated receptor) agonists in previously study (Suh et al., 2008). In the previous study, stereoisomers containing *(S)*-ethoxypropanoic acid (KS11a', KS11b' and KS15') shown to have higher activities on both PPARα and PPARγ than analogs containing *(R)*-ethoxypropanoic acid (Suh et al., 2008). Thus, I compared the effects to the hit chemicals (KS11a, KS11b, KS15) and their stereoisomers (KS11a', KS11b' and KS15') on E-box- or PPAR responsive elements-mediated transcriptional activities for clarification of specificity. As shown in Figure 7C and Table 1, the *(S)*-

ethoxypropanoic acid-containing stereoisomers were much less potent than the hit chemicals on E-box-mediated transcription. By contrast, they exhibited higher enhancing activities on a luciferase reporter driven by multiple PPAR responsive elements than candidates in present study (Fig 8). Taken together, these finding strongly suggest the selectivity of the candidate compound including KS15 in controlling E-box-mediated transactivation.

Notably, the very recently developed compound KL001 reported as a small molecule directly targeting the CRY1/2 (Hirota et al., 2012). But unlike KS15, KL001 represses core loop activity by strengthening the stability of CRY1/2, whereas KS15 enhances core loop activity by inhibiting repressive activity of CRY1/2. Also, KS15 has a distinct scaffold than KL001. KS15 contains 2-ethoxypropanoic acid and two aryl rings connected by an oxime ether linker, while KL001 has a carbazole scaffold (Hirota et al., 2012). More importantly, KL001 has period lengthening changing effect, whereas KS15 is only effective on the amplitude of circadian clock. These differences suggest that KS15 has distinctive mechanism of action than previously reported KL001. Although I examined direct binding of KS15 with CRY1/2, detailed mechanisms for binding of KS15 with CRY proteins remains to be determined.

It is noteworthy that many small compounds such as longdaysin (Hirota et al., 2010) or KL001 (Hirota et al., 2012) were reported as circadian modulator with period changing effect, while KS15 is only effective on the amplitude of circadian clock. Previous studies suggested that single

knockdown of CRY1 leads to shortened periods, while CRY2 knockdown shows lengthened periods of the rhythms generated by Bmal1 promoter-driven luciferase activities (Zhang et al., 2009; Baggs et al., 2009). However, these rhythms were severely attenuated in the case of double knockdown of both CRY1/2 (Baggs et al., 2009). Because KS15 can interact with both CRY1/2 (Fig 18), I hypothesized that KS15 inhibits both CRY1/2 and thereby attenuates the rhythm rather than changing the period length. To prove this, I analyzed the rhythm of Bmal1-dLuc reporter activity with knockdown of each CRY subtype using shRNA. In agreement with previous studies (Zhang et al., 2009; Baggs et al., 2009), single knockdown of CRY1 or CRY2 altered period length, while knockdown of both CRY1/2 severely attenuated amplitude of the rhythm in a dose-dependent manner without significantly changing the period length (Fig 19, Fig 20 and Table 3). These data suggest that KS15 modulates clock-controlled gene transcription by inhibiting both CRY1/2 and thereby attenuates the rhythm without affecting the period. Also, these findings can explain why KS15 did not affect the period length like KL001 (Hirota et al., 2012).

However, unlike results from fibroblast cells, *in vivo* ICV administration of KS15 into mouse causes lengthening of period and delaying of circadian phase. This controversial result can be explained by different regulatory mechanism of central and peripheral clock. It is well-known that even non-SCN cells are autonomous oscillators, however, they may desynchronize from one another in the absence of the SCN as they lack local coupling within tissues (Nagoshi et al., 2004; Welsh et al., 2004, Stratmann and Schibler 2006). In contrast, the neuronal network within the SCN couples its

component single-cell oscillators to produce a coherent circadian oscillation at the tissue level (Aton and Herzog 2005; Welsh et al., 2010). Interestingly, experimental evidences suggest that CRY1 is required for sustained circadian rhythms in dissociated SCN neurons or fibroblasts but not in organotypic SCN slices or at the behavioral level, whereas CRY2 is not required at any of these levels (Liu et al., 2007; Evans et al., 2012). CRY1 is known as a stronger repressor than CRY2, and that this can serve as a biochemical basis for differences in CRY knockout phenotypes (Khan et al., 2012; Hirota et al., 2012). These different natures of central and peripheral clock, especially intracellular coupling of SCN neurons can be reasons for different responses of KS15 to fibroblast and *in vivo*. However, this experiment was performed only in a single dose of KS15 and single injection timing. Analysis of daily activity rhythms with injection of various concentration of KS15 or multiple injection timing will be required for the further investigation.

In conclusion, I developed a novel antagonist for CRY1/2 and validated this compound as circadian modulator for both *in vitro* and *in vivo*. Further optimization of KS15**,** along with functional studies may lead to new therapeutics for a variety of circadian and metabolic disorders develop or linked with the cellular actions of CRYs.

CHAPTER 2

Evaluation of anti-tumor activity of Cryptochrome inhibitor on human breast cancer cell line

ABSTRACT

Among circadian rhythm related tumors, breast cancer is one of the well-known cases that are caused by chronic exposure to disrupting stimuli, such as shift work, on the circadian clock. Cryptochromes (CRYs) are a key component of the molecular circadian clockwork. Increasing evidence has indicated that CRYs affect a variety of genes related with cell cycle regulation and anti-tumor activity. Interestingly, recent studies suggest that inhibition of CRYs enhanced DNA damage response and initiation of apoptosis as a response to genotoxic stress. In addition, mutations within human CRY2 can be risk factors for initiation of breast cancer. Also, expression profiles of CRY2 are differently regulated between normal and breast cancer tissues in human patients. It appears that CRYs can be a novel therapeutic target for the treatment of breast cancer. In the present study, I evaluated the anti-tumor activity of KS15 on human breast cancer cells. KS15 inhibited the proliferation of MCF-7 cells in dose-dependent manner but not in other cell lines (MCF-10A and MDA-MB-231). Sensitivities for the anti-tumor drugs were enhanced only in MCF-7 when co-treated with KS15. On the other hand, adhesion ability on extracellular matrix and metastatic activity were not significantly affected by treatment of KS15. These findings suggest that pharmacological inhibition of CRYs by KS15 has an anti-proliferative effect and increase chemosensitivity to anti-tumor drugs on a specific type of breast cancer. Further investigation on the detailed mechanism and optimization of this anti-tumor activity of KS15 can be a novel therapeutic treatment for breast cancer.

Keywords: Breast cancer, Cryptochrome; Circadian rhythm; Small molecule; Anti-tumor activity

INTRODUCTION

The circadian rhythm has a fundamental role in regulation of physiology and behavior and almost all of biological processes in human are influenced by the circadian clock. Thus, disruption of circadian clock is associated with a variety of adverse affects, including the promotion of oxidative stress and alterations in immune function (Navara et al., 2007). Increasing evidence also suggests that disturbance of circadian rhythm play a major role in various kinds of tumorigenesis processes (Lamont et al., 2007; Stevens et al., 2007). Based on these findings, the IARC concluded that shift work that involves circadian disruption is a possible carcinogen in humans (Group 2A) in 2007 (Straif et al., 2007).

Breast cancer is a type of cancer originating from breast tissue and most common cancer in women in developed countries. Recent studies have indicated that incidence of breast cancer increases significantly in women working nightshifts (Schernhammer et al., 2001). Also, disruption of circadian rhythms through constant light exposure increases the formation of spontaneous mammary tumors in rodents (Aubert et al., 1980; Mhatre et al., 1984). These data suggested that development of breast cancer can be evoked by chronic exposure to disrupting stimuli for circadian clock.

The maintenance of circadian rhythm is largely dependent on a set of core circadian clock genes. (Oster, 2006) These genes form a negative and positive feedback loop, which allows tight control of rhythmic expression of clock controlled genes (CCGs), thereby ensuring that products of these genes will be active in right timing of the circadian cycle (Young and Kay, 2001; Reppert and Weaver, 2001). CCGs include essential cell cycle

regulators and tumor suppressors and circadian control of these genes leads to the coupling of cell proliferation with key tissue functions in vivo (Fu et al., 2002; Panda et al., 2002; Matsuo et al., 2003). Disruption of circadian rhythm in cell proliferation is frequently associated with tumor development and progression in mammals (Bjarnason and Jordan, 2000; Smaaland, 1996).

Cryptochrome (CRY) is one of the core clock genes that essential to the maintenance of circadian rhythm. CRY act as main transcriptional repressor in the negative arm of the circadian clock but also CRY involved in cellular proliferation, including roles in DNA damage checkpoint control (Unsal-Kacmaz et al., 2005) and regulation of genes important for cell cycle progression (Gauger and Sancar, 2005; Matsuo et al., 2003). Recent studies suggested that CRY has important roles in DNA damage response and susceptibility to carcinogenesis. Interestingly, genetically depletion of CRY1/2 showed protective effect on cancer-prone phenotype in response to genotoxic stress (Gauger and Sancar, 2005; Ozturk et al., 2008; Lee et al., 2013). In addition, another studies suggested that single-nucleotide polymorphisms of CRY2 as well as methylation within the CRY2 promoter region were significantly associated with postmenopausal breast cancer risk (Hoffman et al., 2010, Cancer Prev Res). Moreover, knockdown of CRY2 in human breast cancer cell line shows adverse effect on regulation of DNA damage repair and the maintenance of genomic stability. (Hoffman et al., 2010, BMC Cancer) Taken together, these findings suggested that functional modulation of CRY can be a novel therapeutic treatment for breast cancer. In the present study, I evaluate anti-tumor activity of KS15 in human breast cancer cells

MATERIALS AND METHODS

Materials KS15 was dissolved at a concentration of 0.02 M in 100% DMSO as a stock solution, stored at -20 °C, and diluted with medium before each experiment. The final DMSO concentration did not exceed 0.2% DMSO throughout the study (in our study, all the control groups are composed of 0.2% DMSO). Heat-inactivated fetal bovine serum (FBS) was obtained by incubation of normal FBS in 60 °C for 30 min. 3-(4,5-dimethylthiazol-2-yl)-2,5-diphenyltetrazolium bromide (MTT) was obtained from Sigma (St. Louis, Missouri). Before use, MTT dissolved in culture media (0.5 mg/ml). Matrigel was purchased from Becton Dickinson Biosciences (San Jose, California).

Cell culture MCF-7 and MDA-MB-231 human breast carcinoma cells were cultured in DMEM (GIBCO, Invitrogen Corp., Carlsbad, California) supplemented with 10% (v/v) FBS in a humidified atmosphere of 5% CO2 at 37 °C. MCF-10A were cultured in complete MEGM (mammary epithelial growth medium, serum-free) purchased from Clonetics (San Diego, CA) and supplemented with 10% (v/v) FBS in a humidified atmosphere of 5% CO2 at 37 °C.

Cell viability Assay Cells were seeded in a 96-well plate at 5×10^4 cells/well and incubated in 100 μL of medium for 24 h. After incubation, the cells were treated with the 0.5 mg/ml solution of MTT dissolved in culture media and the cells were incubated for 4 h. After removing the medium, 100 μl of DMSO was used to dissolve the MTT formazan crystals. Absorbance from each well was measured at 570 nm.

Adhesion assay 96-well cell culture plates were coated with fibronectin solution (0.5 mg/m in PBS) (Sigma, St. Louis, Missouri) overnight. The wells were blocked for 30 min with 0.5% heat-inactivated FBS. Cells were trypsinized and suspended at a final concentration of 5 × 10^5 cells/ml in serum-free medium. 20 μM and 50 μM of KS15 were given to the cells for 24 h before seeding. 100 μl cell suspension was added to the wells and the plates were incubated at 37 °C for 1 hr. Medium was then carefully suctioned out from each well. Each well was washed three times with PBS. The colorimetric MTT-assay was used to determine the number of remaining cells (adherent cells).

Invasion assay The in vitro invasion assays were carried out using Transwell chamber with 10 mm diameter and 8 μm pore size polycarbonate membrane (Corning Costar, Cambridge, Massachusetts) coated with Matrigel (BD Science). Cells were trypsinized and suspended at a final concentration of 5 × 10^5 cells/ml in serum-free DMEM medium. 20 μM and 50 μM of KS15 were given to the cells for 24 h before seeding. Cell suspension was added into each upper chamber of transwell. The bottom chamber contained medium with 5% FBS to serve as a chemoattractant. After incubation for 24 h at 37 °C under 5% CO2 and 95% air atmosphere, all of the non-invaded cells were removed the upper face of the transwell membrane with a cotton swab; the invaded cells were fixed with 100% methanol and then stained with methylene blue. The invaded cells were counted microscopically. Ten fields were counted for each assay.

RESULTS

Anti-proliferative activity of KS15 to human breast cancer cell lines

To evaluate the effects of CRY inhibitor on cell growth of human breast cancer cells, I cultured the two widely-used human breast cancer cell lines (MCF-7, MDA-MB-231) and normal mammary epithelial cells (MCF-10A) in the absence or presence of KS15 in different concentrations. MCF-7 is estrogen/progesterone receptor (ER/PR) positive type of cancer cell lines with weak invasiveness. Thus, hormonal therapy such as treatment of tamoxifen as well as usual chemotherapy are both effective for this cell lines. On the other hand, MDA-MB-231 is negative for ER, PR and human epidermal growth factor receptor 2 (HER2) and so called as “triple negative breast cancer (TNBC)” type. Therefore, chemotherapy using non-specific anti-tumor drugs Including doxorubicin is only effective for this cell lines. MDA-MB-231 cell line also shows highly invasiveness and thereby widely used for investigating metastatic activity. MCF-10A is immortalized but non-cancerous mammary epithelial cell lines that widely used for cell line model for normal mammary tissues. After 48 hr incubation with various concentration of KS15, MTT assay, a non-radioactive assay that widely used to quantify cell viability and proliferation, was performed. The MTT assay measures cell viability and proliferation based on the ability of the mitochondrial dehydrogenase enzymes to convert the yellow tetrazolium MTT to water-insoluble dark blue formazan by reductive cleavage of the tetrazolium ring. The amount of dye produced is proportional to the number

of metabolically live cells. The results show that KS15 exhibited a significant and a dose-dependent inhibitory effect on viability of MCF-7 cell line, whereas other cell lines (MCF-10A, MDA-MB-231) were not responsive to KS15 (Fig 22A). Moreover, structural analog of KS15 with less potency for inhibition of CRYs (KS25) was failed to show anti-proliferative activity to all three type of cell lines (Fig 22B). These data suggested that pharmacological inhibition of CRYs by application of KS15 has repressive effect on proliferation of MCF-7 human breast cell line.

Enhancement of chemosensitivity by co-treatment of KS15 with anti-tumor drugs

Recent studies Indicated that functional inhibition of CRY1/2 showed protective effect for cancer-prone phenotype of p53 mutant mice and enhanced responses for clonogenic anti-tumor drugs (Gauger and Sancar, 2005; Ozturk et al., 2008; Lee et al., 2013). Based on these findings, I hypothesized that co-treatment of KS15 with anti-cancer drugs can increase susceptibility for these drugs and thereby synergistically inhibits viability of tumor cell lines. To prove this, MCF-7 and MDA-MB-231 cells were treated with KS15 and two different kinds of genotoxicants including doxorubicin and oxaliplatin. Doxorubicin is radiomimetic compound that interacts with DNA by intercalation whereas oxaliplatin is UV mimetic compound that forms both inter- and intra- strand cross links in DNA. In addition, MCF-7 were tested with tamoxifen, an antagonist of the estrogen receptor in breast tissue and thereby widely used for hormone therapy of

ER/PR positive type of breast cancer. After 48 hr incubation, viability of remaining cells was analyzed by MTT assay. As a result, sensitivities of MCF-7 to doxorubicin were significantly increased by co-treatment of KS15 in dose-dependent manner, whereas sensitivities of MDA-MB-231 were not changed (Fig 23). On the other hand, sensitivity to oxaliplatin was not significantly enhanced in both MCF-7 and MDA-MB-231 by co-treatment of KS15 (Fig 24). It should be noted that co-treatment of KS15 with tamoxifen also shows enhanced sensitivity in MCF-7 (Fig 25). Moreover, enhanced efficacies of doxorubicin and tamoxifen with co-treatment of KS15 on MCF-7 cells were analyzed using dose-response curves (Fig 26 and Table 6). These data clearly demonstrated that co-treatment of KS15 reduces IC_{50} values of doxorubicin and tamoxifen in dose-dependent manner. In consistent with Fig 22, these findings suggest that only MCF7, the ER/PR positive type of breast cancer cell line was responsive for enhancing chemosensitivity by treatment of KS15.

KS15 is not effective on both the adhesion ability to fibronectin and metastatic activity of human breast cancer cell lines

Tumor cell adhesion to extracellular matrix (ECM) and basement membranes is considered to be an initial step in the invasive process for metastatic tumor cells (Saiki et al., 1990). I examined the influence of KS15 on the adhesion of human breast cancer cell lines to the substrates pre-coated with human fibronectin, which is a component of basement membranes. After treatment with different concentration of KS15, cells were

incubated with desired periods (30 min, 1 hr, 2 hr) on fibronectin coated culture plate and unattached cells were washed out. Quantification of remaining cells was performed by MTT assay. As a result, the adhesion ability of both MCF-7 and MDA-MB-231 were not significantly changed (Fig. 27).

In addition to cell adhesion ability, cell motility was a measure of metastatic potential of cancer cells. The effect of KS15 on the invasion of human breast cancer cell lines was examined using Matrigel-coated chambers. After treatment with different concentration of KS15, MCF-7 and MDA-MB-231 cells were transferred into upper chamber of transwell. After incubation for 24 hr, all of the non-invaded cells were removed the upper face of the transwell membrane with a cotton swab; the invaded cells were quantified by using MTT assay. In consistent with ability of adhesion to fibronectin, invaded cells from both MCF-7 and MDA-MB-231 were not significantly changed by treatment of KS15 (Fig 28). These findings suggested that pharmacological inhibition of CRYs is only effective for inhibition of tumor growth or enhancing chemosensitivity to other anti-cancer drugs but not effective on metastatic potentials of human breast cancer cells.

Figure 22. Anti-proliferative effect of KS15 on human breast cancer cell lines. (A) Dose-dependent repression of cell viability by treatment of KS15. Note that only MCF-7 cells were inhibited by treatment of KS15, whereas normal cells (MCF10A) and MDA-MB-231 cells were not responds to KS15. (B) Repression of cell viability by treatment of KS25, a structural analog of KS15 with weak potency. (**p<0.01 vs vehicle group) Data were presented as the mean ± S.E.M. from six independent experiments.

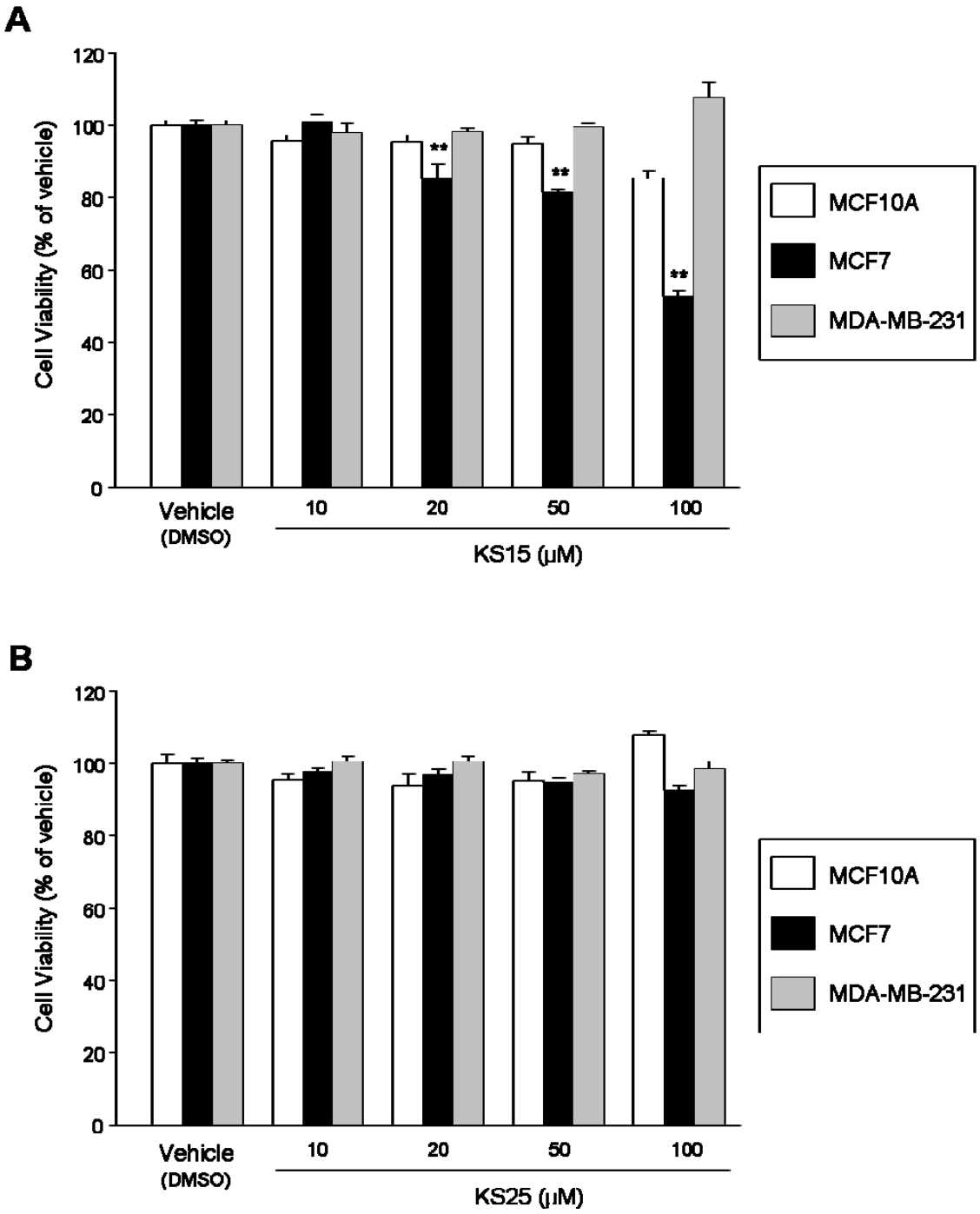
A
120
100
80
60
40
20
0
Cell Viability (% of vehicle)
**
**
**
Vehicle
(DMSO)
10
20
50
100
KS15 (μM)
MCF10A
MCF7
MDA-MB-231
B
120
100
80
60
40
20
0
Cell Viability (% of vehicle)
Vehicle
(DMSO)
10
20
50
100
KS25 (μM)
MCF10A
MCF7
MDA-MB-231

Figure 23. Co-treatment of KS15 and doxorubicin on human breast cancer cell lines. Enhancement of chemosensitivity to doxorubicin by KS15. (A) Cell viability of MCF-7 by co-treatment of doxorubicin (1.5 μM) and a various concentration of KS15. Note that survival of MCF-7 cells after treatment of doxorubicin was decreased by addition of KS15 in dose-dependent manner. (B) Cell viability of MDA-MB-231 by co-treatment of doxorubicin (1.5 μM) and a various concentration of KS15. (*$p<0.05$, **$p<0.01$ vs vehicle group) Data were presented as the mean ± S.E.M. from six independent experiments.

A

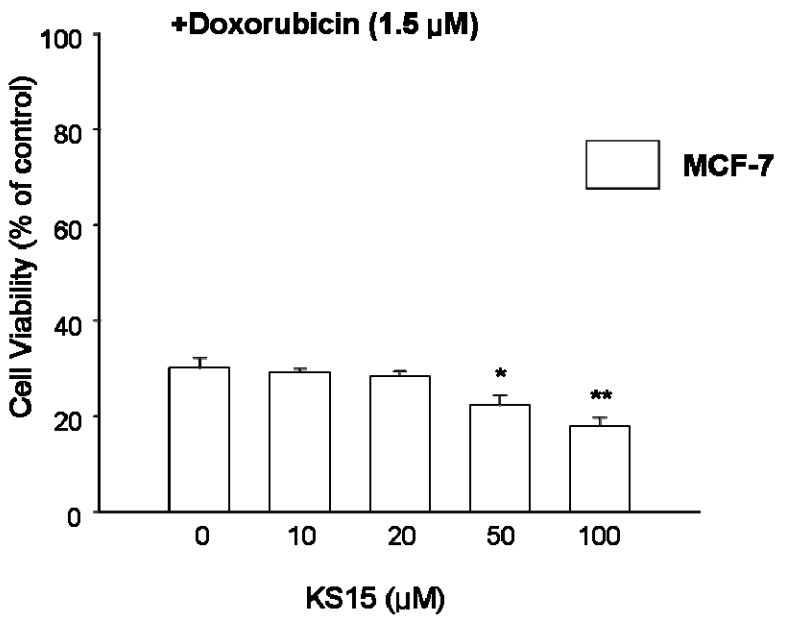
+Doxorubicin (1.5 μM)
MCF-7
Cell Viability (% of control)
100
80
60
40
20
0
*
**
0
10
20
50
100
KS15 (μM)

B

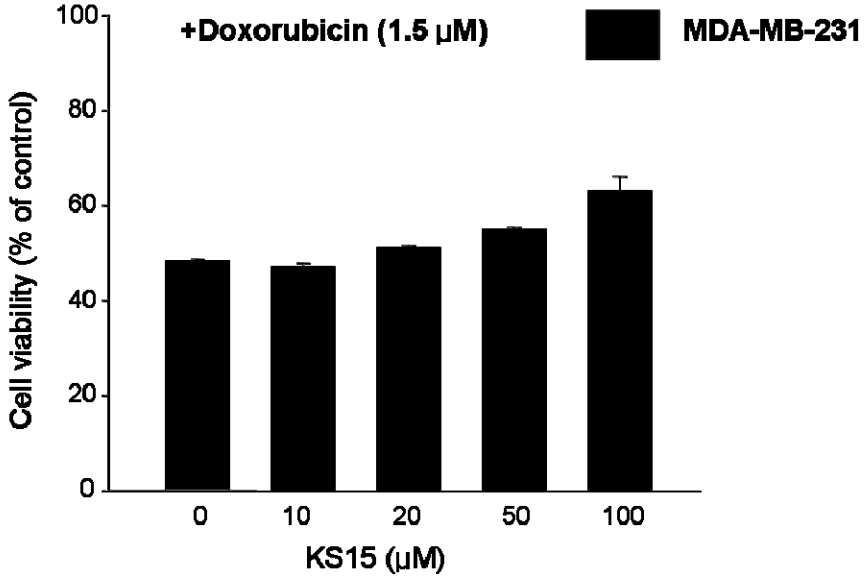
+Doxorubicin (1.5 μM)
MDA-MB-231
Cell viability (% of control)
100
80
60
40
20
0
0
10
20
50
100
KS15 (μM)

Figure 24. Co-treatment of KS15 and oxaliplatin on human breast cancer cell lines. Chemosensitivity to oxaliplatin by co-treatment with KS15. (A) Cell viability of MCF-7 by co-treatment of oxaliplatin (100 μM) and a various concentration of KS15. (B) Cell viability of MDA-MB-231 by co-treatment of oxaliplatn (100 μM) and a various concentration of KS15. Data were presented as the mean ± S.E.M. from six independent experiments.

A

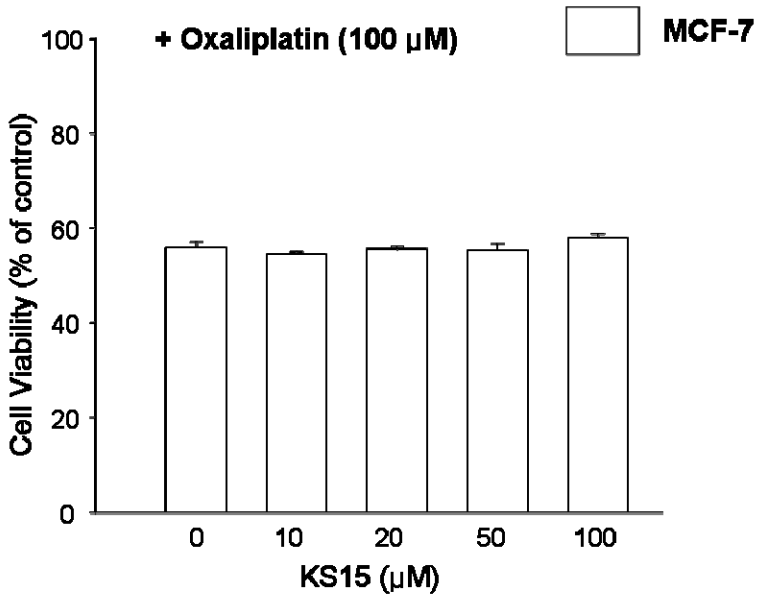
+ Oxaliplatin (100 μM)
MCF-7
Cell Viability (% of control)
100
80
60
40
20
0
0
10
20
50
100
KS15 (μM)

B

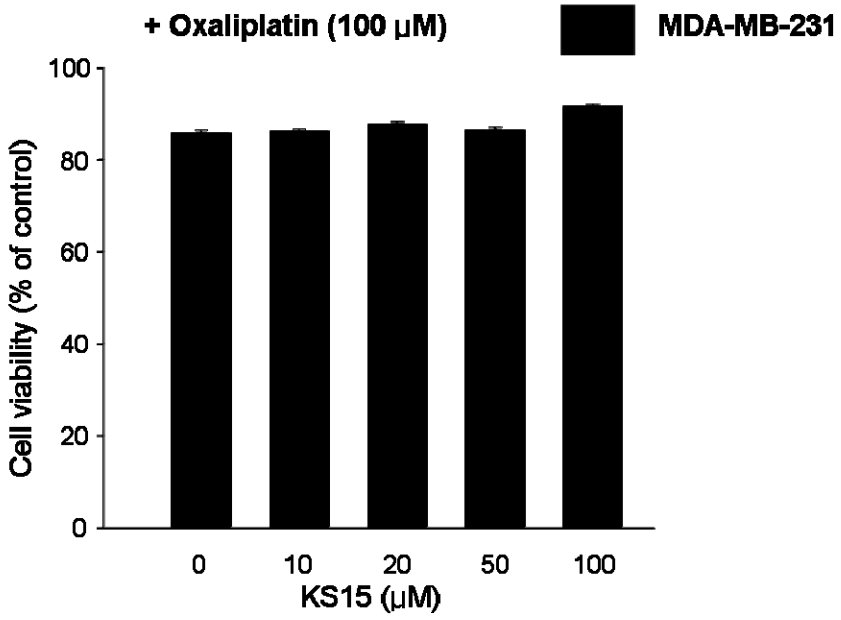
+ Oxaliplatin (100 μM)
MDA-MB-231
Cell viability (% of control)
100
80
60
40
20
0
0
10
20
50
100
KS15 (μM)

Figure 25. Co-treatment of KS15 and tamoxifen on human breast cancer cell lines. Chemosensitivity of MCF-7 cells after co-treatment of tamoxifen and a various concentration of KS15. Note that survival of MCF-7 cells after treatment of tamoxifen (10 μM) was decreased by addition of KS15 in dose-dependent manner. (*$p<0.05$, **$p<0.01$ vs vehicle group) Data were presented as the mean ± S.E.M. from six independent experiments.

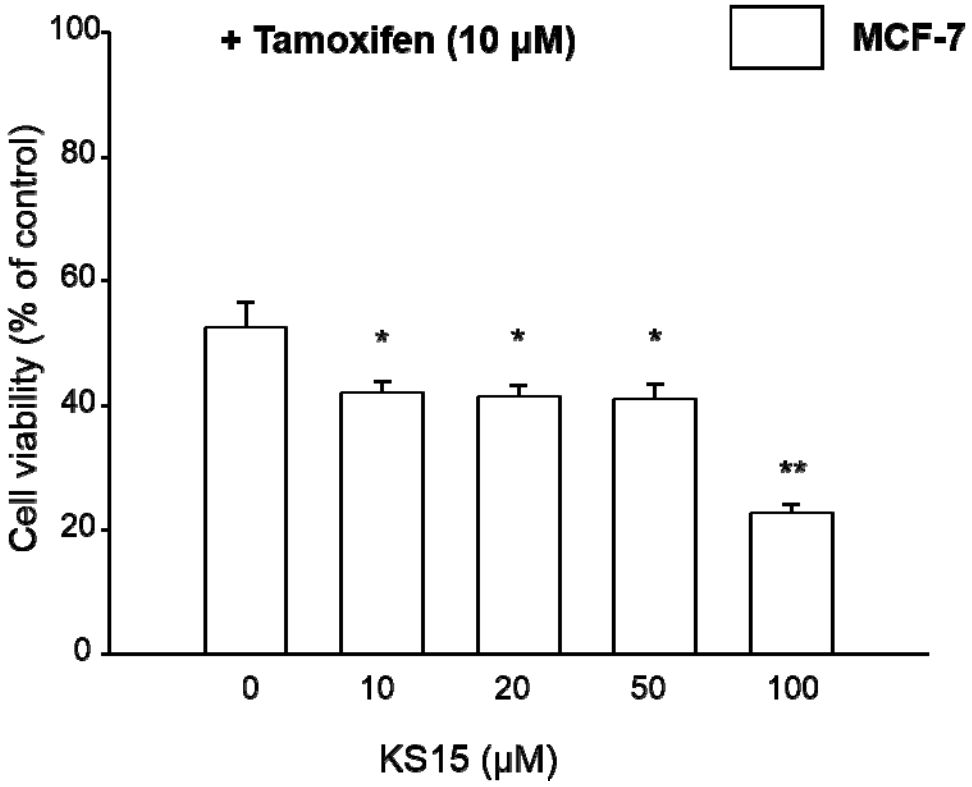
+ Tamoxifen (10 μM)
MCF-7
Cell viability (% of control)
100
80
60
40
20
0
*
*
*
**
0
10
20
50
100
KS15 (μM)

Figure 26. Changes of chemosensitivity by co-treatment of KS15 on MCF-7 cell line. Dose-response curves of anti-tumor drugs with co-treatment of KS15 on MCF-7. Note that survival of MCF-7 cells after treatment of (A) doxorubicin and (B) tamoxifen were decreased by addition of KS15 in dose-dependent manner. Data were presented as the mean ± S.E.M. from four independent experiments.

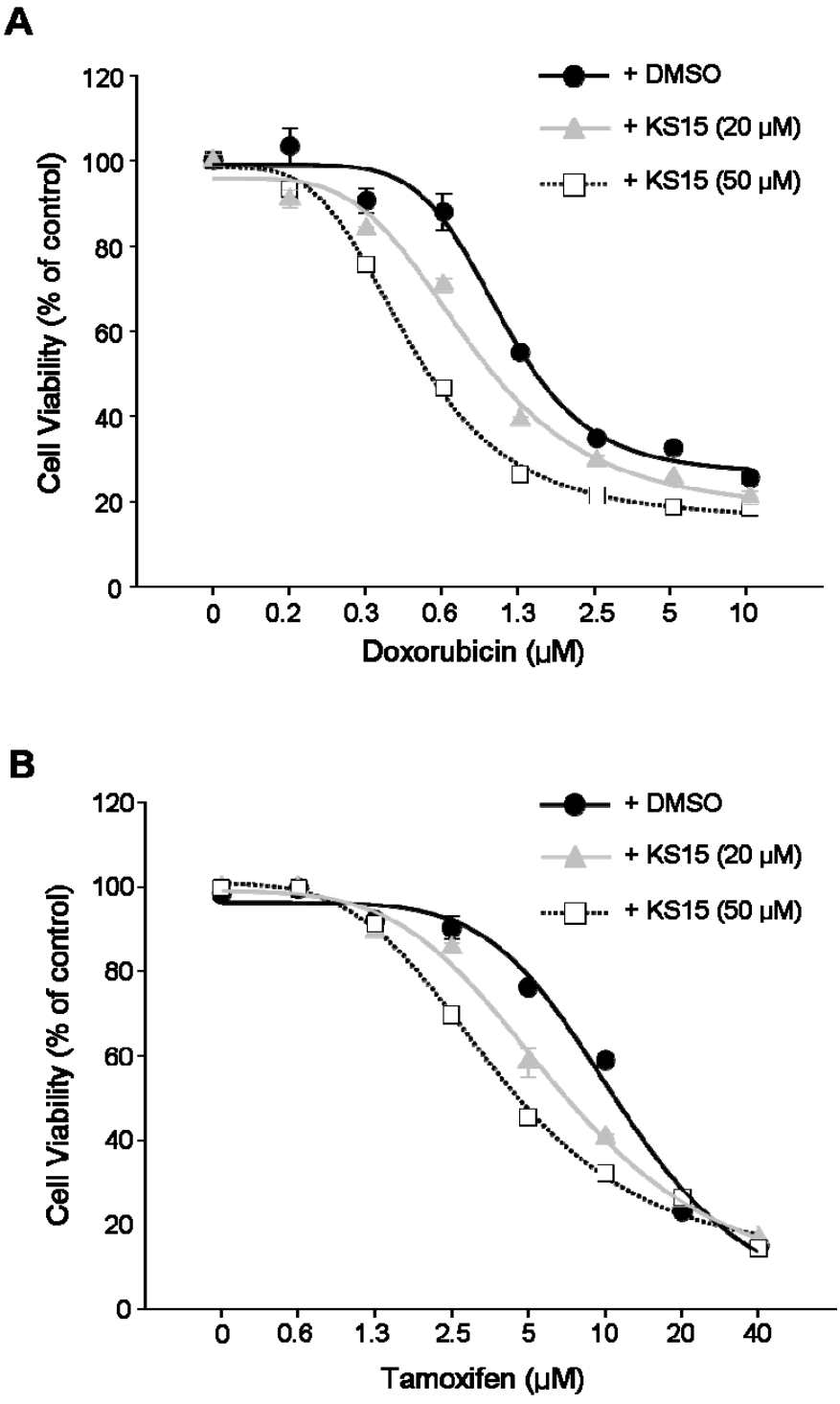
A
+ DMSO
+ KS15 (20 μM)
+ KS15 (50 μM)
Cell Viability (% of control)
120
100
80
60
40
20
0
0
0.2
0.3
0.6
1.3
2.5
5
10
Doxorubicin (μM)
B
+ DMSO
+ KS15 (20 μM)
+ KS15 (50 μM)
Cell Viability (% of control)
120
100
80
60
40
20
0
0
0.6
1.3
2.5
5
10
20
40
Tamoxifen (μM)

Table 6. Chemosensitivity of doxurubicin and tamoxifen with co-treatment of KS15 on MCF-7 cell line. Statistical analysis of efficacy changes by analysis dose-response curves of doxorubicin or tamoxifen with co-treatment of KS15 on MCF-7 cell lines. Efficacy was determined by IC_{50} values that calculated with a logistic 4-parametric equation using the mean values of cell viability.

Compound	Concentration	IC_{50} (doxorubicin)	IC_{50} (tamoxifen)
DMSO	0.2%	1.06 μM	10.83 μM
KS15	20 μM	0.75 μM	5.77 μM
	50 μM	0.46 μM	3.44 μM

Figure 27. Effect of KS15 on human breast cancer cells adhesion to fibronectin. Adhesion of MCF-7 and MDA-MB-231 caner cells to fibronectin after treatment of KS15. Adherent cells after wash out were quantified by MTT assay. Data were presented as the mean ± S.E.M. from six independent experiments.

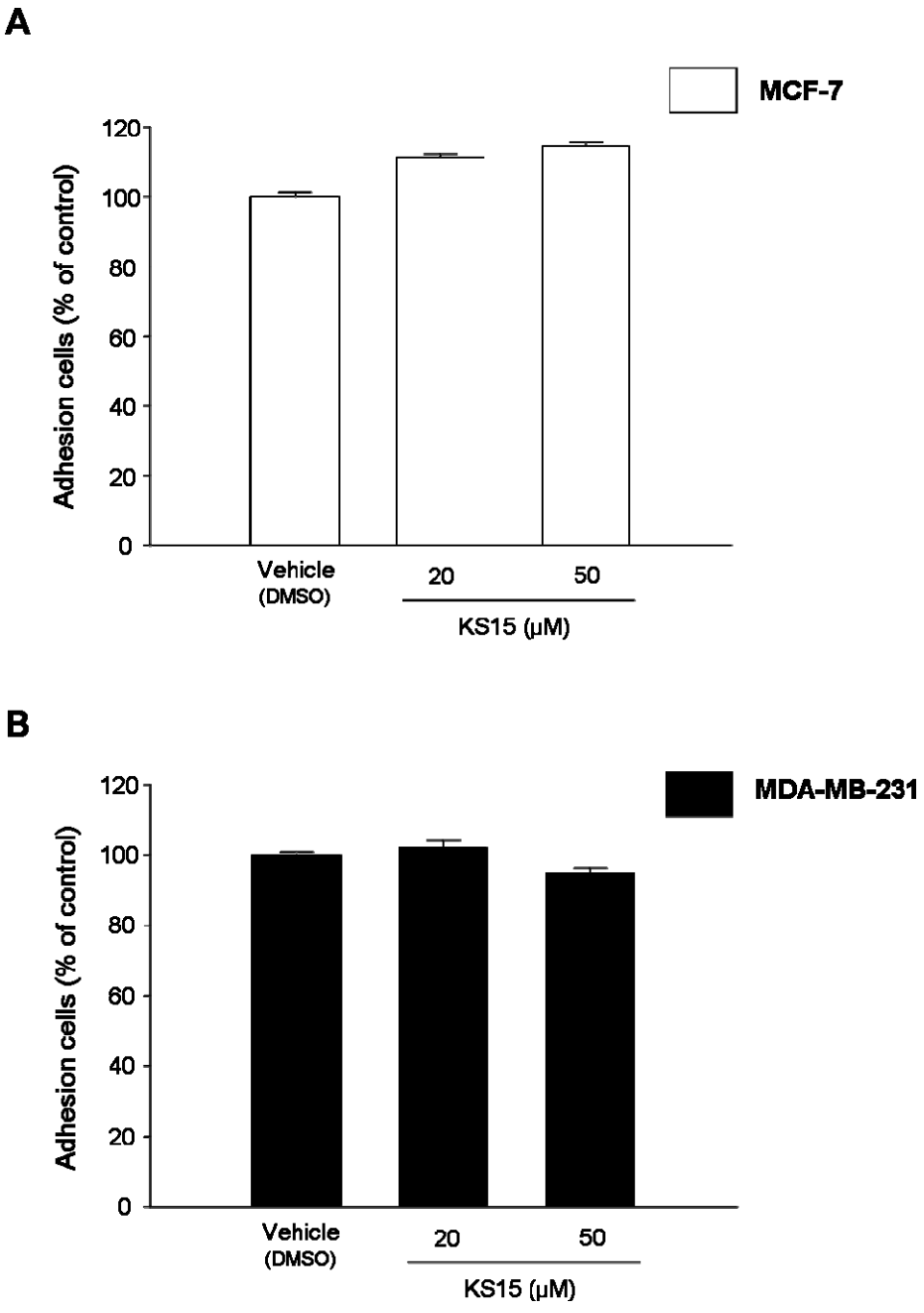
A
MCF-7
Adhesion cells (% of control)
120
100
80
60
40
20
0
Vehicle
(DMSO)
20
50
KS15 (μM)
B
MDA-MB-231
Adhesion cells (% of control)
120
100
80
60
40
20
0
Vehicle
(DMSO)
20
50
KS15 (μM)

Figure 28. Effect of KS15 on human breast cancer cells invasion *in vitro*. Invasion of MCF-7 and MDA-MB-231 caner cells on Matriegel coated transwelll chamber. (A) Photographs of the cell invasion through the polycarbonate membrane. (B) Invasion cells after wash out were quantified by MTT assay. Data were presented as the mean ± S.E.M. from three independent experiments.

A

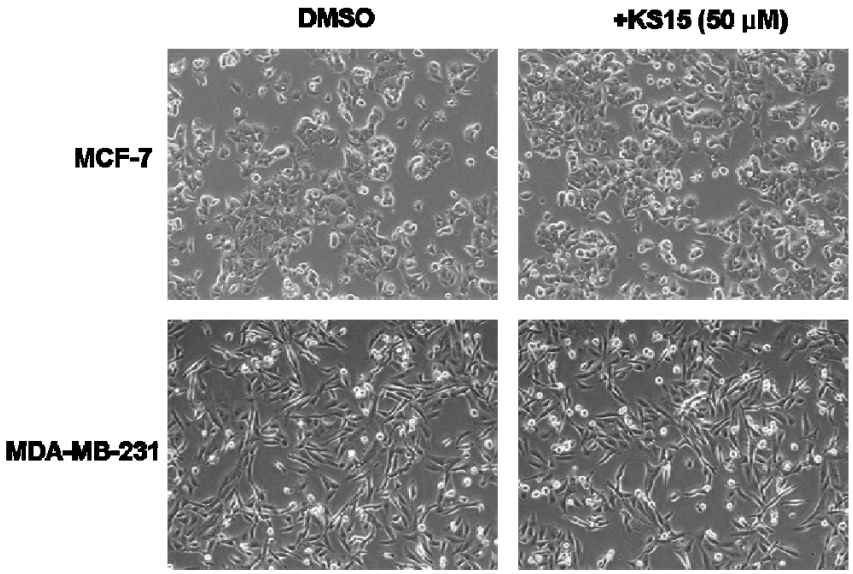
DMSO
+KS15 (50 μM)
MCF-7
MDA-MB-231

B

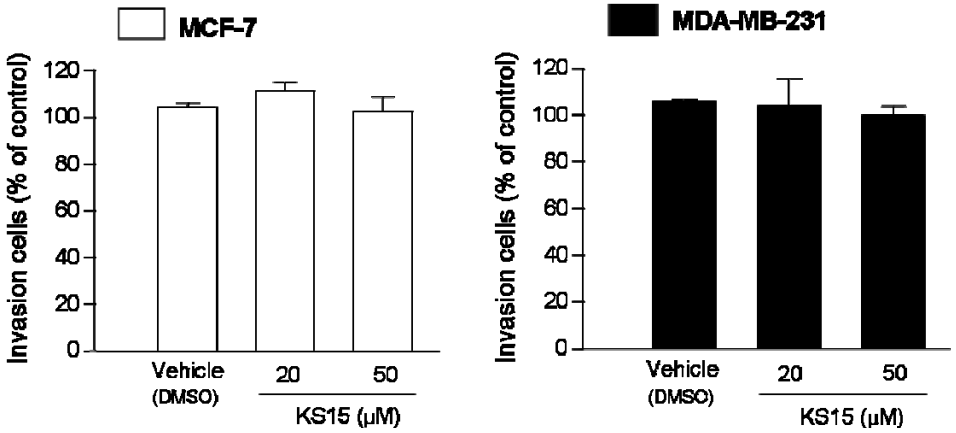
MCF-7
MDA-MB-231
Invasion cells (% of control)
120
100
80
60
40
20
0
Vehicle
(DMSO)
20
50
KS15 (μM)

DISCUSSION

The present study suggests that anti-tumor activity of pharmacological inhibition of CRY1/2 in human breast cancer cells. Development of a novel synthetic circadian clock modulator as well as application of the modulators in disease models are immerging field in last decades. Notably, recent study suggests that selenium compound (L-methyl selenocysteine) showed chemopreventive effect in Bmal1-dependent manner from the systemic toxicity induced by cyclophosphamide (Hu et al., 2011). However, despite the fact that cancer is one of the most well-known circadian rhythm related disorders, studies about administration of synthetic circadian modulator for treatment of cancer were only recently begun. In the present study, I evaluate anti-tumor activity of a novel CRY1/2 inhibitor (KS15) on human breast cancer cells and demonstrated that KS15 can inhibit proliferation and enhance chemosensitivity of ER/PR positive type of human breast cancer cell line (MCF-7).

CRY is a key negative regulator of molecular circadian clockwork as well as closely associated with various cell cycle regulators and oncogenes (Hoffman et al., 2010, Cancer Prev Res; Hoffman et al., 2010, BMC Cancer) Interestingly, CRY1/2 double knockout mice were more resistant to systemic toxicity induced by cyclophosphamide compared to wild-type mice, whereas *Clock* mutant and Bmal1 knockout mice were very sensitive to same drug (Gorbacheva et al., 2005). In contrast, tumors derived from p53 mutant mouse became more sensitive to genotoxic drugs by knockout of CRY1/2 (Lee and Sancar, 2011; Lee et al., 2013). These effects of CRY1/2

knockout might be caused by absence of circadian repression and thereby highly activated CLOCK:BMAL1 transactivation complex (Vitaterna et al., 1999; Okamura et al., 1999). For example, expression of Egr1 is induced in CRY1/2 knockout background because Egr1 is directly regulated by CLOCK:BMAL1 heterodimer activity. Highly elevated Egr1 leads to significantly enhanced DNA damage–inducible p73 transcription and thereby induced apoptosis in response to genotoxic stress (Lee et al., 2013). These studies suggested that functional inhibition of CRYs has the therapeutic potential for treatment of cancer. Although I didn't investigate detailed mechanisms of KS15's action in this study, I hypothesized that treatment of KS15 on breast cancer cell lines may induce similar situation of CRY1/2 knockout background. Further investigation will be required for verifying this hypothesis.

It is of interest to note that among the tested cell lines, only ER/PR-positive type of human breast cancer cell (MCF-7) are responsive to KS15. This specific effect of KS15 can be explained by differences in expression profiles of clock genes between ER/PR positive and negative cell lines. Recent study shows that patients with ER-negative tumors have higher levels of CLOCK gene expression than patients with ER-positive tumors (Hoffman et al., 2010, Cancer Res). If this difference is exist, additional activation of CLOCK:BMAL1 transactivation complex by inhibition of CRYs using KS15 might be less effective for ER-negative tumor cell lines. Moreover, another study suggests that mutations within CRY2 are a risk factor for the ER/PR negative type of tumor, but this association is not significant for ER/PR positive type of breast cancer. This study also shows

that CRY2 expression in breast cancer tissues is differently regulated not only between normal and tumor tissues, but also between ER/PR positive and ER/PR negative tumors (Hoffman et al., 2010, Cancer Prev Res). If the gene structure or expression profiles of CRY2 were different in ER/PR negative cancer cells in compare with ER/PR-positive cancer cells, treatment of KS15 may induce different response from the two cell lines. Taken together, KS15 shows anti-tumor activity on ER/PR-positive breast cancer cell lines selectively. This selectivity is possibly based on the different expression of clock genes, thus further optimization and investigation of detailed mechanism of KS15 can be a novel strategy for selective treatment of ER/PR positive type of breast cancer.

Unlike proliferation or chemosensitivity, administration of KS15 did not affect adhesion and metastasis of both ER/PR positive or negative type of breast cancer cells. Many studies suggest that metastatic activity of cancer is closely related with circadian rhythm, however, most of them were dependent on the action of melatonin (Wu et al., 2012; Mao et al., 2012). Melatonin has anti-tumorigenesis effect as well as inhibition of metastasis and more importantly, secretion of melatonin shows robust circadian rhythm and this patterns is severely affect by disruption of circadian rhythm such as light exposure at night (Wu et al., 2012; Hill et al., 2009; Hill et al., 1988; Mao et al., 2010). Thus, insignificant effect of KS15 on metastasis might be caused by absence of melatonin action. Further investigation of detailed mechanisms including melatonin action on metastasis can be a valuable study for application of KS15 on breast cancer.

Another important issue about the application of KS15 is the effective concentration. The effective concentrations of KS15 on breast cancer cells to inhibit the growth or to increase the chemosensitivity of genotoxic drugs are relatively higher than other chemicals. In previous findings, genetic depletion of CRY1/2 clearly enhanced the chemosensitivity of genotoxicants (Lee and Sancar, 2011; Lee et al., 2013). Although KS15 also inhibits the function of CRY1/2, there is a possibility that inhibition of KS15 on CRY1/2 is weaker than genetic knock-out of CRY1/2. Further optimization of potency and selectivity of KS15 will be needed.

In conclusion, CRY1/2 are novel therapeutic targets for treatment of breast cancer and application of KS15 may be useful for breast cancer therapy. Although these data only shows anti-tumor effect of KS15 and detailed mechanism of action was not included and should be revealed in further study.

REFERENCES

Aubert C, Janiaud P, Lecalvez J (1980) Effect of pinealectomy and melatonin on mammary tumor growth in Sprague-Dawley rats under different conditions of lighting. J Neural Transm 47:121-130.

Balsalobre A, Damiola F, Schibler U (1998) A serum shock induces circadian gene expression in mammalian tissue culture cells. Cell 93:929–937.

Baggs JE, Price TS, DiTacchio L, Panda S, Fitzgerald GA, Hogenesch JB (2009) Network Features of the Mammalian Circadian Clock. PLoS Biol 7:e52.

Bechtold DA, Gibbs JE, Loudon AS (2010) Circadian dysfunction in disease. Trends Pharmacol Sci. 31:191-198.

Boyle P, Levin B (2008) World Cancer Report 2008, pp 1-510, IARC press, Lyon.

Bunger MK, Wilsbacher LD, Moran SM, Clendenin C, Radcliffe LA, Hogenesch JB, Simon MC, Takahashi JS, Bradfield CA (2000) Mop3 is an essential component of the master circadian pacemaker in mammals. Cell 103:1009–1017.

Bugge A, Feng D, Everett LJ, Briggs ER, Mullican SE, Wang F, Jager J, Lazar MA (2012) Rev-erbα and Rev-erbβ coordinately protect the circadian clock and normal metabolic function. Genes Dev 26:657-667.

Buijs RM, van Eden CG, Goncharuk VD, Kalsbeek A (2003) The biological clock tunes the organs of the body: timing by hormones and the autonomic nervous system. J Endocrinol 177:17-26.

Busino L, Bassermann F, Maiolica A, Lee C, Nolan PM, Godinho SI, Draetta GF, Pagano M (2007) SCFFbxl3 controls the oscillation of the circadian clock by directing the degradation of cryptochrome proteins. Science 316:900-904.

Chiu JC, Ko HW, Edery I (2011) NEMO/NLK phosphorylates PERIOD to initiate a time-delay phosphorylation circuit that sets circadian clock speed. Cell 145:357-370.

Cho H, Zhao X, Hatori M, Yu RT, Barish GD, Lam MT, Chong LW, DiTacchio L, Atkins AR, Glass CK, Liddle C, Auwerx J, Downes M, Panda S, Evans RM (2012) Regulation of circadian behaviour and metabolism by REV-ERB-α and REV-ERB-β. Nature 485:123-127.

Chaves I, Yagita K, Barnhoorn S, Okamura H, van der Horst GT, Tamanini F (2006) Functional evolution of the photolyase/cryptochrome protein family importance of the C terminus of mammalian CRY1 for circadian core oscillator performance. Mol Cell Biol 26:1743–1753.

Chen Z, Yoo SH, Takahashi JS (2013) Small molecule modifiers of circadian clocks. Cell Mol Life Sci 70:2985-2998.

Czarna A, Breitkreuz H, Mahrenholz CC, Arens J, Strauss HM, Wolf E (2011) Quantitative analyses of cryptochrome-mBMAL1 interactions: mechanistic insights into the transcriptional regulation of the mammalian circadian clock. J Biol Chem 286:22414–22425.

Dallmann R, Mrosovsky N (2006) Scheduled wheel access during daytime: A method for studying conflicting zeitgebers. Physiol Behav 88:459-465.

Davis S, Mirick DK, Stevens RG (2001) Night shift work, light at night, and

risk of breast cancer. J Natl Cancer Inst 93:1557-1562.

Dunlap JC (1999) Molecular bases for circadian clocks. Cell 96:271-290.

Emens JS, Lewy AJ, Lefler BJ, Sack RL (2005) Relative coordination to unknown "weak zeitgebers" in free-running blind individuals. J Biol Rhythms 20:159-167.

Escobar C, Cailotto C, Angeles-Castellanos M, Delgado RS, Buijs RM (2009) Peripheral oscillators: the driving force for food-anticipatory activity. Eur J Neurosci 30:1665-1675.

Evans JA, Pan H, Liu AC, Welsh DK (2012) Cry1-/- circadian rhythmicity depends on SCN intercellular coupling. J Biol Rhythms 27:443-452.

Gachon F, Nagoshi E, Brown SA, Ripperger J, Schibler U (2004) The mammalian circadian timing system: from gene expression to physiology. Chromosoma 113: 103-112.

Gauger MA, Sancar A (2005) Cryptochrome, circadian cycle, cell cycle checkpoints, and cancer. Cancer Res 65:6828–6834.

Gekakis N, Staknis D, Nguyen HB, Davis FC, Wils-bacher LD, King DP, Takahashi JS, Weitz CJ (1998) Role of the CLOCK protein in the mammalian circadian mechanism. Science 280:1564–1569.

Gorbacheva VY, Kondratov RV, Zhang R, Cherukuri S, Gudkov AV, Takahashi JS, Antoch MP (2005) Circadian sensitivity to the chemotherapeutic agent cyclophosphamide depends on the functional status of the CLOCK/BMAL1 transactivation complex. Proc Natl Acad Sci U S A 102:3407-3412.

Grant D, Yin L, Collins JL, Parks DJ, Orband-Miller LA, Wisely GB, Joshi S, Lazar MA, Willson TM, Zuer-cher WJ (2010) GSK4112, a small

molecule chemical probe for the cell biology of the nuclear heme receptor Rev-erbalpha. ACS Chem Biol. 5:925–932.

Grone BP, Chang D, Bourgin P, Cao V, Fernald RD, Heller HC, Ruby NF (2011) Acute light exposure suppresses circadian rhythms in clock gene expression. J Biol Rhythms 26:78-81.

Harada Y, Sakai M, Kurabayashi N, Hirota T, Fukada Y (2005) Ser-557-phosphorylated mCRY2 is degraded upon synergistic phosphorylation by glycogen synthase kinase-3β. J Biol Chem 280:31714–31721.

Hara R, Wan K, Wakamatsu H, Aida R, Moriya T, Akiyama M, Shibata S (2001) Restricted feeding entrains liver clock without participation of the suprachiasmatic nucleus. Genes Cells 6:269-278.

Hastings MH, Reddy AB, Maywood ES (2003) A clockwork web: circadian timing in brain and periphery, in health and disease. Nat Rev Neurosci 4:649-661.

Hill SM, Blask DE (1988) Effects of the pineal hormone melatonin on the proliferation and morphological characteristics of human breast cancer cells (MCF-7) in culture. Cancer Res 48:6121–6126.

Hill SM, Frasch T, Xiang S, Yuan L, Duplessis T, Mao L (2009) Molecular mechanisms of melatonin anticancer effects. Integr Cancer Ther 8:337–346.

Hirota T, Lee JW, Lewis WG, Zhang EE, Breton G, Liu X, Garcia M, Peters EC, Etchegaray JP, Traver D, Schultz PG, Kay SA (2010) High-throughput chemical screen identifies a novel potent modulator of cellular circadian rhythms and reveals CKIα as a clock regulatory kinase. PLoS Biol 8:e1000559.

Hirota T, Lee JW, St John PC, Sawa M, Iwaisako K, Noguchi T, Pongsawakul PY, Sonntag T, Welsh DK, Brenner DA, Doyle FJ 3rd, Schultz PG, Kay SA (2012) Identification of Small Molecule Activators of Cryptochrome. Science 337:1094–1097

Hoffman AE, Yi CH, Zheng T, Stevens RG, Leaderer D, Zhang Y, Holford TR, Hansen J, Paulson J, Zhu Y (2010) CLOCK in breast tumorigenesis: genetic, epigenetic, and transcriptional profiling analyses. Cancer Res 70:1459-1468.

Hoffman AE, Zheng T, Yi CH, Stevens RG, Ba Y, Zhang Y, Leaderer D, Holford T, Hansen J, Zhu Y (2010) The core circadian gene Cryptochrome 2 influences breast cancer risk, possibly by mediating hormone signaling. Cancer Prev Res 3:539-548.

Hoffman AE, Zheng T, Ba Y, Stevens RG, Yi CH, Leaderer D, Zhu Y (2010) Phenotypic effects of the circadian gene Cryptochrome 2 on cancer-related pathways. BMC Cancer 10:110.

Hogenesch JB, Gu YZ, Jain S, Bradfield CA (1998) The basic-helix-loop-helix-PAS orphan MOP3 forms transcriptionally active complexes with circadian and hypoxia factors. Proc Natl Acad Sci U S A 95:5474–5479.

Hu Y, Spengler ML, Kuropatwinski KK, Comas-Soberats M, Jackson M, Chernov MV, Gleiberman AS, Fedtsova N, Rustum YM, Gudkov AV, Antoch MP (2011) Selenium is a modulator of circadian clock that protects mice from the toxicity of a chemotherapeutic drug via upregulation of the core clock protein, BMAL1. Oncotarget 2:1279-90.

Jin X, Shearman LP, Weaver DR, Zylka MJ, de Vries GJ, Reppert SM

(1999) A molecular mechanism regulating rhythmic output from the suprachiasmatic circadian clock. Cell 96:57-68.

Kondratova AA, Kondratov RV (2012) The circadian clock and pathology of the ageing brain. Nat Rev Neurosci 13:325–335.

Kume K, Zylka MJ, Sriram S, Shearman LP, Weaver DR, Jin X, Maywood ES, Hastings MH, Reppert SM (1999) mCRY1 and mCRY2 are essential components of the negative limb of the circadian clock feedback loop. Cell 98:193-205.

Kojetin D, Wang Y, Kamenecka TM, Burris TP (2011) Identification of SR8278, a synthetic antagonist of the nuclear heme receptor REV-ERB. ACS Chem Biol 6:131–134.

Knutsson A (2003) Health disorders of shift workers. Occup Med 53:103–108.

Lamia KA, Storch KF, Weitz CJ (2008) Physiological significance of a peripheral tissue circadian clock. Proc Natl Acad Sci U S A 105:15172–15177.

Lamia KA, Sachdeva UM, DiTacchio L, Williams EC, Alvarez JG, Egan DF, Vasquez DS, Juguilon H, Panda S, Shaw RJ, Thompson CB, Evans RM (2009) AMPK regulates the circadian clock by cryptochrome phosphorylation and degradation. Science 326:437-440.

Lamont EW, James FO, Boivin DB, Cermakian N (2007) From circadian clock gene expression to pathologies. Sleep Med 8:547–556.

Lee JH, Gaddameedhi S, Ozturk N, Ye R, Sancar A (2013) DNA damage-specific control of cell death by cryptochrome in p53-Mutant ras-transformed cells. Cancer Res 73:785–791.

Lee JH and Sancar A (2011) Circadian clock disruption improves the efficacy of chemotherapy through p73-mediated apoptosis. Proc Natl Acad Sci. U S A 108:10668–10672.

Lee JW, Hirota T, Peters EC, Garcia M, Gonzalez R, Cho CY, Wu X, Schultz PG, Kay SA (2011) A small molecule modulates circadian rhythms through phosphorylation of the period protein. Angew Chem Int Ed 123:10796–10799.

Lin C and Todo T (2005) The cryptochromes. Genome Biol 6:220.

Lipinski CA, Lombardo F, Dominy BW, Feeney PJ (2001) Experimental and computational approaches to estimate solubility and permeability in drug discovery and development settings. Adv Drug Delivery Rev 46:3–26.

Liu AC, Welsh DK, Ko CH, Tran HG, Zhang EE, Priest AA, Buhr ED, Singer O, Meeker K, Verma IM, Doyle 3rd FJ, Takahashi JS, Kay SA (2007) Intercellular coupling confers robustness against mutations in the SCN circadian clock network. Cell 129:605-616.

Matsuo T, Yamaguchi S, Mitsui S, Emi A, Shimoda F, Okamura H (2003) Control mechanism of the circadian clock for timing of cell division in vivo. Science 302:255–259.

Mao L, Dauchy RT, Blask DE, Slakey LM, Xiang S, Yuan L, Dauchy EM, Shan B, Brainard GC, Hanifin JP, Frasch T, Duplessis TT, Hill SM (2012) Circadian gating of epithelial-to-mesenchymal transition in breast cancer cells via melatonin-regulation of GSK3β. Mol Endocrinol 26:1808-1820.

Mao L, Yuan L, Slakey LM, Jones FE, Burow ME, Hill SM (2010) Inhibition of breast cancer cell invasion by melatonin is mediated through

regulation of the p38 mitogen-activated protein kinase signaling pathway. Breast Cancer Res 12:R107.

Maury E, Ramsey KM, Bass J (2010) Circadian rhythms and metabolic syndrome: from experimental genetics to human disease. Circ Res 106:447–462.

Mhatre MC, Shah PN, Juneja HS (1984) Effect of varying photoperiods on mammary morphology, DNA synthesis, and hormone profile in female rats. J Natl Cancer Inst 72:1411-1416.

Mistlberger RE, Skene DJ (2004) Social influences on mammalian circadian rhythms: animal and human studies. Biol Rev Camb Philos Soc 79:533-556.

Moore RY, Silver R (1998) Suprachiasmatic nucleus organization. Chronobiol Int 15:475–487.

Nakahata Y, Sahar S, Astarita G, Kaluzova M, and Sassone-Corsi P (2009) Circadian control of the NAD+ salvage pathway by CLOCK-SIRT1. Science 324:654–657.

Nagano M, Adachi A, Nakahama K, Nakamura T, Tamada M, Meyer-Bernstein E, Sehgal A, Shigeyoshi Y (2003) An abrupt shift in the day/night cycle causes desynchrony in the mammalian circadian center. J Neurosci 23:6141-6151.

Navara KJ, Nelson RJ (2007) The dark side of light at night: physiological, epidemiological, and ecological consequences. J Pineal Res 43:215-224.

Ohta H, Yamazaki S, McMahon DG (2005) Constant light desynchronizes mammalian clock neurons. Nat Neurosci 8:267-269.

Okamura H, Miyake S, Sumi Y, Yamaguchi S, Yasui A, Muijtjens M,

Hoeijmakers JH, van der Horst GT (1999) Photic induction of mPer1 and mPer2 in cry-deficient mice lacking a biological clock. Science 286:2531-2534

O'Neill JS, Maywood ES, Chesham JE, Takahashi JS, Hastings MH (2008) cAMP-dependent signaling as a core component of the mammalian circadian pacemaker. Science 320:949–953.

Oster H (2006) The genetic basis of circadian behavior. Genes Brain Behav 2:73–79.

Ozturk N, Lee JH, Gaddameedhi S, Sancar A (2008) Loss of cryptochrome reduces cancer risk in p53 mutant mice. Proc Natl Acad Sci U S A 106:2841-2846.

Park N, Cheon S, Son GH, Cho S, Kim K (2012) Chronic circadian disturbance by a shortened light-dark cycle increases mortality. Neurobiol Aging 33:1122 e1111–e1122.

Partch CL, Clarkson MW, Ozgür S, Lee AL, Sancar A (2005) Role of structural plasticity in signal transduction by the cryptochrome blue-light photoreceptor. Biochemistry 44:3795–3805.

Pauley SM (2004) Lighting for the human circadian clock: recent research indicates that lighting has become a public health issue. Med Hypotheses 63:588-596.

Preitner N, Damiola F, Lopez-Molina L, Zakany J, Duboule D, Albrecht U, Schibler U (2002) The orphan nuclear receptor REV-ERBalpha controls circadian transcription within the positive limb of the mammalian circadian oscillator. Cell 110:251-260.

Raghuram S, Stayrook KR, Huang P, Rogers PM, Nosie AK, McClure DB, Burris LL, Khorasanizadeh S, Burris TP, Rastinejad F (2007)

Identification of heme as the ligand for the orphan nuclear receptors REV-ERBalpha and REV-ERBbeta. Nat Struct Mol Biol 14:1207–1213.

Ramsey KM, Yoshino J, Brace CS, Abrassart D, Kobayashi Y, Marcheva B, Hong HK, Chong JL, Buhr ED, Lee C, Takahashi JS, Imai S, Bass J (2009) Circadian clock feedback cycle through NAMPT-mediated NAD+ biosynthesis. Science 324:651–654.

Reppert SM (1998) A clockwork explosion! Neuron 21:1-4.

Reppert SM, Weaver DR (2002) Coordination of circadian timing in mammals. Nature 418:935-941.

Ribeiro DC, Hampton SM, Morgan L, Deacon S, Arendt J (1998) Altered postprandial hormone and metabolic responses in a simulated shift work environment. J Endocrinol 158:305-310.

Sahar S, Sassone-Corsi P (2007) Circadian clock and breast cancer: a molecular link. Cell Cycle 6:1329-1331.

Sahar S, Sassone-Corsi P (2009) Metabolism and cancer: the circadian clock connection. Nat Rev Cancer 9:886-896.

Saiki I, Murata J, Nakajima M, Tokura S, Azuma I (1990) Inhibition by sulfated chitin derivatives of invasion through extracellular matrix and enzymatic degradation by metastatic melanoma cells. Cancer Res 50:3631-3637.

Salgado-Delgado R, Angeles-Castellanos M, Buijs MR, Escobar C (2008) Internal desynchronization in a model of nightwork by forced activity in rats. Neuroscience 154:922-931.

Salgado-Delgado R, Angeles-Castellanos M, Saderi N, Buijs RM, Escobar C (2010) Food intake during the normal activity phase prevents

obesity and circadian desynchrony in a rat model of night work. Endocrinology 151:1019-1029.

Sangoram AM, Saez L, Antoch MP, Gekakis N, Staknis D, Whiteley A, Fruechte EM, Vitaterna MH, Shimomura K, King DP, Young MW, Weitz CJ, Takahashi JS (1998) Mammalian circadian autoregulatory loop: a timeless ortholog and mPer1 interact and negatively regulate CLOCK-BMAL1-induced transcription. Neuron 21:1101-1113.

Sanada K, Harada Y, Sakai M, Todo T, Fukada Y (2004) Serine phosphorylation of mCRY1 and mCRY2 by mitogen-activated protein kinase. Genes Cells 9:697–708.

Sariego J (2010) Breast cancer in the young patient. Am Surg 76:1397-400

Schernhammer ES, Laden F, Speizer FE, Willett WC, Hunter DJ, Kawachi I, Colditz GA (2001) Rotating night shifts and risk of breast cancer in women participating in the nurses' health study. J Natl Cancer Inst 93:1563-1568.

Schibler U, Sassone-Corsi P (2002) A web of circadian pacemakers. Cell 111:919-922.

Siepka SM, Yoo SH, Park J, Song W, Kumar V, Hu Y, Lee C, Takahashi JS (2007) Circadian mutant Overtime reveals F-box protein FBXL3 regulation of cryptochrome and period gene expression. Cell 129:1011-1123.

Shuboni D, Yan L (2010) Nighttime dim light exposure alters the responses of the circadian system. Neuroscience 170:1172-1178.

Silver R, LeSauter J, Tresco PA, Lehman MN (1996) A diffusible coupling signal from the transplanted suprachiasmatic nucleus controlling

circadian locomotor rhythms. Nature 382:810–813.

Solt LA, Wang Y, Banerjee S, Hughes T, Kojetin DJ, Lundasen T, Shin Y, Liu J, Cameron MD, Noel R, Yoo SH, Takahashi JS, Butler AA, Kamenecka TM, Burris TP (2012) Regulation of circadian behaviour and metabolism by syn-thetic REV-ERB agonists. Nature 485:62–68.

Son GH, Chung S, Choe HK, Kim HD, Baik SM, Lee H, Lee HW, Choi S, Sun W, Kim H, Cho S, Lee KH, Kim K (2008) Adrenal peripheral clock controls the autonomous circadian rhythm of glucocorticoid by causing rhythmic steroid production. Proc Natl Acad Sci U S A 105:20970–20975.

Spiegel K, Weibel L, Gronfier C, Brandenberger G, Follenius M (1996) Twenty-four-hour prolactin profiles in night workers. Chronobiol Int 13:283-293.

Straif K, Baan R, Grosse Y, Secretan B, El Ghissassi F, Bouvard V, Altieri A, Benbrahim-Tallaa L, Cogliano V (2007) Carcinogenicity of shift-work, painting, and fire-fighting. Lancet Oncol 8:1065–1066.

Stephan FK (2002) The "other" circadian system: food as a Zeitgeber. J Biol Rhythms 17:284-292.

Stevens RG, Blask DE, Brainard GC, Hansen J, Lockley SW, Provencio I, Rea MS, Reinlib L (2007) Meeting report: the role of environmental lighting and circadian disruption in cancer and other diseases. Environ Health Perspect 115:1357–1362.

Suh YG, Kim NJ, Koo BW, Lee KO, Moon SH, Shin DH, Jung JW, Paek SM, Chang DJ, Li F, Kang HJ, Le TV, Chae YN, Shin CY, Kim MK, Lim JI, Ryu JS, Park HJ (2008) Design, synthesis, and biological

evaluation of novel constrained meta-substituted phenyl propanoic acids as peroxisome proliferator-activated receptor alpha and gamma dual agonists. J Med Chem 51:6318–6333.

Takahashi JS, Hong HK, Ko CH, McDearmon EL (2008) The genetics of mammalian circadian order and disorder: implications for physiology and disease. Nat rev Genet 9:764–775.

Takahata S, Sogawa K, Kobayashi A, Ema M, Mimura J, Ozaki N, Fujii-Kuriyama Y (1998) Transcriptionally active heterodimer formation of an Arnt-like PAS protein, Arnt3, with HIF-1a, HLF, and Clock. Biochem Biophys Res Commun 248:789–794.

Takahata S, Sogawa K, Kobayashi A, Ema M, Mimura J, Ozaki N, Fujii-Kuriyama Y (1998) Transcriptionally active heterodimer formation of an Arnt-like PAS protein, Arnt3, with HIF-1a, HLF, and Clock. Biochem Biophys Res Commun 248:789–794.

Todo T, Ryo H, Yamamoto K, Toh H, Inui T, Ayaki H, Nomura T, Ikenaga M (1996) Similarity among the Drosophila (6-4)photolyase, a human photolyase homolog, and the DNA photolyase-blue-light photoreceptor family. Science 272:109–112.

Ueda HR, Chen W, Adachi A, Wakamatsu H, Hayashi S, Takasugi T, Nagano M, Nakahama K, Suzuki Y, Sugano S, Iino M, Shigeyoshi Y, Hashimoto S (2002) A transcription factor response element for gene expression during circadian night. Nature 418:534-539.

Unsal-Kacmaz K, Mullen TE, Kaufmann WK, Sancar A (2005) Coupling of human circadian and cell cycles by the timeless protein. Mol Cell Biol 25:3109–3116

van der Schalie EA, Conte FE, Marz KE, Green CB (2007)

Structure/function analysis of Xenopus cryptochromes 1 and 2 reveals differential nuclear localization mechanisms and functional domains important for interaction with and repression of CLOCK-BMAL1. Mol Cell Biol 27:2120–2129

Vitaterna MH, Selby CP, Todo T, Niwa H, Thompson C, Fruechte EM, Hitomi K, Thresher RJ, Ishikawa T, Miyazaki J, Takahashi JS, Sancar A (1999) Differential regulation of mammalian period genes and circadian rhythmicity by cryptochromes 1 and 2. Proc Natl Acad Sci U S A. 96:12114-12119.

Waterhouse J, Reilly T, Atkinson G, Edwards B (2007) Jet lag: trends and coping strategies. Lancet 369:1117-1129.

Welsh DK, Logothetis DE, Meister M, Reppert SM (1995) Individual neurons dissociated from rat suprachiasmatic nucleus express independently phased circadian firing rhythms. Neuron 14:697-706.

Wu M, Zeng J, Chen Y, Zeng Z, Zhang J, Cai Y, Ye Y, Fu L, Xian L, Chen Z (2012) Experimental chronic jet lag promotes growth and lung metastasis of Lewis lung carcinoma in C57BL/6 mice. Oncol Rep 27:1417-1428

Young MW, Kay SA (2001) Time zones: a comparative genetics of circadian clocks. Nat Rev Genet 2:702–715.

Zhang EE, Liu Y, Dentin R, Pongsawakul PY, Liu AC, Hirota T, Nusinow DA, Sun X, Landais S, Kodama Y, Brenner DA, Montminy M, Kay SA (2010) Cryptochrome mediates circadian regulation of cAMP signaling and hepatic gluconeogenesis. Nat med 16:1152–1156.

Zhang EE, Liu AC, Hirota T, Miraglia LJ, Welch G, Pongsawakul PY, Liu X,

Atwood A, Huss JW 3rd, Janes J, Su AI, Hogenesch JB, Kay SA (2009) A Genome-wide RNAi Screen for Modifiers of the Circadian Clock in Human Cells. Cell 139:199–210.

국문 초록

인간을 포함한 포유동물에서 생체시계는 밤낮의 환경 변화에 적응하기 위해 약 24시간의 주기로 발현하는 생리적, 행동적 변화를 야기하는 내재적인 시간 조절 시스템이다. 이러한 생체시계는 포유동물의 생리기능과 행동을 유지시키는데 매우 중요한 역할을 수행하고 있으며, 이 시스템의 기능이 망가질 경우 암을 포함한 다양한 종류의 질병에 걸릴 위험이 증가한다. 이 때문에 최근에는 생체시계를 표적으로 하는 신규 화합물을 찾으려는 연구들이 많이 진행되고 있다. 그러나 생체시계 유전자의 주요 출력 경로인 E-box를 통한 전사 활성을 촉진시키는 화합물은 아직까지 보고된 바가 없다. 제 1장의 연구에서는 생체시계 핵심 유전자인 Cryprochromes (CRYs)를 표적으로 하여, CRYs에 결합하여 그 기능을 저해하는 신규 약물 (KS15)을 발굴하였다. 제 2장에서는 KS15의 활용성 연구의 일환으로서, 인간 유방암 세포주 모델에 KS15를 적용하여 암세포의 성장, 항암제 감수성 및 전이능력에 미치는 영향을 분석하였다.

제 1장에서는 생체시계 분자기구를 조절할 수 있는 신규 약물을 개발하기 위해 생체시계의 주요 출력 경로인 E-box 매개 전사 활성일 변화시키는 화합물을 선별할 수 있는 세포기반분석법 (cell-based assay)을 설계하고, 이 분석법을 활용하여 약 1000여개의 합성 화합물

라이브러리를 스크리닝하였다. 그 결과 신규 생체시계 조절 화합물인 KS15를 발굴하고, 해당 화합물의 표적 단백질 및 생체시계 기능의 조절 효능을 검증하는 일련의 연구들을 수행하였다. 우선 KS15의 표적 단백질을 분석하기 위해 바이오틴 (biotin) 표지를 부착한 유도체를 이용하여 pull-down assay을 수행한 결과, KS15가 생체시계 핵심 유전자인 Cryptochrome 1, 2(CRY1/2)에 특이적으로 결합하였다. 또한 CRY1/2 유전자 결핍 생쥐 섬유아세포를 이용한 검증 실험을 통해 KS15의 효능이 CRY1/2 유전자에 의존적으로 나타났다. 나아가 KS15를 Per2-Luc 혹은 Bmal1-dLuc 리포터를 발현하는 섬유아세포에 처리하였을 때, 이들의 일주기 리듬 양상을 변화시킬 수 있음을 실시간 생체발광 모니터링을 통해 분석하여 KS15가 CRY1/2의 기능을 억제하여 생체시계 활성을 조절하였다. 마지막으로 KS15를 뇌실내미세주사법 (intracerebroventricular microinjection)을 통해 살아있는 생쥐에 주사했을 때, 일주기 행동 리듬이 변화하였다. 위와 같은 결과들을 통해 신규 개발된 KS15가 생체시계 핵심 유전자인 CRY1/2의 기능을 방해하여 *in vitro* 와 *in vivo* 모델에서 생체시계 리듬을 조절할 수 있는 화합물임을 입증하였다.

여성암 중 가장 흔한 유방암은 생체시계 교란에 의해 발병 위험이 높아지는 대표적인 적응 중 하나이다. 신규 개발된 생체시계 조절

물질의 적용 가능성에 대한 연구의 일환으로써, 제 2장에서는 인간 유방암 세포주 모델을 대상으로 KS15가 유방암의 성장 및 전이성에 미치는 영향에 대한 실험을 수행하였다. 세포 활성 측정의 결과, 단독으로 처리했을 시에 KS15는 인간 유방암 세포주 모델 중 에스트로겐/프로게스테론 수용체 양성 종양의 모델 세포주인 MCF7 세포에서만 성장 억제 효과를 나타냈으며, 정상 유방 세포주 (MCF10A) 및 삼중음성 유방암 세포주 (MDA-MB-231)에서는 억제 효과를 나타내지 못했다. 또한 일반적으로 유방암 치료에 널리 쓰이는 3종의 항암제 (doxorubicin, oxaliplatin, tamoxifen)와 KS15를 동시에 처리했을 때에도 MCF7 세포주에서는 각각 doxorubicin, tamoxifen에 대한 항암제 감수성이 증가하는 효과를 보였으나 MDA-MB-231 세포주에서는 특별한 효능이 관찰되지 않았다. 이상으로 볼 때 신규 개발된 KS15는 약전이성의 에스트로겐/프로게스테론 수용체 양성 타입의 유방암에 대한 치료 효과를 기대할 수 있으며, 후속 연구를 통해 항암 치료의 효과를 증대시키는 보조제로서의 역할이 기대된다고 할 수 있다.

결론적으로 본 연구를 통해 최초의 CRY1/2에 대한 저해제인 KS15가 개발되었으며 이를 통해 생체시계 유전자의 주요 출력 경로인 E-box 매개 전사 활성이 촉진되어 생체시계 활성을 조절할 수 있음이

증명되었다. 또한 그 활용 연구의 일환으로써 인간 유방암 세포주에 대한 KS15의 항암 효과를 분석한 결과, KS15가 MCF-7 세포주에 대해서 성장 억제 효과 및 항암제 감수성 증가 효과를 가짐을 보였다. 해당 화합물의 기능과 항암 효과에 대한 후속 연구를 통해 KS15는 생체시계를 표적으로 하는 새로운 유방암 치료약으로서 개발될 가능성을 기대할 수 있다.

주요어: Cryptochrome (CRY); 생체시계; 저분자화합물; KS15; 세포기반분석법; 유방암; 항암 효능

감사의 글

졸업을 앞두고 길었던 학위 기간을 갈무리하며, 졸문(拙文) 하나 남기고자 합니다. 돌이켜 보면 이 값진 박사 학위는 앞에서 끌어주고 뒤에서 받쳐주던 고마우신 분들의 도움이 없었다면 불가능했으리라 생각합니다. 또 다른 시작인 졸업을 앞둔 이 뜻 깊은 시간에 별처럼 많은 감회와 다짐을 잠시 미뤄두고, 도움 주신 분들께 감사의 말씀 전하고자 합니다.

무엇보다 저를 제자로 받아주시고 이렇듯 박사 학위에 이르기까지 지도해주신 김경진 선생님의 은혜에 감사드립니다. 어둠 속을 항해하는 배처럼 헤매는 제자를 때로는 등대처럼 인도해 주시고 때로는 순풍처럼 신뢰와 격려로 등을 밀어주신 스승님의 은혜는 무엇으로 갚아야 좋을지 모르겠습니다. 또한 바쁘신 와중에도 저의 논문 심사를 맡아주시고 많은 조언을 해주신 정진하 교수님, 이건수 교수님, 최석우 교수님, 선웅 교수님께도 이 지면을 빌어 감사의 말씀을 드리고 싶습니다.

긴 시간 동안 또 하나의 가족처럼 지냈던 실험실 선배님, 후배님들에게도 감사를 드리고 싶습니다. 지금은 교수님으로 나가셨지만, 처음 여기 들어왔을 때부터 지금까지 변함없이 선배 연구자로서, 때로는 인생의 선배로서 물심양면으로 도와주시고 계시는 손기훈 교수님과

정수영 교수님께 감사드리며, 두 분의 복된 앞날을 기원합니다. 그리고 항상 부족한 저를 언제나 따뜻하게 돌봐주시고 지금도 크게 의지가 되어 주시는 김희대 박사님께도 감사드립니다. 비록 지금은 외국에 계시지만 최한경 박사님, 이은정 박사님도 실험실 선배로서뿐만 아니라 인간적으로도 많이 도와주신 분들이기에 감사의 인사를 드립니다. 지금은 자리를 옮겼으나 많은 도움을 주었던 은비와 성식이에게 고맙다고 전하고 싶습니다. 그리고 선배 부탁도 자기 일처럼 여기고 열심히 도와주는 정아와 도연이에게도 감사의 말을 전하며, 후배님들 모두 자기 연구에 좋은 결과 얻길 기원합니다.

마지막으로 가족들에게도 큰절 한번 하는 심정으로 감사의 마음을 남깁니다. 공부를 계속하겠다는 제 뜻을 현실이라는 이름으로 꺾는 대신, 멀리 핀란드에서 일하시면서 제가 공부를 할 수 있도록 묵묵히 지원해주신 아버지, 핀란드와 한국을 왕복하시면서 편찮으신 당신의 몸보다도 못난 자식을 더 아껴주시는 어머니, 두 분께는 제 남은 생을 모두 바쳐 그 은혜를 갚아도 모자랄 것입니다. 그리고 제겐 가장 가까운 인생의 선배이자 친구가 되어준 형님에게도 이 고마움을 전하고 싶습니다. 바쁘다는 핑계로 가족에게 좋은 것 하나 가져오지 못하고 좋은 모습도 보여주지 못한 막내지만, 이 가난한 글로나마 진심으로 감사와 사랑을 전하면서 이만 줄입니다.

이학박사 학위논문

세포기반분석법을 통한
생체시계 조절자의 개발 및 적용 연구

Development of circadian clock modulator

and its application

2014 년 2 월

서울대학교 대학원

생명과학부

전 승 국

세포기반분석법을 통한
생체시계 조절자의 개발 및 적용 연구

Development of circadian clock modulator

and its application

지도교수 김 경 진

이 논문을 이학박사 학위논문으로 제출함
2013년 12월

서울대학교 대학원
생명과학부
전 승 국

전 승 국의 이학박사 학위논문을 인준함

2013년 12월

위 원 장 정 진 하 (인)
부위원장 김 경 진 (인)
위 원 이 건 수 (인)
위 원 최 석 우 (인)
위 원 선 웅 (인)

Development of circadian clock modulator

and its application

A dissertation submitted in partial fulfillment
of the requirement for the degree of

DOCTOR OF PHILOSOPHY

to the Faculty of
School of Biological Sciences
at
Seoul National University
by
Sung Kook Chun

Date Approved

Dec, 2013

ABSTRACT

In mammals, circadian rhythms are found in almost all of biological processes. Based on the physiological and clinical importance of circadian rhythms, identification of novel drugs that can modulate circadian clock is an immerging field. However, small molecule modulators that enhance E box-mediated transcriptional activity have not been reported yet. In Chapter 1, I identified and characterized a novel small molecule KS15 that directly binds to cryptochromes (CRYs) and inhibits its repressive function. In Chapter 2, I investigated the effect of KS15 on proliferation, chemosensitivity and metastatic activity of human breast cancer cells as an application study.

1. In Chapter 1, I aimed to identify novel small molecule modulator influencing the molecular feedback loop of the circadian clock. I designed two-step cell-based screening strategy based on E-box-mediated transcriptional activity to test more than 1,000 drug-like compounds. As a result, KS15 was selected as the most promising drug candidate. I then performed pull-down assays with the biotinylated KS15 and found that both cryptochrome 1 and 2 (CRY1/2), are molecular targets of KS15. In accordance with the binding property, KS15 enhanced E-box-mediated transcription in a CRY1/2-dependent manner, and more importantly, it

attenuated the circadian oscillation of Per2-Luc and Bmal1-dLuc activities in cultured fibroblasts, indicating that KS15 can functionally inhibit the effects of CRY1/2 in the molecular circadian clockwork. Finally, intracerebral injection of KS15 *in vivo* shows delayed phase and lengthened period of circadian rhythm. The present study describes the first novel chemical inhibitor of CRY1/2 that inhibits the repressive function of CRY1/2, thereby modulates circadian clock both *in vitro* and *in vivo*.

2. In Chapter 2, based on recent studies that CRY1/2 are involved in the onset of human breast cancer, I evaluated the anti-tumor activity of KS15 on human breast cancer cells in vitro. First, I treated KS15 in various concentrations to human breast cancer cells (MCF-7 and MDA-MB-231) as well as to a normal mammary epithelial cell (MCF10A). As a result, KS15 inhibited the proliferation of MCF-7 cell line in a dose-dependent manner, but not in other cell lines. Also, sensitivities for the anti-tumor drugs were enhanced only in MCF-7 when co-treated with KS15. On the other hand, adhesion ability on extracellular matrix and metastatic activity were not significantly affected by treatment of KS15. These findings suggest that pharmacological inhibition of CRYs has an anti-proliferative effect and increasing chemosensitivity to anti-tumor drugs on a specific type of breast cancer. It appears that KS15 has the potential to be a candidate for anti-

tumor drugs or an adjuvant to treatment of breast cancer.

In conclusion, I discovered the first novel chemical inhibitor (KS15) of CRY1/2 that inhibits the repressive function of CRY1/2, thereby activating E-box-mediated transcription regulated by CLOCK:BMAL1 heterodimer. As an application study, I evaluated anti-tumor activity of KS15 on proliferation and chemosensitivity of MCF-7 cells. Further investigation on the detailed mechanism and optimization of this anti-tumor activity of KS15 in needed to develop a novel therapeutic drug for breast cancer.

Key words: Cryptochrome (CRY); Circadian rhythm; Small molecule; Cell-based screening; Chemical biology; Breast cancer; Anti-tumor activity

CONTENTS

Page

Chapter 2. Evaluation of anti-tumor activity of Cryptochrome inhibitor on human breast cancer cell lines

LIST OF FIGURES AND TABLES

Background and Purpose

Background and Purpose

1. Mammalian circadian clock

1.1. Circadian rhythm and biological clock

Most living organisms on earth, from cyanobacteria to mammals, have been exposed to day and night cycle due to the earth's rotation. Thus, most organisms have developed an internal time-keeping system, referred to as the 'biological clock' (Dunlap, 1999; Reppert, 1998), to anticipate to these cyclic environmental changes. In mammals, biological clock regulates various essential physiologies and behaviors and therefore, many biological processes display clear daily oscillation. For example, sleep-wake cycles, core body temperature, blood pressure and glucose level as well as hormone levels show robust circadian rhythm. Thus, biological clock allows the organism to prepare for the changes in the environment. Also, this innate time-keeping system provides internal time cues to ensure that a certain physiological change takes place in coordination with others (Gachon et al., 2004). In mammals, the circadian timing is regulated by a hierarchical assembly of multiple oscillators, in which the hypothalamic suprachiasmatic nucleus (SCN) serves as the central pacemaker. (Moore and Silver, 1998; Silver et al., 1996) Most peripheral organs, as well as

extra-SCN brain regions, possess their own molecular oscillators, and these are referred to as peripheral clocks. These clocks have molecular makeup that is similar to the SCN master clock (Lamia et al., 2008; Son et al 2008; Zhang et al., 2010). These oscillators have two general characteristics: First, they are self-sustained and approximately 24-hour rhythm in constant conditions; rhythmicity persists even in the absence of environmental cues such as light. Moreover, oscillation can be observed in dissociated cells from brain (Welsh et al., 1995) as well as in fibroblasts (Balsalobre et al., 1998). Second, autonomous clock can be synchronized by external signals such as light, temperature, or social cues like feeding schedules and maintain the timekeeping system of organism through phase shift and resetting of internal clock. (Reppert and Weaver, 2002; Schibler and Sassone-Corsi, 2002; Schibler et al., 2003).

1.2. Regulation of circadian clock in mammals

Regulation of circadian rhythm in mammal is hierarchical in structure with the master pacemaker located in the SCN of the anterior hypothalamus. SCN is composed by approximately 20,000 neurons and entrained to external light-dark cycle by receiving photic input through the retinohypothalamic tract (RHT). SCN produces a rhythmic output which is composed of neural and hormonal signals that influence physiology and

behavior (Schibler and Sassone-Corsi, 2002). This master pacemaker coordinates countless peripheral clocks within various tissue and cell types. In general, the molecular clock machinery of oscillators within the SCN and the periphery are very similar. The main difference between master and peripheral clocks is how they are synchronized and influenced by various signals. The SCN is entrained by light received through the retina while the peripheral oscillators are often adjusted by chemical signals or by feeding (Dallmann et al., 2012). Elimination of the SCN disrupts circadian rhythm of behavior and hormonal output such as sleep-wake cycle and corticosterone release. Furthermore, implantation of SCN to SCN-lesioned animals rescued circadian pattern in behavior (Ralph et al., 1990; Kriegsfeld et al., 2004). Desynchrony between intrinsic and environmental rhythms has been found to render shortened lifespan in mice (Davidson et al., 2006).

1.3. Molecular mechanism of circadian clock in mammals

The autonomous and self-sustainable nature of circadian timing mainly depends on the molecular circadian clockwork, which is comprised of a subset of clock genes (Fig 1). The clock gene products cooperatively control the rhythmicity of gene expression, primarily by two interlocked positive and negative transcriptional/translational feedback loops (Balsalobre et al., 1998; Bunger et al., 2000; Hogenesch et al., 1998;

Takahata et al., 1998; Gekakis et al., 1998). Circadian Locomotor Output Cycle Kaput (CLOCK) and Brain-Muscle-Arnt-Like protein 1 (BMAL1), which belong to the basic helix-loop-helix–Period-ARNT-SIM (bHLH–PAS) transcription factor superfamily, form a heterodimer to recognize E-box elements on the promoter region of downstream genes, including *Periods* (*Pers*) and *Cryptochromes* (*Crys*), and subsequently activate their transcription. PERs and CRYs proteins translocate into the nucleus and suppress CLOCK:BMAL1-mediated transcription by forming a negative complex that completes the core feedback loop (Jin et al., 1999; Kume et al., 1999; Sangoram et al., 1998). Proteins from core clock genes are not only regulated by transcriptional feedback but also by various post-translational regulations including phosphorylation and ubiquitination. For example, CRYs have been shown to be phosphorylated by AMP-activated kinase AMPK (Lamia et al., 2009) prior to ubiquitination by the F-box E3 ligase FBXL3 (Siepka et al., 2007; Busino et al., 2007). Likewise, phosphorylation by Casein kinase I primes PER proteins for ubiquitination and proteosomal degradation (Chiu et al., 2011). Also, CLOCK and BMAL1 are target of various modifications including phosphorylation, acetylation, ubiquitination (Tamaru et al., 2009; Hirayama et al., 2007; Yoshitane et al., 2009; Kwon et al., 2006). Moreover, a small ubiquitin-related modifier (SUMO)-mediated modification of BMAL1 has also been proposed as another important post-translational regulatory mechanism (Cardone et al.,

Figure 1. Mammalian molecular circadian clockwork. CLOCK and BMAL1 form heterodimer and induce the expression of negative regulators, *Period* and *Cryptochrome* genes by binding to the E-box element in their promoter. PER and CRY form a complex and translocate into the nucleus to inhibit CLOCK/BMAL1-mediated transcription. The CLOCK/BMAL1 heterodimer also induce the transcription of nuclear receptor RORα and REV-ERBα. They control Bmal1 gene expression by binding to ROR response element (RRE) in Bmal1 promoter. RORα activates transcription of *Bmal1* gene, whereas REV-ERBα inhibits *Bmal1* transcription. Also, post-translational modifications of clock genes are also important issue for regulating activity of molecular clockwork. Various kinds of modifications, such as phosphorylation (P), ubiquitination (Ub), Acetylation (A), and SUMOrylation (S) are occurred in core clock genes like CLOCK, BMAL1, PER1/2 and CRY1/2. These modifications regulate their activity and stability and theirby modulate overall activity of molecular circadian clockwork.

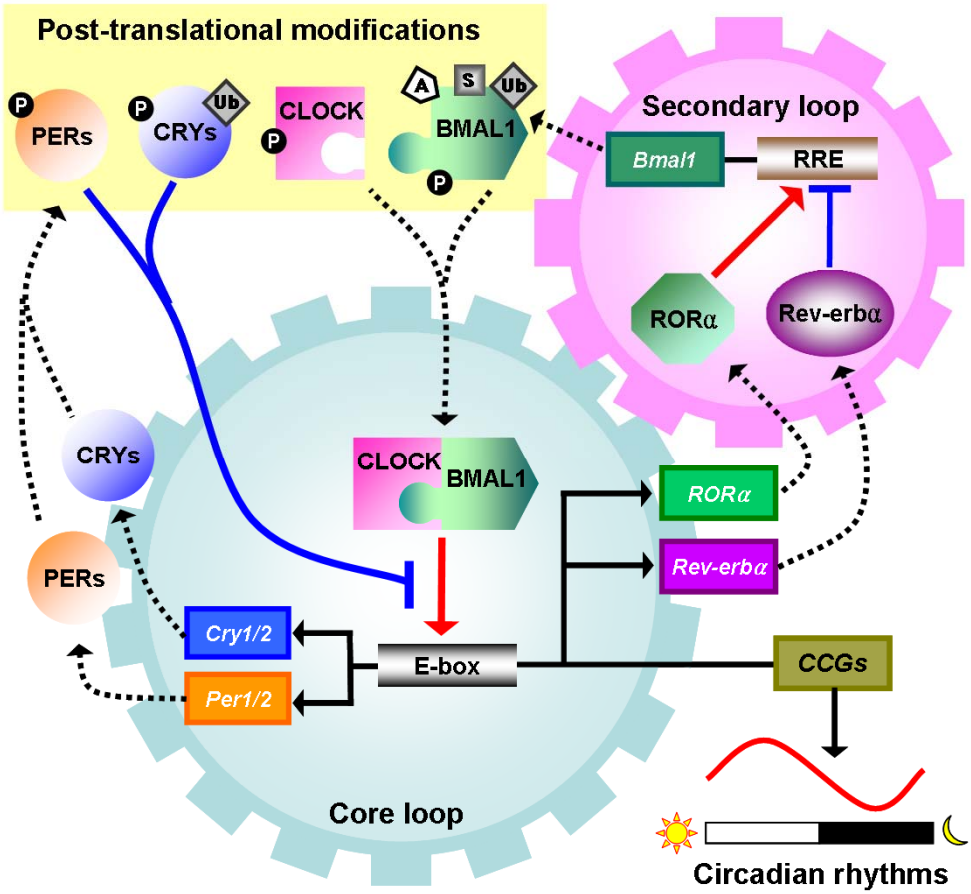
Post-translational modifications
PERs
CRYs
Ub
CLOCK
BMAL1
A
S
Ub
Secondary loop
Bmal1
RRE
RORα
Rev-erbα
CRYs
CLOCK
BMAL1
RORα
Rev-erbα
PERs
Cry1/2
Per1/2
E-box
CCGs
Core loop
Circadian rhythms

2005; Lee et al., 2008). On the other hand, a secondary loop composed of nuclear receptors, including RAR-related Orphan Receptors (RORs) and REV-ERBs, stabilizes the normal cycling of the core clock loop**.** REV-ERBα/β proteins are transcriptional repressors that compete with the RORs in such a manner as to regulate periodic *Bmal1* gene transcription. The RORs and REV-ERBs are also activated by CLOCK:BMAL1-mediated transcription, and this links the secondary loop with the core loop of the circadian molecular clock. (Ueda et al., 2002; Preitner et al., 2002; Bugge et al., 2012; Cho et al., 2012) Taken together, this self-sustained, cell autonomous circadian oscillator is maintained in nearly all mammalian cells and drives physiological alterations by controlling genes that are responsive to components of the molecular circadian clockwork.

2. Disturbance of circadian rhythm and its related disorder

2.1. Disruption of circadian rhythm and its related disorders

Disruption of normal circadian cycling has long been believed to be intimately linked to the onset of various human diseases, including metabolic and mood disorders, cardiovascular diseases, and cancer

(Takahashi et al., 2008; Kondratova and Kondratov, 2012; Maury et al., 2010; Park et al., 2012). People in modern lifestyle especially in highly industrialized society can be easily exposed to these disturbing stimuli for circadian clock system including artificial lights, night feeding, or social activity such as shift work. These are common causes of disturbances in the circadian clock system.

Exposure to light, especially at night, is the most powerful and well-known stimulus for disruption of circadian rhythm. Studies with animal models are providing the consequence of light exposure at night and indicate deleterious effects on behavior and physiology such as accelerated aging, tumorigenesis, propensity to obesity and anxiety-like and depressive-like behaviors (Grone et al., 2011; Shuboni and Yan, 2010; Ohta et al., 2005). Disturbance of circadian rhythms by exposure to various intensities of artificial light also has negative physiological effect in humans (Navara and Nelson, 2007). All this together conforms that the disruption of circadian rhythms consequent to an overexposure to the artificial light may lead to behavioral and physiological dysfunction.

Besides photic signals, there are also non-photic entraining stimuli influencing the biological clock as zeitgebers, such as those given by feeding schedules and physical activity (Dallmann and Mrosovsky, 2006;

Stephan, 2002). Such stimuli can also give temporal signals to the SCN, although they are weak as compared with light inputs (Emens et al., 2005). Although they do not override the light/dark cycle for the adjustment of the SCN, non-photic stimuli, especially food, contribute as potent synchronizers of cells and organs in the periphery, driving them out of phase from the signals transmitted by the SCN, thus resulting in internal desynchrony (Escobar et al., 2009; Hara et al., 2001; Mistlberger and Skene, 2004).

In humans, social activity also acts as important zeitgeber influencing the biological clock. The development of modern technology has promoted a relative independency of social and work activities from the environmental light/dark cycle. Some examples of modern-life habits that alter our biological rhythms are given by the long flights across the continents (jet-lag), shift work, night work, and so forth (Waterhouse et al*.,* 2007; Spiegel et al*.,* 1996; Davis et al., 2001). Animal models simulating similar conditions as night work have confirmed the deleterious effects of activity during the resting hours and circadian desynchrony (Ribeiro et al., 1998; Salgado-Delgado et al*.,* 2008; Salgado-Delgado et al., 2010; Nagano et al., 2003). Even more, the proportion of individuals that stay awake for long intervals in the night, engaged in leisure activities, has importantly increased and has become an important health problem (Pauley, 2004). Exposure to

nontraditional work schedules has been linked with increased risks of colorectal (Schernhammer et al., 2003), breast (Schernhammer et al., 2006), lymphatic (Lahti et al., 2008), and prostate (Kubo et al., 2006) cancers, as well as with obesity (Karlsson et al., 2001), diabetes (Morikawa et al., 2005), stroke (Karlsson et al., 2005), coronary heart disease, atherosclerosis, and heart attack (Tenkanen et al., 1998; Haupt et al., 2008). Individuals reporting poor or disturbed sleep, including shift workers, show increased incidences of diabetes and risk factors for the development of cardiovascular disease (Spiegel et al., 2009). Although the detailed mechanisms for these correlations between shift work exposure and disease are largely unknown, these evidences suggested that disruption of endogenous circadian clock by unnatural activity rhythm is clinically important risk factors.

2.2. Role of circadian clock genes in cancer

Disruption of circadian rhythms is associated with various forms of cancer in humans. Epidemiological studies have revealed that human night-shift workers show an increased risk of breast, colon, lung, endometrial and prostate cancer, hepatocellular carcinoma and non-

Hodgkin's lymphoma (Hansen, 2001; Davis et al., 2001). Loss of circadian rhythm is also associated with accelerated tumor growth in both rodents and human cancer patients (Flipski et al., 2002; Sephton et al., 2000). These findings raise a question of how circadian dysfunction increases the risk of cancers.

There is increasing evidence that links dysfunction of the clockwork with the pathogenesis of cancer. Both positive and negative loops of the molecular clock are involved in cell cycle control. For example, BMAL1 suppresses proto-oncogene c-myc but stimulates the tumor suppressor Wee1 (Fu et al., 2002; Fu et al., 2005). CRY2 indirectly regulates the intra S-check point (Unsal-Kacmaz et al., 2007 ; Unsal-Kacmaz et al., 2005), and PER1 directly interacts with ATM in response to γ-radiation in vitro (Gery et al., 2006). In mice, mutation in Per2 leads to deregulation of DNA-damage response and increased neoplastic growth (Fu et al., 2002; Fu et al., 2005). In humans, deregulation or polymorphism of Per1, Per2, Cry2, Npas2 and Clock is associated with acute myelogenous leukemia, hepatocellular carcinoma, breast, lung, endometrial and pancreatic cancers, and non-Hodgkin's lymphoma (Echave and Nash, 1970; Hoffman et al., 2009; Marino et al., 2008; Zhu et al., 2007; Gery et al., 2005; Chen et al., 2005; Gery et al., 2007; Shih et al., 2006; Pogue-Geile et al., 2006). There

is increasing evidence that links dysfunction of the clockwork with the pathogenesis of cancer. For example, decreased expression levels of Per1 and Per2 genes are observed in sporadic and familiar breast cancers when compared with normal breast tissues. The Per1 gene shows lower expression levels in familiar forms of breast cancer when compared with sporadic forms, suggesting that a potential deregulation of the circadian clock may contribute to the inherited form of the diseases.

3. Pharmacological modulation of circadian rhythm

3.1. Choronopharmacology and circadian rhythm

Recent advances in understanding the molecular control of circadian rhythms and subsequent signaling pathways have allowed for new therapeutic targets to be identified as well as for a better understanding of how to more efficaciously utilize current drugs. In addition to playing a key role in normal physiology and behavior, aberrations in the circadian rhythm are associated with the pathophysiology of diseases including diabetes, cardiovascular disease, psychological disorders and various autoimmune diseases/inflammation (Rybak et al., 2007; Solt et al., 2012), the potency

and efficacy of many drugs is associated with the circadian rhythmicity of expression of their molecular targets and cellular biochemical signals (Ohdo, 2010). A significant fraction of genes are expressed in a circadian fashion (Yan et al., 2008) including many drug targets and drug metabolizing enzymes yielding potential differences in efficacy/side effects based on time of day administration. Applying the knowledge of circadian function and regulation to the relevance of disease has enabled a chronotherapy approach in the timing of administration of conventional drugs in order to synchronize the rhythms in disease activity with the efficacy of the drug. Furthermore, recent advances in targeting the protein components involved in maintenance of the core circadian rhythm have allowed us to examine pharmacological alteration of the core rhythm to examine potential utility for treatment of disease.

3.2. Discovery of small molecule modifiers of circadian clock

Whereas classical genetics produces inherited changes in the sequence and/or abundance of the target protein, most synthetic small molecule modifiers allosterically alter the protein in a reversible, time-controlled and dose-dependent manner. Small molecules may also bind to a particular

domain and consequently modulate the cognate function of a multi-domain protein, leaving the other parts of the protein and associated functions intact. If the binding surface is conserved among multiple paralogous proteins, small molecules can concurrently regulate their activities to circumvent functional redundancy commonly observed in classical genetic studies. Thus, the small molecule-based chemical genetic approach is a powerful tool to perturb the system of interest (Hirota and Kay, 2009; Lehar et al., 2008). Two complementary methods have been utilized to identify small molecule modifiers of the clock. The first approach, based on phenotypic functional assays, interrogates broad chemical space via screening of diverse chemical libraries. In published studies, the reporter assays involved stable cell lines expressing either luciferase alone from an exogenous Bmal1 promoter (Hirota et al., 2012; Lee et al., 2011; Hirota et al., 2010) or PER2::luciferase fusion proteins from the endogenous Per2 promoter (Chen et al., 2012) corresponding to mRNA or protein rhythm, respectively. Bioluminescence is monitored over several days in the so-called kinetic, as opposed to end-point, assay to visualize circadian reporter rhythms. Changes in key clock parameters, including period, phase, and amplitude, can then be measured to identify small molecule modifiers. In these screens, small molecule modifiers may act on an intracellular target

in the upstream input pathway, the core oscillator, or any output pathways with feedback regulatory functions, such as metabolism. Furthermore, novel screening assays targeting additional clock regulatory pathways will likely lead to an enriched repertoire of clock modifiers.

Small molecule modifiers can also be identified based on direct interaction with particular clock proteins or regulatory factors. For example, IC261 and CKI-7 have been shown to lengthen the clock period as expected from their known CKI inhibitory activities (Eide et al., 2005; Vanselow et al., 2006). On the other hand, to generate novel and/or improved ligands for a particular target, it is often necessary to conduct deliberate chemical derivatization of small molecule analogs based on prior knowledge of known ligands and/or binding cavity structures (Vougogiannopoulou et al., 2008). An interesting example is the development of a selective inhibitor of casein kinase Iε, PF-4800567 which confers 20-fold selective inhibition over CKIδ (Walton et al., 2009; Badura et al., 2007; Meng et al., 2010). More recently, this approach has been successfully applied to the nuclear hormone receptors REV-ERBs and RORs, which constitute the stabilization loop of the core oscillator (Solt et al., 2011). Whereas the endogenous ligands are known for these proteins (heme and cholesterols respectively) (Raghuram et al., 2007 ; Yin et al.,

2007 ; Kallen et al., 2004), small molecule ligands are highly desirable to circumvent intracellular complications that altering metabolites commonly incurs, including nonspecific actions, cytotoxicity and redox imbalance (Grant et al., 2010). Starting with privileged scaffolds known to target ligand binding domains of nuclear hormone receptors, investigators were able to identify tertiary amines with three lipophilic substituents as agonists of REV-ERBa (Meng et al., 2008; Gibbs et al., 2012; Solt et al., 2012). Novel RORa/c ligands, most of them sulfonamide derivatives, have also been shown to modulate hepatic metabolism (Wang et al., 2010; Kumar et al., 2011) or to attenuate expression of downstream cytokines and alleviate autoimmune disease symptoms (Kumar et al., 2010; Solt et al., 2011). However, the role of the clock in these settings is currently unknown. In an attempt to correlate bona fide clock effects of small molecules with physiological consequences, I describe below known small molecule clock modifiers based on their activities in modifying the three major clock characteristics, namely period, phase, and amplitude. The classification is based on their primary, most pronounced phenotype since many small molecules are able to co-regulate more than one clock parameter.

4. Purpose

As described above, the circadian clock is a biological process that has physiological and clinical importance. However, the development of small molecule modulators that directly target the core clock machinery of molecular circadian clock has only been recently initiated. In the present study, I aimed to identify novel small molecule modulators influencing the molecular feedback loop of the circadian clock and to discover its clinical implication.

Chapter 1 is designed to identify and characterize a novel circadian clock modulator (KS15) that directly targets Cryptochromes (CRYs) in the molecular circadian clockwork.

Chapter 2 is focused on a potential clinical application of the newly developed circadian modulator. Recent studies suggest that epidemiology of human breast cancer is closely related to disturbance of circadian rhythm. Based on these studies, I hypothesized whether KS15 would affect to regulate induction and progression of human breast cancer. To prove this, I treated KS15 on human breast cancer cell lines and investigated the anti-tumor effect of KS15.

CHAPTER 1

Identification and characterization of a novel small compound modulator that can affect molecular circadian clock, Cryptochrome 1/2

ABSTRACT

Circadian rhythms, biological oscillations with a period of about 24 hours, are maintained by a genetically determined innate time-keeping system called the molecular circadian clockwork. Despite the physiological and clinical importance of the circadian clock, the development of small molecule modulators that directly target the core clock machinery has only been recently initiated. In the present study, I aimed to identify novel small molecule modulators influencing the molecular feedback loop of the circadian clock. I designed two-step cell-based screening strategy based on E-box-mediated transcriptional activity to test more than 1,000 drug-like compounds. As a result, a derivative of 2-ethoxypropanoic acid designated as KS15 was selected as the most promising candidate in terms of both efficacy and potency. I then performed pull-down assays with the biotinylated KS15 and found that both cryptochrome 1 and 2 (CRY1/2), key negative components of the mammalian circadian clock are molecular targets of KS15. In accordance with the binding property, KS15 enhanced E-box-mediated transcription in a CRY1/2-dependent manner, and more importantly, it attenuated the circadian oscillation of Per2-Luc and Bmal1-dLuc activities in cultured fibroblasts, indicating that KS15 can functionally inhibit the activities of CRY1/2 in the molecular circadian clockwork. In addition, intracerebral injection of KS15 *in vivo* caused delay of phase and lengthened period of activity rhythm. In conclusion, the present study describes the first novel chemical inhibitor of CRY1/2 that inhibits the repressive function of CRY1/2, thereby activating CLOCK-BMAL1-evoked E-box-mediated transcription. Further optimizations and subsequent

functional studies about this compound may lead to development of efficient therapeutic strategies for a variety of physiological and metabolic disorders with circadian natures.

Keywords: Cryptochrome; Circadian rhythm; Small molecule; Cell-based screening; Chemical biology

INTRODUCTION

Circadian rhythms with an approximate 24-hour period are found in most biological processes, such as core body temperature, hormone levels, and metabolism, as well as the sleep-wake and activity cycles. To anticipate cyclic environmental changes and coordinate both physiology and behavior so they occur at the appropriate time of day, most organisms from cyanobacteria to mammals have developed an internal time-keeping system referred to as the circadian clock. The mammalian system of circadian timing is organized in a hierarchy of multiple oscillators, in which the hypothalamic suprachiasmatic nucleus (SCN) serves as the central pacemaker (Moore and Silver, 1998; Silver et al., 1996). Most peripheral organs, as well as extra-SCN brain regions, possess their own molecular oscillators, and these are referred to as peripheral clocks. These clocks have molecular makeup that is similar to the SCN master clock (Lamia et al., 2008; Son et al., 2008; Zhang et al., 2010).

Disruption of normal circadian cycling has long been believed to be intimately linked to the onset of various human diseases, including metabolic and mood disorders, cardiovascular diseases, and cancer. Inappropriate light exposure, nighttime food intake, and misalignment of internal and external cycles, such as due to jet lag and shift work, are common causes of disturbances in the circadian clock system (Takahashi et al., 2008; Kondratova and Kondratov, 2012; Maury et al., 2010; Park et al., 2012).

The autonomous and self-sustainable nature of circadian timing mainly depends on the molecular circadian clockwork, which is comprised of a subset of clock genes. The clock gene products cooperatively control the rhythmicity of gene expression, primarily by two interlocked positive and negative transcriptional/translational feedback loops (Balsalobre et al., 1998; Bunger et al., 2000; Hogenesch et al., 1998; Takahata et al., 1998; Gekakis et al., 1998). Circadian Locomotor Output Cycle Kaput (CLOCK) and Brain-Muscle-Arnt-Like protein 1 (BMAL1), which belong to the basic helix-loop-helix–Period-ARNT-SIM (bHLH–PAS) transcription factor superfamily, form a heterodimer to recognize E-box elements on the promoter region of downstream genes, including *Periods* (*Pers*) and *Cryptochromes* (*Crys*), and subsequently activate their transcription. PERs and CRYs proteins translocate into the nucleus and suppress CLOCK:BMAL1-mediated transcription by forming a negative complex that completes the core feedback loop (Jin et al., 1999; Kume et al., 1999; Sangoram et al., 1998). In addition, a secondary loop composed of nuclear receptors, including RAR-related Orphan Receptors (RORs) and REV-ERBs, stabilizes the normal cycling of the core clock loop**.** REV-ERBα/β proteins are transcriptional repressors that compete with the RORs in such a manner as to regulate periodic *Bmal1* gene transcription. The RORs and REV-ERBs are also activated by CLOCK:BMAL1-mediated transcription, and this links the secondary loop with the core loop of the circadian molecular clock (Ueda et al., 2002; Preitner et al., 2002; Bugge et al., 2012; Cho et al., 2012).

Both synthetic compounds and endogenous small molecules have recently been identified as circadian clock modulators. Heme (Raghuram et al., 2007), cAMP (O'Neill et al., 2008) , and NAD (Nakahata et al., 2009; Ramsey et al., 2009) have been shown to affect the periodicity of molecular circadian clock. Synthetic REV-ERBα modulators, including GSK4112 (Grant et al., 2010), SR8278 (Kojetin et al., 2011), SR9009, and SR9011 (Solt et al., 2012), as well as casein kinase I inhibitors such as longdaysin (Hirota et al., 2010) and LH846 (Lee et al., 2011), were recently identified as promising molecular clock modulators. However, despite the physiological and clinical importance of circadian rhythms, small molecule modulators that enhance E box-mediated transcriptional activity have not been reported yet. Notably, the very recently developed compound KL001 is the only one that was reported as a small molecule directly targeting the core clock machinery, but it represses core loop activity by strengthening the negative functions of CRY1/2 (Hirota et al., 2012). In the present study, I identified and characterized a novel small molecule that directly binds to CRY1/2 and inhibits its repressive function, thereby activating E-box-mediated transcriptional activity. This small molecule has a distinct scaffold containing 2-ethoxypropanoic acid and two aryl rings connected by an oxime ether linker, compared with KL001, which has a carbazole scaffold (Hirota et al., 2012).

MATERIALS AND METHODS

Stable transfection Twenty-four hours before transfection, NIH3T3 and Y1 cells (1×10^6 cells per dish) were seeded in 35-mm culture dishes. Cells were co-transfected with luciferase reporter constructs (E-box-Luc or Per2-Luc for NIH3T3 and StARp-Luc for Y1) using Lipofectamine-PLUS reagent (Invitrogen) and a neomycin resistant plasmid (pcDNA3.1) at a molar ratio of 3:1. Two days after transfection, G-418 was added at a final concentration of 1 mg/mL. During 3-weeks of selection, the concentration of G-418 gradually reduced to 250 μg/mL. When resistant colonies became visible, stable transfection was verified by measuring bioluminescence with Cellgraph (ATTO, Tokyo, Japan). Colonies with sufficient luciferase activities were then trypsinized and clonally propagated. Cells were maintained in the culture medium containing G-418 at a final concentration of 100 μg/mL and luciferase activities were measured at every passage.

Luciferase Reporter Assay Stably transfected cells were plated in 48-well plates 12 hours before treatment. After 24 hour of treatment, cells were harvested and lysed with Passive Lysis Buffer (Promega, Madison, WI). Luciferase activities were examined with a commercial reporter assay reagent (Promega) according to the manufacturer's instructions and normalized by protein content, which were measured using Bradford protein assay reagent (Bio-Rad, Hercules, CA). At 24 hours before transfection, MEFs were seeded in 24-well culture plates at 1×10^5 cells/well. Cells were then transiently co-transfected with E-box-Luc (250

ng/well) and a control plasmid (promoterless renilla luciferase expression plasmid, 750 ng/well) using Metafectene easy reagent (Biontex, Martinsried, Germany). Twenty-four hours after transfection, cells were synchronized by a brief treatment with 100 nM dexamethasone (DEX) for 2 hours and then further cultivated for 12 hours. Thereafter, the indicated chemicals were treated for 24 hours and subsequently subjected to luciferase assays with Dual Luciferase Reporter reagent (Promega). E-box-driven firefly luciferase activities were normalized by renilla luciferase levels.

Synthesis Biotin-Conjugated KS15 To a solution of KS15 (62.7 mg, 0.149 mmol) and *N*-(5-aminopentyl)biotinamide trifluoroacetate salt (20.3 mg, 0.0520 mmol) in DMF (2 mL) were added 1-ethyl-3-(3-dimethylaminopropyl)carbodiimide (57.1 mg, 0.298 mmol), triethylamine (0.04 mL, 0.298 mmol) and 1-hydroxybenzotriazole (40.3 mg, 0.298 mmol), and the reaction mixture was stirred at 50 ˚C for 8 h. Then the reaction mixture was cooled to ambient temperature, and the solvent was evaporated *in vacuo*. The residue was diluted with EtOAc, washed with H_2O and brine, dried over $MgSO_4$, filtered, and concentrated *in vacuo*. The resulting residue was purified by flash column chromatography on silica gel (MeOH:CH_2Cl_2 = 1:10) to obtain the biotin-conjugated KS15 (8.2 mg, 23%) as a white solid. FT-IR (thin film, neat) ν_{max} 3297, 3082, 2928, 2859, 1701, 1650, 1535, 1487, 1461, 1403, 1368, 1331 cm^{-1}; ^1H NMR ($CDCl_3$, 400 MHz) δ 7.47 (m, 2H), 7.45 (s, 2H), 7.27 (s, 1H), 7.25 (s, 1H), 7.21 (m, 1H), 6.55 (m, 1H), 5.96 (m, 1H), 5.94 (s, 1H), 5.17 (s, 1H), 5.15 (s, 2H), 4.47 (m, 1H), 4.28 (m, 1H), 3.90 (m, 1H), 3.45 (m, 1H), 3.38 (m, 1H), 3.15 (m, 7H),

2.87 (m, 2H), 2.70 (d, 1H, *J* = 12.7 Hz), 2.22 (s, 3H), 2.17 (t, 2H, *J* = 7.3 Hz), 1.66 (m, 8H), 1.44 (m, 4H), 1.09 (t, 3H, *J* = 7.0 Hz); ^{13}C NMR ($CDCl_3$, 100 MHz) δ 173.0, 172.1, 163.5, 155.3, 137.7, 137.2, 136.2, 131.5, 131.5, 130.5, 129.8, 129.8, 128.2, 127.4, 124.3, 121.6, 81.2, 75.3, 66.6, 61.8, 60.1, 55.5, 40.5, 39.2, 38.9, 38.5, 35.9, 29.7, 29.3, 29.0, 28.1, 25.6, 23.9, 15.2, 12.9; LRMS (FAB) *m*/*z* 730 (M + H^+). HRMS (FAB) calcd for $C_{35}H_{49}BrN_5O_5S$ (M + H^+), 730.2638; found, 730.2638.

Pull-Down Assay HEK293T cells (2 × 10^7 cells per dish) were seeded in 100-mm culture dishes and transiently transfected with CMV promoter-driven expression constructs harboring mouse or human core clock proteins with the indicated epitope-tags (myc-CLOCK, myc-BMAL1, V5-PER1, V5-PER2, flag-CRY1, or flag-CRY2; 32 μg per dish). After 48 hour of transfection, cells were harvested with ice-cold lysis buffer [50 mM Tris (pH 7.4), 2 mM EDTA, 1 mM $MgCl_2$, 0.2% NP-40, 0.1% sodium deoxycholate, 1 mM sodium orthovanadate, 1 mM sodium fluoride, and protease inhibitor cocktail (Sigma−Aldrich, St. Louis, MO)]. Lysates were prepared by sonication followed by centrifugation (7000 × g) at 4 °C for 10 min. The resulting supernatants were diluted with ice-cold 2× binding buffer [100 mM Tris-HCl (pH 7.4), 300 mM NaCl, 0.2% NP-40, 2 mM sodium orthovanadate, 2 mM sodium fluoride and protease inhibitor], pre-cleared with 200 μL (50% slurry) of NeutroAvidin Agarose resin (Thermo Scientific, NYSE, TMO, USA) and then subjected to the pull-down assay. Lysates were incubated at 4 °C with rotation for preclearing. After incubation, beads were removed by centrifugation. The remaining supernatant was split into four samples and

treated with a series of compound mixes: a) only DMSO b) Bait (20 μM), c) Bait 20 μM + KS15 40 μM, and d) Bait (20 μM) + KS16 (40 μM). The final concentration of DMSO was 0.5%. After 30-min incubation with the compounds as indicated, the chemical-bound proteins were isolated by incubating them with activated NeutroAvidin Agarose for 2 hours at 4 °C with continuous agitation. The beads were washed six times with 1× binding buffer, and the bound proteins were eluted with sodium dodecyl sulfate (SDS) sample buffer. The pulled-down samples were separated by SDS-PAGE (8%) and transferred to a PVDF membrane (Millipore, Billerica, MA, USA). Immunoblot analyses were carried out with anti-myc (9E10, Santa Cruz Biotechnology, Santa Cruz , CA, USA), anti-V5 (V8137, Sigma−Aldrich) or anti-flag (M2, Sigma−Aldrich).

Preparation of Purified CRY1 Protein HEK293T cells (2 × 10^7 cells per dish) were seeded in 100-mm culture dishes, and transiently transfected with CMV promoter-driven expression constructs harboring human CRY1 proteins with FLAG and hexa-histidine tag (32 μg per dish). After 48 hour after transfection, cells were harvested with ice-cold lysis buffer [20 mM Tris (pH 7.4), 500 mM NaCl, 5 mM imidazole, 2 mM β-mercaptoethnol, 1% NP-40, 0.1% SDS and protease inhibitor cocktail (Sigma−Aldrich)]. Lysates were prepared by sonication followed by centrifugation (7000 × g) at 4 °C for 10 min. The resulting supernatants were diluted ten times with ice-cold binding buffer [20 mM Tris (pH 7.4), 500 mM NaCl, 5 mM imidazole, 2 mM β-mercaptoethnol, 0.45% NP-40, and protease inhibitor cocktail] and subjected to affinity chromatography using His-Bind Agarose Resin (ELPIS

biotech, Daejeon, Korea). After washing with 10 column volumes of binding buffer, hCRY1 proteins were eluted by using elution buffer [10 mM Tris (pH 7.4), 250 mM NaCl, 500 mM imidazole, and protease inhibitor cocktail]. A single fraction with highest purity was dialyzed against dialysis buffer [10 mM Tris (pH 7.4), 250 mM NaCl, 1 mM phenylmethanesulfonyl fluoride] and used for pull-down assay.

RNA Isolation and RT-PCR mRNA expression analyses were performed as previously described with certain modifications.[2] WT and *Cry1/2*$^{-/-}$ MEFs were suspended and seeded in 6-well culture plates. Cells were synchronized with 100 nM DEX and then changed to normal culture medium. Twelve hours after synchronization, drugs were administrated for a further 24 hours and then harvested. Total RNA was isolated with a single-step acid guanidinium thiocyanate-phenol-chloroform method. Then, 2 μg of each RNA sample were subjected to reverse transcription with MMLV-reverse transcriptase (Promega). mRNA expression profiles were analyzed by quantitative real-time PCR in the presence of SYBR Green I (Sigma−Aldrich). TATA box-binding protein (TBP) was used as an internal control gene transcript. The primer sequences used for real-time RT-PCR were as follows: Per1 up, 5′-GTG TCG TGA TTA AAT TAG TCA G-3′; Per1 dn, 5′-ACC ACT CAT GTC TGG GCC-3′; Per2 up, 5’-ATG CTC GCC ATC CAC AAG A-3′; Per2 dn, 5′-GCG GAA TCG AAT GGG AGA AT-3′; Rev-erbα up, 5′-AGG GCA CAA GCA ACA TTA CC-3′; Rev-erbα dn, 5′-CAC AGG CGT GCA CTC CAT AG-3′; TBP up, 5′-GGG AGA ATC ATG GAC CAG AA-3′; and TBP dn, 5′-CCG TAA GGC ATC ATT GGA CT-3′.

Real-Time Bioluminescence Monitoring Per2-Luc-expressing cells were plated in 35-mm dishes. Cells were synchronized by a treatment with 200 nM DEX for 2 hours, and then the medium was replaced with recording medium [Dulbecco's modified Eagle medium (DMEM) supplemented with 5% fetal bovine serum (FBS), 100 U/mL penicillin/streptomycin, and 0.1 mM luciferin (Promega)] with vehicle (0.2% DMSO) or 20 μM KS15. Light emission was integrated for 1 min at intervals of 10 min using a dish-type wheeled luminometer (Kronos-Dio, ATTO).

Statistical Analysis The CLUSTER (Veldhuis, University of Virginia, Charlottesville, VA) statistical pulse analysis program was used to identify the exact peak timing of Per2-Luc fibroblasts. The number of points for the peak and nadir were set as 3, and both of the T-scores for increase and decrease were set as 3.00. Statistical significance was assessed by Student's *t*-test and is indicated as follows: *, †: $p < 0.05$ and **, ††: $p < 0.01$.

Preparation of ΔCC-Tail Mutant of hCRY1/2 Expression Plasmid Flag−myc−His-tagged human CRY1 and CRY2 expression plasmids were obtained from Addgene (hCRY1: #25843, hCRY2: #25842). The putative coiled-coil (CC) region of hCRY1 and hCRY2 was identified based on the sequence homology of CC regions in mCRY1 and mCRY2, which were defined in a previous study[38]. To generate ΔCC-Tail Mutant of hCRY1/2, we designed the following primers for cloning: 5'- GAT ATC GCC ACC ATG

GGG GTG AAC GCC GTG CAC -3' (hCRY1 mutant, forward), 5'- TCT AGA CAT TGG TTT AGG ATA ATT AAC TCC -3' (hCRY1 mutannt, reverse), 5'- GAT ATC GCC ACC ATG GCG GCG ACT GTG GC -3' (hCRY2 mutant, forward), 5'- TCT AGA GCG CGA AAG CTG CTG GTA AAT C -3' (hCRY2 mutannt, reverse). The forward primer was designed to start before the EcoRV restriction site at the upstream of start codon in the original plasmid. The reverse primer was designed to target immediately before the CC region and harboring the XbaI restriction site, resulting in truncation of the C-terminal region. A PCR-amplified construct was subcloned into a pGEM-T easy vector (Promega) and replaced wild-type hCRY1 or hCRY2 within the original plasmid by using EcoRV/XbaI.

Preparation of ΔCC-Tail Mutant of hCRY1/2 Expression Plasmid To examine the dose-response activity of these compounds on PPAR mediated transcriptional activity, 100 ng per well of DR1-Luc plasmid (a luciferase reporter driven by synthetic promoter containing multiple PPAR responsive elements) and a control plasmid (promoterless renilla luciferase expression plasmid, 500 ng per well) were transfected into NIH3T3 mouse fibroblast cell line and treated with various concentrations of compounds. After 24-hour incubation, cells were harvested and lysed with Passive Lysis Buffer (Promega) and subsequently subjected to luciferase assays with Dual Luciferase Reporter reagent (Promega) according to the manufacturer’s instructions. Luciferase activities were normalized by renilla luciferase levels.

Animal care and handling Wild-type male C57BL/6J mice at 9-12 weeks of ages were obtained from the Laboratoy Animal Center at Seoul National University. Mice were kept in temperature-controlled (22~23˚C) quarters under a 12-hr light and 12-hr dark (LD) photoperiod (light-on at 8:00 a.m.), with standard mouse chow and water availavle *ad libitum*. For dark-dark (DD) conditions, mice were kept in contrast darkness for the indicated duration from the light-off time. Home-cage activities and body temperatures were simultaneously monitored using a VitalView® data acquisition for more than 10-days under LD conditions. All animal procedures were approved by the institutional Animal Care and Use Committee of Seoul National University.

Cannula implantation and microinjection of KS15. Mice were anesthetized with sodium pentobarbital (50 mg/kg, i.p.), mounted on a stereotaxic apparatus (David Kopf Instruments, Tujunga, CA), and unilaterally implanted with 26-gauge stainless steel cannula (model C315G; Plastic Products, Roanoke, VA) into the lateral ventricle (AP -0.4 mm, ML 1.0 mm, DV -1.7 mm). A 32-gauge dummy cannula was inserted into guide cannula to prevent clogging. Two jewelry screws were implanted over the skull to serve as anchors, and the whole assembly was affixed on the skull with dental cement. Mice were given at least 1 week to recover before experimentation. After completion of the experiments, correct placement of the injection cannula tips was verified in all animals. For this purpose, brains were removed from animals and fixed overnight in PBS/4% paraformaldehyde. The fixed brains were coronally sectioned into 100-μm

thicknesses using a vibratome (World Precision Instruments, Sarasota, FL). Sections were then stained with cresyl violet and examined under light microscopy. KS15 dissolved in DMSO (8.4 μg / μl) was administrated unilaterally into the LV via a 33-gauge injector cannula (C315I; Plastic Products) attached to a 10-μl Hamilton syringe. A solution containing 4.2 μg of KS15 in 0.5 μl DMSO was administered. After administration, injector cannula was left in place for an additional minute to allow the solution to diffuse away from the tip.

Circadian Activity Measurements Wheel running activity was recorded at 6-minute intervals using an ER-4000 system (Mini-Mitter) supplemented with a wheel running assembly. For quantitative and statistical analysis, the raw data files generated by VitalView Version 4.0 data acquisition system (Mini-Mitter) were converted to data sets that can readily be applied to the software provided in the textbook, *Circadian Physiology* (CRC Press, Taylor & Francis Group, Boca Raton, FL). The length of periods from each groups were determined by the cosinor fitting analysis of 10-day profiles during entrainment period (light:dark = 12 hrs:12 hrs) and free running period (FRP) in constant dark, as well as post-injection period. Activity onset was characterized by an initial period of activity that: (1) exceeded 10% of the maximum rate for the day; (2) was preceded by at least 4 hours of activity quiescence; and (3) was followed by at least 60 minutes of sustained activity. Phase-shifts were calculated as the difference between the expected times of activity onset from profiles of FRP and actual activity onset timing in post-injection period.

RESULTS

Screen for E-box-mediated transcription modulator

To identify a novel synthetic circadian modulator, I designed a two-step cell-based screening method based on a luciferase reporter system. First, the CLOCK:BMAL1 heterodimer-responsive luciferase reporters were stably expressed in cultured cell lines based on the previous findings of our group. (Son et al., 2008). An artificial reporter (designated as E-box-Luc) was produced by incorporating two E-box elements originated from the mouse steroidogenic acute regulatory protein (StAR) promoter upstream of the SV40 minimal promoter-driven luciferase reporter. The E-box-Luc reporter was then stably expressed in NIH3T3 mouse fibroblasts. To test the effect on the endogenous clock-controlled promoter activities in parallel, mouse StAR promoter-driven luciferase (StAR-Luc) reporter activities were examined in Y1 mouse adrenocortical cell line. Expression profiles of luciferase reporters in these cell lines were verified by bioluminescence imaging device (Cellgraph, ATTO) (Fig 2). Both cell lines expressing luciferase reporters were cultured on 24-well plates for 24 hours, and then treated with 20 μM of more than 1,000 different drug-like compounds. Luciferase activities were analyzed after 24 hours of treatment (Fig 3 and Fig 4). As a result, 72 compounds were finally identified as E-box mediated transcription modulator that either enhanced or suppressed luciferase activities in both reporters (Fig 5). These 72 compounds were proceeding into further verification of compound effect in secondary screening step.

For the second screening, the effects of the selected compounds on E-box-mediated transcriptional activities were compared in mouse embryonic fibroblasts (MEFs) derived from wild-type (WT) and *Bmal1*-deficient mouse to select for compounds dependent on the CLOCK:BMAL1 heterodimer. Both types of MEF cells were synchronized by treatment with 100 nM dexamethasone (DEX) for 2 hours. After 12 hours of further incubation, the selected compounds were treated at 20 μM each for 24 hours. As a result, the compounds KS11a, KS11b, KS15, and KS16 were structurally similar and were shown to BMAL1-dependently enhance E-box-mediated transcription (Fig 6). These compounds were prepared according to the procedures that previously reported (Suh et al., 2008). The intermediate, 3-(3-acetylphenyl)-2-ethoxypropanoic acid is a racemate that was synthesized from commercially available 3-acetylbenzonitrile and then coupled with (*R*)-2-phenylglycinol, followed by chiral resolution. The optically pure (*R*)-3-(3-acetylphenyl)-2-ethoxypropanoic acid was converted into a variety of oxime ethers by condensation with benzyloxy amines. The selected compounds were further tested to determine the potency and dose-response using E-box-Luc-expressing fibroblasts. Efficacy was determined by calculating the maximum change in the luciferase activity at given concentrations. Potency was determined by deducing the EC_{50} from the dose-response curve (Fig 7 and Table 1). I also tested the analogs that both conformationally restricted isoxazoline analogs or stereoisomers containing *(S)*-ethoxypropanoic acid, but they only slightly enhanced E-box-mediated transcription at 20 μM (Fig 7 and Table 1). Among the tested compounds, KS15 was ultimately selected as the E-box-mediated

transcription modulator that was most promising in terms of efficacy and potency.

CRY1/2 are molecular targets of KS15

In the next set of experiments, I sought to identify a molecular target of KS15. I hypothesized that enhanced E-box-mediated transcription is likely to be due to direct binding of KS15 to its target clock protein. In collaboration with professor Youn-Ger Suh and his colleagues, I prepared a biotin-conjugated version of KS15 for pull-down assays, which was conveniently prepared by coupling the carboxyl group of KS15 with a commercially available biotin tag tethered with the amide linker. Derivatives of KS15 with a methyl ester or hexyl amide substituent at the same position (Fig 9) also enhanced E-box-mediated transcriptional activity (Fig 10), suggesting that biotin conjugated probe has same activity of KS15. Then, I carried out pull-down assays using this biotin-conjugated probe as bait in clock protein-expressing HEK293T cell lysates. HEK293T cells were transiently transfected with the tagged core clock proteins-expressing constructs, and cell lysates were prepared 48 hours after transfection and incubated with 20 μM biotin-conjugated KS15 (i.e., the bait) for 30 min in the absence or presence of 40 μM free competitors, and then the bound complexes were isolated by incubating them with avidin-coated beads for 2 hours at 4 °C. The bound proteins were then detected by immunoblotting with tag-specific antibodies. As shown in Figure 11, the biotin-conjugated chemical probe KS15 specifically bound to both CRY1 and CRY2 (Fig 11A),

but not to CLOCK, BMAL1 or PERs amongst the tested core clock proteins (Fig 11B). CRYs binding with biotin-conjugated probe were severely blocked in the presence of free KS15, while KS16, a structural analog of KS15 with weak potency, failed to interrupt CRY binding (Fig 11A). Biotin-conjugated probe also bound to purified CRY1 protein (Fig 12). Moreover, I generated functionally inactive mutants of CRYs and used it in a pull-down assay to find out whether KS15 interacts with an important functional structure/domain of CRYs. The CRYs are composed of highly conserved N-terminal photolyase homology region (PHR) and variable C-terminal extension domain, the tails (Chaves et al., 2006; Partch et al., 2005; Lin et al., 2005; Todo et al., 1996). Also, putative coiled-coil (CC) domain resides in the beginning of C-terminal tail and highly conserved even between CRY1 and CRY2 (Fig 13) (Chaves et al., 2006; Partch et al., 2005). Previous studies suggested that the C-terminal tail, including the CC domain, of CRYs is important for nuclear localization and interaction with other core clock proteins, such as PERs and BMAL1 (Chaves et al., 2006; van der Schalie et al., 2007; Czarna et al., 2011). Also, C-terminal tail is target site of phosphorylation by glycogen synthase kinase-3β (GSK3β) or mitogen-activated protein kinase (MAPK) and regulates stability of CRYs (Harada et al., 2005; Sanada et al., 2004). Based on these findings, I constructed mutants of human CRY1 and CRY2 with truncation of the C-terminal tail and putative CC domain (ΔCC-tail) (Fig 13). Unlike wild-type, both ΔCC-tail mutants of CRY1 and CRY2 were failed to bind biotin-conjugated KS15 (Fig 14). Taken together, these data suggest that KS15 selectively and directly interacts with CRY proteins.

CRYs play a crucial role in the clock gene expression cycle by forming inhibitory complexes with the CLOCK:BMAL1 heterodimer, thus repressing their transcriptional activities (Kume et al., 1999). Because KS15 binds to both CRY1/2, I examined whether the effect of KS15 on the E-box-mediated transcription depends on CRY1/2. WT or *Cry1/2*-knockout MEFs synchronized by DEX treatment were treated with 6.7 μM of KS15, KS16 or KS25 for 24 hours. The effect of KS15 on E-box-mediated transcription, as determined by the E-box-Luc reporter construct, was significantly attenuated in CRY1/2-deficient MEFs (Fig 15A). More importantly, KS15-induced *Per1*, *Per2*, and *Rev-erbα* mRNA expression but these inductions were disappeared in the absence of endogenous CRY1/2 (Fig 15B, C, D). In contrast, the less potent analogs KS16 and KS25 only marginally influenced E-box-mediated transcription, as well as endogenous clock gene expression. In good agreement with the binding assay, these results demonstrate that CRY1/2 are molecular targets of KS15.

Modulation of molecular clock activity by KS15

After identifying binding target of KS15, I examined whether KS15 modulates the circadian periodicity of clock-controlled gene transcription. For this purpose, stable NIH3T3-originated cell line bearing the mouse *Per2* promoter-driven luciferase reporter (Per2-Luc) was synchronized by treatment with DEX, and emitted bioluminescence in the presence of luciferin substrate was non-invasively monitored every 10 min for 96 hours. After synchronization, vehicle (0.2% DMSO) or KS15 (6.7 or 20 μM) was

included in the media (Fig 16). The relative amplitudes of the rhythms were significantly attenuated in a dose-dependent manner, although the periods were not significantly altered (Fig 16 and Table 2). Because the areas under the curves (AUCs) were also changed in same way, it can be postulated that KS15 inhibited CRY-mediated repression of CLOCK:BMAL1 heterodimer transcriptional activities. I also established another stable fibroblast cell line bearing the mouse *Bmal1* promoter-driven destabilized luciferase reporter (Bmal1-dLuc) and analyzed activity in the same way (Fig 17). Like Per2-Luc, the rhythms of Bmal1−dLuc were also attenuated in the presence of KS15 without significantly changing the periods (Fig 17 and Table 3). In addition, I examined the effect of CRY1/2 knockdown on circadian periodicity compared with the effect of KS15 to investigate more detailed mechanism of KS15's action, Small hairpin RNA expression vectors (shRNA) were used for knock down of CRY1/2 expression after verification (Fig 18). As a result, single knockdown of CRY1 or CRY2 altered period length of Bmal1-dLuc reporter activity rhythm, while knockdown of both CRY1/2 severely attenuated amplitude of the rhythm (Fig 19 and Table 3). Moreover, knockdown of CRY1/2 attenuated Bmal1-dLuc reporter activity rhythm in dose-dependent manner without significantly changing the period length (Fig 19 and Table 4). Considering that CRYs are key negative regulators of molecular circadian clockwork (Kume et al., 1999), these findings strongly suggest that the binding of KS15 to both CRY1/2 attenuates circadian clockwork oscillation by inhibiting negative regulators in the core molecular feedback loop.

Modulation of circadian rhythm by KS15 *in vivo*

Finally, I sought to investigate effect of KS15 on circadian rhythms *in vivo*. For this purpose, I designed a set of experiments that monitoring changes of daily activity rhythm of mouse after the intracerebroventricular (ICV) microinjection of KS15. For this purpose, a guide cannula was implanted unilaterally into wild-type male C27/B6 mouse that targeting lateral ventricles of brain. After 1 week of recovery, mice were entrained with normal 12-hr light:12-hr dark cycle with wheel running assembly. By then, free running period (FRP) were monitored in constant dark condition. Then, vehicle (100% DMSO 0.5 μl) or KS15 (4.2 μg in 0.5 μl of DMSO) were administrated by single ICV microinjection through the implanted cannula at two hour before activity onset. After administration, daily activity rhythms in constant dark were monitored another 10 days. As a result, administration of KS15 caused the delay of the activity rhythm than vehicle treated group (Fig 21). KS15 also cause nearly one hour shift of circadian phase than vehicle injected group. These data suggested that ICV administration of KS15 can modulate circadian rhythms *in vivo*.

Figure 2. Establishment of stable cell lines with CLOCK:BMAL1 heterodimer responsive luciferase reporters. (A) Schematic diagram of the promoter region of the mouse StAR gene (-2517 to -1). Previous studies suggested that two E-box elements within the distal region to of the mouse StAR promoter were directly regulated by the CLOCK:BMAL1 heterodimer. (Son et al., 2008) (B) Schematic diagram of transfected cell lines with stable luciferase expression of StARp-Luc and E-box-Luc reporters. E-box-Luc was produced by incorporating two E-box elements originated from the distal region of StAR promoter (around -2140) with SV40 minimal promoter-driven luciferase reporter. The E-box-Luc reporter was then stably expressed in NIH3T3 mouse fibroblasts. StARp-Luc was produced by conjucating 2.5 kb of mouse StAR promoter with luciferase reporter. StARp-Luc was transfected into Y1 mouse adrenocortical cell line for tissue-specificity issue (Y1:StARp-Luc) while E-box-Luc was transfected into NIH3T3 fibroblast cell line (NIH3T3:E-box-Luc) (C) Bioluminescence imaging of cell lines with stable expression of luciferase reporters. Images from NIH3T3:E-box-Luc (upper panel) and Y1:StARp-Luc (lower panel) are presented with both light field image (left) and bioluminescence imaging with pseudocolor coding (right).

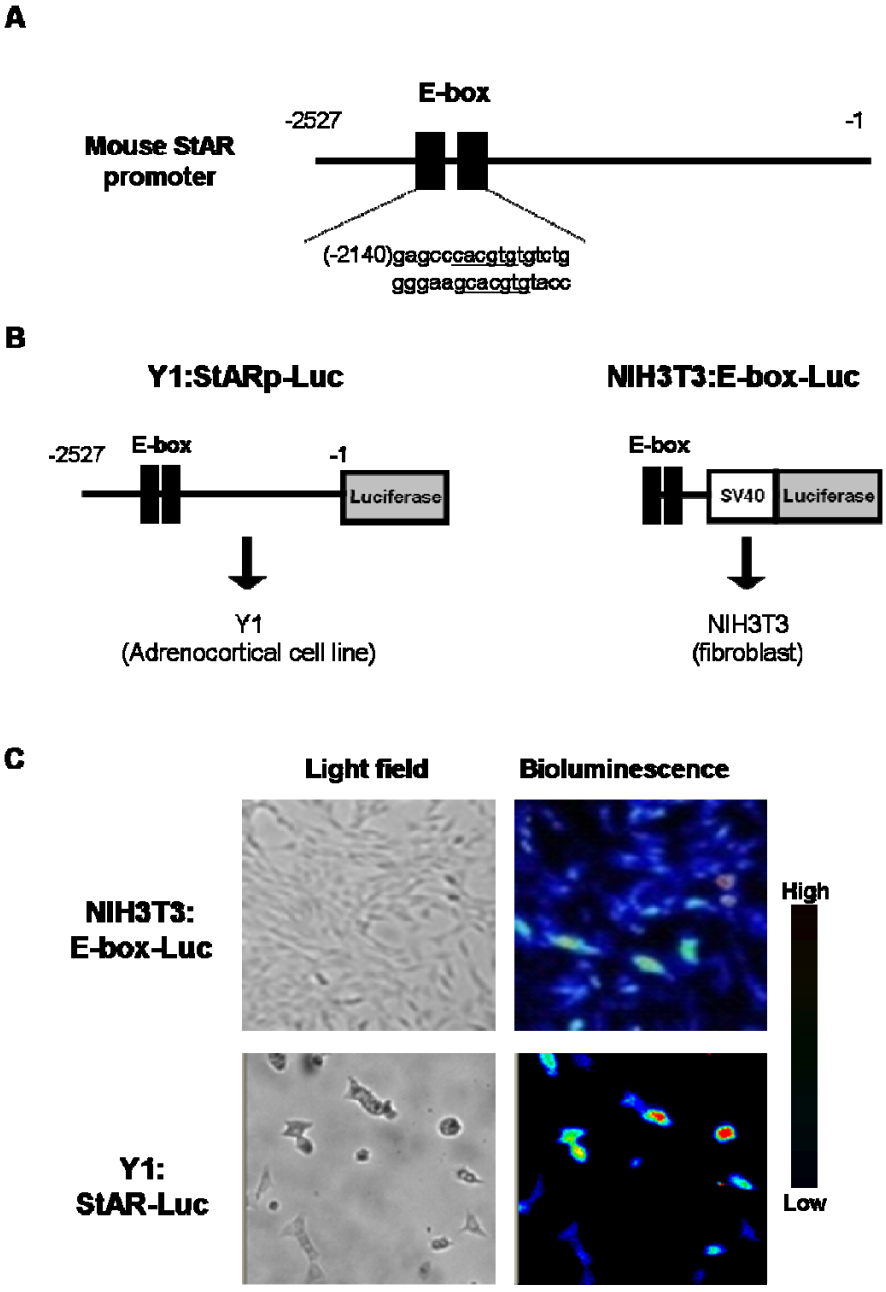
A
E-box
-2527
-1
Mouse StAR promoter
(-2140)gagcccacgtgtgtctg
gggaagcacgtgtacc
B
Y1:StARp-Luc
NIH3T3:E-box-Luc
-2527
E-box
-1
Luciferase
E-box
SV40
Luciferase
Y1
(Adrenocortical cell line)
NIH3T3
(fibroblast)
C
Light field
Bioluminescence
NIH3T3:
E-box-Luc
Y1:
StAR-Luc
High
Low

Figure 3. The primary screening of chemical library by using NIH3T3:E-box-Luc. (A) The distribution of the total 1172 compounds treated to NIH3T3:E-box-Luc stable cell. Changes of luciferase activity caused by compound treatment were normalized by vehicle (0.2% DMSO) treated group and results were presented in scatter plot. The compounds with significant fold change (over 50%) were presented in following colors: over 50% (blue dots), over 100% (orange dots) and over 200% (brown dots) (B) The distribution of whole chemical library presented on a pie graph (left panel). Compounds with inducing effect were shown in orange color, while compounds with inhibiting effect were shown in blue color. The compounds causing cell damage were shown in gray. Also, total chemicals were divided into two pie graphs (right panel). Induction group (compounds with enhancing activity) is composed two groups (over 100% fold change was presented orange color and over 50% change was presented light orange color). Repression group (compounds with repressive activity) is composed of three categories (over 200% fold change was presented dark blue, over 100% fold change was blue and over 50% fold change was presented light blue).

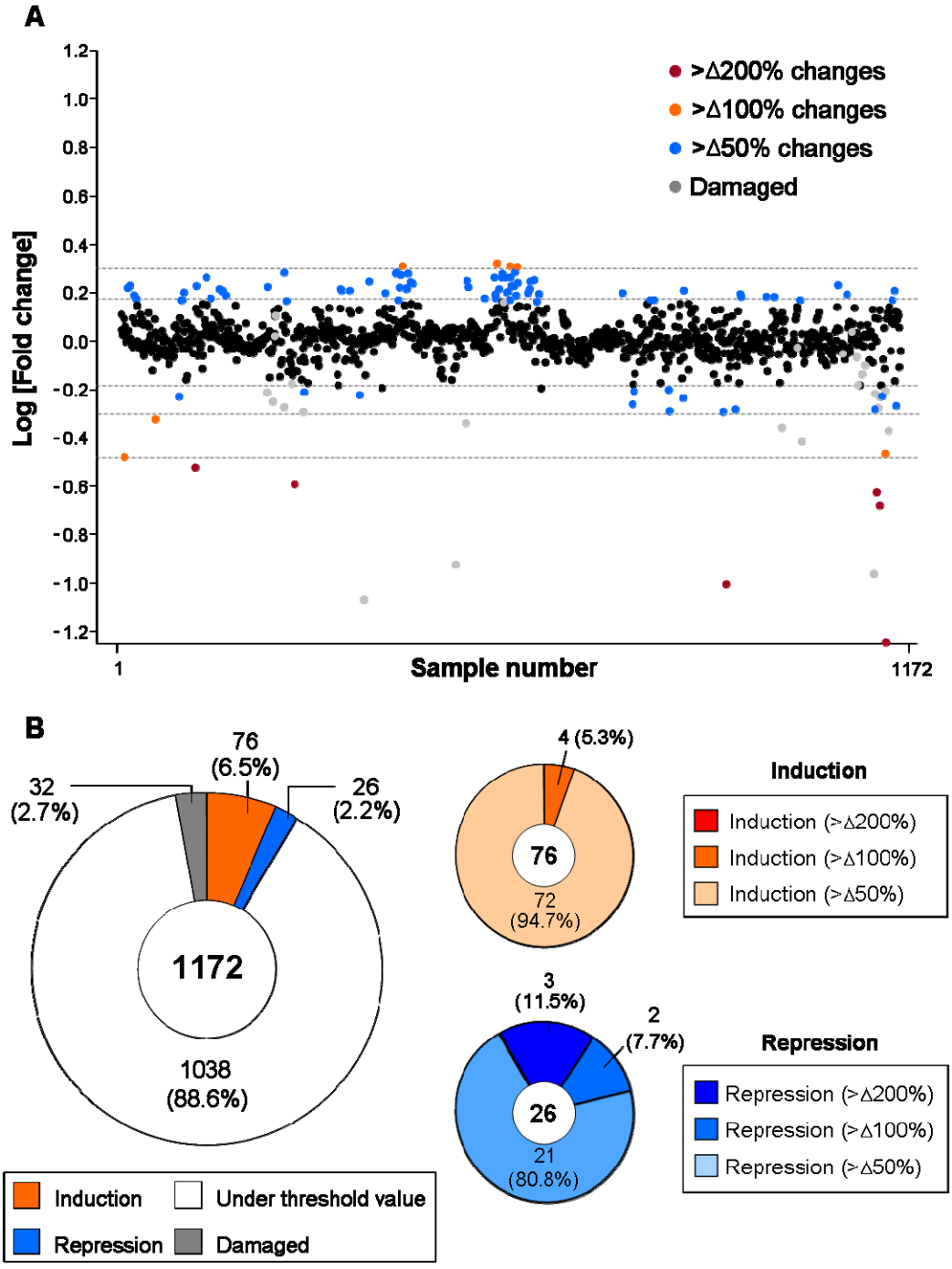
A
>Δ200% changes
>Δ100% changes
>Δ50% changes
Damaged
Log [Fold change]
1.2
1.0
0.8
0.6
0.4
0.2
0.0
-0.2
-0.4
-0.6
-0.8
-1.0
-1.2
1
Sample number
1172
B
76
(6.5%)
32
(2.7%)
26
(2.2%)
1172
1038
(88.6%)
Induction
Under threshold value
Repression
Damaged
4 (5.3%)
76
72
(94.7%)
Induction
Induction (>Δ200%)
Induction (>Δ100%)
Induction (>Δ50%)
3
(11.5%)
2
(7.7%)
26
21
(80.8%)
Repression
Repression (>Δ200%)
Repression (>Δ100%)
Repression (>Δ50%)

Figure 4. The primary screening of chemical library by using Y1:StARp-Luc. (A) The distribution of the total 1172 compounds treated to Y1:StARp-Luc stable cell. Changes of luciferase activity caused by compound treatment were normalized by vehicle (0.2% DMSO) treated group and results were presented in scatter plot. The compounds with significant fold change (over 50%) were presented in following colors: over 50% (blue dots), over 100% (orange dots) and over 200% (brown dots) (B) The distribution of whole chemical library presented on a pie graph (left panel). Compounds with inducing effect were shown in orange color, while compounds with inhibiting effect were shown in blue color. The compounds causing cell damage were shown in gray. Also, total chemicals were divided into two pie graphs (right panel). Induction group (compounds with enhancing activity) is composed three groups (over 200% fold change was presented red color, over 100% fold change was presented orange color and over 50% change was presented light orange color). Repression group (compounds with repressive activity) is also composed of three categories (over 200% fold change was presented dark blue, over 100% fold change was blue and over 50% fold change was presented light blue).

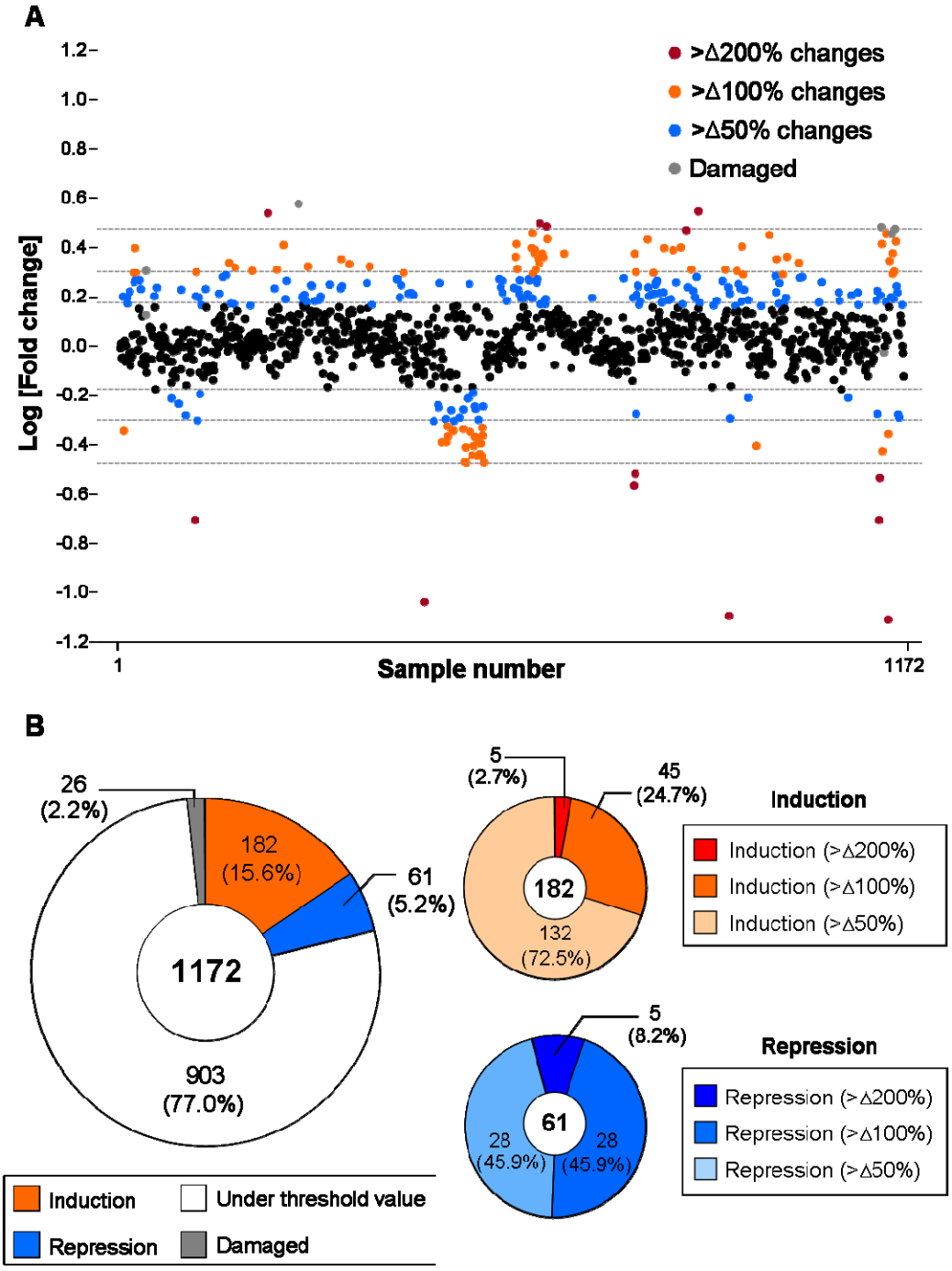
A
>Δ200% changes
>Δ100% changes
>Δ50% changes
Damaged
Log [Fold change]
1.2
1.0
0.8
0.6
0.4
0.2
0.0
-0.2
-0.4
-0.6
-0.8
-1.0
-1.2
1
Sample number
1172
B
26
(2.2%)
182
(15.6%)
61
(5.2%)
1172
903
(77.0%)
Induction
Under threshold value
Repression
Damaged
5
(2.7%)
45
(24.7%)
182
132
(72.5%)
Induction
Induction (>Δ200%)
Induction (>Δ100%)
Induction (>Δ50%)
5
(8.2%)
61
28
(45.9%)
28
(45.9%)
Repression
Repression (>Δ200%)
Repression (>Δ100%)
Repression (>Δ50%)

Figure 5. Selection of hit compounds from primary screening. Hit compounds from primary screening were identified by selecting the compounds that shows enhancing or repressing activities on both reporter systems in same direction. Comparing results from two reporters system, 50 compounds were finally identified as hit compounds with induction effect on both reporters, while 12 compounds were selected as hit compounds with repressive effect on both reporters.


Induction
E-box-Luc
(76 species)
StARp-Luc
(182 species)
24
52
130
Repression
E-box-Luc
(26 species)
StARp-Luc
(61 species)
6
20
41

Figure 6. Identification of the hit compounds by two-step cell-based screening strategy. (A) Representative group of compounds (KS11a-16, KS25) from primary screening. These compounds identified as significantly enhancing both E-box-Luc activities in NIH3T3 cells and StARp-Luc in Y1 cells. (B) Comparison of the effects of KS11a-16 and 25 on E-box-Luc activities in WT and BMAL1-deficient MEFs (*$p < 0.05$, **$p < 0.01$, compared with vehicle (0.1% DMSO)-treated groups (VEH); †$p < 0.05$, ††$p < 0.01$ compared with WT MEF). Data are presented as the mean ± S.E.M. ($n = 3$ for each group). Note that KS11a, KS11b, KS15, and KS16 were found to enhance E-box-mediated transcription in a BMAL1-dependent manner. (C) Structure of KS11a-b, KS15 and KS16.

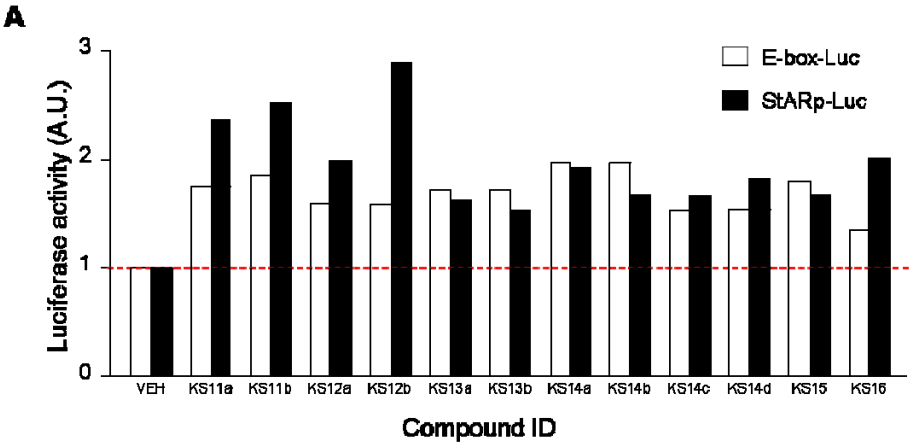
A
Luciferase activity (A.U.)
E-box-Luc
StARp-Luc
VEH
KS11a
KS11b
KS12a
KS12b
KS13a
KS13b
KS14a
KS14b
KS14c
KS14d
KS15
KS16
Compound ID

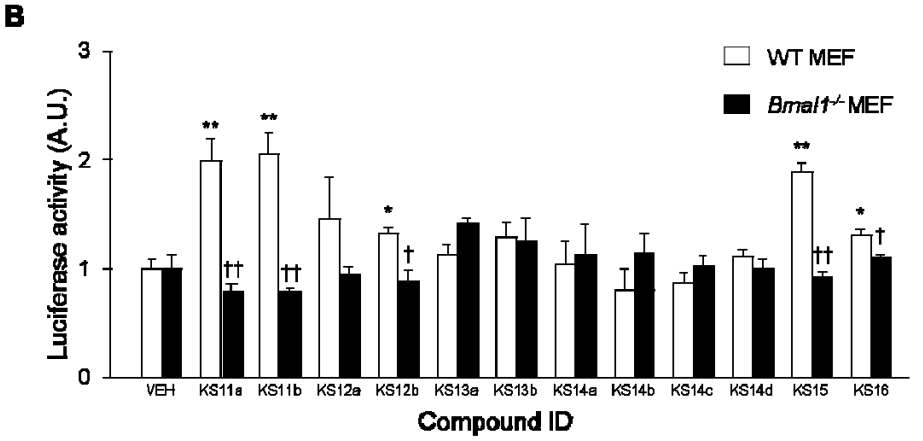
B
Luciferase activity (A.U.)
WT MEF
Bmal1-/- MEF
Compound ID

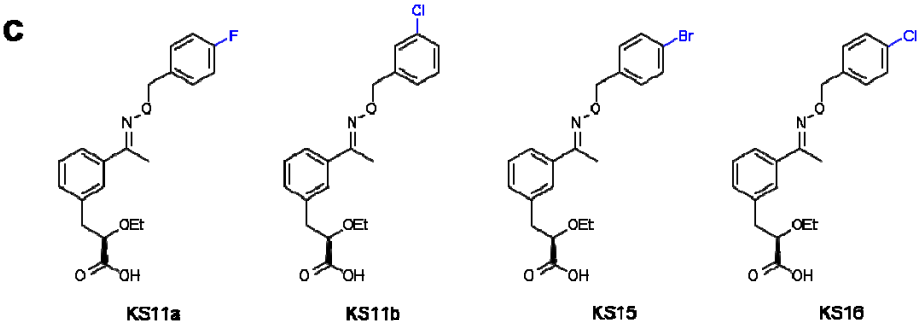
C
KS11a
KS11b
KS15
KS16

Figure 7. Structures and effects of the selected compounds to E-box-mediated transcription. (A) Chemical structure of the selected compounds (**11a**, **11b**, **15**, **16**, and **25**) and their stereoisomers (**11a', 11b'** and **15'**) containing *(S)*-ethoxypropanoic acid**.** (B, C) Dose-response curves of E-box-mediated transcription for the selected compounds (B) and their stereoisomers (C). Data are presented as mean ± S.E.M. (n = 3).

A

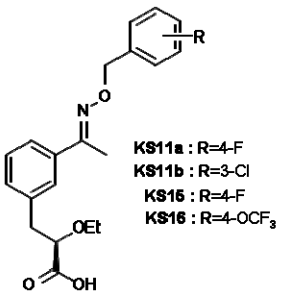

KS11a : R=4-F
KS11b : R=3-Cl
KS15 : R=4-F
KS16 : R=4-OCF3

KS11a, KS11b, KS15, KS16

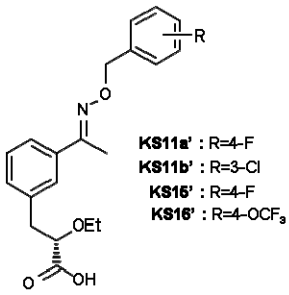

KS11a' : R=4-F
KS11b' : R=3-Cl
KS15' : R=4-F
KS16' : R=4-OCF3

KS11a', KS11b', KS15', KS16'

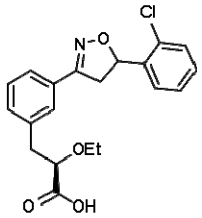

KS25

B

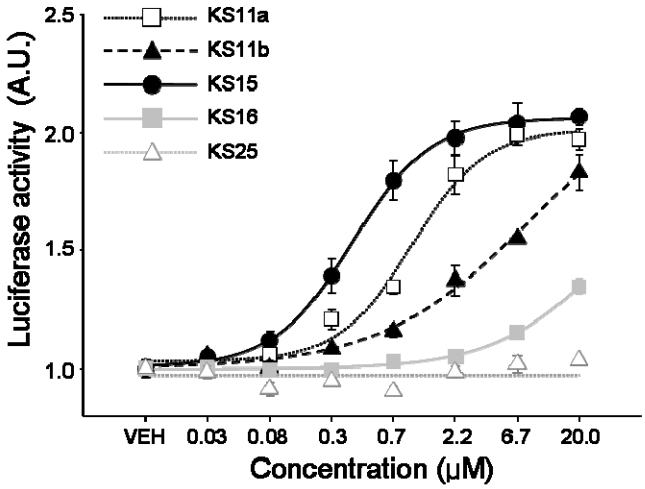

C

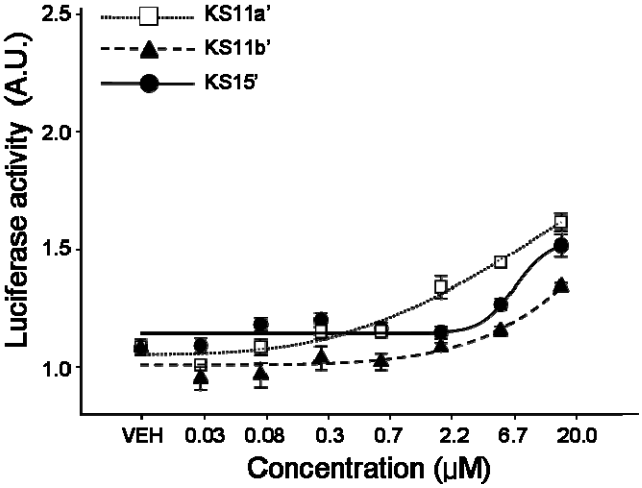

Table 1. Efficacy and potency of the selected analogs in enhancing E-box-Luc activity. KS11a, KS11b, KS15, KS16 and their structural analogs were tested to analyze dose-response curves for E-box-mediated transcription by using NIH3T3:E-box-Luc stable cell line. Efficacy and potency were determined by calculating the maximum change and EC_{50} values from the dose-response curve. Maximum response (MAX.) expressed as the percentage of the vehicle-treated group. EC50 values were calculated with a logistic 4-parametric equation using the mean values of its intrinsic activation. “ND” means that EC_{50} values were not determined within the tested dosages.

ID	Structure	R	Max. (%)	EC_{50} (μM)
11a	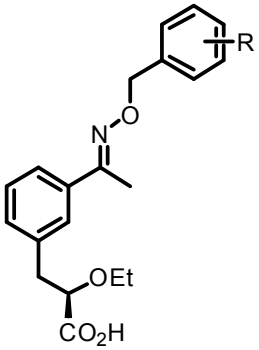	-F (p)	200.55	1.25
11b		-Cl (m)	192.40	2.22
15		-Br (p)	220.98	0.49
16		$-OCF_3$ (p)	140.93	ND
17		-H	193.12	4.02
18		-I (p)	195.94	1.91
19		-Cl (p)	208.10	4.77
20		-OH (p)	138.88	ND
21		-OMe (p)	221.80	3.79
22		$-CF_3$ (p)	143.07	ND
23	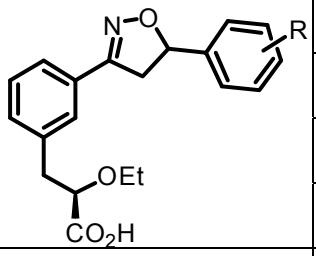	-F (p)	116.20	ND
24		-Cl (m)	99.48	ND
25		-Cl (o)	100.70	ND
26		$-CF_3$ (p)	103.86	ND
11a'	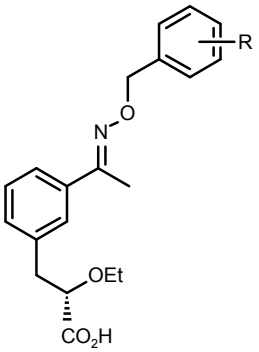	-F (p)	155.30	ND
11b'		-Cl (m)	126.77	ND
15'		-Br (p)	145.05	ND

Figure 8. Dose-response and potency of the selected compounds and their stereoisomers on Peroxisome proliferator-activated receptor (PPAR) mediated transcriptional activity. To examine the dose-response activity of these compounds on PPAR mediated transcriptional activity, DR1-Luc plasmid (a luciferase reporter driven by synthetic promoter containing multiple PPAR responsive elements) and a control plasmid (promoterless renilla luciferase expression plasmid) was transfected into NIH3T3 cells and treated with various concentrations of these compounds. After 24-hour incubation, cells were analyzed by luciferase assay. Dose-response curves of PPAR mediated transcriptional activity for the selected compounds (A) and their stereoisomers (B). Data are presented as mean ± S.E.M. (n = 5).

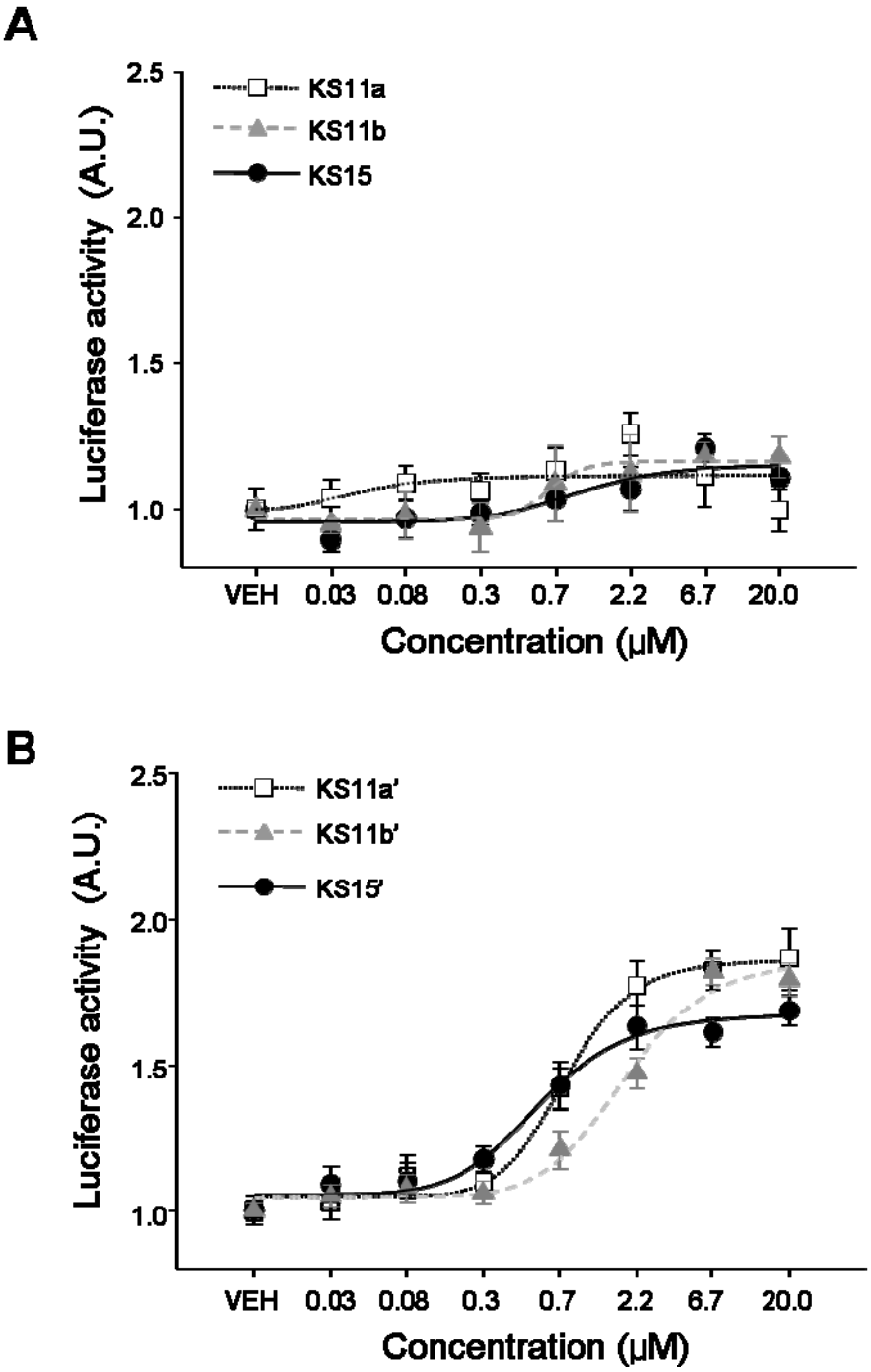
A
2.5
2.0
1.5
1.0
Luciferase activity (A.U.)
KS11a
KS11b
KS15
VEH
0.03
0.08
0.3
0.7
2.2
6.7
20.0
Concentration (μM)
B
2.5
2.0
1.5
1.0
Luciferase activity (A.U.)
KS11a'
KS11b'
KS15'
VEH
0.03
0.08
0.3
0.7
2.2
6.7
20.0
Concentration (μM)

Figure 9. Chemical structure of the derivatives of KS15 with linker from the process of biotinylation. (A) Structure of the original KS15 and its derivatives. The carboxyl group in KS15 was substituted with methyl ester (KS15a) or Hexyl amid (KS15b), the same as the biotin-conjugated probe. (B) Structure of biotin-conjugated KS15.

A

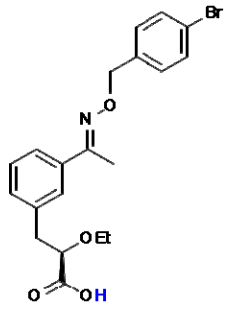

KS15

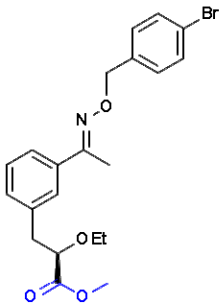

KS15a: Methyl ester

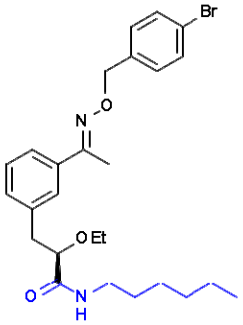

KS15b: Hexyl amide

B

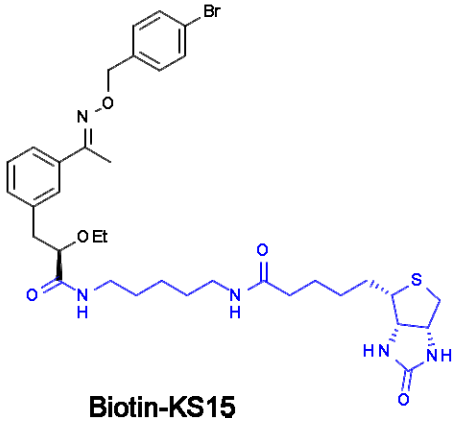

Biotin-KS15

Figure 10. Dose response and potency of the derivatives of KS15 with linker. To examine the dose-response activity of these derivatives on E-box mediated transcription, fibroblast cells stably expressing (A) E-box-Luc or (B) Per2-Luc were treated with various concentrations of these compounds. After 24-hour incubation, cells were analyzed by luciferase assay. Data are presented as mean ± S.E.M. (n = 3).

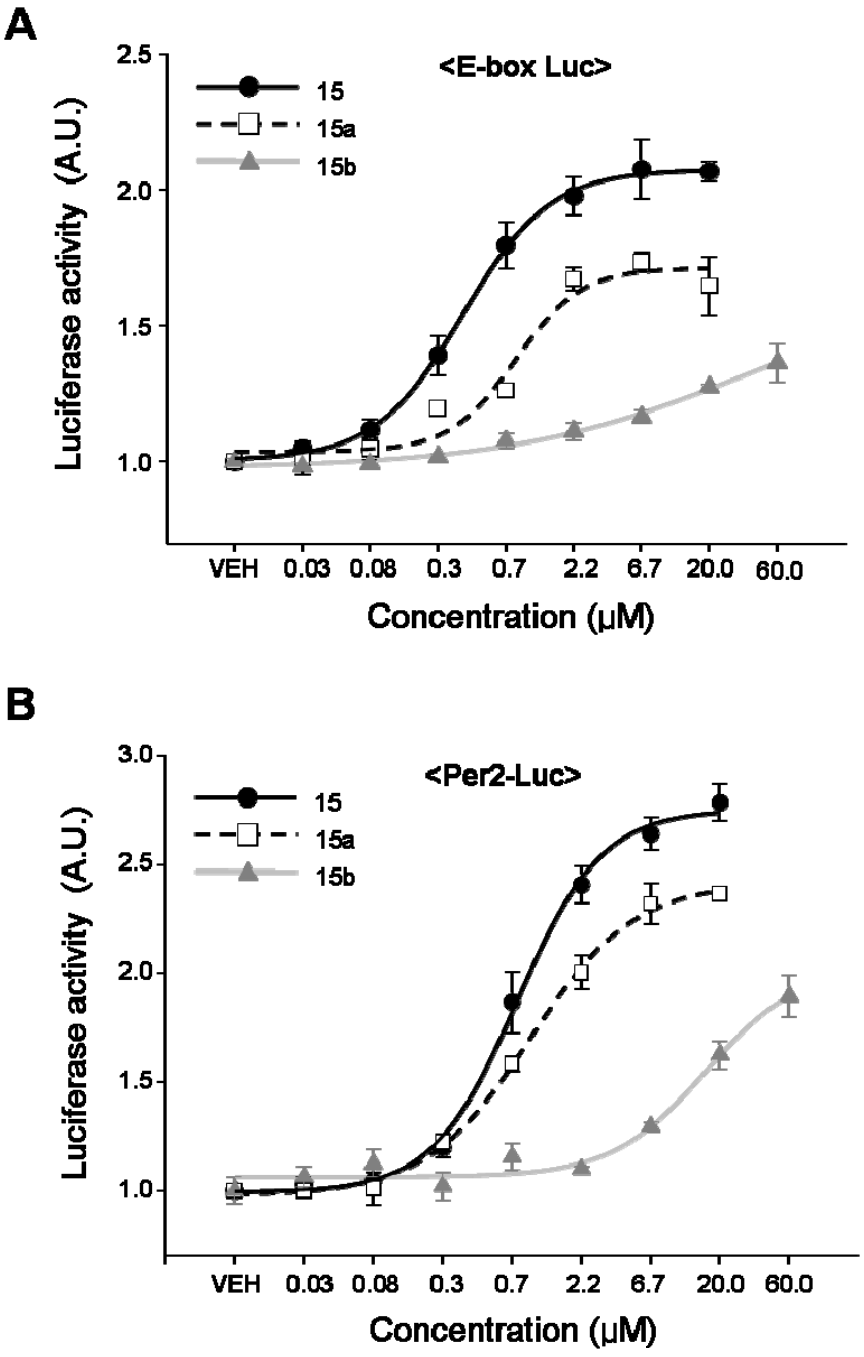
A
<E-box Luc>
15
15a
15b
Luciferase activity (A.U.)
2.5
2.0
1.5
1.0
VEH 0.03 0.08 0.3 0.7 2.2 6.7 20.0 60.0
Concentration (μM)
B
<Per2-Luc>
15
15a
15b
Luciferase activity (A.U.)
3.0
2.5
2.0
1.5
1.0
VEH 0.03 0.08 0.3 0.7 2.2 6.7 20.0 60.0
Concentration (μM)

Figure 11. Identification of binding target of KS15. (A) Pull-down assay of CRY1/2-expressing HEK293T cell lysates. KS15 and KS16 were added for competition. (B) Pull-down assays of core clock proteins. Myc-CLOCK, myc-BMAL1, and V5-PER1/2 were not pulled-down by biotin-conjugated KS15. Bound proteins were visualized by western blot using specific antibodies for the epitopes (anti-FLAG for CRY1/2, anti-myc for CLOCK and BMAL1 and anti-V5 for PER1/2).

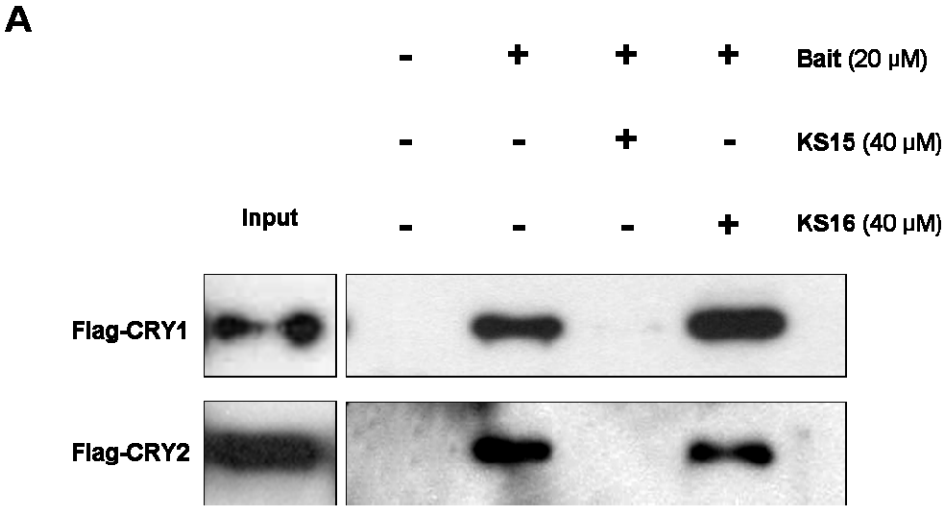
A
- + + + Bait (20 μM)
- - + - KS15 (40 μM)
Input - - - + KS16 (40 μM)
Flag-CRY1
Flag-CRY2

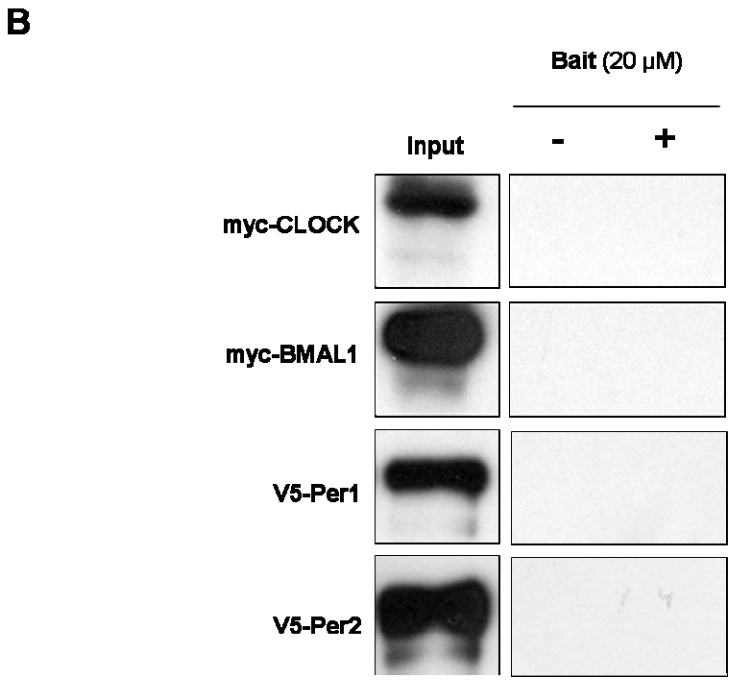
B
Bait (20 μM)
Input - +
myc-CLOCK
myc-BMAL1
V5-Per1
V5-Per2

Figure 12. Pull-down assay of purified CRY1 protein. (A) Purification of CRY1 protein expressed in mammalian cells. Purified CRY1 protein was visualized by Coomassie blue staining (left, CBB staining) or immunolabeling with an anti-FLAG antibody (Right, WB: anti-FLAG). Arrows indicate purified CRY1. More purified fraction of eluate (E2) was used for further experiments. I: Input, F: Flow-through, E1: Eluate fraction 1, E2: Eluate fraction 2. (B) Pull-down assay of purified CRY1 protein. KS15 and KS16 were added for competition.

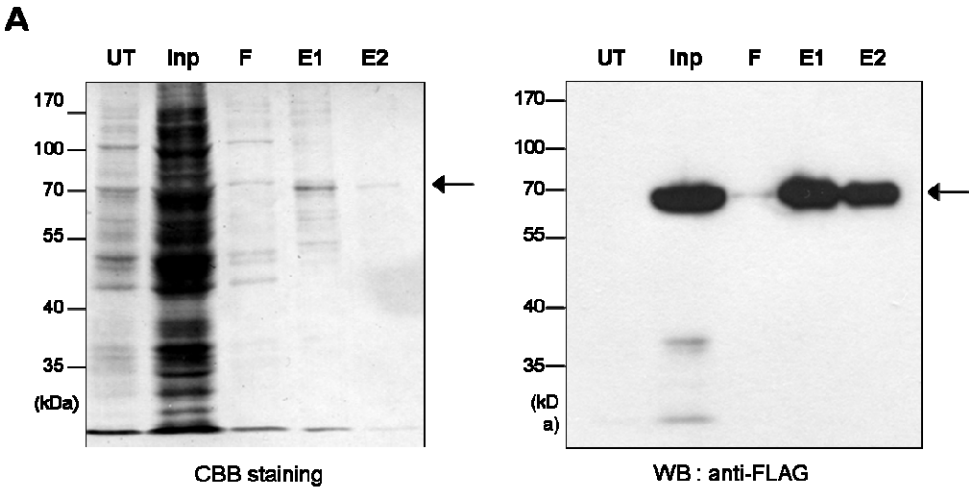
A
UT
Inp
F
E1
E2
170
100
70
55
40
35
(kDa)
CBB staining
WB : anti-FLAG
B
Input
2%
1%
Bait (20 μM)
KS15 (40 μM)
KS16 (40 μM)
Flag-CRY1

Figure 13. Structure of wild-type and functionally inactive mutant (ΔCC-tail) of human CRY1 (hCRY1) and CRY2 (hCRY2) (A) Schematic diagram of the wild-type and ΔCC-tail mutant of hCRY1/2. The N-terminal photolyase-like domain of CRYs are evolutionally conserved, and amino acid sequence homology between hCRY1 and hCRY2 is more than 80%, but the C-terminal extension domains of hCRY1/2 lack sequence homology. The putative coiled-coil domain (CC domain) within hCRY1 and hCRY2 reside at the start of the C-terminal extension domain. (B) Sequence alignment of the mouse and human CRYs: mouse CRYs (mCRYs) and human CRYs (hCRYs). We analyzed sequence homology of mouse and human CRYs by using CLUSTAL Omega (1.2.0) multiple sequence alignment software (Sievers et al., 2011). Putative CC domain and C-terminal extension domain of human CRYs were identified by comparing with predicted C-terminal structure of mCRY1/2 in previous study (Czarna et al., 2011). Unlike C-terminal extension domains, predicted CC domains are highly conserved among the species and subtypes.

A

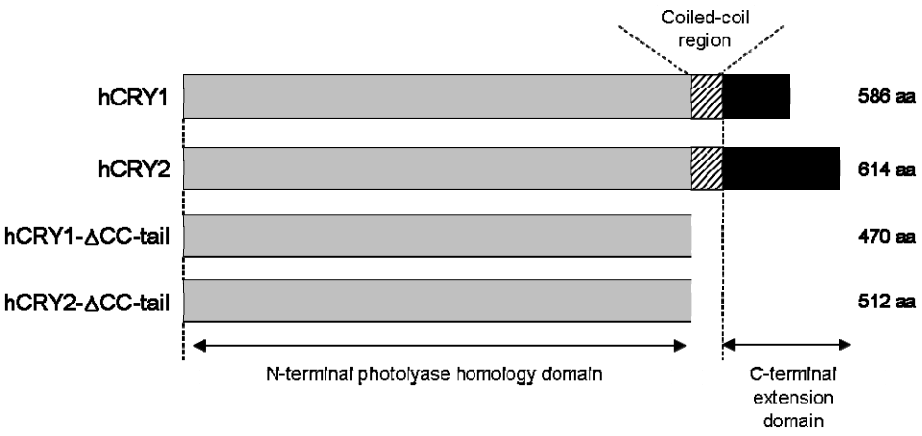
Coiled-coil region
hCRY1
586 aa
hCRY2
614 aa
hCRY1-ΔCC-tail
470 aa
hCRY2-ΔCC-tail
512 aa
N-terminal photolyase homology domain
C-terminal extension domain

B

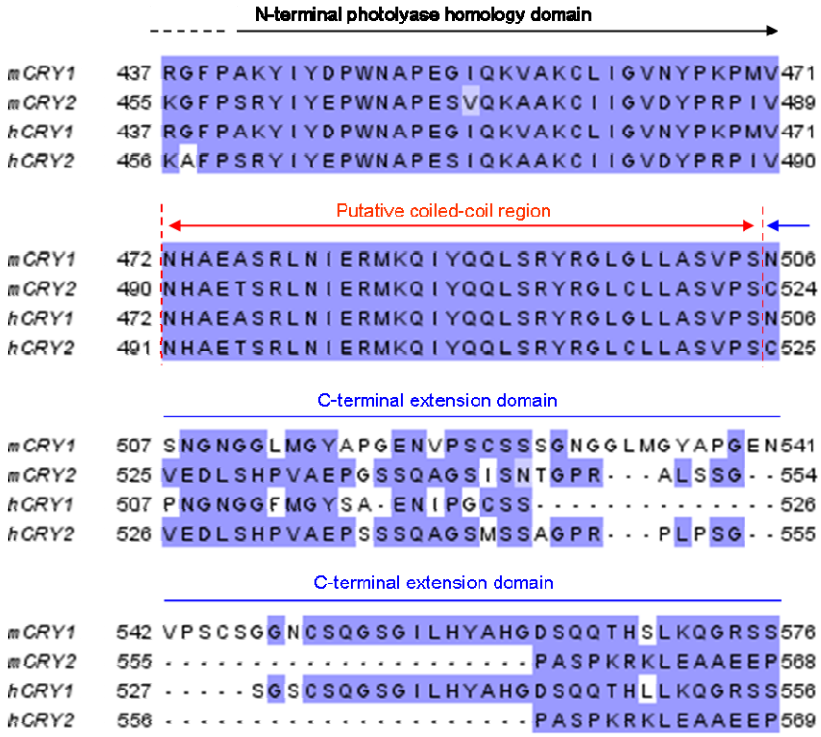
N-terminal photolyase homology domain
mCRY1 437 RGFPAKYIYDPWNAPEGIQKVAKCLIGVNYPKPMV 471
mCRY2 455 KGFPSRYIYEPWNAPESVQKAAKCIIGVDYPRPIV 489
hCRY1 437 RGFPAKYIYDPWNAPEGIQKVAKCLIGVNYPKPMV 471
hCRY2 456 KAFPSRYIYEPWNAPESIQKAAKCIIGVDYPRPIV 490
Putative coiled-coil region
mCRY1 472 NHAEASRLNIERMKQIYQQLSRYRGLGLLASVPSN 506
mCRY2 490 NHAETSRLNIERMKQIYQQLSRYRGLCLLASVPSC 524
hCRY1 472 NHAEASRLNIERMKQIYQQLSRYRGLGLLASVPSN 506
hCRY2 491 NHAETSRLNIERMKQIYQQLSRYRGLCLLASVPSC 525
C-terminal extension domain
mCRY1 507 SNGNGGLMGYAPGENVPSCSSSGNGGLMGYAPGEN 541
mCRY2 525 VEDLSHPVAEPGSSQAGSISNTGPR---ALSSG--554
hCRY1 507 PNGNGGFMGYSA-ENIPGCSS--------------526
hCRY2 526 VEDLSHPVAEPSSSQAGSMSSAGPR---PLPSG--555
C-terminal extension domain
mCRY1 542 VPSCSGGNCSQGSGILHYAHGDSQQTHSLKQGRSS 576
mCRY2 555 ----------PASPKRKLEAAEEP 568
hCRY1 527 -----SGSCSQGSGILHYAHGDSQQTHLLKQGRSS 556
hCRY2 556 ----------PASPKRKLEAAEEP 569

Figure 14. Pull-down assay of mutant CRY1/2. Wild-type and ΔCC-tail mutant of CRY1/2 were individually transfected into HEK293T cell. Whole-cell lysates were harvested for pull-down assay. Note that both ΔCC-tail mutant of CRY1/2 were failed to interact with biotin-conjugated KS15, while wild-type of CRY1/2 successfully bind with bait. V: vehicle (DMSO), B: bait.

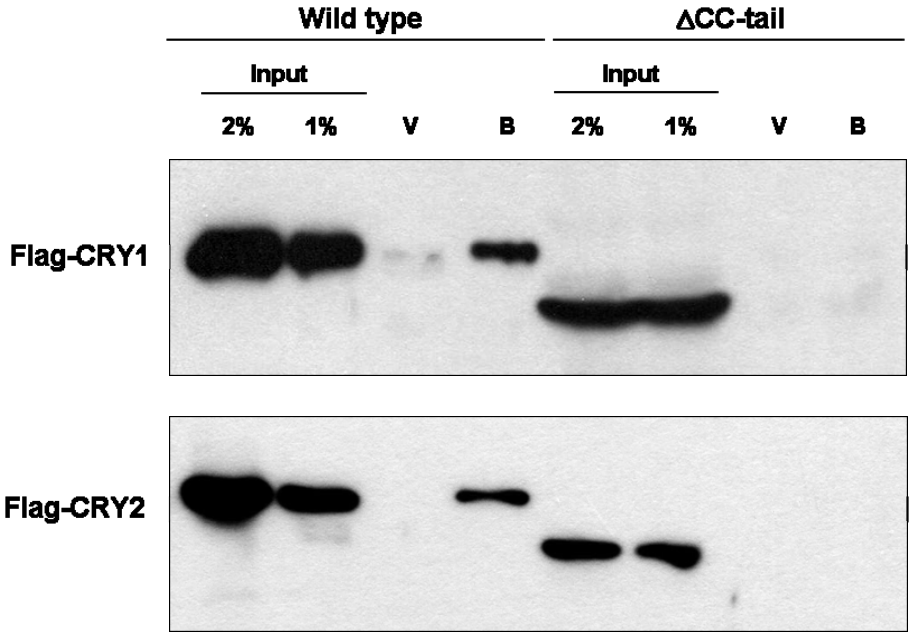
Wild type
ΔCC-tail
Input
Input
2%
1%
V
B
2%
1%
V
B
Flag-CRY1
Flag-CRY2

Figure 15. CRYs-dependent actions of KS15. (A) E-box-Luc reporter activity. Relative *Per1* (B), *Per2* (C) and *Rev-erbα* (D) mRNA expression in WT or CRYs-deficient MEF. ***p* < 0.01 *vs.* Vehicle, ††*p* < 0.01 *vs.* WT with the same treatment. Data are presented as mean ± S.E.M. (n = 4 for each group).

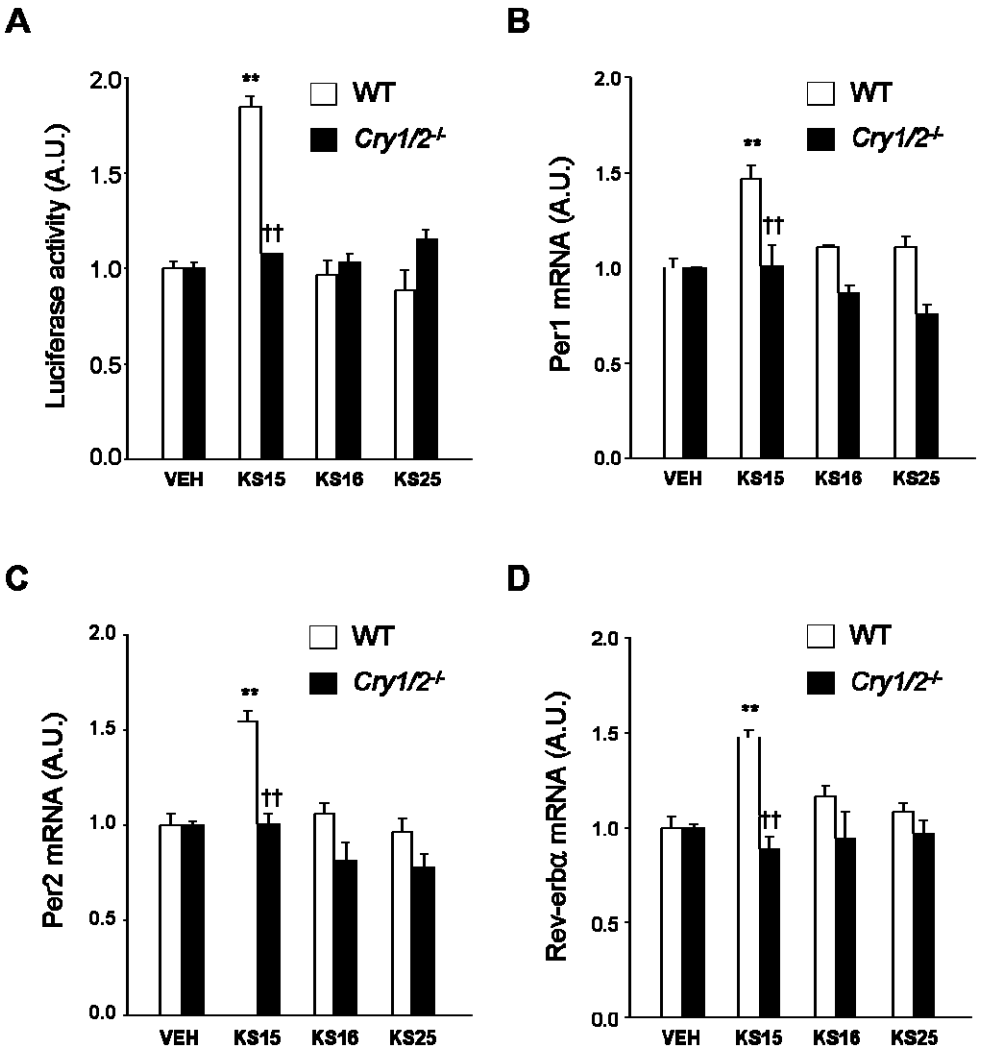
A
B
C
D
WT
Cry1/2-/-
Luciferase activity (A.U.)
Per1 mRNA (A.U.)
Per2 mRNA (A.U.)
Rev-erbα mRNA (A.U.)
2.0
1.5
1.0
0.5
0.0
**
††
VEH
KS15
KS16
KS25

Figure 16. Effect of KS15 on the oscillation of Per2-Luc in fibroblasts. The results of real-time bioluminescence recording are represented in (A) raw or (B) detrended data format. Treatment of KS15 after synchronized by dexamethasone (DEX) decreased Per2-Luc oscillation amplitude compared to the vehicle group. Data are representative of at least five independent experiments.

A

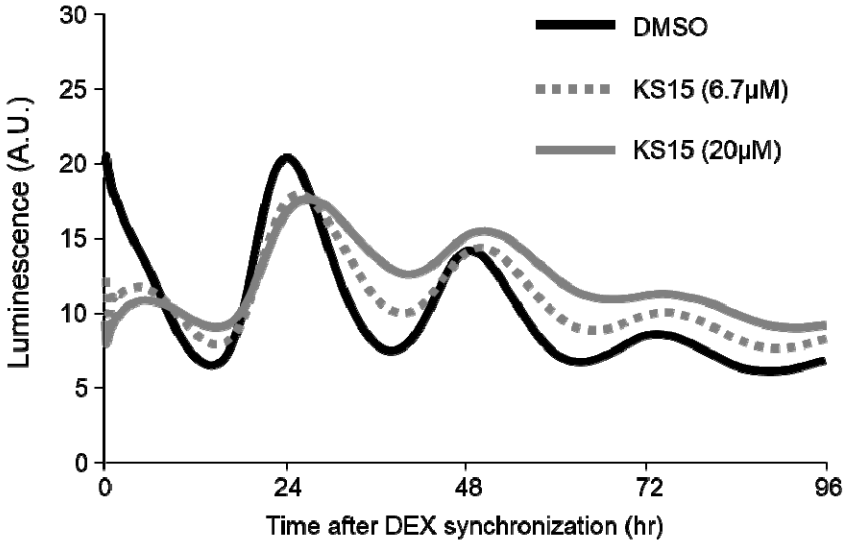
30
25
20
15
10
5
0
Luminescence (A.U.)
0
24
48
72
96
Time after DEX synchronization (hr)
DMSO
KS15 (6.7μM)
KS15 (20μM)

B

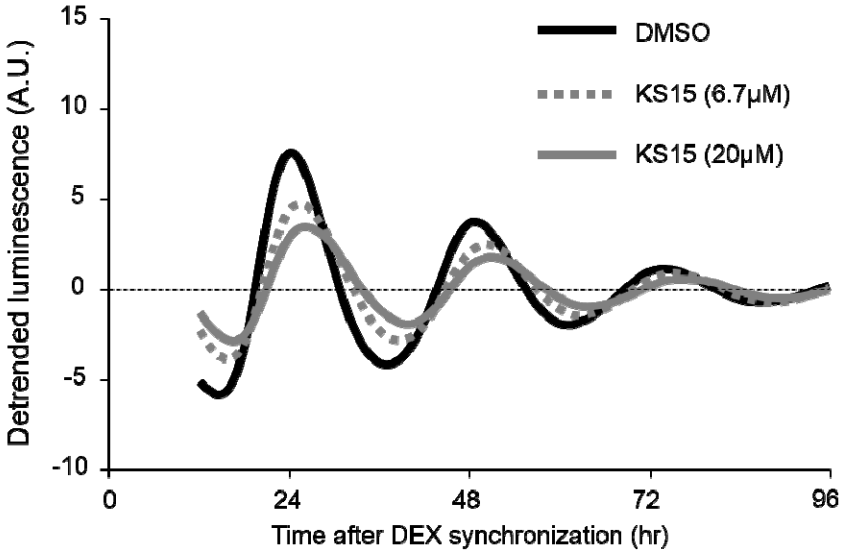
15
10
5
0
-5
-10
Detrended luminescence (A.U.)
0
24
48
72
96
Time after DEX synchronization (hr)
DMSO
KS15 (6.7μM)
KS15 (20μM)

Table 2. Circadian oscillation of Per2-Luc in fibroblasts following treatment with KS15. Statistical analysis of circadian profiles generated by Per2-Luc reporters in fibroblast cell. Average periods were calculated as the mean ± S.E.M. of the inter-peak intervals among the four peaks. Relative amplitudes were calculated as the mean ± S.E.M. of each peak's amplitudes, which were normalized by the amplitudes of the vehicle-treated group. Areas under the curves (AUC) represent the percentage of the vehicle-treated group in raw data format. Each experiment was repeated five times.

Compound	Concentration	Period (hour)	Relative amplitude (%)	AUC (%)
Vehicle (DMSO)	0.20%	24.1 ± 0.03	100	100
KS15	6.7 μM	23.9 ± 0.07	54.2 ± 3.9	111.3 ± 3.0
	20 μM	23.7 ± 0.08	42.6 ± 3.5	115.9 ± 1.7

Figure 17. Effect of KS15 on the oscillation of Bmal1-dLuc in fibroblasts. The results of real-time bioluminescence recording are represented in (A) raw or (B) detrended data format. Treatment of KS15 after DEX synchronization decreased Bmal1-dLuc oscillation amplitude compared to the vehicle group. Data are representative of at least three independent experiments.

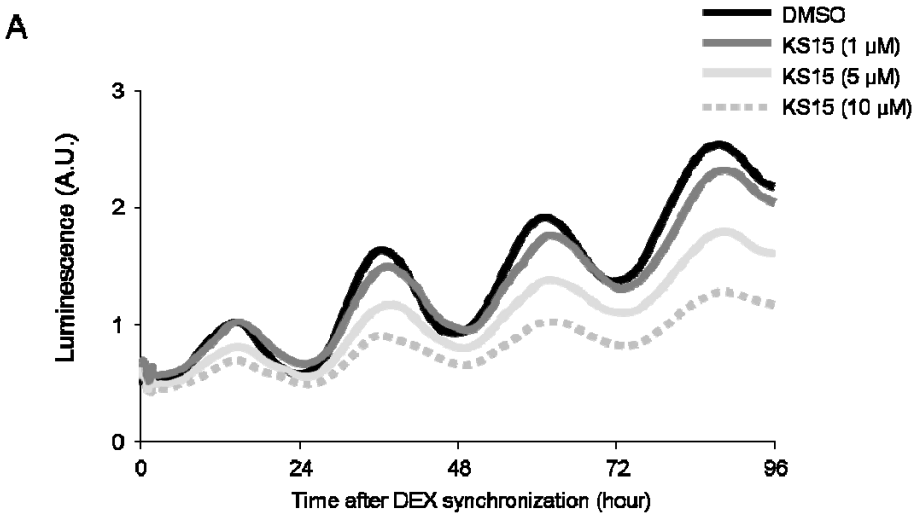
A
DMSO
KS15 (1 μM)
KS15 (5 μM)
KS15 (10 μM)
Luminescence (A.U.)
3
2
1
0
0
24
48
72
96
Time after DEX synchronization (hour)

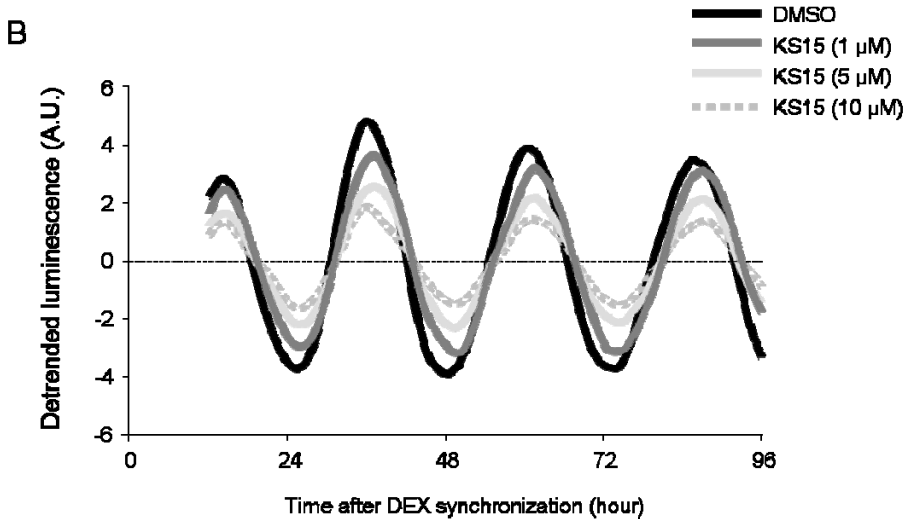
B
DMSO
KS15 (1 μM)
KS15 (5 μM)
KS15 (10 μM)
Detrended luminescence (A.U.)
6
4
2
0
-2
-4
-6
0
24
48
72
96
Time after DEX synchronization (hour)

Table 3. Circadian oscillation of Bmal1-dLuc in fibroblasts following treatment with KS15. Statistical analysis of circadian profiles generated by Bmal1-dLuc reporters in fibroblast cell. Average periods were calculated as the mean ± S.E.M. of the inter-peak intervals among the four peaks. Relative amplitudes were calculated as the mean ± S.E.M. of each peak's amplitudes, which were normalized by the amplitudes of the vehicle-treated group. AUC represent the percentage of the vehicle-treated group in raw data format. Each experiment was repeated three times.

Compound	Concentration	Period (hour)	Relative amplitude (%)	AUC (%)
Vehicle (DMSO)	0.20%	24.6 ± 0.1	100	100
KS15	1 μM	24.5 ± 0.2	71.5 ± 8.3	90.3 ± 2.6
	5 μM	24.5 ± 0.04	60.8 ± 2.9	81.8 ± 2.2
	10 μM	24.1 ± 0.2	39.0 ± 1.7	69.4 ± 3.9

Figure 18. Effect of shCRY1/2 on E-box mediated transcription. E-box-Luc reporter and shCRY1/2 constructs (sc-44835-SH and sc-44836-SH, Santa Cruz Biotechnology) were co-transfected in cultured fibroblasts (NIH3T3) and incubated for 48 hours. Each plasmids were transfected 100 ng per well. After that, cells were harvested and analyzed with luciferase assays. Data are presented as mean ± S.E.M. (n = 3). **: $p < 0.01$ compared with cells transfected with the blank construct.

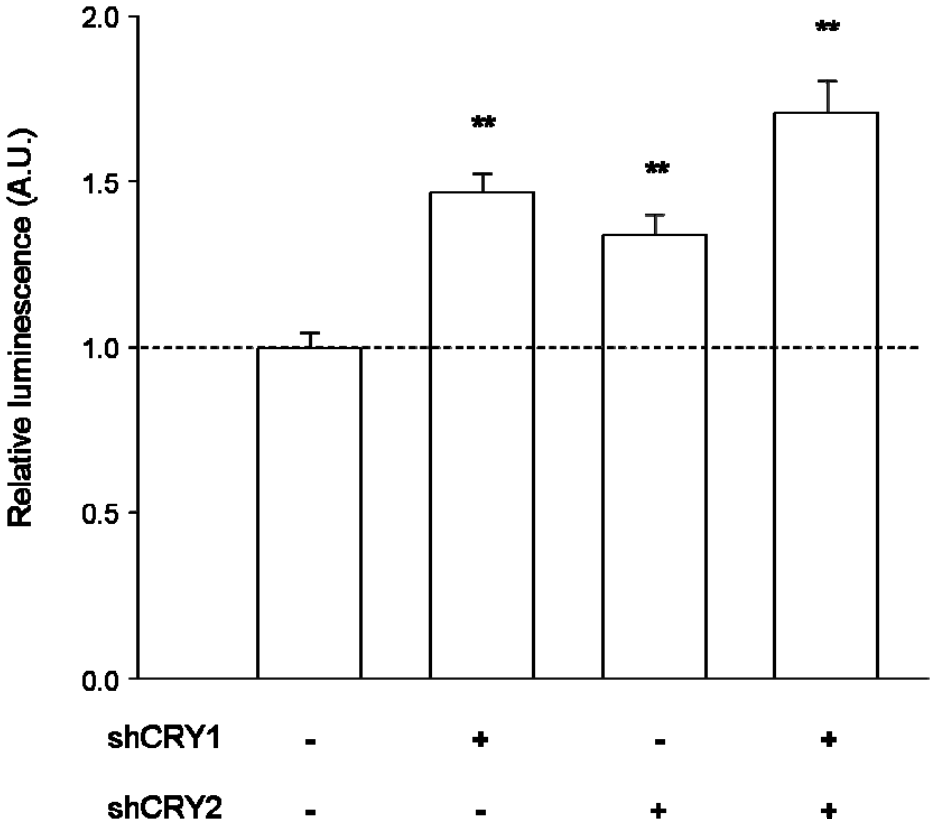
2.0
1.5
1.0
0.5
0.0
Relative luminescence (A.U.)
**
**
**
shCRY1 - + - +
shCRY2 - - + +

Figure 19. The effect of CRY subtype knockdown on Bmal1-dLuc oscillation in fibroblasts. Bmal1-dLuc reporter and shRNA constructs were co-transfected in cultured fibroblasts (NIH3T3) and incubated for 48 hours. Then, cells were synchronized by treatment with DEX, and emitting bioluminescence in the presence of the luciferin substrate was monitored every 10 min for 96 hours. The real-time bioluminescence recording results are represented in raw (A) and detrended data (B) formats. pU6 plasmid was co-transfected with Bmal1-dLuc as a blank construct. Data are representative of at least three independent experiments.

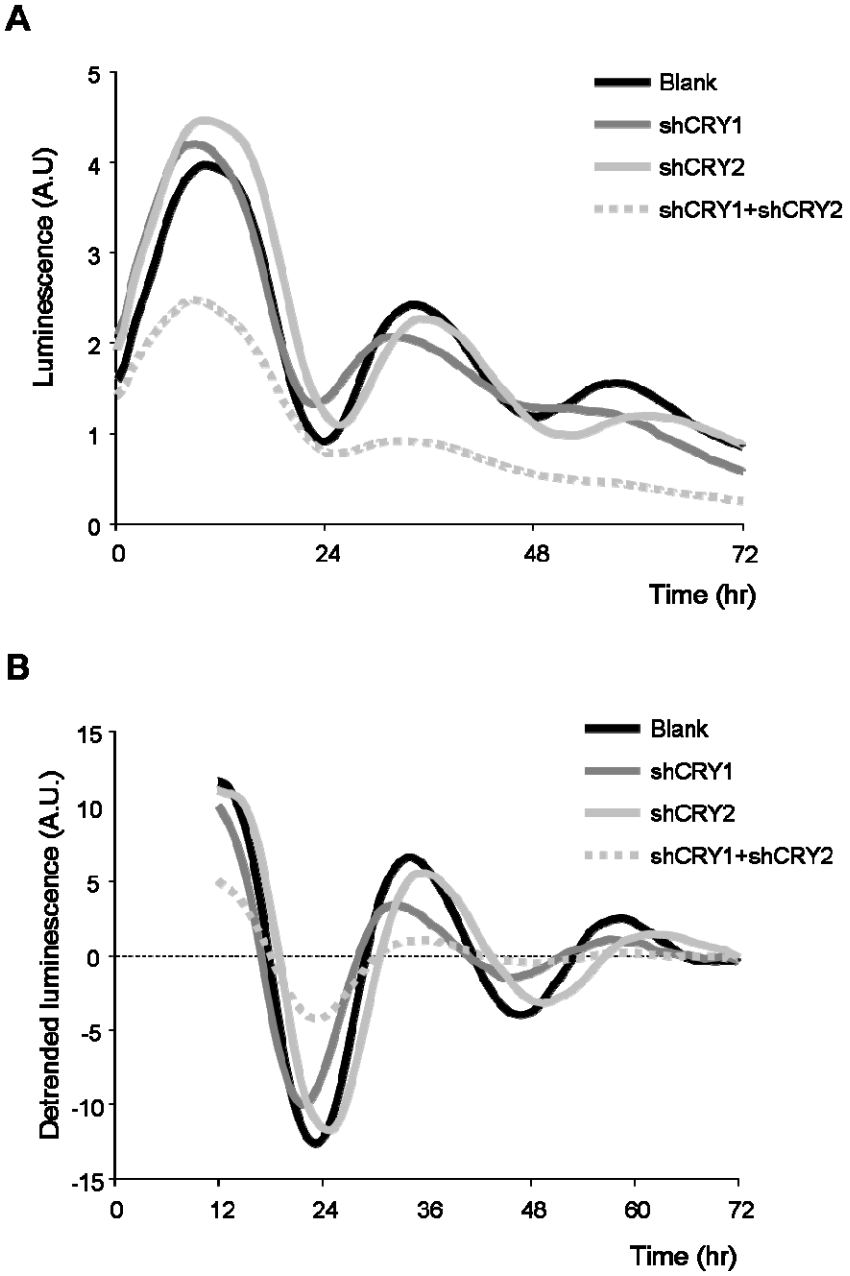
A
Luminescence (A.U)
5
4
3
2
1
0
0
24
48
72
Time (hr)
Blank
shCRY1
shCRY2
shCRY1+shCRY2
B
Detrended luminescence (A.U.)
15
10
5
0
-5
-10
-15
0
12
24
36
48
60
72
Time (hr)
Blank
shCRY1
shCRY2
shCRY1+shCRY2

Table 4. Circadian oscillation of Bmal1-dLuc with co-transfection of shCRY1/2. Statistical analysis of circadian profiles generated by Bmal1-dLuc reporters in fibroblast cell following co-transfection with shCRY1 or shCRY2. Note that single transfection of shCRY1 or shCRY2 were mainly affect on period length whereas co-transfection of shCRY1/2 were not significantly alter period length but severely repressed amplitude of the rhythm. Average periods were calculated as the mean ± S.E.M. of the inter-peak intervals among the four peaks. Relative amplitudes were calculated as the mean ± S.E.M. of each peak's amplitudes, which were normalized by the amplitudes of the vehicle-treated group. AUC represent the percentage of the vehicle-treated group in raw data format. Each experiment was repeated three times.

Construct	Amounts	Period (hour)	Relative amplitude (%)	AUC (%)
Blank	-	23.3 ± 0.2	100	100
shCRY1	200 ng	22.1 ± 0.2	81.6 ± 6.6	83.1 ± 3.8
shCRY2	200 ng	24.9 ± 0.4	96.7 ± 3.4	93.8 ± 2.9
shCRY1 +shCRY2	100 ng + 100 ng	23.6 ± 0.3	46.9 ± 2.8	51.3 ± 1.9

Figure 20. The dose-dependent effect of CRY1/2 double knockdown on Bmal1-dLuc oscillation in fibroblast. Gradually increasing total amounts of shRNA of CRY1/2 were monitored to examine the dose-dependent effect of shCRY1/2 (shCRY1:shCRY2 = 1:1). Procedures for transfection, synchronization and bioluminescence monitoring were same as the experiments in Fig 18. The real-time bioluminescence recording results are represented in raw (A) and detrended data (B) formats. Data are representative of at least three independent experiments.

A

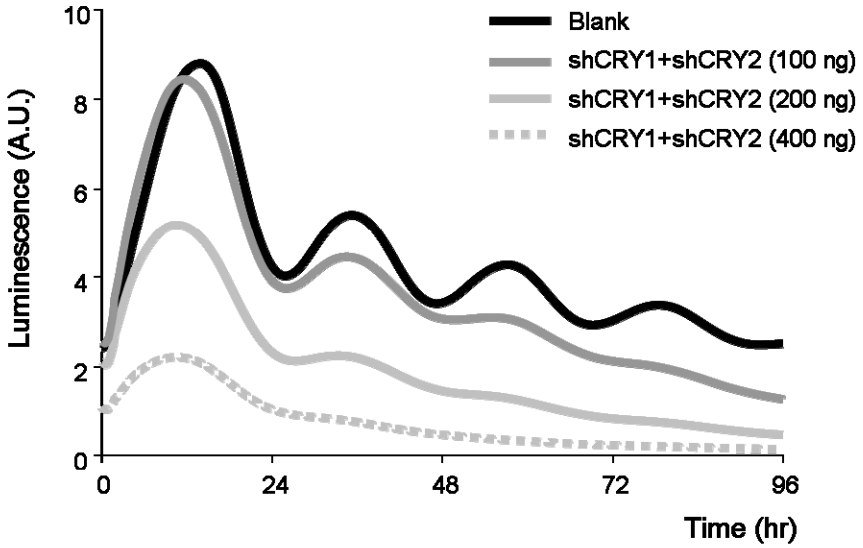
Blank
shCRY1+shCRY2 (100 ng)
shCRY1+shCRY2 (200 ng)
shCRY1+shCRY2 (400 ng)
Luminescence (A.U.)
10
8
6
4
2
0
0
24
48
72
96
Time (hr)

B

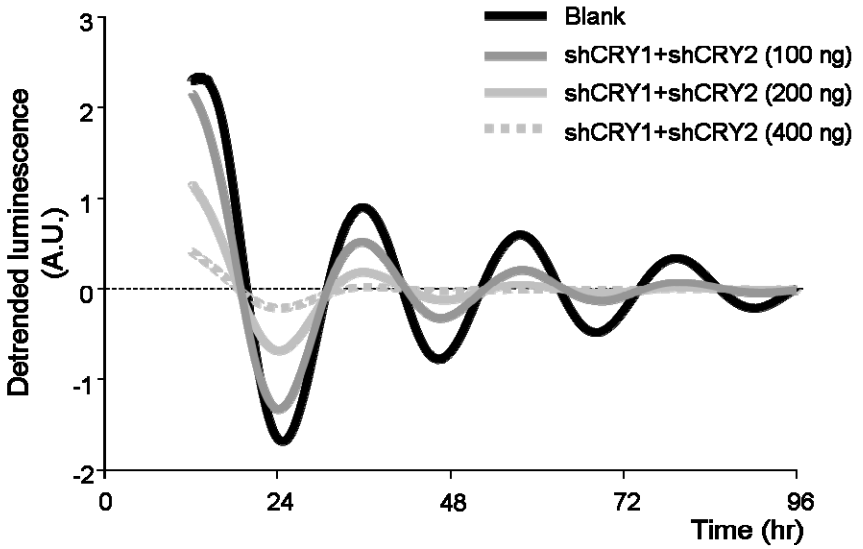
Blank
shCRY1+shCRY2 (100 ng)
shCRY1+shCRY2 (200 ng)
shCRY1+shCRY2 (400 ng)
Detrended luminescence (A.U.)
3
2
1
0
-1
-2
0
24
48
72
96
Time (hr)

Table 5. The dose-dependent effect of CRY1/2 double knockdown on Bmal1-dLuc oscillation in fibroblast. Statistical analysis of circadian profiles that generated by Bmal1-dLuc reporter in fibroblast following co-transfection of both shCRY1 and shCRY2. Note that shCRY1/2 mainly affect on amplitude of Bmal1-dLuc rhythm in dose-dependent manner while period length were not significantly altered. Average periods were calculated as the mean ± S.E.M. of the inter-peak intervals among the four peaks. Relative amplitudes were calculated as the mean ± S.E.M. of each peak's amplitudes, which were normalized by the amplitudes of the vehicle-treated group. AUC represent the percentage of the vehicle-treated group in raw data format. Each experiment was repeated three times.

Construct	Amount	Period (hour)	Relative amplitude (%)	AUC (%)
Blank	-	23.6 ± 0.1	100	100
shCRY1 +shCRY2	100 ng (50 ng + 50 ng)	23.7 ± 0.07	61.9 ± 6.6	74.5 ± 2.7
	200 ng (100 ng + 100 ng)	24.4 ± 0.1	41.2 ± 6.8	51.6 ± 2.1
	400 ng (200 ng + 200 ng)	23.8 ± 0.3	30.3 ± 6.4	26.5 ± 2.9

Figure 21. *In vivo* administration of KS15. Intracerebroventricular (ICV) microinjection of KS15 alters period and phase of activity rhythm. DMSO (vehicle, 0.5 μl) or KS15 (140 μg / kg) of were administrated into mice by single ICV bolus microinjection at two hour before activity onset. (A) Representative 30-day wheel-running double-plot actograms. After 10 days under normal light:dark = 12 hours:12 hours (LD), recording of 10 days under constant dark (FRP, Free-running period), and 10 days after injection of DMSO or KS15 (ICV injection) were shown here. The constant dark phases are illustrated by gray shadows and timings of injection are marked in blank circles within the image. (B) Periods from wheel running activity rhythm of mice with DMSO or KS15 injection. Periods of activity rhythms were determined by the cosinor fitting analysis of 7-day profiles during FRP and post-injection profiles (ICV injection). (**:$p<0.01$ vs vehicle administrated group) (C) Phase-shifts profiles induced by injection of DMSO or KS15. (*:$p<0.05$ vs vehicle administrated group) (D) Relative wheel running activity during FRP and post-injection period. Wheel running activity during entrainment period defined as 100%. All data were presented as the mean ± S.E.M. from three independent experiments.

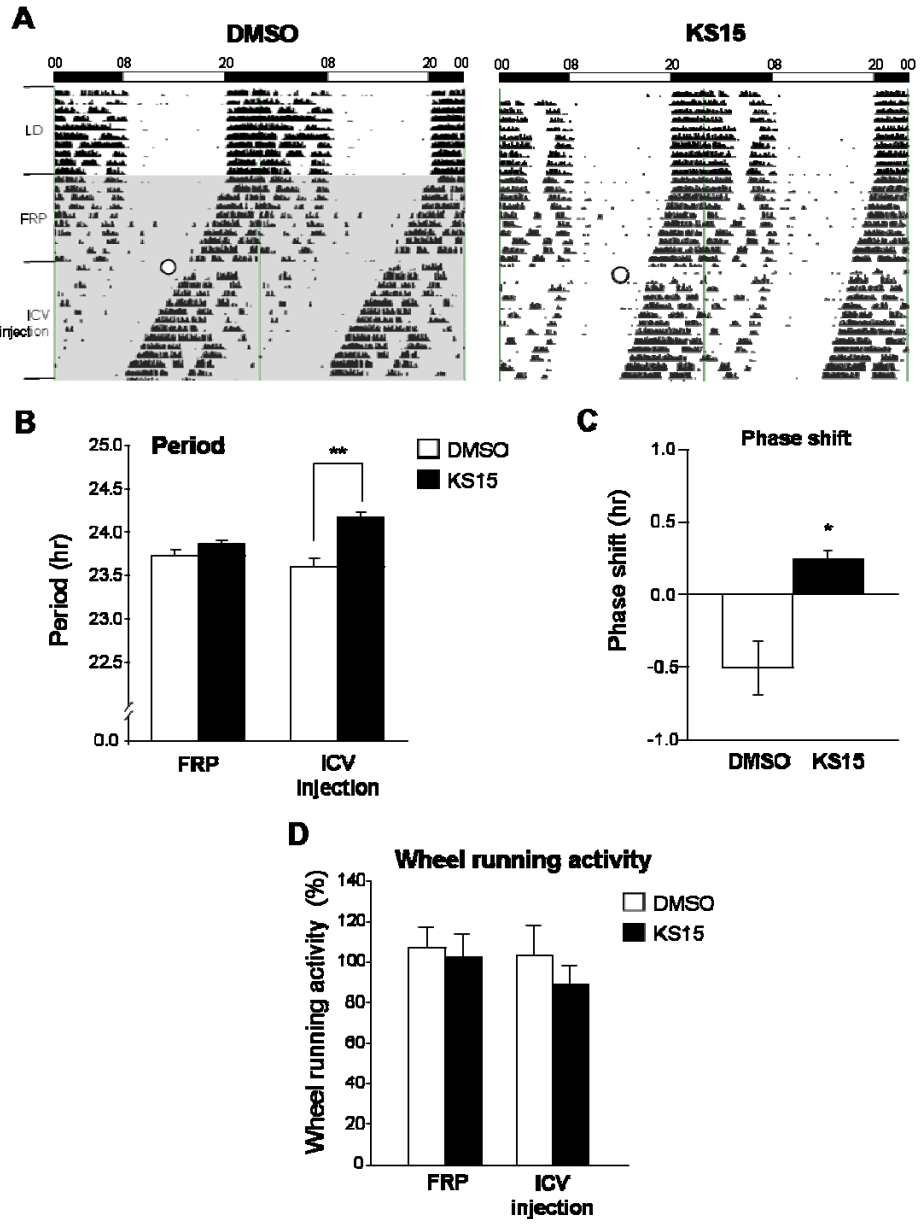
A
DMSO
KS15
00
08
20
08
20
00
LD
FRP
ICV injection
B
Period
**
DMSO
KS15
Period (hr)
25.0
24.5
24.0
23.5
23.0
22.5
0.0
FRP
ICV injection
C
Phase shift
*
Phase shift (hr)
1.0
0.5
0.0
-0.5
-1.0
DMSO
KS15
D
Wheel running activity
Wheel running activity (%)
140
120
100
80
60
40
20
0
DMSO
KS15
FRP
ICV injection

DISCUSSION

The present study was designed to develop a novel synthetic modulator for core clock genes and their functions. In last decades, several synthetic compounds were identified as circadian clock modulators. For example, several agonists and antagonists of REV-ERBα were identified recently and those modulators were used for many physiological and clinical research. SR9009 and SR9011 were identified as REV-ERBα/β agonists and *in vivo* application of these agonists induced enhancement of metabolic functions under normal light-dark cycle as well as affect circadian rhythm without light cues (Solt et al., 2012). This study suggests that circadian clock and its regulatory mechanisms can be novel therapeutic targets for treatment of circadian rhythm-related disorders. However, despite the physiological and clinical importance of circadian rhythms, synthetic compounds that directly regulate E-box mediated transcriptional activity have not been reported yet. Development of circadian clock modulator is immerging field during last decades and many compounds were reported as circadian clock modulator. However, most of them were targeting other than core clock genes (CLOCK, BMAL1, PER1/2, CRY1/2) (Chen et al., 2013). In the present study, I identified and characterized a novel small molecule called as KS15 that directly binds to CRY1/2 and inhibits its repressive function, thereby activating E-box-mediated transcriptional activity. Periodic gene transcription by the CLOCK:BMAL1 heterodimer plays a pivotal role in the cyclic mRNA accumulation of numerous clock-controlled genes, as well as core clock components, such as *Pers* and *Crys*. Therefore, KS15 can be a

novel approach for studying detailed mechanism as well as investigating implication of molecular circadian clockwork on physiology and behavior.

To discover a novel small molecule modulator of the molecular clock, I designed a new cell-based screening method based on E-box-mediated transcriptional activity, the main output of molecular circadian clock. In this method, I used the artificial luciferase reporters selectively regulated by CLOCK:BMAL1 heterodimer and the cultured cell lines with stable expression of these reporters. Establishment of stable cell lines is an important strategy because these stable cell lines are ready-to-use materials for massive screening of chemical library. I also designed the secondary screening step by using BMAL1 knock-out fibroblasts for optimizing selectivity of hit chemicals. Taken together, this two-step screening strategy is a highly efficient method for development of a novel circadian clock modulator.

It should be noted that the hit chemicals (KS11a, KS11b, KS15) from the screening turned out to be stereoisomers of PPAR (peroxisomal proliferator-activated receptor) agonists in previously study (Suh et al., 2008). In the previous study, stereoisomers containing *(S)*-ethoxypropanoic acid (KS11a', KS11b' and KS15') shown to have higher activities on both PPARα and PPARγ than analogs containing *(R)*-ethoxypropanoic acid (Suh et al., 2008). Thus, I compared the effects to the hit chemicals (KS11a, KS11b, KS15) and their stereoisomers (KS11a', KS11b' and KS15') on E-box- or PPAR responsive elements-mediated transcriptional activities for clarification of specificity. As shown in Figure 7C and Table 1, the *(S)*-

ethoxypropanoic acid-containing stereoisomers were much less potent than the hit chemicals on E-box-mediated transcription. By contrast, they exhibited higher enhancing activities on a luciferase reporter driven by multiple PPAR responsive elements than candidates in present study (Fig 8). Taken together, these finding strongly suggest the selectivity of the candidate compound including KS15 in controlling E-box-mediated transactivation.

Notably, the very recently developed compound KL001 reported as a small molecule directly targeting the CRY1/2 (Hirota et al., 2012). But unlike KS15, KL001 represses core loop activity by strengthening the stability of CRY1/2, whereas KS15 enhances core loop activity by inhibiting repressive activity of CRY1/2. Also, KS15 has a distinct scaffold than KL001. KS15 contains 2-ethoxypropanoic acid and two aryl rings connected by an oxime ether linker, while KL001 has a carbazole scaffold (Hirota et al., 2012). More importantly, KL001 has period lengthening changing effect, whereas KS15 is only effective on the amplitude of circadian clock. These differences suggest that KS15 has distinctive mechanism of action than previously reported KL001. Although I examined direct binding of KS15 with CRY1/2, detailed mechanisms for binding of KS15 with CRY proteins remains to be determined.

It is noteworthy that many small compounds such as longdaysin (Hirota et al., 2010) or KL001 (Hirota et al., 2012) were reported as circadian modulator with period changing effect, while KS15 is only effective on the amplitude of circadian clock. Previous studies suggested that single

knockdown of CRY1 leads to shortened periods, while CRY2 knockdown shows lengthened periods of the rhythms generated by Bmal1 promoter-driven luciferase activities (Zhang et al., 2009; Baggs et al., 2009). However, these rhythms were severely attenuated in the case of double knockdown of both CRY1/2 (Baggs et al., 2009). Because KS15 can interact with both CRY1/2 (Fig 18), I hypothesized that KS15 inhibits both CRY1/2 and thereby attenuates the rhythm rather than changing the period length. To prove this, I analyzed the rhythm of Bmal1-dLuc reporter activity with knockdown of each CRY subtype using shRNA. In agreement with previous studies (Zhang et al., 2009; Baggs et al., 2009), single knockdown of CRY1 or CRY2 altered period length, while knockdown of both CRY1/2 severely attenuated amplitude of the rhythm in a dose-dependent manner without significantly changing the period length (Fig 19, Fig 20 and Table 3). These data suggest that KS15 modulates clock-controlled gene transcription by inhibiting both CRY1/2 and thereby attenuates the rhythm without affecting the period. Also, these findings can explain why KS15 did not affect the period length like KL001 (Hirota et al., 2012).

However, unlike results from fibroblast cells, *in vivo* ICV administration of KS15 into mouse causes lengthening of period and delaying of circadian phase. This controversial result can be explained by different regulatory mechanism of central and peripheral clock. It is well-known that even non-SCN cells are autonomous oscillators, however, they may desynchronize from one another in the absence of the SCN as they lack local coupling within tissues (Nagoshi et al., 2004; Welsh et al., 2004, Stratmann and Schibler 2006). In contrast, the neuronal network within the SCN couples its

component single-cell oscillators to produce a coherent circadian oscillation at the tissue level (Aton and Herzog 2005; Welsh et al., 2010). Interestingly, experimental evidences suggest that CRY1 is required for sustained circadian rhythms in dissociated SCN neurons or fibroblasts but not in organotypic SCN slices or at the behavioral level, whereas CRY2 is not required at any of these levels (Liu et al., 2007; Evans et al., 2012). CRY1 is known as a stronger repressor than CRY2, and that this can serve as a biochemical basis for differences in CRY knockout phenotypes (Khan et al., 2012; Hirota et al., 2012). These different natures of central and peripheral clock, especially intracellular coupling of SCN neurons can be reasons for different responses of KS15 to fibroblast and *in vivo*. However, this experiment was performed only in a single dose of KS15 and single injection timing. Analysis of daily activity rhythms with injection of various concentration of KS15 or multiple injection timing will be required for the further investigation.

In conclusion, I developed a novel antagonist for CRY1/2 and validated this compound as circadian modulator for both *in vitro* and *in vivo*. Further optimization of KS15**,** along with functional studies may lead to new therapeutics for a variety of circadian and metabolic disorders develop or linked with the cellular actions of CRYs.

CHAPTER 2

Evaluation of anti-tumor activity of Cryptochrome inhibitor on human breast cancer cell line

ABSTRACT

Among circadian rhythm related tumors, breast cancer is one of the well-known cases that are caused by chronic exposure to disrupting stimuli, such as shift work, on the circadian clock. Cryptochromes (CRYs) are a key component of the molecular circadian clockwork. Increasing evidence has indicated that CRYs affect a variety of genes related with cell cycle regulation and anti-tumor activity. Interestingly, recent studies suggest that inhibition of CRYs enhanced DNA damage response and initiation of apoptosis as a response to genotoxic stress. In addition, mutations within human CRY2 can be risk factors for initiation of breast cancer. Also, expression profiles of CRY2 are differently regulated between normal and breast cancer tissues in human patients. It appears that CRYs can be a novel therapeutic target for the treatment of breast cancer. In the present study, I evaluated the anti-tumor activity of KS15 on human breast cancer cells. KS15 inhibited the proliferation of MCF-7 cells in dose-dependent manner but not in other cell lines (MCF-10A and MDA-MB-231). Sensitivities for the anti-tumor drugs were enhanced only in MCF-7 when co-treated with KS15. On the other hand, adhesion ability on extracellular matrix and metastatic activity were not significantly affected by treatment of KS15. These findings suggest that pharmacological inhibition of CRYs by KS15 has an anti-proliferative effect and increase chemosensitivity to anti-tumor drugs on a specific type of breast cancer. Further investigation on the detailed mechanism and optimization of this anti-tumor activity of KS15 can be a novel therapeutic treatment for breast cancer.

Keywords: Breast cancer, Cryptochrome; Circadian rhythm; Small molecule; Anti-tumor activity

INTRODUCTION

The circadian rhythm has a fundamental role in regulation of physiology and behavior and almost all of biological processes in human are influenced by the circadian clock. Thus, disruption of circadian clock is associated with a variety of adverse affects, including the promotion of oxidative stress and alterations in immune function (Navara et al., 2007). Increasing evidence also suggests that disturbance of circadian rhythm play a major role in various kinds of tumorigenesis processes (Lamont et al., 2007; Stevens et al., 2007). Based on these findings, the IARC concluded that shift work that involves circadian disruption is a possible carcinogen in humans (Group 2A) in 2007 (Straif et al., 2007).

Breast cancer is a type of cancer originating from breast tissue and most common cancer in women in developed countries. Recent studies have indicated that incidence of breast cancer increases significantly in women working nightshifts (Schernhammer et al., 2001). Also, disruption of circadian rhythms through constant light exposure increases the formation of spontaneous mammary tumors in rodents (Aubert et al., 1980; Mhatre et al., 1984). These data suggested that development of breast cancer can be evoked by chronic exposure to disrupting stimuli for circadian clock.

The maintenance of circadian rhythm is largely dependent on a set of core circadian clock genes. (Oster, 2006) These genes form a negative and positive feedback loop, which allows tight control of rhythmic expression of clock controlled genes (CCGs), thereby ensuring that products of these genes will be active in right timing of the circadian cycle (Young and Kay, 2001; Reppert and Weaver, 2001). CCGs include essential cell cycle

regulators and tumor suppressors and circadian control of these genes leads to the coupling of cell proliferation with key tissue functions in vivo (Fu et al., 2002; Panda et al., 2002; Matsuo et al., 2003). Disruption of circadian rhythm in cell proliferation is frequently associated with tumor development and progression in mammals (Bjarnason and Jordan, 2000; Smaaland, 1996).

Cryptochrome (CRY) is one of the core clock genes that essential to the maintenance of circadian rhythm. CRY act as main transcriptional repressor in the negative arm of the circadian clock but also CRY involved in cellular proliferation, including roles in DNA damage checkpoint control (Unsal-Kacmaz et al., 2005) and regulation of genes important for cell cycle progression (Gauger and Sancar, 2005; Matsuo et al., 2003). Recent studies suggested that CRY has important roles in DNA damage response and susceptibility to carcinogenesis. Interestingly, genetically depletion of CRY1/2 showed protective effect on cancer-prone phenotype in response to genotoxic stress (Gauger and Sancar, 2005; Ozturk et al., 2008; Lee et al., 2013). In addition, another studies suggested that single-nucleotide polymorphisms of CRY2 as well as methylation within the CRY2 promoter region were significantly associated with postmenopausal breast cancer risk (Hoffman et al., 2010, Cancer Prev Res). Moreover, knockdown of CRY2 in human breast cancer cell line shows adverse effect on regulation of DNA damage repair and the maintenance of genomic stability. (Hoffman et al., 2010, BMC Cancer) Taken together, these findings suggested that functional modulation of CRY can be a novel therapeutic treatment for breast cancer. In the present study, I evaluate anti-tumor activity of KS15 in human breast cancer cells

MATERIALS AND METHODS

Materials KS15 was dissolved at a concentration of 0.02 M in 100% DMSO as a stock solution, stored at -20 °C, and diluted with medium before each experiment. The final DMSO concentration did not exceed 0.2% DMSO throughout the study (in our study, all the control groups are composed of 0.2% DMSO). Heat-inactivated fetal bovine serum (FBS) was obtained by incubation of normal FBS in 60 °C for 30 min. 3-(4,5-dimethylthiazol-2-yl)-2,5-diphenyltetrazolium bromide (MTT) was obtained from Sigma (St. Louis, Missouri). Before use, MTT dissolved in culture media (0.5 mg/ml). Matrigel was purchased from Becton Dickinson Biosciences (San Jose, California).

Cell culture MCF-7 and MDA-MB-231 human breast carcinoma cells were cultured in DMEM (GIBCO, Invitrogen Corp., Carlsbad, California) supplemented with 10% (v/v) FBS in a humidified atmosphere of 5% CO2 at 37 °C. MCF-10A were cultured in complete MEGM (mammary epithelial growth medium, serum-free) purchased from Clonetics (San Diego, CA) and supplemented with 10% (v/v) FBS in a humidified atmosphere of 5% CO2 at 37 °C.

Cell viability Assay Cells were seeded in a 96-well plate at 5×10^4 cells/well and incubated in 100 μL of medium for 24 h. After incubation, the cells were treated with the 0.5 mg/ml solution of MTT dissolved in culture media and the cells were incubated for 4 h. After removing the medium, 100 μl of DMSO was used to dissolve the MTT formazan crystals. Absorbance from each well was measured at 570 nm.

Adhesion assay 96-well cell culture plates were coated with fibronectin solution (0.5 mg/m in PBS) (Sigma, St. Louis, Missouri) overnight. The wells were blocked for 30 min with 0.5% heat-inactivated FBS. Cells were trypsinized and suspended at a final concentration of 5 × 10^5 cells/ml in serum-free medium. 20 μM and 50 μM of KS15 were given to the cells for 24 h before seeding. 100 μl cell suspension was added to the wells and the plates were incubated at 37 °C for 1 hr. Medium was then carefully suctioned out from each well. Each well was washed three times with PBS. The colorimetric MTT-assay was used to determine the number of remaining cells (adherent cells).

Invasion assay The in vitro invasion assays were carried out using Transwell chamber with 10 mm diameter and 8 μm pore size polycarbonate membrane (Corning Costar, Cambridge, Massachusetts) coated with Matrigel (BD Science). Cells were trypsinized and suspended at a final concentration of 5 × 10^5 cells/ml in serum-free DMEM medium. 20 μM and 50 μM of KS15 were given to the cells for 24 h before seeding. Cell suspension was added into each upper chamber of transwell. The bottom chamber contained medium with 5% FBS to serve as a chemoattractant. After incubation for 24 h at 37 °C under 5% CO2 and 95% air atmosphere, all of the non-invaded cells were removed the upper face of the transwell membrane with a cotton swab; the invaded cells were fixed with 100% methanol and then stained with methylene blue. The invaded cells were counted microscopically. Ten fields were counted for each assay.

RESULTS

Anti-proliferative activity of KS15 to human breast cancer cell lines

To evaluate the effects of CRY inhibitor on cell growth of human breast cancer cells, I cultured the two widely-used human breast cancer cell lines (MCF-7, MDA-MB-231) and normal mammary epithelial cells (MCF-10A) in the absence or presence of KS15 in different concentrations. MCF-7 is estrogen/progesterone receptor (ER/PR) positive type of cancer cell lines with weak invasiveness. Thus, hormonal therapy such as treatment of tamoxifen as well as usual chemotherapy are both effective for this cell lines. On the other hand, MDA-MB-231 is negative for ER, PR and human epidermal growth factor receptor 2 (HER2) and so called as “triple negative breast cancer (TNBC)” type. Therefore, chemotherapy using non-specific anti-tumor drugs Including doxorubicin is only effective for this cell lines. MDA-MB-231 cell line also shows highly invasiveness and thereby widely used for investigating metastatic activity. MCF-10A is immortalized but non-cancerous mammary epithelial cell lines that widely used for cell line model for normal mammary tissues. After 48 hr incubation with various concentration of KS15, MTT assay, a non-radioactive assay that widely used to quantify cell viability and proliferation, was performed. The MTT assay measures cell viability and proliferation based on the ability of the mitochondrial dehydrogenase enzymes to convert the yellow tetrazolium MTT to water-insoluble dark blue formazan by reductive cleavage of the tetrazolium ring. The amount of dye produced is proportional to the number

of metabolically live cells. The results show that KS15 exhibited a significant and a dose-dependent inhibitory effect on viability of MCF-7 cell line, whereas other cell lines (MCF-10A, MDA-MB-231) were not responsive to KS15 (Fig 22A). Moreover, structural analog of KS15 with less potency for inhibition of CRYs (KS25) was failed to show anti-proliferative activity to all three type of cell lines (Fig 22B). These data suggested that pharmacological inhibition of CRYs by application of KS15 has repressive effect on proliferation of MCF-7 human breast cell line.

Enhancement of chemosensitivity by co-treatment of KS15 with anti-tumor drugs

Recent studies Indicated that functional inhibition of CRY1/2 showed protective effect for cancer-prone phenotype of p53 mutant mice and enhanced responses for clonogenic anti-tumor drugs (Gauger and Sancar, 2005; Ozturk et al., 2008; Lee et al., 2013). Based on these findings, I hypothesized that co-treatment of KS15 with anti-cancer drugs can increase susceptibility for these drugs and thereby synergistically inhibits viability of tumor cell lines. To prove this, MCF-7 and MDA-MB-231 cells were treated with KS15 and two different kinds of genotoxicants including doxorubicin and oxaliplatin. Doxorubicin is radiomimetic compound that interacts with DNA by intercalation whereas oxaliplatin is UV mimetic compound that forms both inter- and intra- strand cross links in DNA. In addition, MCF-7 were tested with tamoxifen, an antagonist of the estrogen receptor in breast tissue and thereby widely used for hormone therapy of

ER/PR positive type of breast cancer. After 48 hr incubation, viability of remaining cells was analyzed by MTT assay. As a result, sensitivities of MCF-7 to doxorubicin were significantly increased by co-treatment of KS15 in dose-dependent manner, whereas sensitivities of MDA-MB-231 were not changed (Fig 23). On the other hand, sensitivity to oxaliplatin was not significantly enhanced in both MCF-7 and MDA-MB-231 by co-treatment of KS15 (Fig 24). It should be noted that co-treatment of KS15 with tamoxifen also shows enhanced sensitivity in MCF-7 (Fig 25). Moreover, enhanced efficacies of doxorubicin and tamoxifen with co-treatment of KS15 on MCF-7 cells were analyzed using dose-response curves (Fig 26 and Table 6). These data clearly demonstrated that co-treatment of KS15 reduces IC_{50} values of doxorubicin and tamoxifen in dose-dependent manner. In consistent with Fig 22, these findings suggest that only MCF7, the ER/PR positive type of breast cancer cell line was responsive for enhancing chemosensitivity by treatment of KS15.

KS15 is not effective on both the adhesion ability to fibronectin and metastatic activity of human breast cancer cell lines

Tumor cell adhesion to extracellular matrix (ECM) and basement membranes is considered to be an initial step in the invasive process for metastatic tumor cells (Saiki et al., 1990). I examined the influence of KS15 on the adhesion of human breast cancer cell lines to the substrates pre-coated with human fibronectin, which is a component of basement membranes. After treatment with different concentration of KS15, cells were

incubated with desired periods (30 min, 1 hr, 2 hr) on fibronectin coated culture plate and unattached cells were washed out. Quantification of remaining cells was performed by MTT assay. As a result, the adhesion ability of both MCF-7 and MDA-MB-231 were not significantly changed (Fig. 27).

In addition to cell adhesion ability, cell motility was a measure of metastatic potential of cancer cells. The effect of KS15 on the invasion of human breast cancer cell lines was examined using Matrigel-coated chambers. After treatment with different concentration of KS15, MCF-7 and MDA-MB-231 cells were transferred into upper chamber of transwell. After incubation for 24 hr, all of the non-invaded cells were removed the upper face of the transwell membrane with a cotton swab; the invaded cells were quantified by using MTT assay. In consistent with ability of adhesion to fibronectin, invaded cells from both MCF-7 and MDA-MB-231 were not significantly changed by treatment of KS15 (Fig 28). These findings suggested that pharmacological inhibition of CRYs is only effective for inhibition of tumor growth or enhancing chemosensitivity to other anti-cancer drugs but not effective on metastatic potentials of human breast cancer cells.

Figure 22. Anti-proliferative effect of KS15 on human breast cancer cell lines. (A) Dose-dependent repression of cell viability by treatment of KS15. Note that only MCF-7 cells were inhibited by treatment of KS15, whereas normal cells (MCF10A) and MDA-MB-231 cells were not responds to KS15. (B) Repression of cell viability by treatment of KS25, a structural analog of KS15 with weak potency. (**p<0.01 vs vehicle group) Data were presented as the mean ± S.E.M. from six independent experiments.

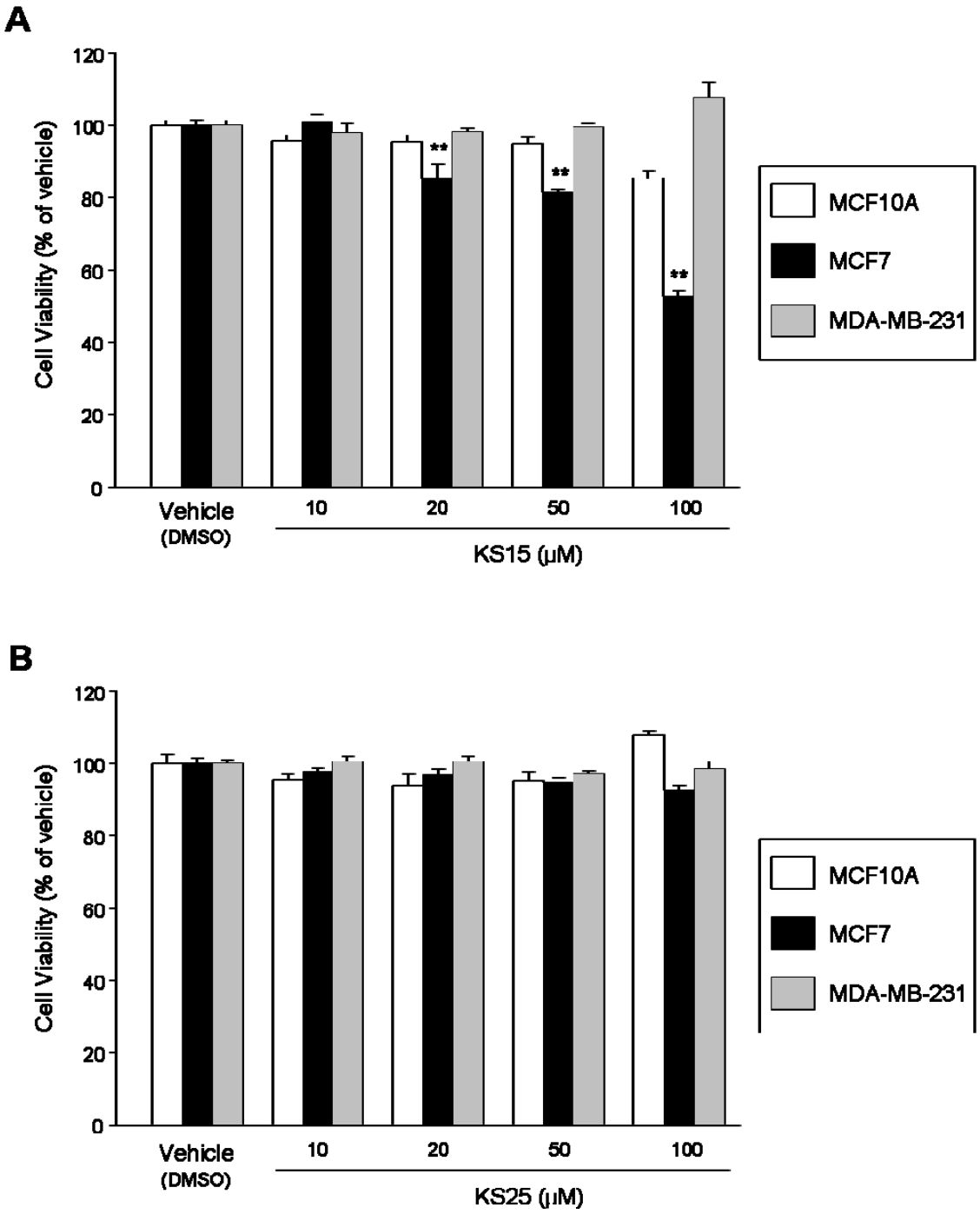
A
120
100
80
60
40
20
0
Cell Viability (% of vehicle)
**
**
**
Vehicle
(DMSO)
10
20
50
100
KS15 (μM)
MCF10A
MCF7
MDA-MB-231
B
120
100
80
60
40
20
0
Cell Viability (% of vehicle)
Vehicle
(DMSO)
10
20
50
100
KS25 (μM)
MCF10A
MCF7
MDA-MB-231

Figure 23. Co-treatment of KS15 and doxorubicin on human breast cancer cell lines. Enhancement of chemosensitivity to doxorubicin by KS15. (A) Cell viability of MCF-7 by co-treatment of doxorubicin (1.5 μM) and a various concentration of KS15. Note that survival of MCF-7 cells after treatment of doxorubicin was decreased by addition of KS15 in dose-dependent manner. (B) Cell viability of MDA-MB-231 by co-treatment of doxorubicin (1.5 μM) and a various concentration of KS15. (*$p<0.05$, **$p<0.01$ vs vehicle group) Data were presented as the mean ± S.E.M. from six independent experiments.

A

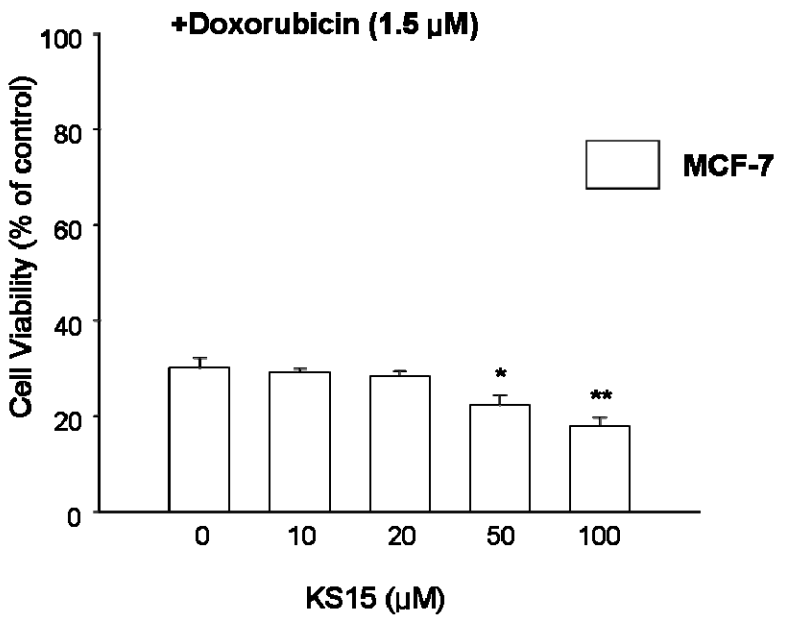
+Doxorubicin (1.5 μM)
MCF-7
Cell Viability (% of control)
100
80
60
40
20
0
*
**
0
10
20
50
100
KS15 (μM)

B

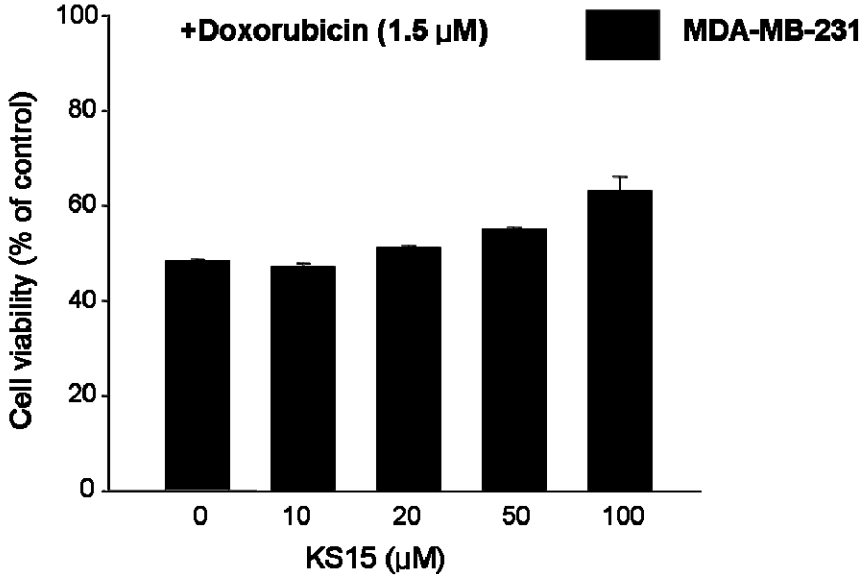
+Doxorubicin (1.5 μM)
MDA-MB-231
Cell viability (% of control)
100
80
60
40
20
0
0
10
20
50
100
KS15 (μM)

Figure 24. Co-treatment of KS15 and oxaliplatin on human breast cancer cell lines. Chemosensitivity to oxaliplatin by co-treatment with KS15. (A) Cell viability of MCF-7 by co-treatment of oxaliplatin (100 μM) and a various concentration of KS15. (B) Cell viability of MDA-MB-231 by co-treatment of oxaliplatn (100 μM) and a various concentration of KS15. Data were presented as the mean ± S.E.M. from six independent experiments.

A

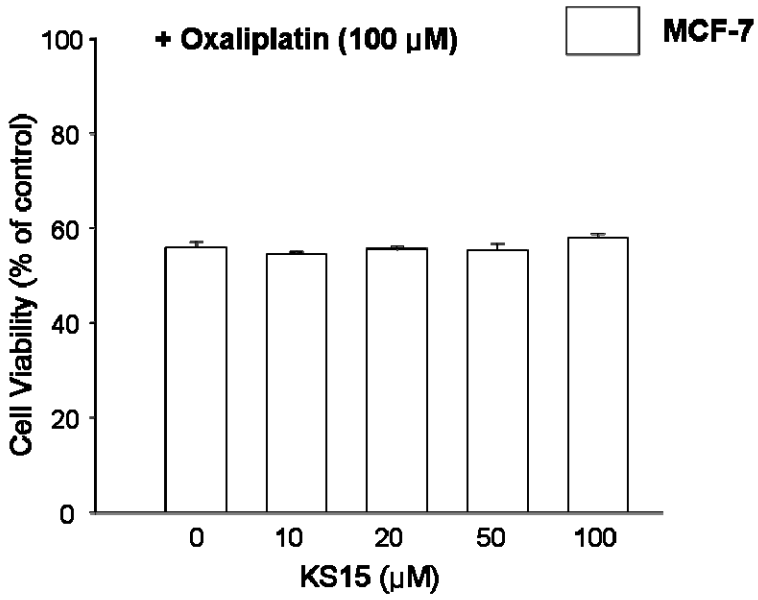
+ Oxaliplatin (100 μM)
MCF-7
Cell Viability (% of control)
100
80
60
40
20
0
0
10
20
50
100
KS15 (μM)

B

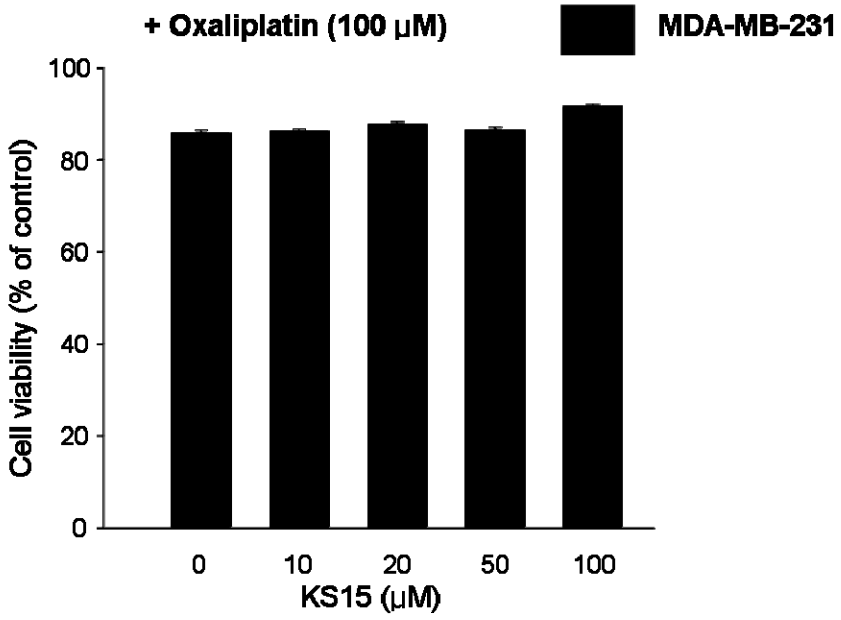
+ Oxaliplatin (100 μM)
MDA-MB-231
Cell viability (% of control)
100
80
60
40
20
0
0
10
20
50
100
KS15 (μM)

Figure 25. Co-treatment of KS15 and tamoxifen on human breast cancer cell lines. Chemosensitivity of MCF-7 cells after co-treatment of tamoxifen and a various concentration of KS15. Note that survival of MCF-7 cells after treatment of tamoxifen (10 μM) was decreased by addition of KS15 in dose-dependent manner. (*$p<0.05$, **$p<0.01$ vs vehicle group) Data were presented as the mean ± S.E.M. from six independent experiments.

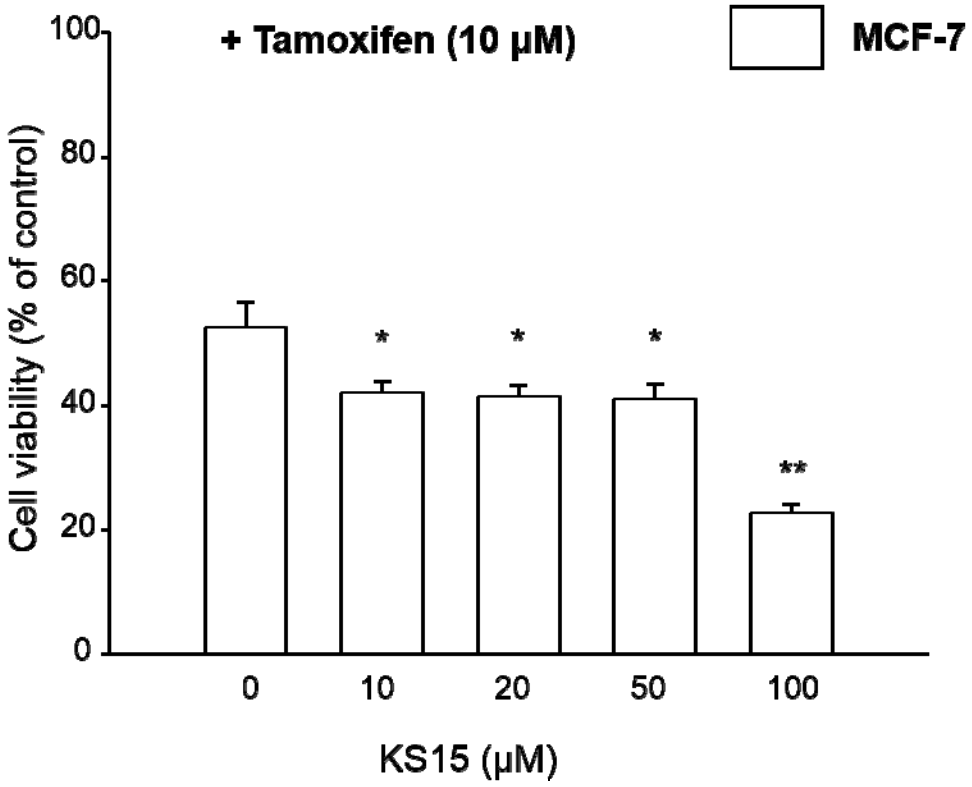
+ Tamoxifen (10 μM)
MCF-7
Cell viability (% of control)
100
80
60
40
20
0
*
*
*
**
0
10
20
50
100
KS15 (μM)

Figure 26. Changes of chemosensitivity by co-treatment of KS15 on MCF-7 cell line. Dose-response curves of anti-tumor drugs with co-treatment of KS15 on MCF-7. Note that survival of MCF-7 cells after treatment of (A) doxorubicin and (B) tamoxifen were decreased by addition of KS15 in dose-dependent manner. Data were presented as the mean ± S.E.M. from four independent experiments.

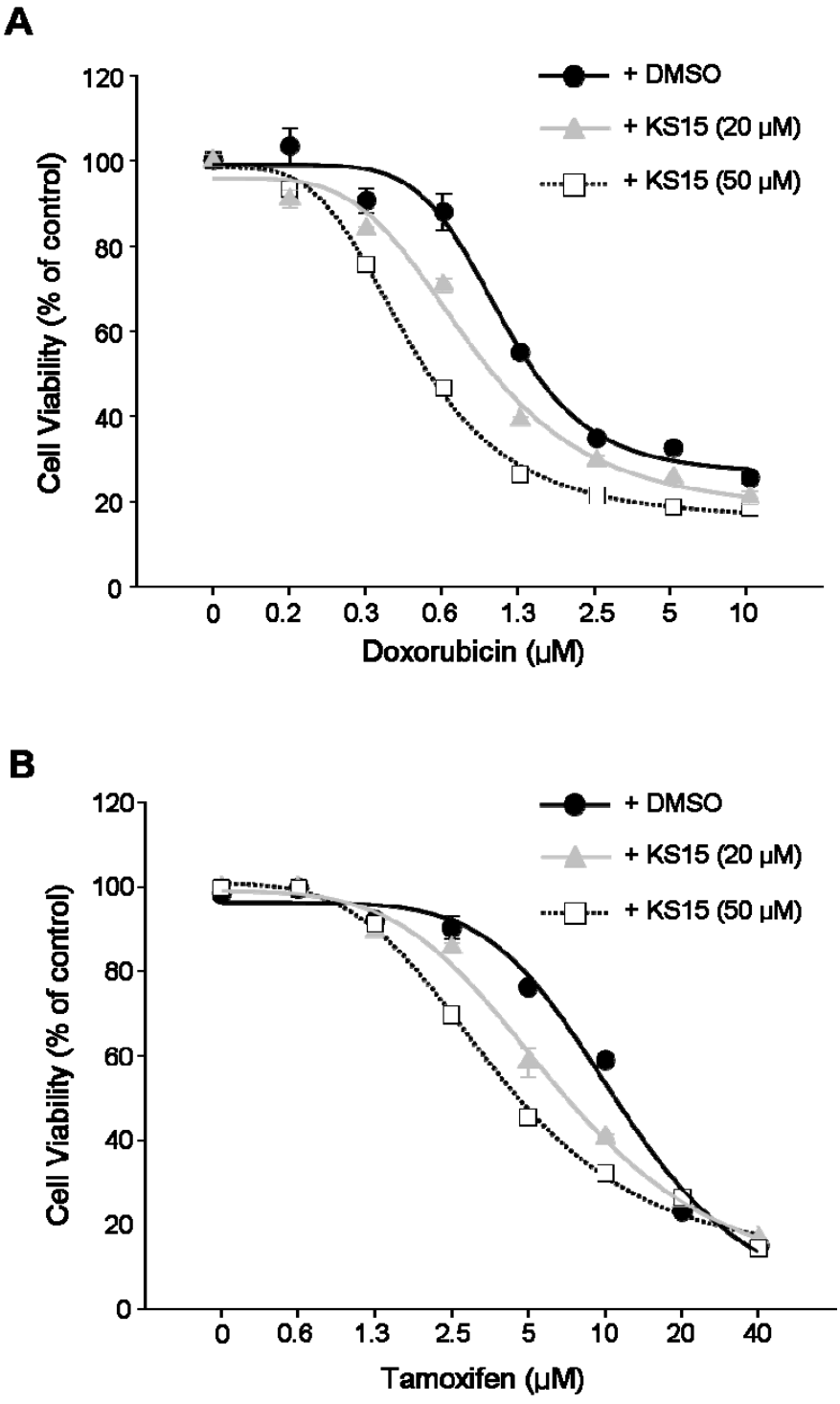
A
+ DMSO
+ KS15 (20 μM)
+ KS15 (50 μM)
Cell Viability (% of control)
120
100
80
60
40
20
0
0
0.2
0.3
0.6
1.3
2.5
5
10
Doxorubicin (μM)
B
+ DMSO
+ KS15 (20 μM)
+ KS15 (50 μM)
Cell Viability (% of control)
120
100
80
60
40
20
0
0
0.6
1.3
2.5
5
10
20
40
Tamoxifen (μM)

Table 6. Chemosensitivity of doxurubicin and tamoxifen with co-treatment of KS15 on MCF-7 cell line. Statistical analysis of efficacy changes by analysis dose-response curves of doxorubicin or tamoxifen with co-treatment of KS15 on MCF-7 cell lines. Efficacy was determined by IC_{50} values that calculated with a logistic 4-parametric equation using the mean values of cell viability.

Compound	Concentration	IC_{50} (doxorubicin)	IC_{50} (tamoxifen)
DMSO	0.2%	1.06 μM	10.83 μM
KS15	20 μM	0.75 μM	5.77 μM
	50 μM	0.46 μM	3.44 μM

Figure 27. Effect of KS15 on human breast cancer cells adhesion to fibronectin. Adhesion of MCF-7 and MDA-MB-231 caner cells to fibronectin after treatment of KS15. Adherent cells after wash out were quantified by MTT assay. Data were presented as the mean ± S.E.M. from six independent experiments.

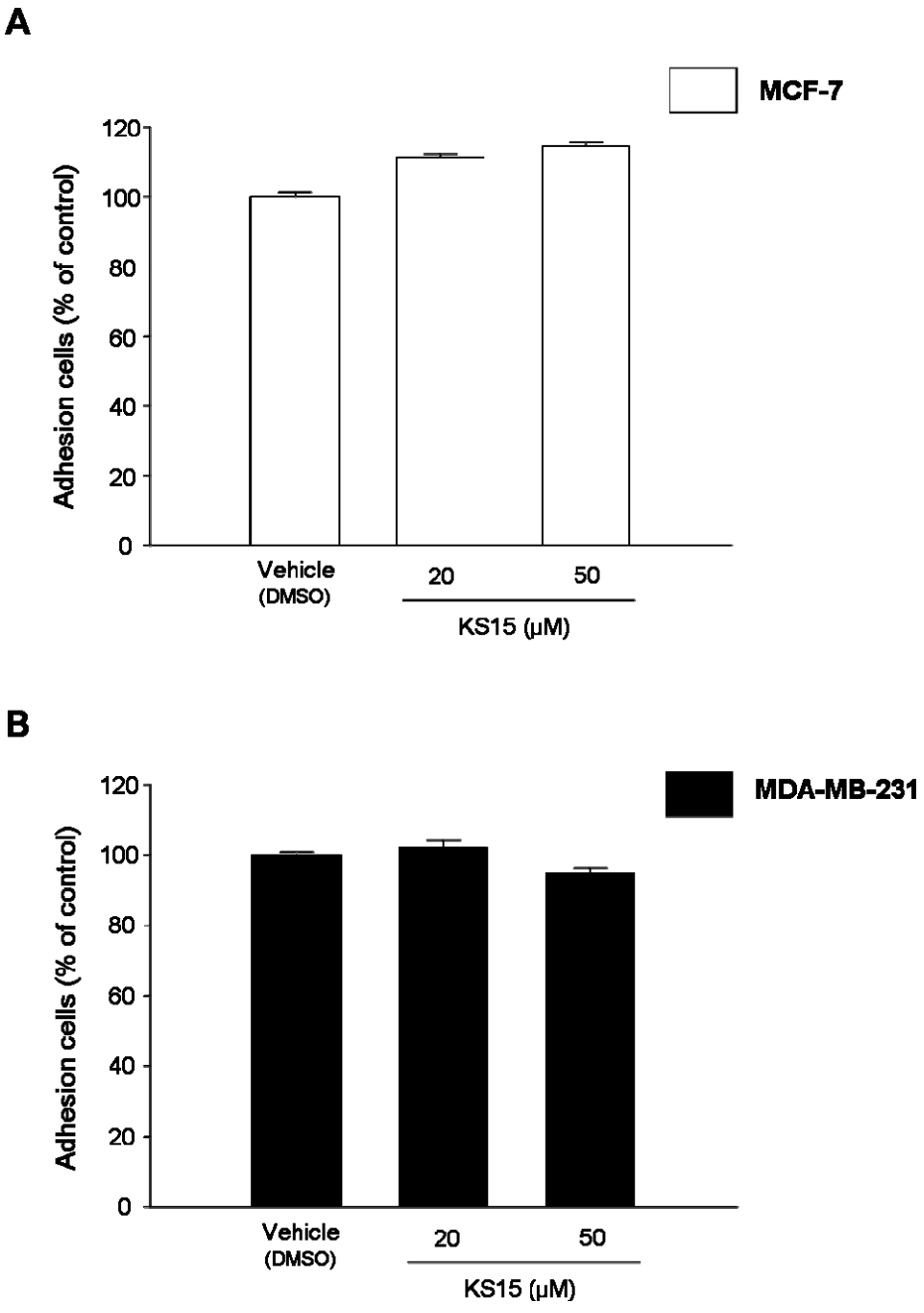
A
MCF-7
Adhesion cells (% of control)
120
100
80
60
40
20
0
Vehicle
(DMSO)
20
50
KS15 (μM)
B
MDA-MB-231
Adhesion cells (% of control)
120
100
80
60
40
20
0
Vehicle
(DMSO)
20
50
KS15 (μM)

Figure 28. Effect of KS15 on human breast cancer cells invasion *in vitro*. Invasion of MCF-7 and MDA-MB-231 caner cells on Matriegel coated transwelll chamber. (A) Photographs of the cell invasion through the polycarbonate membrane. (B) Invasion cells after wash out were quantified by MTT assay. Data were presented as the mean ± S.E.M. from three independent experiments.

A

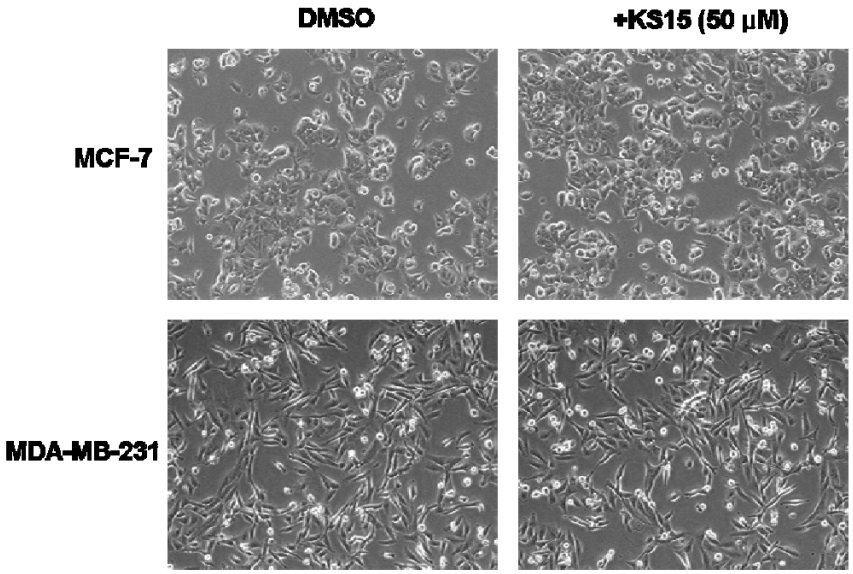
DMSO
+KS15 (50 μM)
MCF-7
MDA-MB-231

B

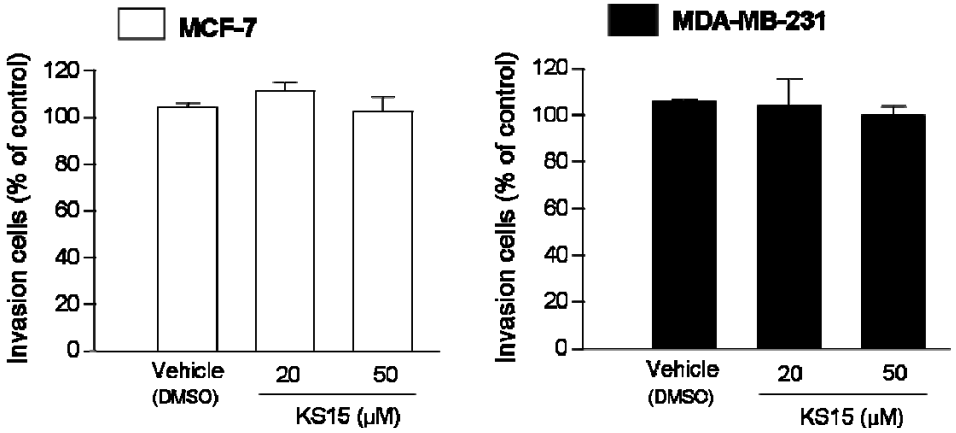
MCF-7
MDA-MB-231
Invasion cells (% of control)
120
100
80
60
40
20
0
Vehicle
(DMSO)
20
50
KS15 (μM)

DISCUSSION

The present study suggests that anti-tumor activity of pharmacological inhibition of CRY1/2 in human breast cancer cells. Development of a novel synthetic circadian clock modulator as well as application of the modulators in disease models are immerging field in last decades. Notably, recent study suggests that selenium compound (L-methyl selenocysteine) showed chemopreventive effect in Bmal1-dependent manner from the systemic toxicity induced by cyclophosphamide (Hu et al., 2011). However, despite the fact that cancer is one of the most well-known circadian rhythm related disorders, studies about administration of synthetic circadian modulator for treatment of cancer were only recently begun. In the present study, I evaluate anti-tumor activity of a novel CRY1/2 inhibitor (KS15) on human breast cancer cells and demonstrated that KS15 can inhibit proliferation and enhance chemosensitivity of ER/PR positive type of human breast cancer cell line (MCF-7).

CRY is a key negative regulator of molecular circadian clockwork as well as closely associated with various cell cycle regulators and oncogenes (Hoffman et al., 2010, Cancer Prev Res; Hoffman et al., 2010, BMC Cancer) Interestingly, CRY1/2 double knockout mice were more resistant to systemic toxicity induced by cyclophosphamide compared to wild-type mice, whereas *Clock* mutant and Bmal1 knockout mice were very sensitive to same drug (Gorbacheva et al., 2005). In contrast, tumors derived from p53 mutant mouse became more sensitive to genotoxic drugs by knockout of CRY1/2 (Lee and Sancar, 2011; Lee et al., 2013). These effects of CRY1/2

knockout might be caused by absence of circadian repression and thereby highly activated CLOCK:BMAL1 transactivation complex (Vitaterna et al., 1999; Okamura et al., 1999). For example, expression of Egr1 is induced in CRY1/2 knockout background because Egr1 is directly regulated by CLOCK:BMAL1 heterodimer activity. Highly elevated Egr1 leads to significantly enhanced DNA damage–inducible p73 transcription and thereby induced apoptosis in response to genotoxic stress (Lee et al., 2013). These studies suggested that functional inhibition of CRYs has the therapeutic potential for treatment of cancer. Although I didn't investigate detailed mechanisms of KS15's action in this study, I hypothesized that treatment of KS15 on breast cancer cell lines may induce similar situation of CRY1/2 knockout background. Further investigation will be required for verifying this hypothesis.

It is of interest to note that among the tested cell lines, only ER/PR-positive type of human breast cancer cell (MCF-7) are responsive to KS15. This specific effect of KS15 can be explained by differences in expression profiles of clock genes between ER/PR positive and negative cell lines. Recent study shows that patients with ER-negative tumors have higher levels of CLOCK gene expression than patients with ER-positive tumors (Hoffman et al., 2010, Cancer Res). If this difference is exist, additional activation of CLOCK:BMAL1 transactivation complex by inhibition of CRYs using KS15 might be less effective for ER-negative tumor cell lines. Moreover, another study suggests that mutations within CRY2 are a risk factor for the ER/PR negative type of tumor, but this association is not significant for ER/PR positive type of breast cancer. This study also shows

that CRY2 expression in breast cancer tissues is differently regulated not only between normal and tumor tissues, but also between ER/PR positive and ER/PR negative tumors (Hoffman et al., 2010, Cancer Prev Res). If the gene structure or expression profiles of CRY2 were different in ER/PR negative cancer cells in compare with ER/PR-positive cancer cells, treatment of KS15 may induce different response from the two cell lines. Taken together, KS15 shows anti-tumor activity on ER/PR-positive breast cancer cell lines selectively. This selectivity is possibly based on the different expression of clock genes, thus further optimization and investigation of detailed mechanism of KS15 can be a novel strategy for selective treatment of ER/PR positive type of breast cancer.

Unlike proliferation or chemosensitivity, administration of KS15 did not affect adhesion and metastasis of both ER/PR positive or negative type of breast cancer cells. Many studies suggest that metastatic activity of cancer is closely related with circadian rhythm, however, most of them were dependent on the action of melatonin (Wu et al., 2012; Mao et al., 2012). Melatonin has anti-tumorigenesis effect as well as inhibition of metastasis and more importantly, secretion of melatonin shows robust circadian rhythm and this patterns is severely affect by disruption of circadian rhythm such as light exposure at night (Wu et al., 2012; Hill et al., 2009; Hill et al., 1988; Mao et al., 2010). Thus, insignificant effect of KS15 on metastasis might be caused by absence of melatonin action. Further investigation of detailed mechanisms including melatonin action on metastasis can be a valuable study for application of KS15 on breast cancer.

Another important issue about the application of KS15 is the effective concentration. The effective concentrations of KS15 on breast cancer cells to inhibit the growth or to increase the chemosensitivity of genotoxic drugs are relatively higher than other chemicals. In previous findings, genetic depletion of CRY1/2 clearly enhanced the chemosensitivity of genotoxicants (Lee and Sancar, 2011; Lee et al., 2013). Although KS15 also inhibits the function of CRY1/2, there is a possibility that inhibition of KS15 on CRY1/2 is weaker than genetic knock-out of CRY1/2. Further optimization of potency and selectivity of KS15 will be needed.

In conclusion, CRY1/2 are novel therapeutic targets for treatment of breast cancer and application of KS15 may be useful for breast cancer therapy. Although these data only shows anti-tumor effect of KS15 and detailed mechanism of action was not included and should be revealed in further study.

REFERENCES

Aubert C, Janiaud P, Lecalvez J (1980) Effect of pinealectomy and melatonin on mammary tumor growth in Sprague-Dawley rats under different conditions of lighting. J Neural Transm 47:121-130.

Balsalobre A, Damiola F, Schibler U (1998) A serum shock induces circadian gene expression in mammalian tissue culture cells. Cell 93:929–937.

Baggs JE, Price TS, DiTacchio L, Panda S, Fitzgerald GA, Hogenesch JB (2009) Network Features of the Mammalian Circadian Clock. PLoS Biol 7:e52.

Bechtold DA, Gibbs JE, Loudon AS (2010) Circadian dysfunction in disease. Trends Pharmacol Sci. 31:191-198.

Boyle P, Levin B (2008) World Cancer Report 2008, pp 1-510, IARC press, Lyon.

Bunger MK, Wilsbacher LD, Moran SM, Clendenin C, Radcliffe LA, Hogenesch JB, Simon MC, Takahashi JS, Bradfield CA (2000) Mop3 is an essential component of the master circadian pacemaker in mammals. Cell 103:1009–1017.

Bugge A, Feng D, Everett LJ, Briggs ER, Mullican SE, Wang F, Jager J, Lazar MA (2012) Rev-erbα and Rev-erbβ coordinately protect the circadian clock and normal metabolic function. Genes Dev 26:657-667.

Buijs RM, van Eden CG, Goncharuk VD, Kalsbeek A (2003) The biological clock tunes the organs of the body: timing by hormones and the autonomic nervous system. J Endocrinol 177:17-26.

Busino L, Bassermann F, Maiolica A, Lee C, Nolan PM, Godinho SI, Draetta GF, Pagano M (2007) SCFFbxl3 controls the oscillation of the circadian clock by directing the degradation of cryptochrome proteins. Science 316:900-904.

Chiu JC, Ko HW, Edery I (2011) NEMO/NLK phosphorylates PERIOD to initiate a time-delay phosphorylation circuit that sets circadian clock speed. Cell 145:357-370.

Cho H, Zhao X, Hatori M, Yu RT, Barish GD, Lam MT, Chong LW, DiTacchio L, Atkins AR, Glass CK, Liddle C, Auwerx J, Downes M, Panda S, Evans RM (2012) Regulation of circadian behaviour and metabolism by REV-ERB-α and REV-ERB-β. Nature 485:123-127.

Chaves I, Yagita K, Barnhoorn S, Okamura H, van der Horst GT, Tamanini F (2006) Functional evolution of the photolyase/cryptochrome protein family importance of the C terminus of mammalian CRY1 for circadian core oscillator performance. Mol Cell Biol 26:1743–1753.

Chen Z, Yoo SH, Takahashi JS (2013) Small molecule modifiers of circadian clocks. Cell Mol Life Sci 70:2985-2998.

Czarna A, Breitkreuz H, Mahrenholz CC, Arens J, Strauss HM, Wolf E (2011) Quantitative analyses of cryptochrome-mBMAL1 interactions: mechanistic insights into the transcriptional regulation of the mammalian circadian clock. J Biol Chem 286:22414–22425.

Dallmann R, Mrosovsky N (2006) Scheduled wheel access during daytime: A method for studying conflicting zeitgebers. Physiol Behav 88:459-465.

Davis S, Mirick DK, Stevens RG (2001) Night shift work, light at night, and

risk of breast cancer. J Natl Cancer Inst 93:1557-1562.

Dunlap JC (1999) Molecular bases for circadian clocks. Cell 96:271-290.

Emens JS, Lewy AJ, Lefler BJ, Sack RL (2005) Relative coordination to unknown "weak zeitgebers" in free-running blind individuals. J Biol Rhythms 20:159-167.

Escobar C, Cailotto C, Angeles-Castellanos M, Delgado RS, Buijs RM (2009) Peripheral oscillators: the driving force for food-anticipatory activity. Eur J Neurosci 30:1665-1675.

Evans JA, Pan H, Liu AC, Welsh DK (2012) Cry1-/- circadian rhythmicity depends on SCN intercellular coupling. J Biol Rhythms 27:443-452.

Gachon F, Nagoshi E, Brown SA, Ripperger J, Schibler U (2004) The mammalian circadian timing system: from gene expression to physiology. Chromosoma 113: 103-112.

Gauger MA, Sancar A (2005) Cryptochrome, circadian cycle, cell cycle checkpoints, and cancer. Cancer Res 65:6828–6834.

Gekakis N, Staknis D, Nguyen HB, Davis FC, Wils-bacher LD, King DP, Takahashi JS, Weitz CJ (1998) Role of the CLOCK protein in the mammalian circadian mechanism. Science 280:1564–1569.

Gorbacheva VY, Kondratov RV, Zhang R, Cherukuri S, Gudkov AV, Takahashi JS, Antoch MP (2005) Circadian sensitivity to the chemotherapeutic agent cyclophosphamide depends on the functional status of the CLOCK/BMAL1 transactivation complex. Proc Natl Acad Sci U S A 102:3407-3412.

Grant D, Yin L, Collins JL, Parks DJ, Orband-Miller LA, Wisely GB, Joshi S, Lazar MA, Willson TM, Zuer-cher WJ (2010) GSK4112, a small

molecule chemical probe for the cell biology of the nuclear heme receptor Rev-erbalpha. ACS Chem Biol. 5:925–932.

Grone BP, Chang D, Bourgin P, Cao V, Fernald RD, Heller HC, Ruby NF (2011) Acute light exposure suppresses circadian rhythms in clock gene expression. J Biol Rhythms 26:78-81.

Harada Y, Sakai M, Kurabayashi N, Hirota T, Fukada Y (2005) Ser-557-phosphorylated mCRY2 is degraded upon synergistic phosphorylation by glycogen synthase kinase-3β. J Biol Chem 280:31714–31721.

Hara R, Wan K, Wakamatsu H, Aida R, Moriya T, Akiyama M, Shibata S (2001) Restricted feeding entrains liver clock without participation of the suprachiasmatic nucleus. Genes Cells 6:269-278.

Hastings MH, Reddy AB, Maywood ES (2003) A clockwork web: circadian timing in brain and periphery, in health and disease. Nat Rev Neurosci 4:649-661.

Hill SM, Blask DE (1988) Effects of the pineal hormone melatonin on the proliferation and morphological characteristics of human breast cancer cells (MCF-7) in culture. Cancer Res 48:6121–6126.

Hill SM, Frasch T, Xiang S, Yuan L, Duplessis T, Mao L (2009) Molecular mechanisms of melatonin anticancer effects. Integr Cancer Ther 8:337–346.

Hirota T, Lee JW, Lewis WG, Zhang EE, Breton G, Liu X, Garcia M, Peters EC, Etchegaray JP, Traver D, Schultz PG, Kay SA (2010) High-throughput chemical screen identifies a novel potent modulator of cellular circadian rhythms and reveals CKIα as a clock regulatory kinase. PLoS Biol 8:e1000559.

Hirota T, Lee JW, St John PC, Sawa M, Iwaisako K, Noguchi T, Pongsawakul PY, Sonntag T, Welsh DK, Brenner DA, Doyle FJ 3rd, Schultz PG, Kay SA (2012) Identification of Small Molecule Activators of Cryptochrome. Science 337:1094–1097

Hoffman AE, Yi CH, Zheng T, Stevens RG, Leaderer D, Zhang Y, Holford TR, Hansen J, Paulson J, Zhu Y (2010) CLOCK in breast tumorigenesis: genetic, epigenetic, and transcriptional profiling analyses. Cancer Res 70:1459-1468.

Hoffman AE, Zheng T, Yi CH, Stevens RG, Ba Y, Zhang Y, Leaderer D, Holford T, Hansen J, Zhu Y (2010) The core circadian gene Cryptochrome 2 influences breast cancer risk, possibly by mediating hormone signaling. Cancer Prev Res 3:539-548.

Hoffman AE, Zheng T, Ba Y, Stevens RG, Yi CH, Leaderer D, Zhu Y (2010) Phenotypic effects of the circadian gene Cryptochrome 2 on cancer-related pathways. BMC Cancer 10:110.

Hogenesch JB, Gu YZ, Jain S, Bradfield CA (1998) The basic-helix-loop-helix-PAS orphan MOP3 forms transcriptionally active complexes with circadian and hypoxia factors. Proc Natl Acad Sci U S A 95:5474–5479.

Hu Y, Spengler ML, Kuropatwinski KK, Comas-Soberats M, Jackson M, Chernov MV, Gleiberman AS, Fedtsova N, Rustum YM, Gudkov AV, Antoch MP (2011) Selenium is a modulator of circadian clock that protects mice from the toxicity of a chemotherapeutic drug via upregulation of the core clock protein, BMAL1. Oncotarget 2:1279-90.

Jin X, Shearman LP, Weaver DR, Zylka MJ, de Vries GJ, Reppert SM

(1999) A molecular mechanism regulating rhythmic output from the suprachiasmatic circadian clock. Cell 96:57-68.

Kondratova AA, Kondratov RV (2012) The circadian clock and pathology of the ageing brain. Nat Rev Neurosci 13:325–335.

Kume K, Zylka MJ, Sriram S, Shearman LP, Weaver DR, Jin X, Maywood ES, Hastings MH, Reppert SM (1999) mCRY1 and mCRY2 are essential components of the negative limb of the circadian clock feedback loop. Cell 98:193-205.

Kojetin D, Wang Y, Kamenecka TM, Burris TP (2011) Identification of SR8278, a synthetic antagonist of the nuclear heme receptor REV-ERB. ACS Chem Biol 6:131–134.

Knutsson A (2003) Health disorders of shift workers. Occup Med 53:103–108.

Lamia KA, Storch KF, Weitz CJ (2008) Physiological significance of a peripheral tissue circadian clock. Proc Natl Acad Sci U S A 105:15172–15177.

Lamia KA, Sachdeva UM, DiTacchio L, Williams EC, Alvarez JG, Egan DF, Vasquez DS, Juguilon H, Panda S, Shaw RJ, Thompson CB, Evans RM (2009) AMPK regulates the circadian clock by cryptochrome phosphorylation and degradation. Science 326:437-440.

Lamont EW, James FO, Boivin DB, Cermakian N (2007) From circadian clock gene expression to pathologies. Sleep Med 8:547–556.

Lee JH, Gaddameedhi S, Ozturk N, Ye R, Sancar A (2013) DNA damage-specific control of cell death by cryptochrome in p53-Mutant ras-transformed cells. Cancer Res 73:785–791.

Lee JH and Sancar A (2011) Circadian clock disruption improves the efficacy of chemotherapy through p73-mediated apoptosis. Proc Natl Acad Sci. U S A 108:10668–10672.

Lee JW, Hirota T, Peters EC, Garcia M, Gonzalez R, Cho CY, Wu X, Schultz PG, Kay SA (2011) A small molecule modulates circadian rhythms through phosphorylation of the period protein. Angew Chem Int Ed 123:10796–10799.

Lin C and Todo T (2005) The cryptochromes. Genome Biol 6:220.

Lipinski CA, Lombardo F, Dominy BW, Feeney PJ (2001) Experimental and computational approaches to estimate solubility and permeability in drug discovery and development settings. Adv Drug Delivery Rev 46:3–26.

Liu AC, Welsh DK, Ko CH, Tran HG, Zhang EE, Priest AA, Buhr ED, Singer O, Meeker K, Verma IM, Doyle 3rd FJ, Takahashi JS, Kay SA (2007) Intercellular coupling confers robustness against mutations in the SCN circadian clock network. Cell 129:605-616.

Matsuo T, Yamaguchi S, Mitsui S, Emi A, Shimoda F, Okamura H (2003) Control mechanism of the circadian clock for timing of cell division in vivo. Science 302:255–259.

Mao L, Dauchy RT, Blask DE, Slakey LM, Xiang S, Yuan L, Dauchy EM, Shan B, Brainard GC, Hanifin JP, Frasch T, Duplessis TT, Hill SM (2012) Circadian gating of epithelial-to-mesenchymal transition in breast cancer cells via melatonin-regulation of GSK3β. Mol Endocrinol 26:1808-1820.

Mao L, Yuan L, Slakey LM, Jones FE, Burow ME, Hill SM (2010) Inhibition of breast cancer cell invasion by melatonin is mediated through

regulation of the p38 mitogen-activated protein kinase signaling pathway. Breast Cancer Res 12:R107.

Maury E, Ramsey KM, Bass J (2010) Circadian rhythms and metabolic syndrome: from experimental genetics to human disease. Circ Res 106:447–462.

Mhatre MC, Shah PN, Juneja HS (1984) Effect of varying photoperiods on mammary morphology, DNA synthesis, and hormone profile in female rats. J Natl Cancer Inst 72:1411-1416.

Mistlberger RE, Skene DJ (2004) Social influences on mammalian circadian rhythms: animal and human studies. Biol Rev Camb Philos Soc 79:533-556.

Moore RY, Silver R (1998) Suprachiasmatic nucleus organization. Chronobiol Int 15:475–487.

Nakahata Y, Sahar S, Astarita G, Kaluzova M, and Sassone-Corsi P (2009) Circadian control of the NAD+ salvage pathway by CLOCK-SIRT1. Science 324:654–657.

Nagano M, Adachi A, Nakahama K, Nakamura T, Tamada M, Meyer-Bernstein E, Sehgal A, Shigeyoshi Y (2003) An abrupt shift in the day/night cycle causes desynchrony in the mammalian circadian center. J Neurosci 23:6141-6151.

Navara KJ, Nelson RJ (2007) The dark side of light at night: physiological, epidemiological, and ecological consequences. J Pineal Res 43:215-224.

Ohta H, Yamazaki S, McMahon DG (2005) Constant light desynchronizes mammalian clock neurons. Nat Neurosci 8:267-269.

Okamura H, Miyake S, Sumi Y, Yamaguchi S, Yasui A, Muijtjens M,

Hoeijmakers JH, van der Horst GT (1999) Photic induction of mPer1 and mPer2 in cry-deficient mice lacking a biological clock. Science 286:2531-2534

O'Neill JS, Maywood ES, Chesham JE, Takahashi JS, Hastings MH (2008) cAMP-dependent signaling as a core component of the mammalian circadian pacemaker. Science 320:949–953.

Oster H (2006) The genetic basis of circadian behavior. Genes Brain Behav 2:73–79.

Ozturk N, Lee JH, Gaddameedhi S, Sancar A (2008) Loss of cryptochrome reduces cancer risk in p53 mutant mice. Proc Natl Acad Sci U S A 106:2841-2846.

Park N, Cheon S, Son GH, Cho S, Kim K (2012) Chronic circadian disturbance by a shortened light-dark cycle increases mortality. Neurobiol Aging 33:1122 e1111–e1122.

Partch CL, Clarkson MW, Ozgür S, Lee AL, Sancar A (2005) Role of structural plasticity in signal transduction by the cryptochrome blue-light photoreceptor. Biochemistry 44:3795–3805.

Pauley SM (2004) Lighting for the human circadian clock: recent research indicates that lighting has become a public health issue. Med Hypotheses 63:588-596.

Preitner N, Damiola F, Lopez-Molina L, Zakany J, Duboule D, Albrecht U, Schibler U (2002) The orphan nuclear receptor REV-ERBalpha controls circadian transcription within the positive limb of the mammalian circadian oscillator. Cell 110:251-260.

Raghuram S, Stayrook KR, Huang P, Rogers PM, Nosie AK, McClure DB, Burris LL, Khorasanizadeh S, Burris TP, Rastinejad F (2007)

Identification of heme as the ligand for the orphan nuclear receptors REV-ERBalpha and REV-ERBbeta. Nat Struct Mol Biol 14:1207–1213.

Ramsey KM, Yoshino J, Brace CS, Abrassart D, Kobayashi Y, Marcheva B, Hong HK, Chong JL, Buhr ED, Lee C, Takahashi JS, Imai S, Bass J (2009) Circadian clock feedback cycle through NAMPT-mediated NAD+ biosynthesis. Science 324:651–654.

Reppert SM (1998) A clockwork explosion! Neuron 21:1-4.

Reppert SM, Weaver DR (2002) Coordination of circadian timing in mammals. Nature 418:935-941.

Ribeiro DC, Hampton SM, Morgan L, Deacon S, Arendt J (1998) Altered postprandial hormone and metabolic responses in a simulated shift work environment. J Endocrinol 158:305-310.

Sahar S, Sassone-Corsi P (2007) Circadian clock and breast cancer: a molecular link. Cell Cycle 6:1329-1331.

Sahar S, Sassone-Corsi P (2009) Metabolism and cancer: the circadian clock connection. Nat Rev Cancer 9:886-896.

Saiki I, Murata J, Nakajima M, Tokura S, Azuma I (1990) Inhibition by sulfated chitin derivatives of invasion through extracellular matrix and enzymatic degradation by metastatic melanoma cells. Cancer Res 50:3631-3637.

Salgado-Delgado R, Angeles-Castellanos M, Buijs MR, Escobar C (2008) Internal desynchronization in a model of nightwork by forced activity in rats. Neuroscience 154:922-931.

Salgado-Delgado R, Angeles-Castellanos M, Saderi N, Buijs RM, Escobar C (2010) Food intake during the normal activity phase prevents

obesity and circadian desynchrony in a rat model of night work. Endocrinology 151:1019-1029.

Sangoram AM, Saez L, Antoch MP, Gekakis N, Staknis D, Whiteley A, Fruechte EM, Vitaterna MH, Shimomura K, King DP, Young MW, Weitz CJ, Takahashi JS (1998) Mammalian circadian autoregulatory loop: a timeless ortholog and mPer1 interact and negatively regulate CLOCK-BMAL1-induced transcription. Neuron 21:1101-1113.

Sanada K, Harada Y, Sakai M, Todo T, Fukada Y (2004) Serine phosphorylation of mCRY1 and mCRY2 by mitogen-activated protein kinase. Genes Cells 9:697–708.

Sariego J (2010) Breast cancer in the young patient. Am Surg 76:1397-400

Schernhammer ES, Laden F, Speizer FE, Willett WC, Hunter DJ, Kawachi I, Colditz GA (2001) Rotating night shifts and risk of breast cancer in women participating in the nurses' health study. J Natl Cancer Inst 93:1563-1568.

Schibler U, Sassone-Corsi P (2002) A web of circadian pacemakers. Cell 111:919-922.

Siepka SM, Yoo SH, Park J, Song W, Kumar V, Hu Y, Lee C, Takahashi JS (2007) Circadian mutant Overtime reveals F-box protein FBXL3 regulation of cryptochrome and period gene expression. Cell 129:1011-1123.

Shuboni D, Yan L (2010) Nighttime dim light exposure alters the responses of the circadian system. Neuroscience 170:1172-1178.

Silver R, LeSauter J, Tresco PA, Lehman MN (1996) A diffusible coupling signal from the transplanted suprachiasmatic nucleus controlling

circadian locomotor rhythms. Nature 382:810–813.

Solt LA, Wang Y, Banerjee S, Hughes T, Kojetin DJ, Lundasen T, Shin Y, Liu J, Cameron MD, Noel R, Yoo SH, Takahashi JS, Butler AA, Kamenecka TM, Burris TP (2012) Regulation of circadian behaviour and metabolism by syn-thetic REV-ERB agonists. Nature 485:62–68.

Son GH, Chung S, Choe HK, Kim HD, Baik SM, Lee H, Lee HW, Choi S, Sun W, Kim H, Cho S, Lee KH, Kim K (2008) Adrenal peripheral clock controls the autonomous circadian rhythm of glucocorticoid by causing rhythmic steroid production. Proc Natl Acad Sci U S A 105:20970–20975.

Spiegel K, Weibel L, Gronfier C, Brandenberger G, Follenius M (1996) Twenty-four-hour prolactin profiles in night workers. Chronobiol Int 13:283-293.

Straif K, Baan R, Grosse Y, Secretan B, El Ghissassi F, Bouvard V, Altieri A, Benbrahim-Tallaa L, Cogliano V (2007) Carcinogenicity of shift-work, painting, and fire-fighting. Lancet Oncol 8:1065–1066.

Stephan FK (2002) The "other" circadian system: food as a Zeitgeber. J Biol Rhythms 17:284-292.

Stevens RG, Blask DE, Brainard GC, Hansen J, Lockley SW, Provencio I, Rea MS, Reinlib L (2007) Meeting report: the role of environmental lighting and circadian disruption in cancer and other diseases. Environ Health Perspect 115:1357–1362.

Suh YG, Kim NJ, Koo BW, Lee KO, Moon SH, Shin DH, Jung JW, Paek SM, Chang DJ, Li F, Kang HJ, Le TV, Chae YN, Shin CY, Kim MK, Lim JI, Ryu JS, Park HJ (2008) Design, synthesis, and biological

evaluation of novel constrained meta-substituted phenyl propanoic acids as peroxisome proliferator-activated receptor alpha and gamma dual agonists. J Med Chem 51:6318–6333.

Takahashi JS, Hong HK, Ko CH, McDearmon EL (2008) The genetics of mammalian circadian order and disorder: implications for physiology and disease. Nat rev Genet 9:764–775.

Takahata S, Sogawa K, Kobayashi A, Ema M, Mimura J, Ozaki N, Fujii-Kuriyama Y (1998) Transcriptionally active heterodimer formation of an Arnt-like PAS protein, Arnt3, with HIF-1a, HLF, and Clock. Biochem Biophys Res Commun 248:789–794.

Takahata S, Sogawa K, Kobayashi A, Ema M, Mimura J, Ozaki N, Fujii-Kuriyama Y (1998) Transcriptionally active heterodimer formation of an Arnt-like PAS protein, Arnt3, with HIF-1a, HLF, and Clock. Biochem Biophys Res Commun 248:789–794.

Todo T, Ryo H, Yamamoto K, Toh H, Inui T, Ayaki H, Nomura T, Ikenaga M (1996) Similarity among the Drosophila (6-4)photolyase, a human photolyase homolog, and the DNA photolyase-blue-light photoreceptor family. Science 272:109–112.

Ueda HR, Chen W, Adachi A, Wakamatsu H, Hayashi S, Takasugi T, Nagano M, Nakahama K, Suzuki Y, Sugano S, Iino M, Shigeyoshi Y, Hashimoto S (2002) A transcription factor response element for gene expression during circadian night. Nature 418:534-539.

Unsal-Kacmaz K, Mullen TE, Kaufmann WK, Sancar A (2005) Coupling of human circadian and cell cycles by the timeless protein. Mol Cell Biol 25:3109–3116

van der Schalie EA, Conte FE, Marz KE, Green CB (2007)

Structure/function analysis of Xenopus cryptochromes 1 and 2 reveals differential nuclear localization mechanisms and functional domains important for interaction with and repression of CLOCK-BMAL1. Mol Cell Biol 27:2120–2129

Vitaterna MH, Selby CP, Todo T, Niwa H, Thompson C, Fruechte EM, Hitomi K, Thresher RJ, Ishikawa T, Miyazaki J, Takahashi JS, Sancar A (1999) Differential regulation of mammalian period genes and circadian rhythmicity by cryptochromes 1 and 2. Proc Natl Acad Sci U S A. 96:12114-12119.

Waterhouse J, Reilly T, Atkinson G, Edwards B (2007) Jet lag: trends and coping strategies. Lancet 369:1117-1129.

Welsh DK, Logothetis DE, Meister M, Reppert SM (1995) Individual neurons dissociated from rat suprachiasmatic nucleus express independently phased circadian firing rhythms. Neuron 14:697-706.

Wu M, Zeng J, Chen Y, Zeng Z, Zhang J, Cai Y, Ye Y, Fu L, Xian L, Chen Z (2012) Experimental chronic jet lag promotes growth and lung metastasis of Lewis lung carcinoma in C57BL/6 mice. Oncol Rep 27:1417-1428

Young MW, Kay SA (2001) Time zones: a comparative genetics of circadian clocks. Nat Rev Genet 2:702–715.

Zhang EE, Liu Y, Dentin R, Pongsawakul PY, Liu AC, Hirota T, Nusinow DA, Sun X, Landais S, Kodama Y, Brenner DA, Montminy M, Kay SA (2010) Cryptochrome mediates circadian regulation of cAMP signaling and hepatic gluconeogenesis. Nat med 16:1152–1156.

Zhang EE, Liu AC, Hirota T, Miraglia LJ, Welch G, Pongsawakul PY, Liu X,

Atwood A, Huss JW 3rd, Janes J, Su AI, Hogenesch JB, Kay SA (2009) A Genome-wide RNAi Screen for Modifiers of the Circadian Clock in Human Cells. Cell 139:199–210.

국문 초록

인간을 포함한 포유동물에서 생체시계는 밤낮의 환경 변화에 적응하기 위해 약 24시간의 주기로 발현하는 생리적, 행동적 변화를 야기하는 내재적인 시간 조절 시스템이다. 이러한 생체시계는 포유동물의 생리기능과 행동을 유지시키는데 매우 중요한 역할을 수행하고 있으며, 이 시스템의 기능이 망가질 경우 암을 포함한 다양한 종류의 질병에 걸릴 위험이 증가한다. 이 때문에 최근에는 생체시계를 표적으로 하는 신규 화합물을 찾으려는 연구들이 많이 진행되고 있다. 그러나 생체시계 유전자의 주요 출력 경로인 E-box를 통한 전사 활성을 촉진시키는 화합물은 아직까지 보고된 바가 없다. 제 1장의 연구에서는 생체시계 핵심 유전자인 Cryprochromes (CRYs)를 표적으로 하여, CRYs에 결합하여 그 기능을 저해하는 신규 약물 (KS15)을 발굴하였다. 제 2장에서는 KS15의 활용성 연구의 일환으로서, 인간 유방암 세포주 모델에 KS15를 적용하여 암세포의 성장, 항암제 감수성 및 전이능력에 미치는 영향을 분석하였다.

제 1장에서는 생체시계 분자기구를 조절할 수 있는 신규 약물을 개발하기 위해 생체시계의 주요 출력 경로인 E-box 매개 전사 활성일 변화시키는 화합물을 선별할 수 있는 세포기반분석법 (cell-based assay)을 설계하고, 이 분석법을 활용하여 약 1000여개의 합성 화합물

라이브러리를 스크리닝하였다. 그 결과 신규 생체시계 조절 화합물인 KS15를 발굴하고, 해당 화합물의 표적 단백질 및 생체시계 기능의 조절 효능을 검증하는 일련의 연구들을 수행하였다. 우선 KS15의 표적 단백질을 분석하기 위해 바이오틴 (biotin) 표지를 부착한 유도체를 이용하여 pull-down assay을 수행한 결과, KS15가 생체시계 핵심 유전자인 Cryptochrome 1, 2(CRY1/2)에 특이적으로 결합하였다. 또한 CRY1/2 유전자 결핍 생쥐 섬유아세포를 이용한 검증 실험을 통해 KS15의 효능이 CRY1/2 유전자에 의존적으로 나타났다. 나아가 KS15를 Per2-Luc 혹은 Bmal1-dLuc 리포터를 발현하는 섬유아세포에 처리하였을 때, 이들의 일주기 리듬 양상을 변화시킬 수 있음을 실시간 생체발광 모니터링을 통해 분석하여 KS15가 CRY1/2의 기능을 억제하여 생체시계 활성을 조절하였다. 마지막으로 KS15를 뇌실내미세주사법 (intracerebroventricular microinjection)을 통해 살아있는 생쥐에 주사했을 때, 일주기 행동 리듬이 변화하였다. 위와 같은 결과들을 통해 신규 개발된 KS15가 생체시계 핵심 유전자인 CRY1/2의 기능을 방해하여 *in vitro* 와 *in vivo* 모델에서 생체시계 리듬을 조절할 수 있는 화합물임을 입증하였다.

여성암 중 가장 흔한 유방암은 생체시계 교란에 의해 발병 위험이 높아지는 대표적인 적응 중 하나이다. 신규 개발된 생체시계 조절

물질의 적용 가능성에 대한 연구의 일환으로써, 제 2장에서는 인간 유방암 세포주 모델을 대상으로 KS15가 유방암의 성장 및 전이성에 미치는 영향에 대한 실험을 수행하였다. 세포 활성 측정의 결과, 단독으로 처리했을 시에 KS15는 인간 유방암 세포주 모델 중 에스트로겐/프로게스테론 수용체 양성 종양의 모델 세포주인 MCF7 세포에서만 성장 억제 효과를 나타냈으며, 정상 유방 세포주 (MCF10A) 및 삼중음성 유방암 세포주 (MDA-MB-231)에서는 억제 효과를 나타내지 못했다. 또한 일반적으로 유방암 치료에 널리 쓰이는 3종의 항암제 (doxorubicin, oxaliplatin, tamoxifen)와 KS15를 동시에 처리했을 때에도 MCF7 세포주에서는 각각 doxorubicin, tamoxifen에 대한 항암제 감수성이 증가하는 효과를 보였으나 MDA-MB-231 세포주에서는 특별한 효능이 관찰되지 않았다. 이상으로 볼 때 신규 개발된 KS15는 약전이성의 에스트로겐/프로게스테론 수용체 양성 타입의 유방암에 대한 치료 효과를 기대할 수 있으며, 후속 연구를 통해 항암 치료의 효과를 증대시키는 보조제로서의 역할이 기대된다고 할 수 있다.

결론적으로 본 연구를 통해 최초의 CRY1/2에 대한 저해제인 KS15가 개발되었으며 이를 통해 생체시계 유전자의 주요 출력 경로인 E-box 매개 전사 활성이 촉진되어 생체시계 활성을 조절할 수 있음이

증명되었다. 또한 그 활용 연구의 일환으로써 인간 유방암 세포주에 대한 KS15의 항암 효과를 분석한 결과, KS15가 MCF-7 세포주에 대해서 성장 억제 효과 및 항암제 감수성 증가 효과를 가짐을 보였다. 해당 화합물의 기능과 항암 효과에 대한 후속 연구를 통해 KS15는 생체시계를 표적으로 하는 새로운 유방암 치료약으로서 개발될 가능성을 기대할 수 있다.

주요어: Cryptochrome (CRY); 생체시계; 저분자화합물; KS15; 세포기반분석법; 유방암; 항암 효능

감사의 글

졸업을 앞두고 길었던 학위 기간을 갈무리하며, 졸문(拙文) 하나 남기고자 합니다. 돌이켜 보면 이 값진 박사 학위는 앞에서 끌어주고 뒤에서 받쳐주던 고마우신 분들의 도움이 없었다면 불가능했으리라 생각합니다. 또 다른 시작인 졸업을 앞둔 이 뜻 깊은 시간에 별처럼 많은 감회와 다짐을 잠시 미뤄두고, 도움 주신 분들께 감사의 말씀 전하고자 합니다.

무엇보다 저를 제자로 받아주시고 이렇듯 박사 학위에 이르기까지 지도해주신 김경진 선생님의 은혜에 감사드립니다. 어둠 속을 항해하는 배처럼 헤매는 제자를 때로는 등대처럼 인도해 주시고 때로는 순풍처럼 신뢰와 격려로 등을 밀어주신 스승님의 은혜는 무엇으로 갚아야 좋을지 모르겠습니다. 또한 바쁘신 와중에도 저의 논문 심사를 맡아주시고 많은 조언을 해주신 정진하 교수님, 이건수 교수님, 최석우 교수님, 선웅 교수님께도 이 지면을 빌어 감사의 말씀을 드리고 싶습니다.

긴 시간 동안 또 하나의 가족처럼 지냈던 실험실 선배님, 후배님들에게도 감사를 드리고 싶습니다. 지금은 교수님으로 나가셨지만, 처음 여기 들어왔을 때부터 지금까지 변함없이 선배 연구자로서, 때로는 인생의 선배로서 물심양면으로 도와주시고 계시는 손기훈 교수님과

정수영 교수님께 감사드리며, 두 분의 복된 앞날을 기원합니다. 그리고 항상 부족한 저를 언제나 따뜻하게 돌봐주시고 지금도 크게 의지가 되어 주시는 김희대 박사님께도 감사드립니다. 비록 지금은 외국에 계시지만 최한경 박사님, 이은정 박사님도 실험실 선배로서뿐만 아니라 인간적으로도 많이 도와주신 분들이기에 감사의 인사를 드립니다. 지금은 자리를 옮겼으나 많은 도움을 주었던 은비와 성식이에게 고맙다고 전하고 싶습니다. 그리고 선배 부탁도 자기 일처럼 여기고 열심히 도와주는 정아와 도연이에게도 감사의 말을 전하며, 후배님들 모두 자기 연구에 좋은 결과 얻길 기원합니다.

마지막으로 가족들에게도 큰절 한번 하는 심정으로 감사의 마음을 남깁니다. 공부를 계속하겠다는 제 뜻을 현실이라는 이름으로 꺾는 대신, 멀리 핀란드에서 일하시면서 제가 공부를 할 수 있도록 묵묵히 지원해주신 아버지, 핀란드와 한국을 왕복하시면서 편찮으신 당신의 몸보다도 못난 자식을 더 아껴주시는 어머니, 두 분께는 제 남은 생을 모두 바쳐 그 은혜를 갚아도 모자랄 것입니다. 그리고 제겐 가장 가까운 인생의 선배이자 친구가 되어준 형님에게도 이 고마움을 전하고 싶습니다. 바쁘다는 핑계로 가족에게 좋은 것 하나 가져오지 못하고 좋은 모습도 보여주지 못한 막내지만, 이 가난한 글로나마 진심으로 감사와 사랑을 전하면서 이만 줄입니다.